

NATIONAL COOPERATIVE  
HIGHWAY RESEARCH PROGRAM REPORT

**299**

# **FATIGUE EVALUATION PROCEDURES FOR STEEL BRIDGES**

TRANSPORTATION RESEARCH BOARD  
NATIONAL RESEARCH COUNCIL

## TRANSPORTATION RESEARCH BOARD EXECUTIVE COMMITTEE 1987

### *Officers*

#### Chairman

LOWELL B. JACKSON, *Executive Director, Colorado Department of Highways*

#### Vice Chairman

HERBERT H. RICHARDSON, *Vice Chancellor and Dean of Engineering, Texas A & M University*

#### Secretary

THOMAS B. DEEN, *Executive Director, Transportation Research Board*

### *Members*

RAY A. BARNHART, *Federal Highway Administrator, U.S. Department of Transportation* (ex officio)  
JOHN A. CLEMENTS, *Vice President, Sverdrup Corporation* (Ex officio, Past Chairman, 1985)  
DONALD D. ENGEN, *Federal Aviation Administrator, U.S. Department of Transportation* (ex officio)  
FRANCIS B. FRANCOIS, *Executive Director, American Association of State Highway and Transportation Officials* (ex officio)  
E. R. (VALD) HEIBERG III, *Chief of Engineers and Commander, U.S. Army Corps of Engineers, Washington, D.C.* (ex officio)  
LESTER A. HOEL, *Hamilton Professor and Chairman, Department of Civil Engineering, University of Virginia* (ex officio, Past Chairman, 1986)  
RALPH STANLEY, *Urban Mass Transportation Administrator, U.S. Department of Transportation* (ex officio)  
DIANE STEED, *National Highway Traffic Safety Administrator, U.S. Department of Transportation* (ex officio)  
GEORGE H. WAY, *Vice President for Research and Test Department, Association of American Railroads* (ex officio)  
ALAN A. ALTSHULER, *Dean, Graduate School of Public Administration, New York University*  
JOHN R. BORCHERT, *Regents Professor, Department of Geography, University of Minnesota*  
ROBERT D. BUGHER, *Executive Director, American Public Works Association*  
DANA F. CONNORS, *Commissioner, Maine Department of Transportation*  
C. LESLIE DAWSON, *Secretary, Kentucky Transportation Cabinet*  
PAUL B. GAINES, *Director of Aviation, Houston Department of Aviation*  
LOUIS J. GAMBACCINI, *Assistant Executive Director/Trans-Hudson Transportation of The Port Authority of New York and New Jersey*  
JACK R. GILSTRAP, *Executive Vice President, American Public Transit Association*  
WILLIAM J. HARRIS, *Snead Distinguished Professor of Transportation Engineering, Dept. of Civil Engineering, Texas A & M University*  
WILLIAM K. HELLMAN, *Secretary, Maryland Department of Transportation*  
RAYMOND H. HOGREFE, *Director—State Engineer, Nebraska Department of Roads*  
THOMAS L. MAINWARING, *Consultant to Trucking Industry Affairs for Ryder System, Inc.*  
JAMES E. MARTIN, *President and Chief Operating Officer, Illinois Central Gulf Railroad*  
DENMAN K. McNEAR, *Chairman, President and Chief Executive Officer, Southern Pacific Transportation Company*  
LENO MENGHINI, *Superintendent and Chief Engineer, Wyoming Highway Department*  
WILLIAM W. MILLAR, *Executive Director, Port Authority Allegheny County, Pittsburgh*  
MILTON PIKARSKY, *Distinguished Professor of Civil Engineering, City College of New York*  
JAMES P. PITZ, *Director, Michigan Department of Transportation*  
JOE G. RIDEOUTTE, *South Carolina Department of Highways and Public Transportation*  
TED TEDESCO, *Vice President, Resource Planning, American Airlines, Inc., Dallas/Fort Worth Airport*  
CARL S. YOUNG, *Broome County Executive, New York*

## NATIONAL COOPERATIVE HIGHWAY RESEARCH PROGRAM

### *Transportation Research Board Executive Committee Subcommittee for NCHRP*

LOWELL B. JACKSON, *Colorado Department of Highways* (Chairman)  
HERBERT H. RICHARDSON, *Texas A & M University*  
LESTER A. HOEL, *University of Virginia*

FRANCIS B. FRANCOIS, *Amer. Assn. of State Hwy. & Transp. Officials*  
RAY A. BARNHART, *U.S. Dept. of Transp.*  
THOMAS B. DEEN, *Transportation Research Board*

### *Field of Design*

#### *Area of Bridges*

#### *Project Panel, C12-28(3)*

WILLIAM CROZIER, *California Department of Transportation* (Chairman)  
MARK BOWMAN, *Purdue University*  
GEORGE A. CHRISTIAN, *New York State Department of Transportation*  
WALTER JESTINGS, *Consultant*

KARL KLIPPSTEIN, *University of Pittsburgh*  
ANDREW LALLY, *Andrew Lally, PC, Consulting Engineers*  
C. W. ROEDER, *University of Washington*  
JERAR NISHANIAN, *FHWA Liaison Representative*  
GEORGE W. RING, III, *TRB Liaison Representative*

### *Program Staff*

ROBERT J. REILY, *Director, Cooperative Research Programs*  
ROBERT E. SPICHER, *Associate Director*  
LOUIS M. MACGREGOR, *Program Officer*  
IAN M. FRIEDLAND, *Senior Program Officer*

CRAWFORD F. JENCKS, *Senior Program Officer*  
DAN A. ROSEN, *Senior Program Officer*  
HARRY A. SMITH, *Senior Program Officer*  
HELEN MACK, *Editor*

# **FATIGUE EVALUATION PROCEDURES FOR STEEL BRIDGES**

**F. MOSES, C. G. SCHILLING, and K. S. RAJU**  
Case Western Reserve University  
Cleveland, Ohio

RESEARCH SPONSORED BY THE AMERICAN  
ASSOCIATION OF STATE HIGHWAY AND  
TRANSPORTATION OFFICIALS IN COOPERATION  
WITH THE FEDERAL HIGHWAY ADMINISTRATION

**AREAS OF INTEREST:**

Structures Design and Performance  
Maintenance  
(Highway Transportation, Public Transit, Rail Transportation)

**TRANSPORTATION RESEARCH BOARD**  
NATIONAL RESEARCH COUNCIL  
WASHINGTON, D.C.

NOVEMBER 1987

## **NATIONAL COOPERATIVE HIGHWAY RESEARCH PROGRAM**

Systematic, well-designed research provides the most effective approach to the solution of many problems facing highway administrators and engineers. Often, highway problems are of local interest and can best be studied by highway departments individually or in cooperation with their state universities and others. However, the accelerating growth of highway transportation develops increasingly complex problems of wide interest to highway authorities. These problems are best studied through a coordinated program of cooperative research.

In recognition of these needs, the highway administrators of the American Association of State Highway and Transportation Officials initiated in 1962 an objective national highway research program employing modern scientific techniques. This program is supported on a continuing basis by funds from participating member states of the Association and it receives the full cooperation and support of the Federal Highway Administration, United States Department of Transportation.

The Transportation Research Board of the National Research Council was requested by the Association to administer the research program because of the Board's recognized objectivity and understanding of modern research practices. The Board is uniquely suited for this purpose as: it maintains an extensive committee structure from which authorities on any highway transportation subject may be drawn; it possesses avenues of communications and cooperation with federal, state, and local governmental agencies, universities, and industry; its relationship to the National Research Council is an insurance of objectivity; it maintains a full-time research correlation staff of specialists in highway transportation matters to bring the findings of research directly to those who are in a position to use them.

The program is developed on the basis of research needs identified by chief administrators of the highway and transportation departments and by committees of AASHTO. Each year, specific areas of research needs to be included in the program are proposed to the National Research Council and the Board by the American Association of State Highway and Transportation Officials. Research projects to fulfill these needs are defined by the Board, and qualified research agencies are selected from those that have submitted proposals. Administration and surveillance of research contracts are the responsibilities of the National Research Council and the Transportation Research Board.

The needs for highway research are many, and the National Cooperative Highway Research Program can make significant contributions to the solution of highway transportation problems of mutual concern to many responsible groups. The program, however, is intended to complement rather than to substitute for or duplicate other highway research programs.

## **NCHRP REPORT 299**

Project 12-28(3) FY '85

ISSN 0077-5614

ISBN 0-309-04568-1

L. C. Catalog Card No. 88-50046

**Price \$10.40**

### **NOTICE**

The project that is the subject of this report was a part of the National Cooperative Highway Research Program conducted by the Transportation Research Board with the approval of the Governing Board of the National Research Council. Such approval reflects the Governing Board's judgment that the program concerned is of national importance and appropriate with respect to both the purposes and resources of the National Research Council.

The members of the technical committee selected to monitor this project and to review this report were chosen for recognized scholarly competence and with due consideration for the balance of disciplines appropriate to the project. The opinions and conclusions expressed or implied are those of the research agency that performed the research, and, while they have been accepted as appropriate by the technical committee, they are not necessarily those of the Transportation Research Board, the National Research Council, the American Association of State Highway and Transportation officials, or the Federal Highway Administration, U.S. Department of Transportation.

Each report is reviewed and accepted for publication by the technical committee according to procedures established and monitored by the Transportation Research Board Executive Committee and the Governing Board of the National Research Council.

### **Special Notice**

The Transportation Research Board, the National Research Council, the Federal Highway Administration, the American Association of State Highway and Transportation Officials, and the individual states participating in the National Cooperative Highway Research Program do not endorse products or manufacturers. Trade or manufacturers' names appear herein solely because they are considered essential to the object of this report.

Published reports of the

### **NATIONAL COOPERATIVE HIGHWAY RESEARCH PROGRAM**

are available from:

Transportation Research Board  
National Research Council  
2101 Constitution Avenue, N.W.  
Washington, D.C. 20418

Printed in the United States of America

## FOREWORD

*By Staff  
Transportation  
Research Board*

This report contains guidance for the fatigue evaluation of existing steel bridges. The report includes recommended revisions to the fatigue evaluation requirements presently in the *AASHTO Manual for Maintenance Inspection of Bridges*, along with a companion commentary. Probabilistic limit-states concepts are used in the development of the recommended procedures. In addition, fatigue design procedures in the same format as the evaluation procedures are also presented in the report. The contents of this report will be of immediate interest and use to bridge engineers, researchers, specification writing bodies, and others concerned with the fatigue evaluation and design of existing steel highway bridges.

---

The fatigue provisions in the current *AASHTO Standard Specifications for Highway Bridges* are based on approximations of actual conditions in steel bridges. These provisions combine an artificially high stress range with an artificially low number of stress cycles to produce a reasonable design. Furthermore, the current AASHTO provisions were intended for design applications and not for rating or assessing the remaining fatigue life of existing steel bridges, and do not provide consistent levels of reliability for different cases.

In recent years, much information has been developed on variable-amplitude fatigue behavior, high-cycle, long-life fatigue behavior, actual traffic loadings, load distribution for fatigue, inspection and assessment of material properties and structural conditions, and other important parameters related to fatigue. This new information, together with the extensive information previously accumulated on the fatigue behavior of various steel bridge details, is sufficient to permit the development of realistic procedures for fatigue evaluation.

NCHRP Project 12-28(3), "Fatigue Evaluation Procedures for Steel Bridges," was initiated in 1985 with the objective of developing practical procedures that more accurately reflect the actual fatigue conditions in steel bridges, and that can be applied for evaluation of existing bridges or design of new bridges. The procedures were intended to permit determination of fatigue-load ratings and estimation of remaining life for existing bridges. This report documents that work and provides recommended revisions to the fatigue evaluation requirements in the *AASHTO Manual for Maintenance Inspection of Bridges*. In addition, recommended revisions to the design requirements in the *AASHTO Standard Specifications for Highway Bridges* are presented, in a similar format.

The procedures presented in this report were developed using probabilistic limit-states concepts. The advantages of the procedures developed in the study include: a

more realistic assessment of the fatigue conditions in bridges; consistency in the procedures for designing new bridges and evaluation of existing bridges; consistent and appropriate levels of reliability developed from bridge performance histories; and the ability to quantify the effect of different levels of effort in reducing uncertainties and improving the prediction of remaining life. The procedures use the same detail categories and corresponding fatigue strength data, and the same methods of calculating stress ranges, as the present AASHTO specifications. The report also contains numerous examples demonstrating the use of the recommended procedures.

It is expected that AASHTO will review the recommended evaluation and design specifications for consideration for adoption during 1988.

## CONTENTS

1	SUMMARY
	<b>PART I</b>
5	CHAPTER ONE Introduction Fatigue Behavior of Actual Bridges, 5 Concepts of Fatigue Safety, 7 Proposed Fatigue Design or Evaluation Procedures, 8 Report Organization, 10
11	CHAPTER TWO Proposed Evaluation Procedure Format, 11 General, 11 Stress Range, 11 Remaining Life, 16
22	CHAPTER THREE Proposed Design Procedure Format, 22 Reliability Factors, 22 Design Stress Range, 22 Simplified Design Procedure, 25 Permissible Stress Range for a Desired Design Life, 23 Annualized Costs, 25
28	CHAPTER FOUR Structural Reliability and Calibration of Safety Analysis Introduction, 28 Probability Theory, 29 Reliability Theory, 30 Calibration, 31 Fatigue Reliability Model, 31 Statistical Data Base, 33 Example, 35 Target Betas for Evaluation Procedure, 36 Safety Factors for Evaluation Procedure, 38 Safety Factors for Design Procedure, 42 Fatigue Limit, 42 Infinite Life Safety Margin, 43 Sensitivity Studies, 44
45	CHAPTER FIVE Examples Evaluation, 45 Design, 55 Summary, 58
59	CHAPTER SIX Conditions not Considered in the Evaluation Procedure Secondary Bending, 59 Cracked Members, 61 Corrosion and Mechanical Damage, 65 Case Histories, 67
67	CHAPTER SEVEN Conclusion and Suggested Research Conclusions and Implementation, 67 Suggested Research, 67
	<b>PART II</b>
70	APPENDIX A Proposed Fatigue Evaluation Procedures
74	APPENDIX B Proposed Fatigue Design Procedure
77	APPENDIX C Alternative Procedures
84	APPENDIX D Traffic Loading Data
84	APPENDIX E Bridge Response Data
85	APPENDIX F References and Bibliography

## **ACKNOWLEDGMENTS**

The research documented in this report was conducted under NCHRP Project 12-28(3). The co-principal investigators were Fred Moses, Professor of Civil Engineering, Case Western Reserve University, and Charles G. Schilling, Consulting Engineer. K. S. Raju, a graduate student in Civil Engineering at Case made extensive contributions to this research. The NCHRP Project Panel assisted greatly with valuable comments and suggestions along with contributions from members of the AASHTO Highway Subcommittee on Bridges and Structures. In

addition, this research was ably assisted in preparing examples and reviewing reports by project consultants Dr. Abba Lichtenstein of A. G. Lichtenstein and Associates and Dr. John Fisher of Lehigh University. Special thanks are also extended to Baidar Bakht of Ontario Ministry of Transportation who provided examples of lateral distribution factors, Dr. Michel Ghosn of City University of New York who assisted with development of the load data base, and William Nyman and John Gobieski, graduate students, who assembled fatigue data and performed reliability modeling.



# FATIGUE EVALUATION PROCEDURES FOR STEEL BRIDGES

## SUMMARY

The primary purpose of this study was to develop improved procedures for the fatigue evaluation of existing steel bridges. A secondary objective was to develop improved procedures for the fatigue design of new steel bridges. The evaluation procedures are recommended for inclusion as Section 6 in the AASHTO *Manual for Maintenance Inspection of Bridges* and the design procedures are recommended for inclusion as Articles 10.3.1 and 10.3.2 in the AASHTO *Standard Specifications for Highway Bridges*.

### *Background*

Present AASHTO design procedures do not reflect actual fatigue conditions in bridges; instead, they combine an artificially high stress range with an artificially low number of stress cycles. Furthermore, present procedures are somewhat rigid, do not reflect recent fatigue research findings, do not provide consistent levels of reliability for different cases, do not permit calculation of the remaining fatigue life, and are not suitable for evaluating existing bridges.

Advantages of the procedures developed in this study include the following:

1. They realistically reflect actual fatigue conditions in bridges.
2. They provide consistent procedures for evaluating existing bridges and designing new bridges.
3. They permit suitable flexibility in making designs and evaluations.
4. They include procedures for calculating the remaining fatigue life and permit these calculations to be updated in the future to reflect changes in traffic conditions.
5. They provide consistent and appropriate levels of reliability developed from performance histories.
6. They are based on extensive recent research and can be conveniently modified in the future to reflect future research.
7. They permit different levels of effort to reduce uncertainties and improve predictions of remaining life.
8. They utilize the same detail categories and corresponding fatigue strength data as the present AASHTO specifications.
9. They utilize methods of calculating stress ranges that are similar to present AASHTO methods.

Most of the fatigue damage in a bridge is caused by passages of single trucks across the bridge. The total number of truck passages in the 75- to 100-year life of a bridge can exceed 100 million, but is often much less. The effective stress range rarely exceeds 5 ksi and is usually 1 to 3 ksi. Traffic volumes usually grow at an annual rate of about 3 to 5 percent until they reach a very high limiting value. Traffic volumes on some urban highways are presently at such high levels.

Static strength design must be based on the worst conditions expected to occur over the life of the bridge because a single occurrence exceeding a critical level causes collapse or unacceptable damage. Fatigue checks, on the contrary, should be based

on typical conditions that occur, often because many repetitions are required to cause a failure. In a fatigue check, permissible stress conditions are related to particular design lives, and exceeding these permissible conditions merely shortens that life rather than causing an immediate failure.

In strength design procedures, a conservative assumption is often made in each step to account for the worst conditions expected in that step. Because the worst conditions will not occur simultaneously in all steps, this can lead to an excessive overall safety level. A reliability analysis can be used to interrelate the individual safety levels from each step and assess the overall safety they provide. Such reliability analyses were used in developing the new fatigue design and evaluation procedures.

### *Evaluation Procedures*

These procedures apply only to uncracked members subjected to primary stresses that are normally calculated in design.

The stress range is calculated first and used to predict the remaining mean and safe fatigue lives. The remaining mean life is the best possible estimate of the actual remaining life. The remaining safe life is a more conservative estimate which provides a level of reliability comparable to present AASHTO fatigue provisions. Alternatives that may be used at the option of the Engineer are given for several steps in the procedure. Each detail must be considered individually.

*Stress Range.* The stress range for the fatigue evaluation can be calculated by the following steps or, alternatively, can be determined from field measurements.

*Fatigue Truck.* A fatigue truck is used to represent the variety of trucks of different types and weights in the actual traffic. This truck has a constant spacing of 30 ft, rather than a variable spacing, between main axles. This spacing approximates that for the 4- and 5-axle semitrailers that do most of the fatigue damage to bridges. The gross weight of the fatigue truck is 54 kip; this weight was developed from extensive recent weigh-in-motion data. Alternatively, the gross weight can be calculated from a truck-weight histogram obtained from weigh station or weigh-in-motion data for the site by using an equation based on extensive variable-amplitude fatigue tests of simulated bridge members. Alternative axle spacings and weight distributions based on site data are also permitted.

*Truck Superpositions.* The effects of more than one truck on the bridge at a time can be neglected unless there are special conditions that cause bunching of the trucks. For such special conditions, the gross weight of the fatigue truck is increased by 15 percent; this percentage is based on judgment supported by field data.

*Impact.* The impact factors caused by different trucks on a given bridge usually vary considerably. The "typical" or "average" factor, rather than the maximum factor, affects the fatigue evaluation. Also, the impact factor used for fatigue evaluation is for stress range rather than peak stress. Field data indicate that a factor of 10 percent is appropriate for fatigue evaluations. Poor joint or pavement conditions, however, require higher values.

*Moment Range.* The fatigue evaluation is based on the moment or axial load range caused by the passage of the fatigue truck across the bridge.

*Lateral Distribution.* The lateral distribution factors for the fatigue evaluation are based on a single truck at the centerline of a traffic lane rather than on trucks in all lanes. These factors approximate those developed from extensive analytical studies and are consistent with available field data. Alternatively, lateral distribution factors can be determined by more refined analytical methods.

*Member Section.* Many field tests have shown that the bending strength of actual bridges is usually well above that calculated by normal procedures, which conserv-

actively neglect such effects as unintended composite action, contributions from non-structural elements such as parapets, unintended partial end fixity at abutments, and direct transfer of load through the slab to the supports. To account for these beneficial effects, the computed section modulus is increased by appropriate percentages for composite and noncomposite sections, respectively.

*Reliability Factors.* Reliability factors are provided to assure adequate safety and consistent levels of reliability in calculating the remaining safe life for various different cases. Basic factors are recommended for redundant and nonredundant members. The corresponding probabilities that the actual remaining fatigue life will exceed the calculated remaining safe life are about 97.7 percent and 99.9 percent, respectively. The reliability factor is 1.0 for calculating the remaining mean life.

*Compressive Dead Load Stresses.* If the compressive dead load stress is high enough so that essentially all of the stress cycles caused by normal traffic are completely in compression, the fatigue life is assumed to be infinite. This occurs when the compressive dead load stress is equal to the tension portion of the (factored) stress range caused by the heaviest truck in the traffic. For this estimate it is assumed that the heaviest truck weighs twice as much as the fatigue truck; less than 0.2 percent of trucks weigh more than this value.

*Fatigue Limit.* If the maximum stress range in tension falls below the fatigue limit for a particular detail, crack growth will not occur and infinite fatigue life may be assumed. This situation, which applies primarily to higher detail categories (C and above), is checked by comparing the factored stress range with a fatigue limit value calibrated to provide an adequate reliability that crack initiation will not occur. This fatigue limit value is equal to 0.367 times the present AASHTO allowable stress range for the over-two-million cycle category. When the factored stress range is below this value, substantially all of the stress cycles in the spectrum are below the constant-amplitude fatigue limit.

*Finite Remaining Life.* If a given detail does not satisfy the infinite life check, the remaining mean or safe fatigue life (in years) corresponding to the factored stress range is calculated for a lifetime average truck volume and a selected number of stress cycles per truck passage. Alternatively, more refined procedures that involve growth rates and changes in truck weights with time can be used to calculate the remaining fatigue life. The factors involved in the basic and alternative procedures are discussed in the following paragraphs.

*Detail Constants.* Detail constants are given for the detail categories in the present AASHTO specifications. Except for Category F, these detail constants define SN curves that are consistent with the present AASHTO allowable stress ranges.

The SN curve for Category F (shear on throat of fillet weld) uses the same slope as the curves for the other categories instead of the different slope implied by the present AASHTO allowable stress ranges. Because Category F rarely governs, use of the different slope is not justified. This approach is conservative for the lives that actually occur in bridges.

*Cycles Per Truck Passage.* The passage of the fatigue truck across a short-span bridge usually produces a complex stress cycle that has two major peaks (corresponding to the main axles) and a valley between. The exact shape of the complex cycle can be determined from an influence line, and the net effect of the complex cycle can be represented by an equivalent number of individual cycles. The equivalent number of stress cycles per truck passage, determined in this way, is given for various cases. Alternatively, the cycles per passage can be calculated directly for the bridge under consideration.

*Lifetime Average Truck Volume.* The lifetime average truck volume may be either estimated by the Engineer or obtained from graphs involving (1) the present truck volume at the site, (2) the present age of the bridge, and (3) the annual growth rate.

The present truck volume at a site can be calculated from the average daily traffic (ADT) volume by applying factors for the percentage of trucks in the traffic and the percentage of trucks in the outer lane.

*Options If Remaining Life Is Inadequate.* The evaluation procedure gives four options that may be pursued if the Engineer considers the calculated remaining safe fatigue life to be inadequate. These include (1) calculating fatigue life more accurately (2) restricting traffic on the bridge, (3) repairing the bridge, or (4) instituting periodic inspections.

#### *Design Procedure*

The design procedure utilizes most of the same concepts as the evaluation procedure, but is in a format convenient for design. Specifically, the factored design stress range must be less than a permissible stress range for the desired design life unless essentially all of the stress cycles caused by normal traffic are entirely in compression.

*Reliability Factors.* The reliability factors for redundant and nonredundant members correspond to probabilities of about 85 percent and 99.9 percent, respectively, that the actual fatigue life will exceed the design life. These probabilities are considered adequate because (1) the consequences of exceeding the factored permissible stress range is a shorter life rather than immediate failure, (2) the fatigue safety of the bridge can be periodically reassessed in the future, and (3) significantly higher reliability factors would have caused fatigue to govern some designs that would not have been governed by fatigue under current AASHTO specifications.

*Design Stress Range.* The design stress range is calculated by the same procedures as were used in the evaluation procedure. In the design procedure, an impact factor of 15 percent is used instead of 10 percent because of the greater uncertainty about joint and pavement conditions over the life of the bridge.

*Permissible Stress Range.* The permissible stress range for a desired design life (in years) is calculated by an equation that involves the detail constant, the stress cycles per truck passage, and the design truck volume. The provisions regarding the detail constant and the cycles per truck passage are the same as those in the evaluation procedure. In addition, for the higher detail categories (C and above) a permissible stress range corresponding to the infinite life fatigue limit may control. These limiting stress ranges are 0.367 times the constant amplitude fatigue limit and define a lower limit for the permissible stress range.

*Design Truck Volume.* Three options are presented for determining the truck volume, which is the average daily truck volume in the shoulder lane over the design life of the bridge. In the first option, the Engineer estimates the design truck volume, probably in conjunction with the traffic department. In the second, the design volume is obtained from a table based on the expected traffic volume at the bridge opening. This table was developed for a design life of 75 years and an annual growth rate of 3 percent. In the third, the design volume is calculated from the starting truck volume by equations that involve a constant annual growth and a limiting truck volume discussed below. The factors used to calculate the starting truck volume from the starting ADT are the same as those used in the evaluation procedure. This report gives simple graphs for determining the design truck volume that are not included in the design procedure.

*Limiting Truck Volume.* It is unrealistic to project traffic growth indefinitely into the future because traffic volume tends to be self-limiting. Therefore, a limiting truck volume is used in calculating the remaining life. This limiting truck volume is obtained by applying factors (for the percentage of trucks in traffic and the percentage of

trucks in the outer lane) to the maximum practical traffic volume (ADT), which assumed to be 20,000 vehicles per day per lane. This value was obtained from recent data on selected urban highways that carry extremely high traffic volumes.

## CHAPTER ONE

# INTRODUCTION

The maintenance and safety of existing bridges is an important concern of all highway agencies. To assure adequate safety and to assist in assessing maintenance needs, highway bridges are periodically inspected, usually at 2-year intervals. In conjunction with such inspections, a safety rating is established by procedures given in the *AASHTO Manual for Maintenance Inspection of Bridges* (hereinafter referred to as the *Manual*). The *Manual* presents detailed procedures for rating the (nonfatigue) strength capacity of steel bridges but does not give detailed procedures for assessing the safety with respect to fatigue. Instead, it suggests that the *AASHTO Standard Specifications for Highway Bridges* (hereinafter referred to as the *Specifications*) be used as a guide in assessing fatigue strength.

The fatigue provisions in the *Specifications* were originally adopted before adequate information was available on the fatigue conditions in actual bridges. Therefore, these provisions do not reflect the fatigue conditions that actually occur. Instead, they combine an artificially high stress range with an artificially low number of stress cycles to produce a reasonable design. Furthermore, the fatigue provisions in the *Specifications* are presented in terms of allowable stresses and do not indicate how to calculate the remaining life of an existing bridge, which is needed to make cost-effective decisions regarding inspection, repair, rehabilitation, and replacement. Neither the *Manual* nor the *Specifications* considers secondary bending effects or cracked or repaired members.

The objective of the present study is to develop practical fatigue evaluation procedures that:

1. Realistically reflect the actual fatigue conditions in highway bridges.
2. Give an accurate estimate of the remaining fatigue life of a bridge and permit this estimate to be updated in the future to reflect changes in traffic conditions.
3. Provide consistent and reasonable levels of reliability.
4. Permit different levels of effort to reduce uncertainties and improve predictions of remaining life.
5. Apply consistently to both the evaluation of existing bridges and the design of new bridges.
6. Can be conveniently modified to reflect future research.
7. Are suitable for inclusion in the AASHTO maintenance manual and design specifications.

This report describes the development of such procedures for virgin (uncracked and unrepaired) members. As background

for this development, the fatigue behavior of actual bridges is described, several concepts relating to fatigue safety are discussed, and fatigue design and evaluation procedures proposed in the past are summarized. The report also provides information and references on several factors that are not considered directly in the proposed evaluation and design procedures: (a) secondary bending, (b) cracked members, and (c) corrosion and mechanical damage.

## FATIGUE BEHAVIOR OF ACTUAL BRIDGES

### Stress Cycles

**Magnitude.** The stress ranges that occur at critical locations in actual bridges under normal traffic have been extensively measured. A summary of all available results (193) as of 1982 is given in Table E-1 of Appendix E. The results include 215 individual histograms for 41 bridges in 11 states. The bridges included composite and noncomposite simple-span, continuous-span, and cantilever steel girder or beam bridges; no truss bridges are included. The locations of the measurements were not tabulated. Because most of the measurements were made to study fatigue behavior, however, it is assumed that most were made at critical fatigue locations such as near a cover plate end (on the side with the smaller section modulus). The average peak stress range for the 215 histograms was 4.3 ksi. The single highest stress range in any of the histograms was 10.5 ksi, and the next highest was 9.0 ksi. The effective stress range for a variable-amplitude spectrum is defined as the equivalent constant-amplitude stress range that provides the same fatigue damage as the variable-amplitude spectrum (196, 198). The average effective stress range for the 215 histograms is only 1.8 ksi. The single highest effective stress range is 4.9 ksi and the next highest is 4.4 ksi. These data suggest that the peak stress range for histograms for steel girder or beam bridges is almost always below 10 ksi and that the effective stress range is almost always below 4.5 ksi.

Design stress ranges calculated by present AASHTO procedures (209) are usually well above these measured stress ranges. Many factors contribute to the difference. Some of these result from the use in fatigue calculations of static-design procedures that are based on extreme conditions. Fatigue damage actually results from typical, or average, rather than extreme conditions. Specifically, the AASHTO HS-20 truck, the AASHTO lateral

distribution factors, and the AASHTO impact factors are too conservative for fatigue calculations. Similarly, for short and medium span bridges it is inappropriate to use lane loadings in fatigue calculations (195).

Many other factors that contribute to the difference between design and measured stresses are difficult to calculate and are conservatively ignored in design calculations. These include (1) unintended composite action; (2) contributions to strength from nonstructural elements, such as parapets; (3) unintended partial end fixity at abutments; (4) catenary tension forces due to "frozen" joints or rigid end supports; (5) longitudinal distribution of moment; (6) direct transfer of load through the slab to the supports; and (7) direct transfer of load through the deck to supports in truss bridges. Although these factors are difficult to calculate, they consistently combine to produce actual stresses well below those calculated by normal procedures.

**Number.** Average daily traffic volumes (ADT) of 120,000 are not unusual on major six-lane highways in large cities (106). The corresponding traffic volume in one direction is 60,000. About 10 percent of urban traffic is composed of trucks and about 75 percent of these trucks are in the shoulder lanes (195). Thus, the average daily truck traffic (ADTT) in the shoulder lane may exceed 4,500 in some cases. This truck volume applied over a 50-year life results in 82 million truck passages, and the same volume applied over a 100-year life results in 164 million passages. Many bridges put into service in the 1930's are now 50 years old, and some major bridges put into service in the early 1900's are approaching an age of 100 years. In most cases, each truck passage causes one stress cycle, but in some cases it

may cause 1.5 or 2.0 equivalent stress cycles. Thus, well over 100 million stress cycles, and perhaps as high as 300 million cycles, can be expected to occur in some bridges. The cyclic life categories used in selecting the AASHTO allowable fatigue stresses are generally well below this number, for example, 2 million cycles.

On many bridges the traffic volume would be much less. Again, however, considerable growth and uncertainty in traffic volume should be expected over a 50- to 100-year life. Even a very low truck volume of 550 per day applied over a 50-year life corresponds to about 10 million passages. Thus, it is expected that most bridges will be subjected to more than 10 million stress cycles.

### Region of Concern

The foregoing discussion shows that actual bridges are subjected to a very large number of relatively small stress cycles. The region of concern is shown on the log-log chart in Figure 1; effective stress range is the ordinate and number of stress cycles is the abscissa. The region of concern is enclosed within a rectangle bounded by an effective stress range of 5 ksi and cyclic lives of 10 million and 300 million cycles. The value of 5 ksi represents an approximate upper bound on the effective stress ranges for the stress spectra observed on actual bridges. Most of the effective stress ranges for the observed spectra were between 1 and 3 ksi (see Appendix E). The expected number of stress cycles in most bridges is between 10 million

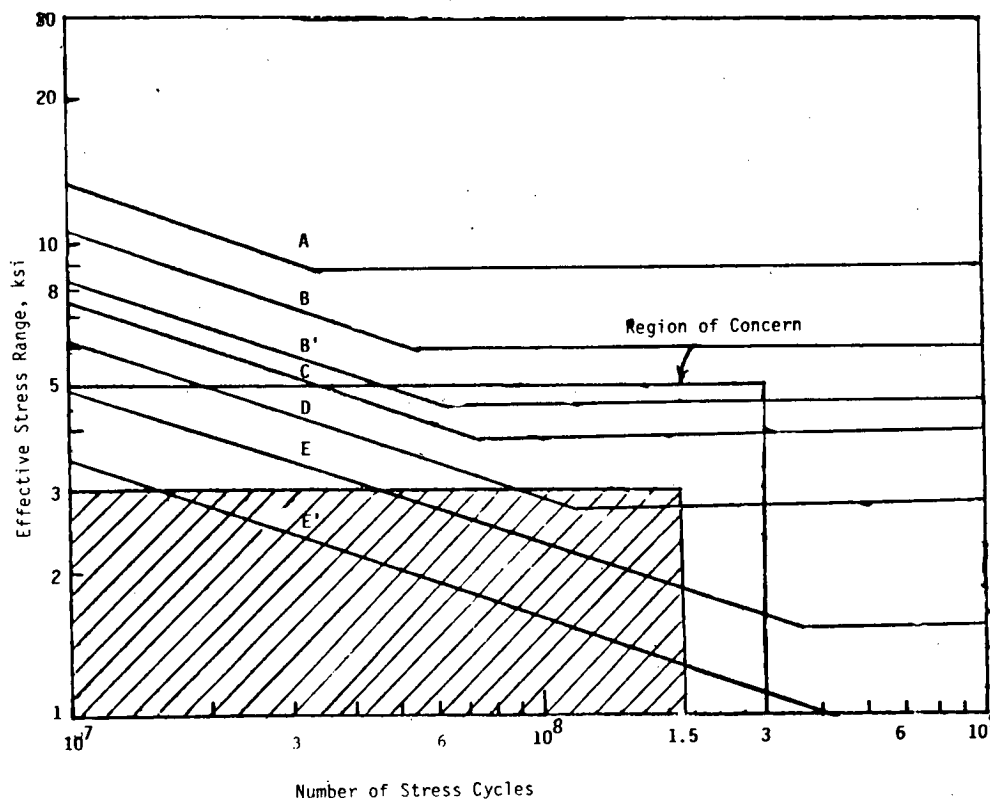


Figure 1. Region of concern for fatigue in highway bridges.

and 150 million cycles. Therefore, an inner region of greater concern is shown as a cross hatched rectangle in Figure 1; it is bounded by effective ranges of 3 and 1 ksi, and cyclic lives of 10 million and 150 million cycles.

The latest AASHTO design SN curves for the various detail categories are also plotted in Figure 1. These curves are conservatively extended below the constant-amplitude fatigue limits because recent research has suggested that the beneficial effects of the constant-amplitude fatigue limit should be ignored if even a few cycles in the spectrum are above this limit. The design SN curves approximate the lower 95 percent confidence limits from test results; the mean curves from these tests are significantly higher.

The design SN curves for Categories A through C are mostly above the inner region of concern; the corresponding mean curves are completely above this inner region. Therefore, very few fatigue problems would be expected for these detail categories. In contrast, much of the design SN curves for Categories D through E' are within the inner region of concern; this is especially true for Category E'. Consequently, many more fatigue problems would be expected with these detail categories. This is consistent with experience; fatigue failures have not been reported for Categories A through C, but have occurred in Categories E and E'. It is fortunate that the SN curves for Categories A through C are above the main region of concern because such details can generally not be eliminated from bridges. On the other hand, Categories D, E, and E' generally can be eliminated, if necessary, by changes in design.

## CONCEPTS OF FATIGUE SAFETY

The concept of safety as applied to repetitive loads that cause fatigue damage is quite different from the concepts of safety that are applied in the normal rating or strength design of a bridge with respect to maximum static (nonrepetitive) loads. An understanding of the differences is needed in selecting suitable fatigue evaluation and design procedures for bridges. Therefore, the differences are discussed here.

A single occurrence of a loading exceeding the corresponding static strength causes unacceptable permanent damage or collapse due to excessive yielding, buckling, or fracture. The critical condition for static rating or design is the worst combination of loads that can occur simultaneously during the life of the bridge; for example, heavy trucks with full impact effect in the worst positions in all lanes at the same time. Only one occurrence of this critical condition needs to be considered and must have a correspondingly small probability of occurrence.

For fatigue, many loading repetitions are required to produce a failure at some time in the future, usually far in the future. Generally, all truck loading stresses, whether above or below the allowable stress range value, cause fatigue damage that could result in a failure in the far future. An exception to this is the case in which all stress range cycles are below the fatigue limit.

To achieve adequate safety, static loading must be kept below the maximum rating or design loading. In contrast, it is not necessary to keep the fatigue loading below any particular value to assure adequate safety. The only effect of increasing or decreasing the fatigue loading is to shorten or lengthen the life of the bridge. Therefore, the effects of fatigue loading on an existing bridge can best be defined in terms of the remaining safe fatigue life of the bridge. Similarly, the effects of fatigue loading on a

new bridge can best be defined in terms of the total life of the bridge, although it may be convenient to use a permissible stress range corresponding to a desired design life to facilitate the reportioning of members that do not have an adequate life. Safety factors can be applied in calculating the remaining or total life to assure that the actual life will exceed the calculated life with a desired degree of probability or reliability.

## Fatigue-Life Approach

The fatigue-life (remaining life) approach can be applied in several ways to existing bridges to achieve adequate safety. If an evaluation of an existing bridge reveals that the calculated remaining fatigue life is less than desired, the Engineer has four options. First, he could recalculate the remaining life using more accurate data. For example, he could use more accurate calculations of lateral distributions. Also, he could make a traffic survey to obtain site-specific data on the volume and weight distribution of trucks rather than using general values. Second, he could restrict the weight and/or volume of trucks to increase the fatigue life. Third, he could modify the bridge to improve its fatigue life. For example, if a particular detail caused the short fatigue life, it could be retrofitted to improve its fatigue characteristics. Alternatively, the stress level in the bridge could be reduced by adding cross section or by other means; this would also increase the fatigue life. Fourth, he could institute periodic inspections at appropriate intervals to assure that fatigue cracks could be detected before components actually failed. Estimates of the remaining lives of various details would be helpful in selecting appropriate inspection intervals and allocating inspection efforts. With any of these four options, the bridge can be easily reevaluated at any time in the future to reflect changes in traffic or other conditions.

An accurate estimate of the remaining fatigue life of a bridge also has other important uses. Such an estimate is needed in bridge management systems that are used to make cost-effective decisions regarding inspection, maintenance, repair, rehabilitation, and replacement of existing bridges. Estimates of remaining fatigue life would also be very useful in assessing permit-vehicle policy or determining the effects of permitting a certain class of overloaded vehicles to use the highways. Similarly, remaining-life estimates could be used in assessing legislative policies such as permissible truck weights.

The fatigue-life approach can also be applied in the design of new bridges. Generally, any particular detail that does not provide the desired life would be redesigned in the same way that it would be with allowable-stress procedures. To facilitate the redesign, it may be convenient to use a permissible stress range corresponding to a desired safe design life. Instead of redesigning, however, the designer might alternatively choose to recalculate the life with more accurate data or decide the calculated life is acceptable for that particular bridge. The latter may be a logical decision for, say, a rehabilitation job. The estimated life of a new bridge must be based on assumptions regarding future conditions, especially traffic loadings, which are likely to change significantly over the 50- to 100-year life of a typical bridge. Since the bridge can be periodically re-evaluated in the future on the basis of the actual conditions that have occurred, it is not realistic to impose unnecessarily rigid requirements for the calculated total fatigue life of a new bridge being designed.

Defining the effects of fatigue in terms of fatigue life is a

much more useful approach than imposing rigid allowable fatigue stresses. The fatigue-life approach provides the following advantages: (1) it defines the actual effects of fatigue loadings on a bridge, (2) it permits the Engineer to choose from among many suitable options to assure adequate safety, (3) it permits the Engineer to react in a rational way to future changes in fatigue loadings or other pertinent factors, (4) it replaces the rigid go/no-go approach imposed by allowable-stress procedures with a flexible approach that is more appropriate for the uncertain and changing conditions that affect fatigue, and (5) it helps the practicing engineer to recognize that fatigue loadings affect safety in a far different way than do static (nonrepetitive) loadings.

### Reliability

In developing and utilizing design procedures, it is normal and appropriate to make conservative assumptions at each step. Many of these conservative assumptions are hidden in various specification parameters and equations. The conservative assumptions are intended to account for uncertainties in each step of the design process by using the most conservative value that could reasonably be expected to occur in that step. Of course, it is highly unlikely that the values for all steps will be at their worst in the same bridge.

A reliability analysis (50, 160) is often made to assess the safety of a specification that contains safety factors as well as other conservative assumptions. Such an analysis usually defines the degree of safety in terms of a safety index that relates to the probability that a particular limit state condition, such as the strength of a column, will be exceeded (50). A reliability analysis can also be applied to predictions of remaining life in a fatigue evaluation. A safety index can be calculated to indicate the probability that the actual life will be less than the predicted life. It is important to note, however, that the practical consequences of violating this safety parameter, that is, of having an actual life shorter than predicted, is much less severe than the consequences of violating a static-design safety parameter, such as exceeding the strength of a column. Violating the static-design safety parameter can lead to a failure. Violating the fatigue safety parameter means only that the remaining life is shorter than expected.

One of the most important benefits of a reliability analysis is that it shows the interrelationship of the various conservative assumptions that are made at each step in a design or evaluation procedure. Such an analysis helps to put into proper perspective the consequences of exceeding a conservative design value in a single step; usually this detrimental effect will be counteracted at some other step so that the overall safety parameter will not be violated. For example, in a fatigue evaluation, a larger than expected truck loading may be counteracted by a smaller than expected lateral distribution factor so that the actual life will still exceed the predicted life. Another view of this same analysis is that the overall safety (or fatigue life) can be assured with a very high degree of certainty (say, with a risk of failures of only  $10^{-5}$ ) even though the value of the variable in each step is known with much less certainty (say, a  $10^{-2}$  probability level) provided the interrelationship of all variables is properly accounted for in the reliability model. This has an important impact on the overall required safety factor as well as the amount and quality of statistical data needed to produce estimates with high confidence.

## PROPOSED FATIGUE DESIGN OR EVALUATION PROCEDURES

Two comprehensive European fatigue specifications have been adopted in recent years: (1) the ECCS fatigue specifications (172) and (2) the British fatigue code (212). These are discussed below. Numerous other fatigue design or evaluation procedures have been proposed in the literature; these procedures are summarized briefly in subsequent sections.

### Specifications

The fatigue provisions of the present AASHTO design specifications (209) and maintenance-inspection manual (132) were discussed earlier in this chapter and will not be discussed further here.

**ECCS.** For several years the European Convention for Constructional Steelwork (ECCS) has been preparing recommendations (172) for the fatigue design of steel structures, which are intended to apply to highway and railway bridges, crane and machinery supports, and other structures. The ECCS recommendations follow the AASHTO approach of classifying structural details according to their fatigue strength; however, ECCS uses 14 different detail categories instead of the 7 presently used by AASHTO, and includes some details not covered by AASHTO. Furthermore, ECCS gives a complete design SN curve (stress range vs. life) for each category instead of allowable stresses corresponding to specific life categories. These curves are similar to those used to develop the AASHTO allowable stress range values.

The ECCS uses an effective stress range concept similar to that developed in NCHRP Project 12-12 (198) to define variable-amplitude spectra. This effective stress range is based on Miner's Law (139). In the fatigue check, the effective stress range corresponding to the design loading is used with the appropriate SN curve. For highway bridges, ECCS also uses the fatigue-truck concept developed in the NCHRP project (196, 198); in this concept the variety of trucks in typical traffic is represented by standard fatigue vehicles. The fatigue check can be made in terms of either stress or life and rigid allowable stresses are not imposed.

A typical ECCS design SN curve is shown in Figure 2. The dashed horizontal line represents the constant-amplitude fatigue limit for the detail. If all of the stress cycles in a variable-amplitude spectrum are below this limit the life is assumed to be infinite and no further fatigue check is required. The level of the horizontal line is set at the point where the sloping finite-life portion of the curve intersects a life of 5 million cycles. It is assumed that the break between the sloping and horizontal portions of an SN curve occurs at this same life of 5 million cycles for all details. However, this contrasts with data that suggest the break life increases with the severity of the detail (119). For example, the break life for AASHTO category E' details is about 22 million cycles (119).

If some of the cycles in a variable-amplitude spectrum are above the constant-amplitude fatigue limit while others are below, the fatigue life can be determined from the solid curve shown in Figure 2. The sloping portion that is below the constant-amplitude fatigue limit has a slope of 5. The lower horizontal line is drawn at the level where this sloping portion intersects 100 million cycles. This lower cutoff line is at a level



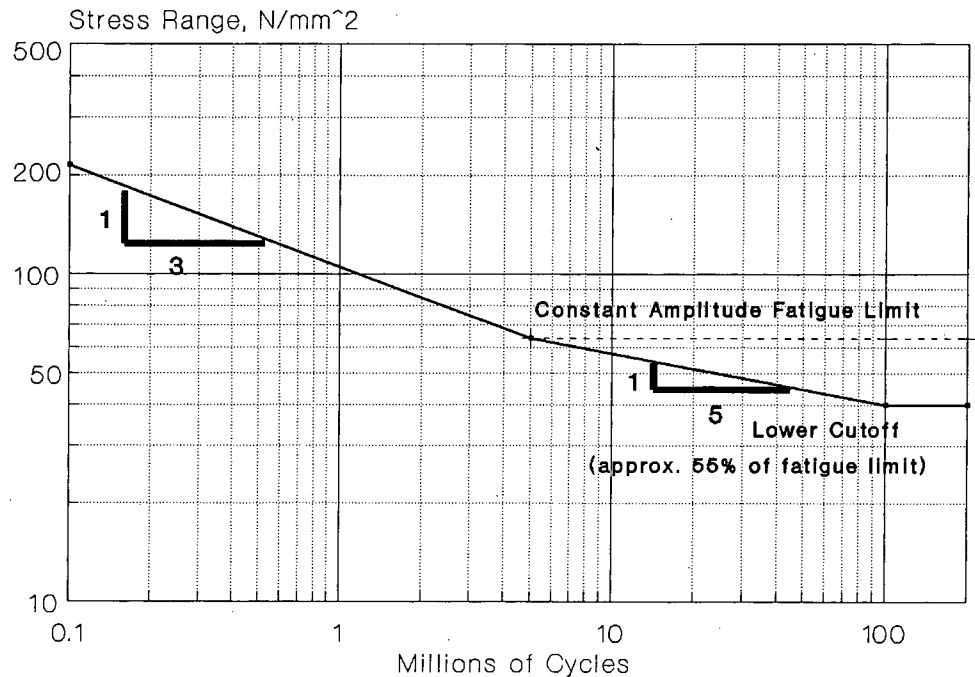


Figure 2. Typical SN curve from ECCS recommendation.

approximately 55 percent of the constant-amplitude fatigue limit for each detail. Alternatively, a slope of 3 may be used between the constant-amplitude fatigue limit and the cutoff line; this is a simpler and more conservative approach. All stress cycles below the lower cut-off line may be ignored.

For welded members, the ECCS recommendations treat compression cycles, in which the applied stress varies in magnitude but is always compressive, the same as tension cycles, in which a portion or all of the applied cycle is in tension. The rationale for this provision is that tensile residual stresses in welded members shift the applied compressive stress cycles into the tension region.

**British.** The recent British fatigue code (212), which applies to both highway and railway bridges, gives three different procedures of varying complexity for highway bridges. All three procedures use the same design SN curves to define the fatigue strengths of various detail categories. The classification of details into categories is similar to that used in the ECCS recommendations (172). Also, the finite-life portions of the SN curves for the various categories are generally about the same as those used by ECCS (172). In the British code, however, the constant-amplitude fatigue limit for each category is taken as the stress range at a life of 10 million cycles and the SN curve is projected below this stress range at a slope of 5. There is no cutoff level below which stress cycles have no effect. For welded members, the British code treats compression cycles the same as tension cycles.

In the simplest of the three procedures, an effective applied stress range for each detail is calculated by loading the bridge with standard fatigue trucks that represent typical truck traffic. This calculated effective stress range must be below an allowable stress range corresponding to a life of 120 years and to a truck volume that is defined for various types of highway. Each truck passage is assumed to cause one stress cycle. The highest of the specified truck volumes is 2 million per year in one lane; this

corresponds to 240 million stress cycles over the expected 120-year life of the bridge. The effective stress range and fatigue truck concepts used in this procedure are based on concepts developed in a previous NCHRP study (198) and are consistent with Miner's Law (139).

The other two procedures are much more complex and permit the direct calculation of the fatigue damage caused by each truck passage. Miner's Law (139) is used to assess the cumulative fatigue damage caused by such passages.

#### Proposed Design or Evaluation Procedures

Many references describing fatigue design or evaluation procedures, which have been proposed for various structural applications, are included in the bibliography in Appendix F. These procedures are intended to realistically reflect the actual fatigue conditions that occur in the structure under consideration. Consequently, they generally involve three steps: (1) calculate the variable-amplitude stress spectrum caused by the actual loading, (2) relate this variable-amplitude stress spectrum to an equivalent or effective constant-amplitude stress by some cumulative damage approach, and (3) compare the resulting applied stress parameter with a fatigue strength (SN) curve to get the fatigue life or to show that the applied stress is below an allowable stress value corresponding to a desired design life. In many of the design procedures, probabilistic methods are used to define the degree of uncertainty in the calculations and to provide consistent levels of safety for various design cases. These approaches are consistent with the probabilistic or reliability approaches used in various static-design codes. Stress range is the main stress parameter in most of the proposed procedures; some also consider the effects of mean stress. Factors of safety may be applied to the applied stress, the strength parameter and/or the design life.

The uncertainty in the calculated variable-amplitude stress

spectrum depends on how accurately the loading can be defined and on how accurately stresses can be calculated from the loading. For highway bridges, truck traffic is the main fatigue loading and a gross weight histogram for such traffic is the most important parameter defining this loading. Therefore, most of the proposed procedures define a typical histogram and/or permit the use of an actual histogram for the site. The wheel spacings and distributions of the gross weights to various axles are also important and are defined in most of the proposed procedures. Calculation of the stresses from the loading involves factors to account for lateral distribution, impact, and truck superpositions. These parameters are usually covered in some way in the proposed procedures.

Miner's Law (139) is used in almost all of the proposed procedures to relate variable-amplitude fatigue behavior to constant-amplitude behavior. Although Miner's Law is often criticized by researchers, especially those dealing with special types of loadings, an extensive NCHRP study (198) of simulated bridge members showed that it is unbiased for such members and that the scatter in predicting the life is not large. For convenience, many of the proposed procedures use the effective stress range concept that was developed in the NCHRP study (198) and is based on Miner's Law. In this concept, a variable-amplitude spectrum is represented by an equivalent constant-amplitude stress cycle. Several of the proposed methods carry this concept one step further and use an effective fatigue truck to represent typical truck traffic (198).

In most of the proposed procedures pertaining to highway bridges, the effective stress range is compared with fatigue strength curves that are consistent with the present AASHTO allowable fatigue stresses (209) for various detail categories. The finite-life portion of these curves represents the approximate lower 95 percent confidence limit for the worst detail in each category. Mathematical expressions are often given to define the curves, and parallel lines representing other confidence levels are sometimes provided. Some of the proposed procedures give allowable stresses for various details that are based on the fatigue strength curves; generally, these allowable stresses are based on heavy traffic volumes that are considered appropriate for specified types of highways and on a particular design life. For example, the Connecticut Department of Transportation (51) includes such a fatigue check in its bridge evaluation rating procedures. Some procedures, however, give allowable stresses for any estimated lifetime average truck volume and desired design life. Thus, truck volumes appropriate for the actual site can be used. Some of the procedures recognize that a truck passage may cause more than one stress cycle and give procedures to define the appropriate number of stress cycles per truck passage. None of the procedures include methods of assessing the effects of increases in truck volume and weights over the life of the bridge.

Some of the proposed procedures use a variable-amplitude fatigue limit that is some fraction of the constant-amplitude fatigue limit. If the effective stress range for the spectrum is

below this variable-amplitude fatigue limit, the fatigue life is assumed to be infinite. Other procedures project the finite-life portion of the fatigue strength curve downward without limit and thus assume that the constant-amplitude fatigue limit has no effect on the fatigue life. Since the effect of fatigue limit is still under study, the more recent proposals generally adopted the conservative approach of extending the fatigue curve downwards without a limit. Generally, a uniform slope of 3 is used for the sloping portions of the log-log SN curves. Some of the proposed procedures assume that the fatigue life is infinite if all of the stress cycles in the variable-amplitude spectrum are always in compression. This is consistent with the present AASHTO (209) approach.

Many of the proposed procedures use probabilistic concepts for assessing safety. Some of the procedures are intended to indicate the probability that the actual fatigue life will exceed a particular value. Many procedures use reliability calculations to assess or adjust the level of safety associated with a particular design procedure or to obtain a consistent level of safety over a range of design cases. The values of key parameters in a design procedure can be adjusted to improve this consistency. Some factors that affect the fatigue stresses in actual bridges, such as unintended end fixity at abutments, may also be included in the design procedure or reliability analysis to assure uniformity in safety levels.

## REPORT ORGANIZATION

Chapter Two discusses each step in the proposed evaluation procedure and explains the basis for the equations and factors used in that step. The evaluation procedure as it would appear in the AASHTO *Manual for Maintenance Inspection of Bridges* is given in Appendix A. Chapter Three is composed of the proposed design procedure, which is given in Appendix B, as it would appear in the AASHTO *Standard Specifications for Highway Bridges*. Chapter Four presents structural reliability background, a reliability model for fatigue life prediction and calibration of the proposed evaluation and design methods. Chapter Five contains examples of the application of the proposed evaluation and design procedures, and compares these procedures with current AASHTO methods. Chapter Six includes information and references on several factors that are not considered directly in the proposed evaluation and design procedures, such as secondary bending, cracked members, and corrosion and mechanical damage. Chapter Seven contains a summary of the conclusions and suggestions for further research. Appendix C gives alternative procedures that are permitted in the evaluation procedure, but are not described in detail in Appendix A. Appendixes D and E provide a summary of traffic loading and bridge response data, respectively, to support the proposed fatigue evaluation and design procedures. Cited references and bibliography are provided in Appendix F.

## CHAPTER TWO

## PROPOSED EVALUATION PROCEDURE

## FORMAT

A proposed fatigue evaluation procedure for existing steel highway bridges is given in Appendix A in the form it might appear in the 1983 AASHTO *Manual for Maintenance Inspection of Bridges* (132). The development of the procedure is discussed in this chapter. First, the overall format is discussed in general. Then each step in the procedure is discussed in detail. Additional explanations and supporting data are given in Appendixes D and E.

The evaluation procedure contains a relatively simple basic procedure for calculating both the remaining mean life and the remaining safe life of a detail. More complicated alternative procedures that may be used at the option of the Engineer are also included. Most of the alternative procedures require more effort than the basic procedure, but generally result in less uncertainty and hence a longer calculated remaining safe life. For each step, the basic procedure is presented first and may be followed by one or more numbered alternative procedures. Some of the more involved alternative procedures are not described in detail in the evaluation procedure itself, but are given in Appendix C. To follow the relatively simple basic procedure, the Engineer merely ignores all of the numbered alternative procedures. The evaluation procedure also presents options that can be pursued by the Engineer if he considers the calculated remaining life to be inadequate.

## GENERAL

## Scope

The evaluation procedure is applicable to virgin (uncracked and unrepaired) members subjected to primary stresses that are normally calculated in design. It does not cover (1) the effects of secondary bending that is not normally calculated in design, (2) the evaluation and repair of cracked members, or (3) the effects of corrosion and mechanical damage. However, information and references on these effects are given in Chapter Six. The evaluation procedure does apply to members that have received normal repairs during fabrication.

## Approach

The remaining fatigue life for a detail is obtained by first determining a nominal stress range for the truck traffic crossing the bridge and then calculating the life corresponding to this stress range based on an estimated truck volume. Two different estimates of remaining life can be obtained: (1) the remaining mean life and (2) the remaining safe life. These two different estimates of remaining life provide a useful indication of fatigue safety and facilitate reasonable cost-effective decisions regarding repair, rehabilitation, or replacement.

The remaining mean life is the best possible estimate of the actual remaining life; there is a 50 percent probability that the actual remaining life will exceed the remaining mean life. The remaining mean life is the same for redundant and nonredundant members.

The remaining safe life provides a much higher degree of safety. The remaining safe life is different for redundant and nonredundant members because different levels of safety are provided for the two cases. Specifically, the probability that the actual remaining life will exceed the remaining safe life is 97.7 percent for redundant members and 99.9 percent for nonredundant members. These levels of safety approximate those associated with the present AASHTO fatigue design provisions (209) as discussed in Chapter Four. To achieve these desired levels of safety, appropriate reliability or safety factors are applied to the stress range calculated by the basic procedure. To account for improved analysis accuracy, lower safety factors are applied for alternative procedures used in calculating the stress range. However, these lower safety factors, still yield the same probabilities of failure as the basic procedure.

The ratio of the total mean fatigue life, in cycles to failure, to the total safe fatigue life is constant for various cases (different bridges, details, etc.). This ratio is about 5 for redundant members and 10 for nonredundant members. These large ratios are required to provide a degree of safety consistent with present AASHTO fatigue design provisions (209). The ratios of the stress ranges corresponding to the mean and safe lives are equal to the cube roots of these life ratios: about 1.7 for redundant members and 2.2 for nonredundant members.

For two reasons, the ratios of the remaining mean and safe lives in years are not the same as the ratios of the total lives in cycles to failure. First, the life in years is not directly proportional to the number of cycles to failure if a compound growth rate is involved. Second, the same number (the age of the bridge) must be subtracted from the total mean and safe lives to get the remaining mean and safe lives.

## STRESS RANGE

## General Procedure

In the basic procedure, the nominal stress range is calculated from general information or from specific site data by the steps discussed in subsequent paragraphs. As an alternative, however, the nominal stress range can be calculated from a stress-range histogram obtained from field measurements on the bridge under normal traffic. The equation used to calculate the effective stress range was developed from extensive fatigue tests of details under simulated traffic loadings (198), and is given as:

$$S_r = (\sum f_i S_{ri}^3)^{1/3} \quad (1)$$

where  $f_i$  = fraction of stress ranges within an interval  $i$ ,  $S_{ri}$  = midwidth of stress interval  $i$ , and  $S_r$  = effective stress range.

The fatigue damage caused by a given number of cycles of the effective stress range is the same as the damage caused by an equal number of the different stress ranges defined by the histogram or stress spectrum. This root-mean-cube formula is based on Miner's Law (139) and a slope of 3 for a straight line log  $S$  vs. log  $N$  fatigue curve. This slope has been adopted as the basis for the AASHTO allowable fatigue stresses for all detail categories except F. Miner's Law is used because it has been shown to provide reasonably accurate results for a broad range of applications and is easy to use. Furthermore, extensive fatigue tests of simulated bridge members confirmed that it is applicable for such members (198).

## Fatigue Truck

### Axle Configuration

The fatigue truck used in the evaluation procedure (Figure 6.2.2A in Appendix A) was proposed by Schilling (196, 198) to represent the variety of trucks of different types and weights in actual traffic. Because a high percentage of the fatigue damage in a typical bridge in the United States is done by 4- and 5-axle semitrailers (195), the axle spacing and axle load distribution of the proposed fatigue truck approximate the spacing and load distribution for such trucks. Measurements of actual trucks (195, 205) showed that the spacing of main axles is about 30 ft. The dual axles on the semitrailers are represented by single axles on the fatigue truck.

Other possible fatigue trucks, such as the AASHTO HS-20 truck, a vehicle proposed by Pavia (146), and the AASHTO legal rating vehicles (3S2), were investigated along with the proposed fatigue truck to see which best represents the actual traffic. The criteria for evaluating these possible fatigue trucks are based on a moment ratio that is defined as the average value of the influence factor (maximum moment divided by gross weight) for the actual traffic divided by the influence factor of the fatigue truck. The gross weight of the fatigue truck is determined from the actual traffic as explained in the next section; consequently, the moment ratio defines the effects of axle configuration alone.

The moment ratios depend on (1) the type of bridge (continuous or simple), (2) the span length, (3) the location along the span, and (4) the percentages of different types of trucks in the traffic. Ideally, the axle configuration of the fatigue truck should provide a moment ratio that is close to 1.0 and varies as little as possible with the span length and type of bridge. As demonstrated in Appendix E, the fatigue truck used in the evaluation procedure satisfies these criteria better than the other trucks that were considered. The variation in the effect of axle configuration with span length and type of bridge is included in the reliability calibration. Although a constant 30-ft spacing of main axles is required to accurately assess fatigue life, it is sometimes convenient to use a variable spacing of 14 to 30 ft, which corresponds to the spacing for the AASHTO HS-20 truck (209). If this variable spacing is used, the moment caused by the fatigue truck can be obtained from that caused by the HS-20 truck by multiplying by the ratio of gross weights. It is always conservative to use the variable spacing, but the calculated fatigue life will be considerably reduced if the span length

is small. For example, on a 60-ft simple-span bridge, using the 14-ft spacing increases the maximum midspan moment by 55 percent and reduces the calculated life by a factor of 3.7.

### Gross Weight

The gross weight of the fatigue truck used in the basic procedure is 54 kip. This is an effective weight that represents the actual truck traffic spectrum from recent (1981) WIM studies (205) that included 30 sites nationwide and more than 27,000 observed trucks. Earlier FHWA loadometer data (195) had suggested a gross weight of 50 kip for the fatigue truck. The increase can be attributed to two main factors. First, the WIM measuring systems are undetectable to drivers and, hence, include some overweight trucks not found in typical FHWA loadometer studies. Second, part of the increase may reflect real growth in truck weights with time.

The effective weight for a given truck traffic is selected so that the fatigue damage caused by a given number of passages of a truck of this weight is the same as the fatigue damage caused by an equal number of passages of trucks of different weights in the actual traffic. An equation (similar to Eq. 1) defining the effective gross weight  $W$  is given below.

$$W = (\sum f_i W_i^3)^{1/3} \quad (2)$$

where  $f_i$  = fraction of gross weights within interval  $i$ , and  $W_i$  = midwidth of interval  $i$ .

Equation 2 was used to calculate the effective gross weight of 54 kip from the WIM data, and also effective weights from other data discussed in Appendix D.

To recognize the considerable region-to-region and site-to-site differences in truck weight population, four alternatives for determining the gross weight of the fatigue truck are permitted in the evaluation procedure: (1) adjust the gross weight based on judgment supported by a knowledge of traffic at the site, (2) calculate the gross weight from weigh station data, (3) calculate the gross weight from local weigh-in-motion data, and (4) calculate the gross weight from traffic survey data that include the percentages of various types of trucks in the traffic but not a gross weight histogram. Equation 2 is used in these calculations. The partial safety factors applied for weigh station and WIM data differ because weigh station data tend to be biased toward lower weights as a result of efforts to evade load-limit enforcement (205).

Alternatives 2, 3, and 4 state that the histograms used to calculate the effective weight should be based on the truck traffic excluding panel, pickup, and other 2-axle/4-wheel trucks. This same definition of a truck is used later with respect to truck volume. An inconsistency is introduced into the fatigue calculation if the same definition is not used to define both the truck volume and the truck-weight histogram. For example, if 2-axle/4-wheel trucks were included, the truck volume would be considerably higher, but the effective truck weight would be correspondingly lower. The definition that was chosen is convenient and reasonable because the excluded vehicles cause very little fatigue damage. To use a definition based on excluding trucks weighing less than a certain amount would be inconvenient because traffic volume data are usually given in terms of types of vehicles.

### Truck Superpositions

Most trucks cross short- and medium-span bridges individually with no other trucks on the bridge at the same time. Therefore, fatigue evaluations should generally be based on the passage of a single fatigue truck across the bridge in the lane under consideration. A recent study (189, 193) using data on the frequency of occurrence of various spacings in combination with calculations of fatigue damage caused by such spacings showed that the net effect of closely spaced trucks is small for normal traffic conditions. Therefore, for such conditions, the effect of truck superpositions need not be considered by the Engineer in making a fatigue evaluation. This applies to span lengths typically covered by present AASHTO procedures. A headway factor, however, is introduced into the calibration procedure described in Chapter Four to account for possible small increases in stress due to truck superpositions in some cases.

For conditions that tend to cause unusual bunching of trucks, the nominal stress range should be increased by 15 percent to account for the possible detrimental effects of the unusually large percentage of close spacings. Such conditions include a traffic signal on or near the bridge and a steep hill on a two-lane bridge.

The factor of 15 percent is based on judgment supported by the following conservative example for a multilane bridge with multiple girders. Assume that trucks make up 10 percent of the traffic. With "unusual site conditions" causing bunching of trucks, there will always be some vehicle alongside a truck in the shoulder lane. Because trucks make up about 10 percent of the traffic, 10 percent of the time there would be trucks side-by-side on the bridge. If the stress range in the critical girder due to a single truck in the shoulder lane of the bridge is  $S$ , the contribution from the truck in the adjacent lane can be conservatively taken as an additional 0.8 $S$  (80 percent increase in stress due to a simultaneous truck crossing in the adjacent lane). The corresponding effective stress range is given by Eq. 3 where the fraction of time two trucks are present is 0.1; otherwise the fraction is 0.9.

$$S_{re} = [(0.1)(1.8S)^3 + 0.9(S)^3]^{1/3} = 1.14S \quad (3)$$

Limited available field data on multilane bridges suggest a somewhat lower factor. Specifically, for eight carefully monitored test sites (145, 148), the average contribution to a critical girder from an adjacent lane loading was found to be only 42 percent rather than 80 percent. The corresponding bunching factor is 1.06 if there are 10 percent trucks in the traffic; and 1.11, if there are 20 percent trucks in the traffic.

### Long Span Loadings

A recent study (171) investigated the fatigue conditions in long-span cable-stayed bridges. Loading guidelines were presented for cable-stay design and testing compatible with AASHTO specifications. Simulations of traffic loadings were made from truck traffic data supplied from WIM studies. Based on this work it was concluded that present lane loadings are inappropriate for fatigue checks of long-span bridges. As a result, the Post-Tensioning Institute (PTI) recommends that AASHTO truck loading, instead of lane loading, be used for calculating fatigue stresses.

The study (171) also quotes a report on load measurements on a cable-stayed highway bridge over a 3-month period. The maximum values of axial cable stresses recorded under moving traffic were only 13 percent of the design cable stresses due to the specified lane traffic loading (based on DIN 1072). Under an artificially produced, extremely unfavorable traffic jam, 37 percent of the design stresses from lane traffic loading were reached. This confirms that it is inappropriate to use lane loading in calculating fatigue stresses for cable-stayed bridges. However, further work may be needed to establish the appropriate number of cycles for the truck loading and the corresponding safety factor needed. In actual long-span bridges, the traffic loading often causes long periods of continuous stresses of varying magnitude rather than large numbers of individual cycles. The equivalent number of cycles for such periods of continuous stresses may need to be investigated.

As discussed earlier, individual truck passages control fatigue behavior for short- and medium-span bridges, and there is no reason to consider lane loadings in a fatigue evaluation of such bridges. As the span length increases, the relative importance of individual trucks decreases while the relative importance of groups of trucks increases because the effect of such groups depends on the ratio of spacings to span length.

### Impact

For fatigue evaluations, the impact factor should define the increase in stress range, rather than peak stress, caused by dynamic effects. The impact factors for different trucks crossing a particular bridge vary considerably. The impact factor used for fatigue is intended to be an effective value that averages all trucks in the traffic rather than a safe extreme value, such as is used in static design. Theoretically, the effective value for a particular bridge could be obtained by a root-mean-cubed relationship similar to the relationship for effective stress range, but a sufficient quantity of data would rarely be available to permit such a calculation.

The effective impact factor for fatigue also varies considerably among different bridges, but does not appear (161) to be a function of the natural frequency of the bridge as specified for static design in the Ontario bridge code (164) or of the span length as specified for static design in the AASHTO specifications (209). Instead, it depends mainly on the surface roughness or "bump" at the end of the bridge (161).

The value of the impact factor in the basic procedure is intended to represent an average value of the effective impact factor for bridges with a normal amount of surface roughness and a good joint at the bridge abutment. Because the factor amplifies stress range, it includes both an increase in the peak stress and a reduction in the minimum stress caused by a single vehicle crossing. The impact factor of 10 percent used in the evaluation procedure is based on available data from field measurements (161, 191). Specifically, Moses and Nyman reported an average value of 1.12 (161) and Schilling (191) reported average values of 1.15 and 1.17, respectively, for simple- and continuous-span bridges. These values are averaged over different sites and do not account for the roughness of the road surface. Consequently, the evaluation procedure uses an impact factor of 1.10 for smooth surfaces and a factor ranging from 1.10 to 1.30 for rough surfaces.

### Moment Range

The stress range should be based on the passage of the fatigue truck across the bridge in the lane under consideration. Therefore, the corresponding moment range (or axial load range for trusses) for longitudinal members should be obtained by placing the truck alternately in positions that cause the algebraic maximum and minimum moments at the detail under consideration.

For transverse members, the correct stress spectrum could be obtained by making separate moment calculations with the truck in each lane and assigning the frequency of occurrence of each moment according to the percentage of the truck volume that normally uses that lane. (Usually, 80 percent or more of the truck volume (195) is in the shoulder lane.) This procedure, however, is cumbersome and probably would not be justified in most cases. Therefore, the evaluation procedure conservatively specifies that the fatigue truck be placed at the center of the lane resulting in the highest transverse moment. Thus, it is assumed that all the truck volume travels in that lane.

### Lateral Distribution

For longitudinal bending members, a lateral distribution factor,  $DF$ , is applied to the total fatigue truck moment to get the portion of this moment carried by the member under consideration. It is not appropriate to use the AASHTO (209) lateral distribution factors for fatigue evaluations because they are based on all lanes being loaded simultaneously. Further, the AASHTO values consider the worst possible transverse location of the truck with respect to maximum moment. In contrast, the lateral distribution factors for fatigue should be based on typical conditions that occur often. Specifically, they should be based on a single truck positioned at the center of one of the traffic lanes; usually the shoulder lane is critical because most of the truck traffic is in that lane.

For I-shaped members, the basic evaluation procedure specifies that the truck moment be distributed by simple-beam action if there are only two members, and gives separate provisions for lateral distribution to exterior and interior girders if there are more than two members.

For box-shaped members, the basic procedure permits the member cross section to be divided into two equivalent I-shaped members. This is conservative because it neglects the torsional rigidity of the box, which can provide considerable lateral distribution.

Three alternatives to the basic procedure are permitted for I-shaped or box-shaped members. The first two are approximate procedures based on a single truck at the centerline of a traffic lane. The third alternative is a rigorous analysis, again based on a single truck at the centerline of a traffic lane.

The two alternative approximate procedures are given in Appendix C. Both were developed empirically from extensive studies covering a wide range of pertinent parameters as described in Appendix E. One of the studies (14) used orthotropic-plate analytical procedures to develop the lateral distribution factors used in the Ontario bridge code (164). From the results of this study, Bakht developed empirical curves that can be conveniently used to get the lateral distribution factors for a single truck. The other study (192, 193, 194) used finite element procedures to develop lateral distribution factors specifically for use in fatigue checks. As discussed in Appendix E, these ap-

proximate procedures agree reasonably well with lateral distribution factors measured on actual bridges.

The lateral distribution factors used in the basic procedure were developed in the present study; they are based on the alternative orthotropic-plate procedure given in Appendix C and agree reasonably well with measured lateral distribution factors. These factors are given in the familiar AASHTO S/D format. For convenience, however, the S/D factors are based on the full truck moment rather than  $\frac{1}{2}$  of the truck moment as the present AASHTO factors. Development of the basic method is shown in Appendix E. Although separate provisions are given for interior and exterior girders, the factors resulting from these provisions are generally the same unless the bridge has a large overhang and a small shoulder.

For interior girders, the basic procedure gives an upper limit of  $(S-3)/S$  for the lateral distribution factor. This limit prevents the basic factor, which was developed empirically, from exceeding a factor obtained by distributing wheel loads to the two adjacent girders by simple-beam action. This simple-beam distribution to adjacent girders represents a theoretical upper-bound because some of the moment is actually distributed beyond the adjacent girders. The maximum simple-beam distribution to a girder occurs when the centerline of the truck is directly over the girder, and this distribution remains the same as long as the truck centerline is within 3 ft of the girder centerline. Consequently, the limiting simple-beam distribution is  $(S-3)/S$ .

The position of the truck with respect to the exterior girder affects  $DF$  for this girder. It is satisfactory to use the same  $DF$  for both interior and exterior girders provided the truck position is not too close to, or outside of, the exterior girder. Otherwise, a larger  $DF$  must be used for the exterior girder. Bridge dimensions that affect the truck position with respect to the exterior girder are defined in Figure 3. The truck is assumed to be at the center of the shoulder lane. The  $DF$  for the exterior girder must be calculated if the overhang is more than 1 ft and the shoulder width is less than 4 ft. Simple empirical equations are given to calculate the  $DF$  for these unusual cases. These equations are the same as those used for exterior girders in the first alternative procedure (finite element study) given in Appendix C.

Figure 4 shows when the  $DF$  for the exterior girders exceeds that for the interior girders. This figure is conservatively based on an overhang of  $\frac{1}{2}$  the girder spacing—about the maximum used in girder bridges. The solid lines in the figure define the

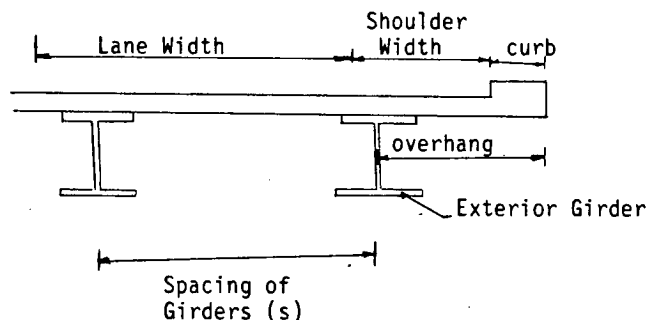


Figure 3. Bridge dimensions that affect distribution factor for exterior girders.

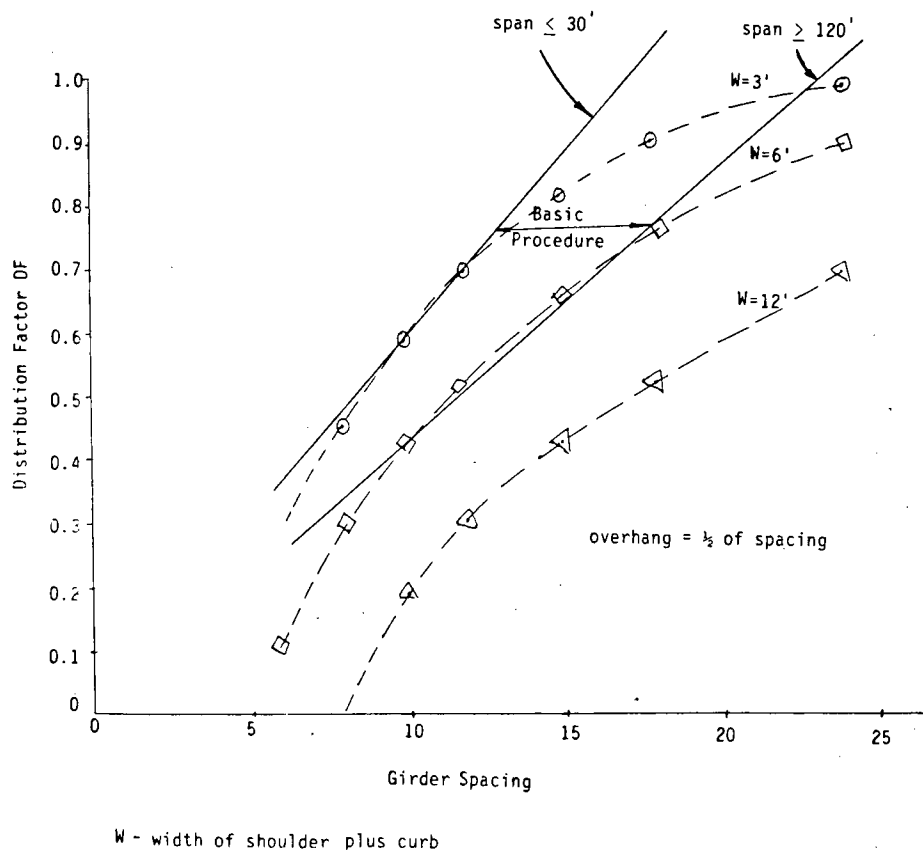


Figure 4. Effect of shoulder width plus curb width.

range of  $DF$  values given by the basic procedure for interior girders of various spans. The dashed lines show the  $DF$  given by the empirical equations (192, 193) for exterior girders; these factors depend on the shoulder plus curb width,  $W$ , but not on the span length. When the shoulder plus curb width is 6 ft or more, the  $DF$  for the exterior girders is less than, or equal to, that of the interior girders. The curb width is generally 1.5 ft or more and the empirical equations for exterior girders are conservative. Therefore, the basic procedure uses the same  $DF$  for interior and exterior girders when the shoulder width is 4 ft or more.

If the overhang is small, as it is in many older bridges, the  $DF$  for the exterior girders is less than that for the interior girders. Therefore, the basic procedure also uses the same  $DF$  for interior and exterior girders when the distance from the face of the curb to the exterior girder is 1 ft or less.

The empirical equations for exterior girders are based on the stiffnesses of the girders alone. In actual bridges, however, curbs and parapets often contribute additional stiffness along the edge of the bridge and thereby reduce the stresses in the exterior girders. Consequently, if normal calculation procedures indicate a problem with the exterior girders, it might be desirable to verify the beneficial effects of the curb or parapet through special calculations or measurements rather than making costly improvements to these girders.

Alternative 2 in the evaluation procedure permits a rigorous analysis for determining the lateral distribution. Generally, this

analysis should be performed with a single truck at the centerline of the shoulder lane because most of the truck traffic is in this lane. Lateral distribution factors should be calculated for the exterior girder and the first interior girder. The factor for the first interior girder can generally be applied to other interior girders. The effect of trucks in other lanes need not be considered in this analysis because it is included in the factor  $F_L$  used in Appendix A, Article 6.3.5.1 of the evaluation procedure to determine the effective truck volume for the evaluation.

A more refined evaluation could be made by determining individual distribution factors for all girders when the truck is at the centerline of each traffic lane and combining stress cycles according to the actual truck volume in each lane. In this way a different stress spectrum could be determined for each girder and used to calculate an effective stress range for that girder. Because of the many uncertainties in the evaluation procedure, such a refined analysis would generally not be justified.

#### Member Section

In the basic evaluation procedure, the section modulus of a beam is obtained by dividing the beam moment of inertia by the distance from the neutral axis to the expected crack initiation location in the detail, and this section modulus is used to calculate the stress range,  $S_r$ . For truss members the cross-sectional area is used to get the stress range,  $S_r$ .

Many field tests have shown that the bending stress in actual bridges is usually well below that calculated by normal procedures, which conservatively neglect such beneficial effects as unintended composite action, contributions from nonstructural elements, unintended partial end fixity at abutments, and direct transfer of load through the slab to the supports. (Some allowance for such beneficial effects is indirectly included in the present AASHTO fatigue provisions.) These beneficial effects are equivalent to an increase in section modulus. Therefore, the proposed procedure permits the Engineer to increase the section modulus in certain cases. Measured values of the beneficial effects from four different sites are shown in Appendix E for composite decks and for noncomposite decks that had no visual separation between deck and girder. Table E-10 gives the proposed increases in section modulus for the above two cases. Because the data are limited to positive bending regions, the increase in section modulus is permitted only for such regions. The provisions for calculating the section modulus are summarized below.

For composite decks, the Engineer can use the AASHTO composite section increased by 15 percent in positive bending regions and a section including the longitudinal reinforcing steel in negative bending regions. The AASHTO composite section is defined in Article 10.38.3 of the AASHTO specifications (209). For noncomposite decks, only the steel section should be used to compute the section modulus. However, if there is no visual separation between the deck and the girder, the computed section modulus in positive bending regions may be increased by 30 percent. As an alternative to increasing the section modulus by 30 percent, the Engineer is permitted to use the AASHTO composite section in positive bending regions. Table E-10 gives data supporting these increases.

### Reliability Factor

In calculating the remaining mean life, it is not necessary to apply a reliability or safety factor to the calculated stress range because this is the best estimate of the actual stress range. In calculating the remaining safe life, in contrast, a reliability, or safety, factor is applied to the calculated stress range to achieve a desired level of safety; that is, a desired probability that the actual life will exceed the safe life. A measure of this probability is given by the safety index, which is a statistical parameter denoted as  $\beta$  (the precise definition is given in Chapter Four). It gives the number of standard deviations contained within the mean safety margin. The correlation between  $\beta$  and risk that the actual life will be less than the calculated life is given in Chapter Four from a standard normal probability table.

The safety factors are calibrated in Chapter Four to achieve certain target values. For most structural applications,  $\beta$  values are in the range from 2 to 4. For fatigue evaluations, a relatively low  $\beta$  is justified because the safety concern associated with  $\beta$  is remaining fatigue life rather than a strength failure such as is used in static design procedures. The consequence of violating this safety parameter is shorter life rather than possible immediate failure.

The target  $\beta$  values for the evaluation procedure are 2.0 and 3.0 for redundant and nonredundant members, respectively. (The AASHTO definition of redundant member, which is based on the judgment of the Engineer, is used so that no additional calculations are required to determine redundancy.) The cor-

responding overall safety factors determined in Chapter Four are 1.35 and 1.75. These factors incorporate the respective uncertainties of loading, analysis, and fatigue life. The corresponding probabilities that the calculated life will exceed the actual life are 97.7 percent and 99.9 percent. The remaining mean life, which is the best estimate of the remaining life, is much greater than the remaining safe life defined above. Examples illustrating the relationship between the mean and safe lives are given in Chapter Five.

As discussed previously, a separate partial safety factor is applied for each alternative method that is used. These factors account for reductions in scatter or bias in the evaluation procedure resulting from using the alternative in place of the basic (or default) procedure. This reduced uncertainty allows the required safety index to be achieved with lower partial safety factors. Specific values of the partial safety factors are determined in the reliability calibration in Chapter Four.

## REMAINING LIFE

### Infinite Life

The remaining life is infinite, and no further fatigue check is required if the factored stress range is below either of two limiting values. The first is based on the constant-amplitude fatigue limit and the second is based on the assumption that a fatigue check is not required when all stress cycles are entirely in compression.

### Fatigue Limit

It is generally accepted that the fatigue life for a variable-amplitude spectrum is infinite if all of the cycles in the spectrum are below the constant-amplitude fatigue limit. Therefore, a variable-amplitude fatigue limit can be obtained by dividing the constant-amplitude fatigue limit by a peak ratio, which is the maximum stress range for the spectrum divided by the effective stress range for the spectrum. If the calculated effective stress range is below this variable-amplitude fatigue limit, the life is taken as infinite; otherwise, the life is finite and must be calculated. Thus, the variable-amplitude fatigue limit serves as a screening level to determine whether a detailed life analysis is required.

Both the peak ratio and the constant-amplitude fatigue limit are random variables. Therefore, the fatigue limit check involves statistical variability and can be expressed as:

$$\gamma S_r < \frac{\text{Fatigue limit}}{\phi} = \frac{S_{FD}}{\phi}$$

where  $\gamma$  = reliability factor defined above (it is different for redundant and nonredundant members);  $S_r$  = effective stress range computed from fatigue truck loading;  $S_{FD}$  = allowable stress range for the AASHTO "over 2 million" cycles category (this is assumed to be the 95 percent confidence level for the fatigue limit); and  $\phi$  = factor to account for the statistical variation in the maximum range divided by the effective stress range.

The reliability factor,  $\gamma$ , is the same value used for the finite life check. The quantity  $S_{FD}/\phi$  corresponds to the variable-amplitude fatigue limit,  $S_{rL}$ ; values of this limit for the various



detail categories are given in the evaluation procedure and are discussed further in the section on "Detail Constants" and in Chapter Four.

### Compression Cycling

The AASHTO specifications (209) do not require a fatigue check for applied stress cycles that are entirely in compression. In contrast, European fatigue specifications (172, 212) generally require a fatigue check for such cycles. For welded members, the compression cycles are treated the same as tension cycles (172, 212). For nonwelded, or fully stress-relieved members, compression cycles are either ignored or are multiplied by a factor of 0.6 (172).

Test results (72, 198) show that fatigue cracks initiate in regions where the applied cyclic stresses are completely in compression. In such regions, constant tensile residual stresses are superimposed on the applied compressive stresses to produce cycles that are partly or fully in tension (190). The fatigue cracks usually stop growing when they reach a region of compressive residual stresses and generally do not cause failures (72, 198). In a few variable-amplitude tests, however, beams cycled in bending failed as a result of cracks in flanges subjected only to compressive applied stresses (198). There have been no reports of failures resulting from compression cycling in actual bridges (54).

In a highway bridge, the applied stresses are entirely in compression when the compressive dead load stress at the detail exceeds the tensile portion of the stress cycle caused by the heaviest truck in the traffic. It is assumed that the heaviest truck weighs twice as much as the fatigue truck. Thus, the stress cycles are completely in compression when  $2 R_s S_t < S_c$ ;  $S_t$  is the tension portion of the stress cycle caused by the fatigue truck,  $S_c$  is the compressive dead load stress, and  $R_s$  is the reliability factor. Less than 0.2 percent of the trucks in an extensive WIM study (205) weighed more than twice as much as the fatigue truck for this traffic. This small percentage of cycles that are partly within the tensile region is not expected to significantly affect fatigue behavior. Furthermore, an additional margin of safety is provided by the reliability factor.

### Finite Life

If the calculated stress range multiplied by the reliability factor is above the limiting value for infinite life, the remaining fatigue life must be calculated. A basic procedure, and one alternative procedure, for calculating the remaining life is given in the evaluation procedure itself. In addition, four other more refined procedures are permitted; these four are given in Appendix C.

In all of these procedures, the remaining life corresponding to the calculated stress range is determined from the fatigue strength (SN) curve, or equation, for the detail under consideration. The fatigue strength curves for detail Categories A to E were developed by Fisher (70, 71, 72) and are the basis for the present AASHTO (209) allowable fatigue stresses. These allowable SN curves approximate the lower 95 percent confidence limits for test data in each category. The mean life for a particular stress range is about twice the life from the allowable SN curve. The allowable SN curves are discussed further under "Detail Constants."

### Basic Procedure

Either the remaining safe or mean life in years corresponding to the factored stress range,  $R_s S_r$ , can be calculated from

$$Y_f = \frac{f K \times 10^6}{T_a C (R_s S_r)^3} - a \quad (4)$$

in which  $T_a$  is the estimated lifetime average daily truck volume,  $C$  is the cycles per truck passage,  $a$  is the age of the bridge in years,  $R_s S_r$  is the factored stress range,  $K$  is a detail discussed later, and  $f$  is a factor to account for the difference between the mean and allowable SN curves. In calculating the remaining safe life,  $f = 1$  and  $R_s$  is above 1. In calculating the remaining mean life,  $f = 2$  and  $R_s = 1$ . This equation uses a mathematical relationship to define the SN curve for the detail.

The lifetime average daily truck volume may be estimated by the Engineer or obtained from a chart that involves the present truck volume,  $T$ , the present age of the bridge,  $a$ , and the compound annual growth rate,  $g$ , for the truck volume. Procedures for determining the lifetime average daily truck volume are discussed later under a separate heading.

### First Alternative

A more accurate estimate of remaining safe or mean life can be obtained by dividing the total fatigue life into two periods in which the truck volume and fatigue truck weight remain constant: A past period from the opening of the bridge to the present and a future period from the present to the end of the fatigue life.  $Y_p$  denotes the past period in which the truck volume,  $T_p$ , and the effective truck weight,  $W_p$ , were constant.  $Y_f$  denotes the future period in which the truck volume,  $T_N$ , and effective truck weight,  $W_N$ , are also assumed constant.  $Y_1$  and  $Y_N$  are the fatigue lives in years based on the past and future traffic conditions, respectively. Fatigue damage in the past period is given by  $Y_p/Y_1$  while fatigue damage in the future period is given by  $Y_f/Y_N$ . Failure occurs when the total damage equals one, or

$$1 = \frac{Y_p}{Y_1} + \frac{Y_f}{Y_N} \quad (5)$$

where  $Y_1$  and  $Y_N$  are given by  $fK \times 10^6/[T_p C(R_s S_r W_p/W)^3]$  and  $fK \times 10^6/[T_N C(R_s S_r W_N/W)^3]$  respectively. Therefore,

$$Y_f = Y_N [1 - Y_p/Y_1] \quad (6)$$

The Engineer must supply appropriate values of  $T_p$ ,  $T_N$ ,  $W_p$ , and  $W_N$  from his knowledge of conditions at the site.

### Other Alternatives

Four, more refined, alternative procedures for calculating the remaining safe or mean fatigue life are permitted. These procedures are given in Appendix C. By including a growth rate and/or permitting more calculation periods, these procedures more accurately account for the increases in truck volume and weight that occur over the life of a bridge. These changes have a major influence on fatigue behavior as discussed in Appendix D.

In the first procedure, the remaining life is calculated by dividing the total fatigue life into two periods in which the truck-volume growth rate and fatigue truck weight both remain constant. The first period is from the opening of the bridge to the present, and the second is from the present to the end of the fatigue life. In the second procedure, the remaining life is calculated by dividing the total fatigue life into several (more than two) periods in which the truck-volume growth rate and fatigue truck weight both remain constant. In the third procedure, the remaining life is calculated by dividing the total fatigue life into several (more than two) periods in which the truck volume and fatigue truck weight both remain constant. In the fourth procedure, a record of accumulated fatigue damage for the bridge is maintained in conjunction with the normal 2-year maintenance inspections; this record can be used at any time to calculate the remaining life.

The derivations of the equations used in these four alternative procedures are given in Appendix C. In all of these procedures, the total fatigue life,  $Y$ , for present traffic conditions (truck volume,  $T$ , and fatigue truck weight,  $W$ ) is calculated. The fatigue damage,  $D_i$ , that actually occurs during any calculation period is related to the damage that would have occurred under present traffic conditions. Specifically,

$$D_i = Y_i \left( \frac{N_i}{N} \right) \left( \frac{W_i}{W} \right)^3 \quad (7)$$

in which  $Y_i$  is the length of the calculation period in years,  $N_i$  is the actual number of cycles for the period,  $N$  is the number of cycles for the period based on present traffic conditions, and  $W_i$  is the fatigue truck weight for the period. For constant-growth periods,  $N_i$  is calculated from the growth rates. A limiting truck volume discussed in Appendix D and Chapter Three is used to account for the self-limiting nature of traffic. When the  $\Sigma D_i = Y$ , the fatigue life is exhausted.

### Detail Constants

#### Mean and Allowable SN Curves

Calculation of the remaining fatigue life for a detail is based on allowable fatigue stresses proposed in studies at Lehigh University (119) and adopted by AASHTO (209). The total number of cycles,  $N$ , that a member can sustain before it fails depends mainly on the nominal stress range at the detail and the stress concentration. To account for different degrees of stress concentration, different types of members are classified into 8 detail categories, namely, A, B, B', C, D, E, E', and F. The mean stress range,  $S$ , the member can sustain for a given number of cycles,  $N$ , is given by

$$NS^b = c \quad (8)$$

When plotted on a log-log scale, a straight line with an intercept  $c$  and a negative slope  $b$  is obtained.

There is considerable scatter in the fatigue data on which Eq. 8 is based. It is normally assumed that the scatter in stress range values follows a log normal statistical distribution (161) for a given  $N$ . Consequently, for design purposes allowable nominal stress ranges are usually defined two-standard deviations below the mean stress ranges. This design curve is defined as

$$NS_{95}^b = A \quad (9)$$

in which  $S_{95}$  is the stress range two-standard deviations below the mean and  $A$  is the intercept for this allowable design curve.

For all detail categories except F, Fisher et al. (119) proposed that the slope  $b$  be taken as 3.0. Fisher (119) also proposed values of  $A$  for each detail category, where  $A$  is the intercept at 2,000,000 cycles. The value of  $A$ , together with the slope of 3.0, defines the fatigue strength of each detail category, and is the basis for the present AASHTO (209) allowable fatigue stresses for that category. For convenience in calculating the remaining life in years, a new detail constant,  $K$ , is used in the proposed fatigue evaluation procedure. This constant is related to  $A$  by

$$K = \frac{A}{365 \times 10^6} \quad (10)$$

Values of  $K$  are given in Article 6.3.3 of the evaluation procedure (Appendix A).

The allowable and mean SN curves for a given detail are assumed to be parallel on a log-log plot. Consequently, the ratio of stress ranges for the two curves is the same at all cyclic lives. This ratio is given in Table 8 for all detail categories. For categories B through E', the ratio of mean to allowable stress range does not vary greatly and averages 1.243. Because of the power of 3 in the SN curve, the corresponding ratio of mean to safe lives is equal to 1.243 cubed, or 1.92. The average ratio of mean to safe lives including Category A is  $1.27^3 = 2.05$ . Thus, the value of  $f$  is taken as 2.0 while calculating mean life in the proposed evaluation procedure.

The ratio of mean life to safe life in the evaluation procedure can be obtained by combining the stress range ratio for the allowable and mean SN curves with the reliability factor that is applied to the stress range. For redundant members, this reliability factor is 1.35 and the corresponding ratio of mean and safe lives is  $(1.35 \times 1.243)^3 = 4.73$ , or about 5 as mentioned earlier. For nonredundant members, this reliability factor is 1.75 and the corresponding ratio of mean and safe lives is  $(1.75 \times 1.243)^3 = 10.29$ , or about 10.

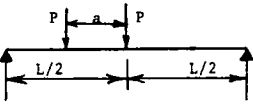
#### Limiting Stress Range for Infinite Life

In the evaluation procedure, the fatigue life of a detail is infinite if the factored stress range,  $R_s S_r$ , is below the variable-amplitude fatigue limit,  $S_{FL}$ , that is listed in Article 6.3.3. The listed values of  $S_{FL}$  are derived in Chapter Four. The result obtained is similar to multiplying the present AASHTO constant-amplitude fatigue limit by the factor 1.1/3, or 0.367. The present AASHTO (209) allowable stress ranges for the over-two-million cycle category for redundant members correspond to lowerbound constant-amplitude fatigue limits for the various details. The levels of  $S_{FL}$  used in the evaluation procedure are justified in four different ways as explained below: (1) a simplified reliability analysis, (2) a direct comparison with the present AASHTO fatigue limit check, (3) a study of the peak ratio (peak/effective) for a nationwide truck weight spectrum, and (4) a study of peak ratios (peak/effective) for measured stress spectrums. Extensive research on the effect of the constant-amplitude fatigue limit on variable-amplitude fatigue behavior is presently being conducted under the sponsorship of NCHRP and FHWA. The proposed levels of  $S_{FL}$  can be mod-

**Table 1. Ratio of calculated stresses (AASHTO/proposed) for simple spans.**

Factor	Span = 50'	Span = 100'	Span = 200'
W (weight)	72/54 = 1.333	72/54 = 1.333	72/54 = 1.333
M (moment)	18/12.5 = 1.440	43/35 = 1.229	93/85 = 1.094
I (impact)	1.29/1.10 = 1.73	1.22/1.10 = 1.109	1.15/1.10 = 1.045
D (distribution)	19.55/14 = 1.393	22.3/14 = 1.593	23/14 = 1.643
S (section)	1.15/1.00 = 1.150	1.15/1.00 = 1.150	1.15/1.00 = 1.150
Total Ratio	3.61	3.33	2.88

M factor:



$$\text{moment at } \frac{L}{2} = \frac{PL}{4} + \left( \frac{L/2 - a}{L} \right) \cdot \frac{L}{2} P$$

$$\frac{m}{P} = \frac{L}{4} + \frac{L - a}{2} = \frac{L}{2} - \frac{a}{2}$$

$a$  = spacing of main axles (14' for AASHTO, 30' for proposed);  
not less than  $L/2$

**D factor:** AASHTO factor is  $S/7$  for 1/2 truck or  $S/14$  for full truck

**S factor:** is for composite sections

ified in the future if justified by the results of this and other research.

A simplified reliability analysis is made in Chapter Four to develop levels of  $S_{FL}$  that provide a high probability that all, or substantially all, of the stress ranges in the spectrum will be below the constant-amplitude fatigue limit. This analysis considers all of the uncertainties in calculating the stress range that are considered in the main reliability calibration. In addition, this analysis considers the uncertainty in the level of the constant-amplitude fatigue limit and the value of the peak ratio, which is the peak stress range in the spectrum divided by the effective stress range for the spectrum. The reliability analysis suggests that  $S_{FL}$  should be about  $1/2.75$ , or 0.364, times the constant-amplitude fatigue limit.

Present AASHTO (209) fatigue design procedures require a fatigue limit check for high traffic volumes ( $ADTT > 2,500$ ) by specifying that the calculated stress range be below the allowable value based on the constant-amplitude fatigue limit. A lateral distribution factor of  $S/7$  is used in calculating this stress range. Stress ranges calculated by these AASHTO procedures are roughly 3 times the unfactored stress ranges calculated by the proposed evaluation procedures, as illustrated in Tables 1 and 26(a). Therefore, the proposed procedure provides about the same level of safety with respect to the fatigue limit check if it uses an  $S_{FL}$  value equal to  $1/3$  of the AASHTO limiting value (constant-amplitude fatigue limit).

The factor of 3 is reasonable in relationship to the nationwide WIM truck weight spectrum (205) as described in Appendix D (Figure D-18). A truck weight of 162 kip is obtained by applying this factor to the effective weight of 54 kip for the spectrum. Only 0.023 percent of the trucks in the spectrum weigh more than this value. Thus, substantially all of the stress ranges caused

by this truck spectrum will be below the constant-amplitude fatigue limit if the unfactored stress range corresponding to the effective truck weight is kept below  $1/3$  of the constant-amplitude fatigue limit.

The factor of 3 is also reasonable in relationship to the peak ratios for the measured stresses listed in Table E-1. The average value of the peak ratio for all histograms is 2.67. The peak ratios for some individual histograms substantially exceeded 3; however, these high ratios typically resulted from a single occurrence (out of several thousand) that was considerably higher than all other occurrences. Thus, it is reasonable to use a peak ratio of 3 in defining  $S_{FL}$ .

#### Category F

This detail category applies only to shear on the throat of fillet welds. It rarely governs a design, because the shear stresses in the weld are usually low enough so that cracks do not occur in the weld itself (70). Instead, fatigue cracks usually occur at the weld toe termination (70) as a result of the stresses in the connected material, and these cracks control the fatigue strength. No fatigue cracking due to shear in a fillet weld has been reported in actual bridge members.

The present AASHTO (209) allowable fatigue stresses for this category are based on an SN curve with a slope of 5.86 instead of the slope of 3.0 used for all other detail categories. This SN curve is based on tests (235) of small plate specimens with specially designed welds purposely subjected to high shear stresses (70). Consequently, Lehigh University (119) has suggested that "Studies are needed to provide rational design criteria for welds in shear."

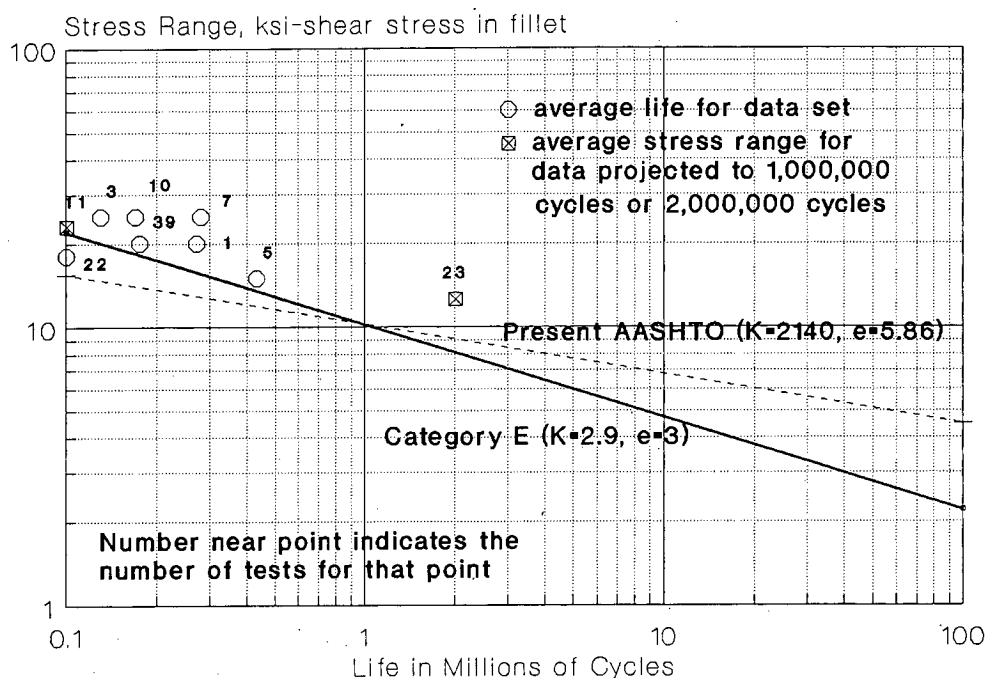


Figure 5. Fatigue strength of Category F.

The available data, and the AASHTO SN curve, for Category F are plotted in Figure 5; the data points represent mean values for sets of data (152). These data are for longitudinal and transverse fillet welds, plug and slot welds, and combinations of these weldments. The data are for the high-stress low-life region below 2 million cycles. The AASHTO SN curve for Category E, which is also plotted in the figure, conservatively represents the data except at very short lives. At long lives, such as occur in actual bridges, the Category E SN curve is considerably below the present Category F SN curve. Therefore, the Category E SN curve could be safely used for Category F, although it may be overly conservative for the longer lives. Because Category F rarely governs and because the use of a different slope for Category F complicates the evaluation procedure, the SN curve for Category E is used in this procedure to define the fatigue strength of fillet welds in shear. The value of  $S_{FL}$  for Category F is based on the present AASHTO (209) constant amplitude fatigue limit for this category.

#### Cycles Per Truck Passage

For very short simple-span bridges (less than 30 ft), the passage of the fatigue truck across the bridge produces two individual stress cycles corresponding to the main axles (189, 193). For longer simple-span bridges, the passage generally causes one complex stress cycle with two major peaks and a valley between. The exact shape of the complex cycle can be calculated for a given span by using an influence line, and the net effect of the complex cycle can be represented by an equivalent number of individual cycles. By using this approach, the equivalent number of cycles was plotted as a function of span for several different cases (189, 193). The table of stress cycles

per truck passage in the evaluation procedure was developed from these plots. In many cases, the number of cycles per truck passage is 1.0, but in other cases the number is greater than 1.0.

Near an interior support in a continuous-span bridge, two individual cycles are produced when a single concentrated load crosses over the support from one adjacent span to the other. For long spans, the equivalent number of cycles for the fatigue truck approaches this value of 2. For shorter spans, however, the equivalent number of cycles is considerably less than 2 and varies approximately linearly with the span. Therefore, a simple empirical equation is used for this case in the basic procedure.

A study (189, 193) of the small vibration stresses caused in typical bridges by the passage of a truck showed they are generally small enough to be neglected except in cantilever (suspended span) girder bridges and possibly a few other unusual types of bridges. In such bridges, the vibration stresses may be large so that a single truck passage can cause several equivalent cycles (189, 193). Therefore, a value of 2 has been used for such bridges. If this value proves excessive for a given situation, the Engineer should consider a simple field test to verify the presence of the large vibration stresses.

A procedure for calculating the equivalent number of cycles corresponding to a particular complex cycle is given in Appendix C. In Alternative 1, it can be used in conjunction with an influence line to calculate the equivalent number of cycles directly, and in Alternative 2 it can be used to calculate the equivalent number of stress cycles from field measurements.

#### Lifetime Average Daily Truck Volume

The lifetime average daily truck volume used in calculating the remaining life either can be estimated directly by the En-

gineer or obtained from a chart. Because of the importance of this parameter in the fatigue evaluation, the Engineer should always use whatever site data are available for making this estimate either directly or from the chart. Regardless of whether the estimate is made directly or obtained from the chart, it must be based on excluding panel, pickup, and other 2-axle/4-wheel trucks to be consistent with the procedure used in calculating the fatigue truck weight.

The lifetime average daily truck volume is intended to represent the truck volume in the shoulder lane plus a small additional volume to account for the effects of the truck volume in other lanes. The shoulder lane is generally the most critical for fatigue evaluations because most of the truck volume is in that lane. The evaluation of all girders is conservatively based on the truck volume in this critical lane. A factor  $F_L$  is given in Appendix A Article 6.3.5.1 of the evaluation procedure to obtain the truck volume in the shoulder lane from the total truck volume on the bridge. This factor should be used in estimating the lifetime average volume either directly or from the chart.

The factor  $F_L$  is based on the truck-volume lane distributions, as discussed in Appendix D, and includes the volume in the shoulder lane plus 15 percent of the volume in the adjacent lane. This percentage is based on the reduction in stress range (in the critical girder under the shoulder lane) that occurs when a truck travels in the adjacent lane rather than in the shoulder lane. The reduction depends on the lateral distribution characteristics of the bridge and varies with the parameters that affect this distribution. A finite-element study (194) of various cases suggested that 50 percent is a reasonable conservative value for this reduction. This value is also conservative with respect to the measured lateral distribution from an adjacent lane that was discussed under the heading "Truck Superpositions." The equivalent truck volume corresponding to this 50 percent stress reduction is equal to 0.5 cubed or 0.125, which was conservatively rounded to 15 percent. The effect of trucks in lanes further from the shoulder lane is small enough to be neglected.

The chart giving the lifetime average daily truck volume (Figure 6.3.5A in the evaluation procedure) involves (1) the present truck volume, (2) the present age of the bridge, and (3) the compound annual growth rate for the truck volume. The present truck volume and the annual growth rate are discussed under subsequent headings. As explained in Appendix D, the lifetime average volume from the chart is based on a constant growth rate from the opening of the bridge to a time 30 years from the present. Thus, the chart is conservative for projections up to 30 years into the future, but is somewhat unconservative for longer projections if volume actually grows at the assumed rate. Of course, there is considerable uncertainty in such longer projections. Consequently, in the evaluation of existing bridges, the Engineer is usually concerned primarily with projections of 30 years or less. Furthermore, these projections will be periodically updated in the future. Therefore, the chart is appropriate for the fatigue evaluation of existing bridges.

#### *Present Truck Volume*

The present truck volume can be calculated from the known or assumed ADT at the site by applying factors to account for (1) the percentage of trucks in the traffic and (2) the percentage of trucks in the shoulder lane. Of course, panel, pickup, and

other 2-axle/4-wheel trucks must be excluded from the percentage of trucks in traffic to be consistent with the procedures used in calculating the fatigue truck weight. If the percentage of trucks in traffic is unknown, it is conservatively taken as 20 percent for rural Interstate highways, 15 percent for other rural highways and urban Interstate highways, and 10 percent for other urban highways (109, 122, 195). Data on these percentages from several different sources are given in Appendix D. More data are needed, especially on the percentages by highway category. Such data may be obtained as a part of NCHRP Project 12-28(11), "Development of Site-Specific Load Models for Bridge Evaluation and Rating." The factor  $F_L$ , which was discussed earlier, should be used to define the percentage of trucks in the shoulder lane.

#### *Truck-Volume Growth Rate*

It is intended that the Engineer estimate past and future growth rates from a knowledge of local conditions. Appendix D provides guidance in making such estimates. Generally, the Engineer can make the best possible estimates by combining his knowledge of local conditions with the historical data on growth rates given in the Appendix D. For example, the Engineer may know that the growth rate at the site of a particular bridge on an Interstate highway is greater than normal and, therefore, use a growth rate of 6 percent instead of the average rate of 4.5 percent for such highways.

#### *Limiting Truck Volume*

Small truck-volume growth rates projected far into the future can result in unrealistically high values because of the self-limiting nature of traffic; motorists avoid congested highways and/or demand improvements in these highways. Therefore, a limiting truck volume is used in several of the alternative procedures given in Appendix C for calculating the remaining fatigue life. (A limiting truck volume is not used in the basic procedure or in Alternative 1 because the growth rate is not used in calculating remaining life by these procedures.) Truck volumes obtained by projecting the present truck volume into the future are not allowed to exceed this limiting value.

The limiting truck volume is the maximum practical annual-average truck volume on a highway and is obtained by applying factors to the maximum practical total traffic volume. These factors, which account for the percentage of trucks in the traffic and the percentage of trucks in the shoulder lane, are the same as those used in calculating the present truck volume. From a study of extreme ADT volumes actually observed on highways (106, 107) a value of 20,000 vehicles per day per lane was established as the maximum practical traffic volume. The value of 20,000 vehicles per day per lane is well below the theoretical capacity of 2,000 vehicles per hour per lane often used by traffic engineers (107, 223), because this high volume is not sustained over a long period of time.

In projecting future truck volumes, the growth rate is assumed to remain constant until it reaches the limiting volume. Actually, the growth rate would be expected to diminish as the volume approaches the limiting value. However, this effect has been conservatively neglected to avoid complicating the alternative evaluation procedures excessively.

### Options If Remaining Life Is Inadequate

The proposed evaluation procedure gives four options that may be pursued by the Engineer if he considers the calculated remaining safe fatigue life to be inadequate: (1) recalculate the remaining life using one of the alternative procedures to get a

more accurate (probably longer) estimated life, (2) restrict the traffic on the bridge to increase the remaining life in years, (3) modify the bridge to improve its fatigue strength, or (4) institute appropriate periodic inspections to assure adequate safety without other changes.

## CHAPTER THREE

# PROPOSED DESIGN PROCEDURE

### FORMAT

A draft of a proposed fatigue design procedure for steel highway bridges is given in Appendix B in the form it might appear in the *AASHTO Standard Specifications for Highway Bridges* (209). The development of this design procedure, and its relationship to the proposed evaluation procedure, are discussed in this chapter.

The proposed design procedure is consistent with the proposed evaluation procedure and utilizes many of the same concepts. However, it is presented in a format convenient for design. First, a design stress range,  $S_r$ , is calculated for each detail in a manner similar to that used in the evaluation procedure. The design stress range is multiplied by a reliability factor,  $R_s$ , to provide an acceptable probability that the actual fatigue life of the member will exceed the desired fatigue life. The factored stress range, however, is not used to calculate a safe fatigue life as in the evaluation procedure. Instead, the Engineer compares it with a permissible stress range for a desired design life. If the calculated (factored) design stress range is less than the permissible stress range, there is a high probability that the actual fatigue life will exceed the desired design life. Otherwise, the member can be redesigned to reduce the (factored) design stress range to the permissible level and increase the corresponding safe life to the desired value. Most of the alternative procedures permitted in the evaluation procedure are not appropriate for the design of new bridges and are not included.

### RELIABILITY FACTORS

Reliability (safety) factors,  $R_s$ , of 1.1 and 2.0 are used for redundant and nonredundant members, respectively. These factors correspond respectively to safety indices,  $\beta$ , of 1.0 and 3.0, and to probabilities of about 85 percent and 99.9 percent that the actual fatigue life will exceed the design life. These levels of reliability are considered adequate because (1) the consequences of exceeding the factored permissible stress range is a shorter life rather than an immediate failure, (2) the fatigue safety of the bridge can be periodically reassessed, and (3) significantly higher reliability factors would have caused fatigue to govern some designs that would not be governed by fatigue under the current AASHTO specifications.

The design procedure does not give a best estimate of the fatigue life of the bridge that would be comparable to the mean life in the evaluation procedure. If the calculated (factored) stress range for a detail is at the permissible level, however, a best estimate of the actual life can be obtained by multiplying the design life by a factor that is calculated in the same way as the ratio of the mean and safe lives in the evaluation procedure. For redundant members, this factor is  $(1.1 \times 1.243)^3 = 2.56$ , or about  $2\frac{1}{2}$ . For nonredundant members, this factor is  $(2.0 \times 1.243)^3 = 15.4$ , or about 15. If the calculated (factored) stress range for the detail is below the permissible level, the best estimate of the actual fatigue life is even greater. This occurs when the cross section at the detail is controlled by static design rather than fatigue.

### DESIGN STRESS RANGE

The design stress range is calculated in the same way as the stress range in the evaluation procedure. The identical fatigue truck is used. The gross weight can be taken as 54 kip or calculated from a gross-weight histogram by using the following equation:

$$W = (\sum f_i W_i^3)^{1/3} \quad (10)$$

where  $W$  = effective gross weight of fatigue truck,  $f_i$  = fraction of gross weights within a weight interval  $i$ , and  $W_i$  = gross weight at midwidth of interval  $i$ .

As explained in Chapter Two, it is important that the definitions of "truck" are consistent for estimating both the truck volume and fatigue truck weight. For convenience, panel, pickup, and other 2-axle/4-wheel trucks should be excluded from both the gross-weight histogram and the truck volume data. For special traffic conditions that can cause bunching, the gross weight of the fatigue truck is increased by 15 percent as explained in Chapter Two. Such conditions include (1) a traffic signal on or near the bridge and (2) a steep hill when the bridge is on a two-lane highway.

As discussed in Chapter Two, it is always conservative to use a variable spacing of 14 to 30 ft instead of a constant spacing

of 30 ft for the main axles of the fatigue truck. However, this can substantially increase the design stress range and cause fatigue to govern in cases where it would not otherwise govern. For example, on a 60-ft simple-span bridge, using a 14-ft spacing increases the maximum midspan moment and corresponding stress range by 55 percent.

An impact factor of 15 percent is used instead of 10 percent because of the greater uncertainty about joint and pavement conditions over the life of the bridge. The moment range is calculated by positioning the fatigue truck in the same way as in the evaluation procedure. The same procedures are specified for lateral distribution factors, but a rigorous analysis is also permitted. The lateral distribution factor multiplied by the total moment range due to the fatigue truck gives the moment range in the critical girder. The moment range in the girder is divided by section modulus to obtain the design stress range.

In calculating section modulus, steel sections alone should be used for noncomposite sections (where the deck is not connected to the steel section by shear connectors). For composite sections, an effective section equal to 1.15 times the full composite section (as defined in Article 10.38 of AASHTO *Standard Specifications for Highway Bridges*) can be used in positive bending regions and a section including the longitudinal rebars can be used for negative bending regions. This 15 percent increase in the effective section in positive bending regions is intended to account for beneficial effects, such as contributions from nonstructural elements, that are not calculated directly. This is consistent with the evaluation procedure described in Chapter Two.

#### PERMISSIBLE STRESS RANGE FOR A DESIRED DESIGN LIFE

No further fatigue check of a detail is required if the compressive dead load stresses are high enough so that essentially all of the stress cycles caused by the traffic are completely in compression. Otherwise, a permissible stress range for the desired design life must be calculated as explained in subsequent paragraphs.

#### Simplified Procedure

The permissible stress range may be obtained by either a simplified procedure or a general procedure. The simplified procedure is based on a design life of 75 years and gives normalized permissible stress ranges in Table 10.3.3.1A (Appendix B) for four different traffic volume categories. These normalized values are the actual permissible stress ranges for Category C details if the cycles per truck passage is 1. For other detail categories and/or cycles per truck passage, the actual permissible stress range is obtained by multiplying the value in the table by appropriate factors. The normalized permissible stress ranges given in the table for a particular volume category (ADT) vary with the number of lanes and type of traffic (one way or two way) because the truck volume in the critical lane depends on these parameters as discussed later.

#### General Procedure

In the general procedure, the Engineer can select the desired safe design life for the bridge. A high design life of about 75 to

100 years is generally appropriate because major bridges put into service in the early 1900's are now approaching an age of 100 years, and many bridges put into service in the 1930's are now 50 years old. The British fatigue code (212) uses a design life of 120 years and uses a damage accumulation sum to satisfy the requirement (42). An example is given at the end of this chapter to illustrate how the choice of a design life affects the annualized costs for a bridge. This example suggests that these costs are often lower for a design life of 75 years than for a design life of 50 years.

The permissible stress range for a particular life is given by an equation that involves (1) the detail constant, (2) the number of stress cycles per truck passage, and (3) the design truck volume. The detail constant defines the fatigue strength of the detail under consideration. The detail constants used in the design procedure are the same as those used in the evaluation procedure and are based on present AASHTO (209) allowable fatigue stresses. Similarly, the design procedure uses the numbers of stress cycles per truck passage that were defined for various cases in the evaluation procedure.

#### Fatigue Limit

The permissible stress range need not be taken as less than the proposed variable-amplitude fatigue limits given in the evaluation section and discussed in Chapter Two. Therefore, the design procedure includes the same limiting  $S_{FL}$  values as the evaluation procedures.

Table 2 shows when the limiting fatigue limit value governs. This table gives the permissible stress ranges,  $S_{pr}$ , from Article 10.3.3.1 (without regard to  $S_{FL}$ ) for all detail categories for the four traffic volume categories. The listed values are for  $C = 1.0$  (cycle per truck passage); for higher  $C$  values, the listed permissible stress ranges would be lower. The table also gives the limiting stress ranges,  $S_{FL}$ , for each detail category. When  $S_{FL}$  is greater than the permissible stress range, it governs and the permissible stress range in the table is enclosed in parentheses. For Categories A through C (stiffeners),  $S_{FL}$  generally governs for the heavy traffic volume categories. For Categories D through E',  $S_{FL}$  does not govern for any of the traffic volume categories because the break life (life at which the SN curve breaks from a sloping line to a horizontal line) is very high. If  $C$  exceeds 1.0,  $S_{FL}$  governs more cases.

#### Design Truck Volume

The design truck volume is analogous to the lifetime average daily truck volume used in the evaluation procedure. It is intended to represent the truck volume in the shoulder lane plus a small additional volume to account for the effects of the truck volume in other lanes. Panel, pickup, and other 2-axle/4-wheel trucks must be excluded from the truck volume to be consistent with the procedures used in calculating the fatigue truck weight.

The design truck volume can be obtained by any of the following three methods: (1) It can be estimated directly by the Engineer. (2) It can be obtained from a table that depends on the expected traffic volume (ADT) at the opening of the bridge. (3) It can be calculated from equations that depend on the expected growth rate of the truck volume. Each of these methods is discussed in the following paragraphs.

Table 2. Permissible stress ranges.

Detail Category	$S_{FL}$	Traffic Type	Lanes	Permissible Stress Range			
				VHT	HT	LT	VLT
A	8.80	2-way	2	(7.23)	(7.62)	8.88	14.01
			4	(6.32)	(6.66)	(7.84)	12.28
			6	(5.74)	(6.05)	(7.12)	11.17
			8	(5.21)	(5.50)	(6.47)	10.14
		1-way	1	(7.68)	(8.09)	9.55	14.97
			2	(6.44)	(6.79)	(8.00)	12.54
			3	(5.74)	(6.05)	(7.12)	11.17
			4	(5.21)	(5.50)	(6.47)	10.14
		2-way	2	(5.68)	5.99	7.06	11.01
			4	(4.96)	(5.23)	6.16	9.65
			6	(4.51)	(4.75)	(5.60)	8.78
			8	(4.10)	(4.32)	(5.08)	7.97
B	5.87	2-way	1	6.04	6.36	7.51	11.77
			2	(5.06)	(5.33)	6.29	9.85
			3	(4.51)	(4.75)	(5.60)	8.78
			4	(4.10)	(4.32)	(5.08)	7.97
		1-way	2	4.55	4.80	5.66	8.82
			4	(3.88)	(4.20)	4.84	7.73
			6	(3.61)	(3.81)	4.49	7.04
			8	(3.28)	(3.46)	(4.08)	6.39
		2-way	1	4.84	5.10	6.02	9.43
			2	(4.05)	(4.28)	5.04	7.90
			3	(3.61)	(3.81)	4.49	7.04
			4	(3.28)	(3.46)	(4.08)	6.39
C	3.67 4.40	2-way	2	4.05	4.27	5.04	7.86
			4	(3.54)	3.74	4.40	6.89
			6	(3.22)	(3.39)	3.99	6.27
			8	(2.92)	(3.08)	(3.63)	5.69
		1-way	1	4.31	4.54	5.36	8.40
			2	(3.61)	3.81	4.49	7.03
			3	(3.22)	(3.39)	3.99	6.27
			4	(2.92)	(3.08)	(3.63)	5.69
		2-way	2	3.22	3.39	4.00	6.24
			4	2.81	2.96	3.49	5.47
			6	(2.55)	2.69	3.17	4.97
			8	(2.32)	(2.45)	2.88	4.51
D	2.57	1-way	1	3.42	3.60	4.25	6.67
			2	2.87	3.02	3.56	5.58
			3	(2.55)	2.69	3.17	4.97
			4	(2.32)	(2.45)	2.88	4.51
		2-way	2	2.53	2.66	3.14	4.89
			4	2.21	2.33	2.74	4.29
			6	2.00	2.11	2.49	3.90
			8	1.82	1.92	2.26	3.54
		1-way	1	2.68	2.83	3.34	5.23
			2	2.25	2.37	2.80	4.38
			3	2.00	2.11	2.49	3.90
			4	1.82	1.92	2.26	3.54
E	1.65	2-way	2	1.83	1.93	2.27	3.54
			4	1.60	1.68	1.98	3.10
			6	1.45	1.53	1.80	2.83
			8	1.32	1.39	1.64	2.56
		1-way	1	1.94	2.05	2.42	3.79
			2	1.63	1.72	2.02	3.17
			3	1.45	1.53	1.80	2.83
			4	1.32	1.39	1.64	2.56
		2-way	2	1.83	1.93	2.27	3.54
			4	1.60	1.68	1.98	3.10
			6	1.45	1.53	1.80	2.83
			8	1.32	1.39	1.64	2.56
E'	0.95	2-way	2	1.83	1.93	2.27	3.54
			4	1.60	1.68	1.98	3.10
			6	1.45	1.53	1.80	2.83
			8	1.32	1.39	1.64	2.56
		1-way	1	1.94	2.05	2.42	3.79
			2	1.63	1.72	2.02	3.17
			3	1.45	1.53	1.80	2.83
			4	1.32	1.39	1.64	2.56
		2-way	2	1.83	1.93	2.27	3.54
			4	1.60	1.68	1.98	3.10
			6	1.45	1.53	1.80	2.83
			8	1.32	1.39	1.64	2.56

*Direct Estimate*

In estimating the design truck volume directly, the Engineer should use the factor  $F_L$  to get the truck volume in the shoulder lane from the total truck volume on the bridge. This factor is tabulated in the design procedure and is the same as the lane factor used in the evaluation procedure. It includes the effects of traffic in other lanes. The estimated design truck volume, of course, must include the expected growth over the life of the bridge.

*Table*

In the table (Table 10.3.3.5A in Appendix B), the design truck volume is given as a function of traffic type (1-way or 2-way), number of lanes on the bridge, and traffic volume category. Four different traffic volume categories are included in the table. The "Very Heavy Traffic" category assumes an ADT

of 20,000 veh per lane at the opening of the bridge. "Heavy Traffic," "Light Traffic," and "Very Light Traffic" categories assume starting ADT values of 8,000 veh per lane, 2,000 veh per lane and 500 veh per lane, respectively. The design truck volumes given in the table were calculated from the growth equations in the third method. These design volumes are based on (1) a design life of 75 years, (2) a compound annual growth rate of 3 percent, (3) a limiting traffic volume of 20,000 veh per day per lane, and (4) factors defining the percentage of trucks in the traffic,  $F_T$ , and the percentage of trucks in the shoulder lane,  $F_L$ . These parameters are discussed below.

Seventy-five years is a reasonable minimum design life for a bridge as discussed earlier in this chapter. The growth rate data in Appendix D suggest that 3 percent is a reasonable rate for design purposes, but particular sites may have higher or lower rates. The growth equations rather than the table should be used to get the design truck volume if the Engineer wants to base the design on a different growth rate.

As discussed in Chapter Two, 20,000 veh per day per lane



is a reasonable limiting traffic volume based on available data. A limiting truck volume was obtained from this limiting traffic volume by applying the factors  $F_T$  and  $F_L$ . In calculating the design volume, the truck volume was assumed to grow at a rate of 3 percent until it reached the limiting value, and then was assumed to remain constant. For the "Very Heavy Traffic" category, it was assumed that the truck volume was at the limiting value throughout the life of the bridge.

The tabulated values of  $F_L$  discussed earlier were used in calculating the design truck volumes in the table. For the "Very Heavy Traffic" and "Heavy Traffic" categories,  $F_T$  was taken as 10 percent because this heavy traffic usually occurs in urban areas where the percentage of trucks (excluding 2-axle/4-wheel trucks) is relatively small. For the "Light Traffic" and "Very Light Traffic" categories,  $F_T$  was taken as 15 percent. A sample calculation is shown below to illustrate how the Table 10.3.3.5A values were obtained.

1. *Given:*

- Heavy Traffic Category, 2-way traffic, 2 lanes.

2. *Assumptions:*

- Starting ADT = 8,000 veh per lane.
- Three percent annual growth rate.
- 20,000 veh per lane limiting traffic volume.
- Design life of 75 years.
- $F_T = 0.10$ .
- $F_L = 0.60$  (for 2-lane 2-way traffic from Article 10.3.3.5 of the design procedure).

3. *Calculations:*

- Total starting ADT on the bridge =  $8,000 \times \text{no. of lanes}$  = 16,000 vehicles.
- Starting truck volume (ADT) in outer lane = (starting total volume)  $F_T F_L = (16,000)(0.10)(0.60) = 960$  trucks per day.
- Figure 6 (reproduced from Appendix D, Figure D-5) gives the relation between  $V_a/V$  and  $V/V_L$  for different growth rates.  $V_a$ ,  $V$ ,  $V_L$  are the design truck volume (average over lifetime), starting truck volume, and the limiting truck volume, respectively. Thus  $(V)(F_T)/(V_L)(F_T) = (8,000)(0.10)/(20,000)(0.10) = 0.40$ .
- From Figure 6,  $V_a/V = 2.14$  for a growth rate of 3 percent.
- Therefore,  $V_a = 2.14(960) = 2054$  trucks per day. This value is rounded to 2,050 trucks per day.

### Equations

The third method of obtaining the design truck volume is based on the growth equations developed in Appendix D. By using this method, the Engineer can calculate the design truck volume for any values of (1) the design life, (2) the starting ADT, (3) the growth rate, and (4) the percentage of trucks in traffic. Again, the calculation involves the limiting truck volume and the tabulated values of  $F_L$ . The Engineer can also use these equations to assess the effects of various possible growth rates on the fatigue life of the member.

Graphs based on these equations are given in Figures 6 and 7 (reproduced from Appendix D, Figures D-5 and D-6) for lives of 75 and 100 years, respectively. These graphs can be conveniently used to obtain the design truck volumes corresponding to various growth rates.

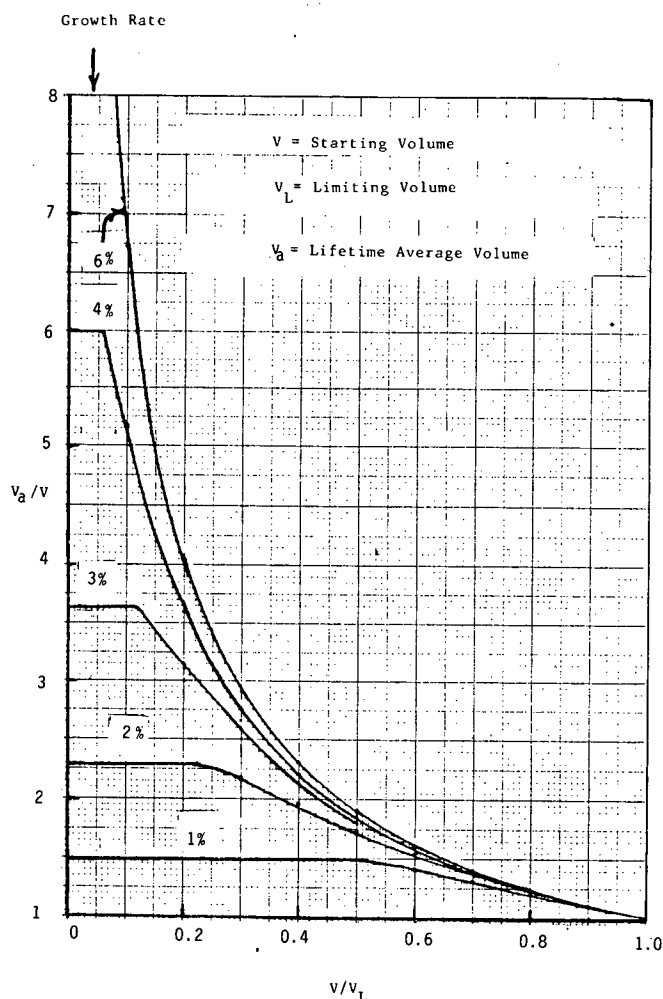


Figure 6. Average truck volume over a 75-year life.

### SIMPLIFIED DESIGN PROCEDURE

Table 3 gives a simplified version of the design rules to show how easily it can be applied to normal design cases. The actual design procedure is longer because it (1) permits greater flexibility in selecting design life, growth rates, truck traffic characteristics, and other parameters that affect the design, (2) defines various terms such as the span length for continuous girders, and (3) covers various additional cases such as box girders and decks with large overhangs.

The flexibility permitted by the design procedure is very desirable and does not cause problems in applying the procedure because the Engineer can merely ignore the more complex provisions he does not want to use for a particular design. The design procedure provides a good balance between simplicity and adequately defining terms and covering various cases.

### ANNUALIZED COSTS

It is possible to formulate an economic optimization which considers present worth costs for achieving future benefits cor-

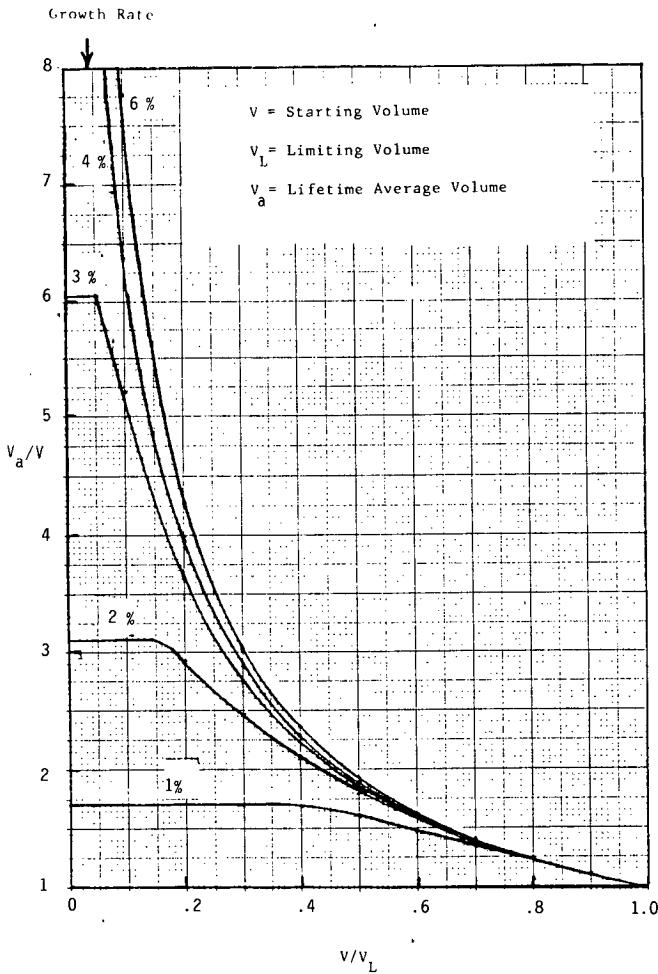


Figure 7. Average truck volume over a 100-year life.

responding to longer bridge lives. A sample calculation using one such optimization model is shown below. It illustrates that a design life of 75 years is more economical than a design life of 50 years for most design cases.

Consider two bridges: Bridge A is designed for a life of 50 years, and Bridge B is designed for a life of 75 years. Assuming the same truck conditions (truck weight, volume, and so on) and bridge conditions (impact, distribution factors) for both bridges, the only differences lie in the total number of cycles the bridge must sustain over its life. As the ratio of the fatigue lives for Bridges A and B is in the ratio of 1:1.5, the total number of cycles on the member would also be in the ratio of 1:1.5. This simple comparison ignores the growth rate in volume over the last 25 years of life.

It was shown in Chapter Two that the fatigue strength curves have a slope of 3.0 on a log-log scale. Therefore, the permissible stress ranges for Bridges A and B are in the ratio of  $(1.5)^{1/3}:1.0$  or 1.145:1.0. This calculation assumes that the infinite life fatigue limit,  $S_{FL}$ , does not govern. Because the required section modulus varies inversely with the permissible stress range, the required section moduli for Bridges A and B will be in the ratio of 1:1.145. Assuming that the weight per foot of a member is directly proportional to section modulus (see illustration in Ta-

ble 4) the ratio of the girder material costs for Bridges A and B would be 1:1.145. If the cost of material for Bridge A is  $C_1$ , the cost of material for Bridge B would be  $1.145C_1$ . If the cost of fabrication and construction is  $C_c$  (assume same for both bridges), the corresponding total costs of Bridges A and B would be  $C_1 + C_c$ , and  $1.145C_1 + C_c$ , respectively. The annual cost of the bridge is given by

$$\text{Annual cost} = \text{Total cost} [\text{capital recovery factor } (i, n)] \quad (11)$$

where  $i$  is real rate of interest, i.e., actual rate minus inflation rate; and  $n$  is the useful life of the structure.

Let,

$$C_c = aC_1 \quad (12)$$

where  $a$  is a constant for a given problem and usually ranges between 1.0 and 3.0. Substituting Eq. 12 into the total costs gives

$$\begin{aligned} \text{Total Cost of Bridge A} &= C_1 + aC_1 \\ &= (1 + a)C_1 \end{aligned} \quad (13)$$

$$\begin{aligned} \text{Total Cost of Bridge B} &= 1.145C_1 + aC_1 \\ &= C_1(1.145 + a) \end{aligned} \quad (14)$$

For a given  $a$ , annual costs in terms of  $C_1$  can be found for Bridges A and B by using Eqs. 12 to 14. Figure 8 shows a plot of  $a$  as a function of annual costs for Bridges A and B for an interest rate of 3 percent. Figure 9 shows a similar plot for an interest rate of 5 percent. Figures 8 and 9 show that designing for 75 years is more economical than designing for 50 years in the normal range of  $a$  (1.0 to 3.0).

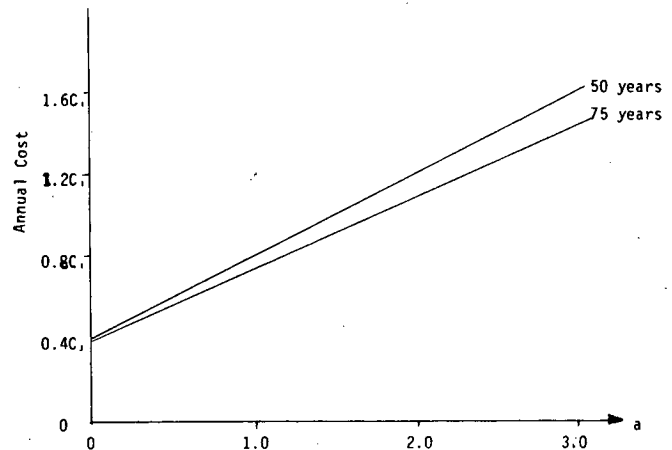


Figure 8. Annual costs for interest rate of 3 percent.

Table 3. Simplified fatigue design check.

1. Use Fatigue Design Truck with axle spacings and weight distribution shown in Fig. 1 [The gross weight of 54 kips may be changed to reflect data available from site].
2. Increase gross weight of truck by 15% to account for impact.
3. Place vehicle on span to obtain maximum moment (or force) range.
4. If a deck is supported by two members, distribute the moment assuming the deck acts as a simple beam with a single truck placed at the center of the outer traffic lane. If there are more than two members, use distribution factor (DF) as follows:

$$DF = S/D$$

Where D may be found from rigorous analysis or interpolated from the following table and S is the girder spacing in feet.

Span, ft	30	40	60	90	120
D	17	19	20	22	23

5. Section properties shall be those used in static design except that it may be increased by 15% for composite sections in positive bending regions.
6. Compute the design stress range ( $S_r$ ) at critical sections. This shall satisfy the following equation:

$$R_s S_r \leq S_{rp}$$

Where  $R_s = 1.1$  for redundant and 2.0 for nonredundant members

$S_{rp}$  = permissible stress range given on the next page for various detail categories

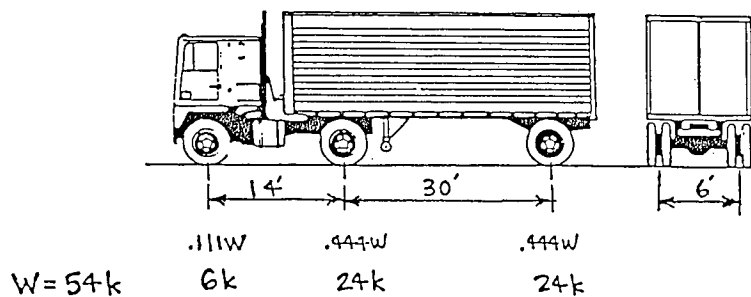


Figure 1 Fatigue Design Truck

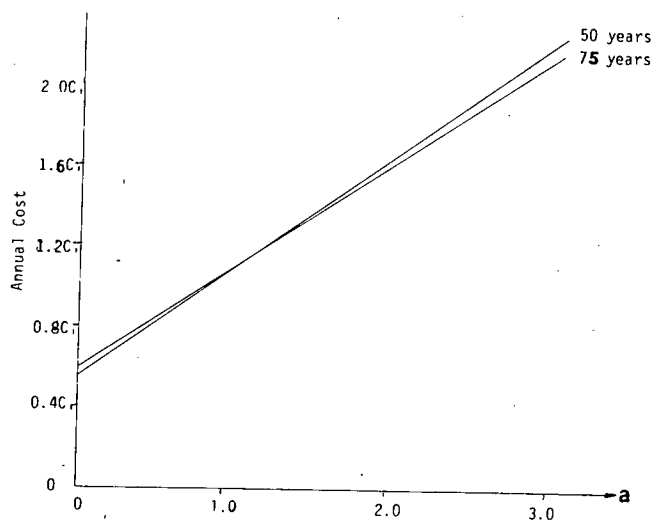


Figure 9. Annual costs for interest rate of 5 percent.

Table 4. Illustrations of weight/foot vs. section modulus.

Case No	Section Designation	Wt per foot	$S_x$	Weight Ratio $\frac{W_1}{W}$	Section Modulus Ratio $\frac{S_{x1}}{S_x}$
1	W36 x 300	300	1110	BASECASE	
2	W36 x 280	280	1030	.93	.93
3	W36 x 260	260	953	.87	.86
4	W36 x 245	245	895	.82	.81
5	W36 x 230	230	837	.77	.75

Note: Weight ratio is similar to section modulus ratio

Table 3. Continued

$$S_{rp} = F S_{rpo} / C^{1/3} \text{ but not less than } S_{rL}$$

Detail Category:	A	B	B'	C	D	E	E'
F =	1.78	1.40	1.12	1.00	.79	.45	.62
$S_{rL}$ =	8.80	5.87	4.40	*3.67	2.57	.95	2.93

\*Use 4.40 for stiffeners only

$$S_{rpo}, \text{ ksi}^*$$

Traffic Type	Lanes on Bridge	Very Heavy Traffic (ADT>8000/lane)	Heavy Traffic (ADT>2000/lane) (ADT<8000/lane)	Light Traffic (ADT>500/lane) (ADT<2000/lane)	Very Light Traffic (ADT<500/lane)
2-way	2	4.05	4.27	5.04	7.86
	4	3.54	3.74	4.40	6.89
	6	3.22	3.39	3.99	6.27
	8	2.92	3.08	3.63	5.69
1-way	1	4.31	4.54	5.36	8.40
	2	3.61	3.81	4.49	7.03
	3	3.22	3.39	3.99	6.27
	4	2.92	3.08	3.63	5.69

\* Based on (a) an annual ADT growth rate of 3%, (b) a design life of 75 years, and (c) 10% trucks for the Very Heavy and Heavy Traffic categories and 15% for the Light and Very Light Traffic categories.

C, the number of stress cycles per truck may be found as follows:

For longitudinal members:

- (a) Simple-span girders:
  - Above 40-ft span = 1.0
  - Below 40-ft span = 1.8
- (b) Continuous-span girders within a distance equal to 0.1 of the span on each side of an interior support:
  - Above 80-ft span =  $1 + (\text{Span}-80)/400$  in feet
  - Above 40-ft but below 80-ft span = 1.0
  - Below 40-ft span = 1.5
- (c) Continuous-span girders elsewhere:
  - Above 40-ft span = 1.0
  - Below 40-ft span = 1.5
- (d) Cantilever (suspended span) girders = 2.0
- (e) Trusses = 1.0

For transverse members:

- (a) Above 20-ft spacing = 1.0
- (b) Below 20-ft spacing = 2.0

## CHAPTER FOUR

# STRUCTURAL RELIABILITY AND CALIBRATION OF SAFETY ANALYSIS

## INTRODUCTION

Historically, safety factors have evolved in structural engineering based on performance evaluation and the expectations of engineers with regard to loading and the strength of materials. Safety factors were supposed to account for uncertainties in load intensity, calculation of load effects, quality of materials, and member and system strength prediction theories. Even without formal probability theories, code writers developed sound rules for flexible safety factors based on relative uncertainties in magnitudes and the influence of combinations of variables. For example, higher safety factors were used in checking foundations

compared to steel members. Similarly, reductions in safety factors were specified in multilane bridges where it is highly unlikely that all lanes will be simultaneously loaded at their extreme levels.

In recent years, structural code writing groups have found it advantageous to consider formal probabilistic techniques in assessing the reliability of existing provisions and in introducing new code checking formats. These methods fall in the general framework of structural reliability techniques. The goals for these methods are to assure code writers that their provisions provide consistent and uniform reliability across the full range

of code utilization. Some specific areas of applications include the following:

1. Adjusting safety factors between different materials so the same reliability level is achieved.
2. Allowing for redundancy in selecting factors.
3. Balancing load factors between dead, live, and environmental load effects.
4. Adjusting safety factors between main members and attachments (welds, bolts, etc.) to achieve consistent economy.
5. Providing provisions for special applications, such as safety factors during construction, or other short-term exposure cases.
6. Permitting the introduction of new technologies in materials or construction and developing suitable safety factors.

Examples of the adoption of structural reliability to assist code writers include the recently issued AISC-LRFD for design of steel buildings, RP2A-LRFD for design of offshore platforms and the *Ontario Highway Bridge Design Code*. In general, reliability principles are transparent to designers who receive deterministic code provisions in the traditional sense. It is only the code writers or researchers who use reliability to formulate code provisions and select safety factors.

## PROBABILITY THEORY

The concept of random variables is important as a first step leading to structural reliability theory. A variable may be a material property (modulus or yield stress), analysis (e.g., a stress concentration factor), or a consequence of loading (truck weight, impact). A variable is characterized by several parameters which define the uncertainty associated with these variables. Figure 10 shows a frequency distribution of truck weights at a site which characterizes how a large number of observations of the variable would appear. A measure of the central location

of the variable is the mean or average value. For a series of discrete observations of a variable, the mean is simply the average value. (Other measures of this central tendency are the mode, which corresponds to the value with the highest frequency, and the median, which is the value such that 50 percent of values fall below and 50 percent fall above.)

A measure of the uncertainty in the occurrence of a random variable is the standard deviation (or sigma value). This is defined as the square root of the variance,  $VAR$ , where:

$$\sigma_x^2 = VAR [X] = \int (x - \bar{X})^2 f(x) dx \quad (16)$$

where  $f(x)$  is the frequency or probability density,  $\bar{X}$  is the mean and  $\sigma_x$  the sigma value (22). Sigma is a measure of the spread or dispersion of the probability distribution away from the mean.

Equation 16 is similar to the calculation of the moment of inertia of the area under the frequency distribution curve about its mean value. A larger spread of the frequency distribution leads to a larger sigma. See illustration in Figure 11. A non-dimensional measure of this uncertainty is the coefficient of variation, or  $cov$ , often written with the parameter  $V$ ,

$$V_x = \frac{\sigma_x}{\bar{X}} \quad (17)$$

where  $V_x = cov$  of random variable  $X$ ,  $\sigma_x$  = standard deviation of  $X$ , and  $\bar{X}$  = mean value of  $X$ .

Another measure of a random variable used in practice is the nominal or safe value. It is usually located some number of standard deviations on the safe side of the mean value. For example, an A36 steel has a nominal value of 36 ksi used in design calculations. Tests of plates show a true mean of about 40 ksi and a sigma of about 3 ksi. Thus, the nominal value is some 1.33 sigma below the mean. A measure of the nominal value is the bias defined as:

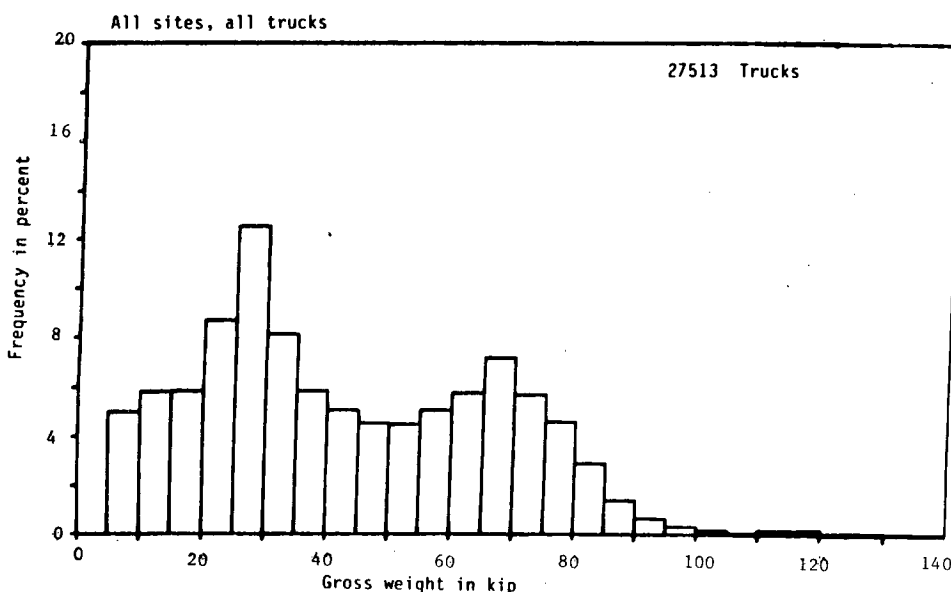


Figure 10. Truck weight histogram summary from WIM data.

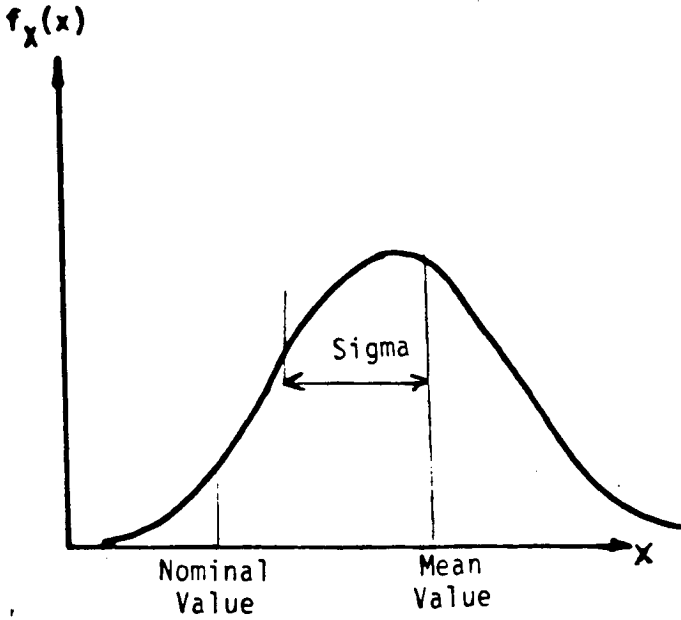


Figure 11. Probability density function ( $X$ —random variable).

$$\text{Bias} = \frac{\text{Mean Value of } X}{\text{Nominal Value}} \quad (18)$$

The mean (or bias) and coefficient of variation (or sigma) of a variable are sometimes referred to as the first two statistical moments. They provide a great deal of description of the uncertainty of a variable. A full description requires a probability distribution function such as the normal or log normal density curve or one of many other available distributions. Typically, there may not be enough data to accurately distinguish which distribution function is more representative of a particular random variable. Considerable progress in structural reliability applications has been made in using only the two moments cited above without any probability distribution. More exact reliability assessment in actuarial or statistical confidence terms does require such probability laws.

## RELIABILITY THEORY

The simplest model of reliability is the case of a load,  $S$ , and resistance,  $R$ . The structure is safe if the resistance exceeds the load. Thus, reliability,  $R_o$ , or the probability of survival, can be written as

$$R_o = \Pr [R > S] \quad (19)$$

Where  $\Pr$  should be read as probability. In terms of failure probability,  $P_f$ .

$$P_f = \Pr [R < S] \quad (20)$$

This model is shown in Figure 12. Both  $R$  and  $S$  are random variables. Failure probability occurs because of the overlap of

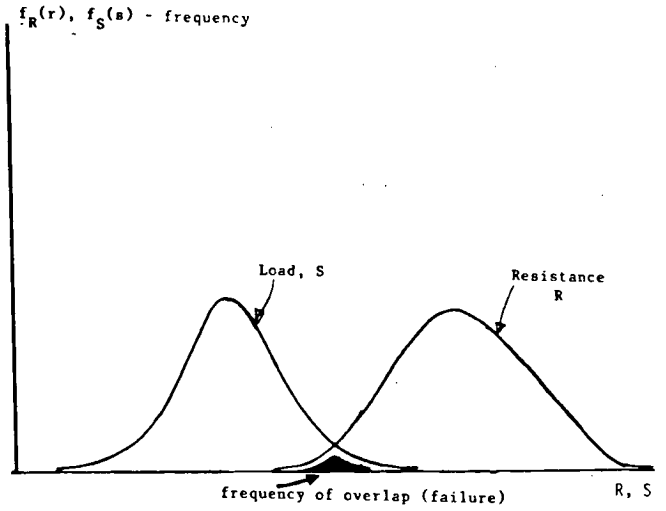


Figure 12. Fundamental reliability example.

the  $R$  and  $S$  probability densities. One way to formulate the failure probability is to define a margin of safety,  $Z$ , as:

$$Z = R - S \quad (21)$$

The statistical moments of  $Z$  are easily expressed as:

$$\text{mean, } \bar{Z} = \bar{R} - \bar{S} \quad (22)$$

$$\text{sigma, } \sigma_Z = (\sigma_R^2 + \sigma_S^2)^{1/2} \quad (23)$$

where  $\bar{R}$ ,  $\bar{S}$ , and  $\sigma_R$ ,  $\sigma_S$  are the respective means and sigmas of  $R$  and  $S$ .

An exact expression for  $P_f$  results if both  $R$  and  $S$  are normal distributions because  $Z$  would then also be normal, i.e.,

$$P_f = \Pr [Z < 0] = \phi^{-1} \left( \frac{0 - \bar{Z}}{\sigma_Z} \right) \quad (24)$$

Where  $\phi$  is the normal table available in any statistics text and  $\phi^{-1}$  is its inverse value. Note that  $P_f$  decreases as the mean safety margin  $\bar{Z}$  increases or the uncertainty in  $R$  or  $S$  expressed by their sigma value decreases. This allows the possibility in safety checking of trading off a lower safety factor with a more in-depth analysis which reduces the overall uncertainty and yet keeps the same reliability level. This is the basis for the decisions about safety factors which follow in the fatigue evaluation.

In much of the structural reliability application a convenient measure of the reliability ( $-\bar{Z}/\sigma_Z$ ) from Eq. 24 is denoted as the *safety index*, or beta as commonly called because of the use of the greek symbol  $\beta$ . The safety index may be defined as (100):

$$\text{Safety Index, } \beta = \frac{\text{Mean Value of safety margin of } (\bar{Z})}{\text{Standard deviation of } Z (\sigma_Z)}$$

For log normal distributions of  $R$  and  $S$ , provided  $V_R$  and  $V_S$  are not too large, a convenient expression is:

$$\beta = \frac{\ln \bar{R} / \bar{S}}{\sqrt{V_R^2 + V_S^2}} \quad (25)$$

$\beta$  is illustrated in Figure 13. It is the number of standard deviations between the mean of  $Z$  and the safe value of  $Z$ . If  $Z$  is assumed to be normal, the risks corresponding to  $\beta$  are:

Safety Index, $\beta$	Risk, $P_f$
1.5	0.07
2	0.023
2.5	0.006
3	0.001
3.5	0.0002
4	0.00003
5	$10^{-7}$
6	$10^{-9}$

Beta typically falls in the 1 to 4 range in most applications. Although the table is exact only if  $R$  and  $S$  are normal, research has shown that the results can be generalized with  $Z$  being any function such that  $Z > 0$  means safety.  $Z$  is normally a function of several random variables and is expressed as:

$$Z = f(X_1, X_2, \dots, X_n) \quad (26)$$

where  $X_1, X_2, \dots, X_n$  are the random variables in the analysis. The expression for  $\beta$  is exact if the function  $Z$  is linear and the variables are normal. If the variables are not normal, computer programs are available to map the function  $Z$  to be a function of equivalent normal variables. Similarly, if  $Z$  is not a linear function, it can be linearized. The point about which it is linearized is called the *design point* (or failure point). It generally corresponds to the most likely combination of variables  $X^*$  for the failure event with the highest probability. For example, in Figure 12 the most likely failure point is the value of  $R$  and  $S$  corresponding to the largest failure density in the shaded overlap region. This failure point is denoted as  $R^* = S^*$ . Computer programs such as appear in the National Bureau of Standards NBS Spec. Pub. 577 (50) are available to compute  $\beta$  for general distributions of random variables and failure functions  $Z$ . The programs automatically output the safety index,  $\beta$ , and the most likely failure values  $X^*$ . The latter helps to visualize the presence in the failure event from each random variable and highlight any possible requirements for further data.

It should be noted that the accuracy requirements in characterizing the statistics of any single variable will decrease as the total number of variables increase as, say, in the fatigue model which follows. For example, if we have a risk of  $10^{-5}$  and there are, say, 5 variables, the  $X^*$  value for each variable may fall in only the  $10^{-2}$  range. Thus, realistic and accurate assessments of reliability can be made without requiring an unrealistic amount of data. This will be seen below.

## CALIBRATION

Code writers have several tasks in conjunction with the reliability framework. A major responsibility is selecting a consistent target safety index, or  $\beta$ , for a code check. One approach is to base the decision on economics, i.e., an optimum failure rate occurs when the cost trade-off of increasing the safety factor

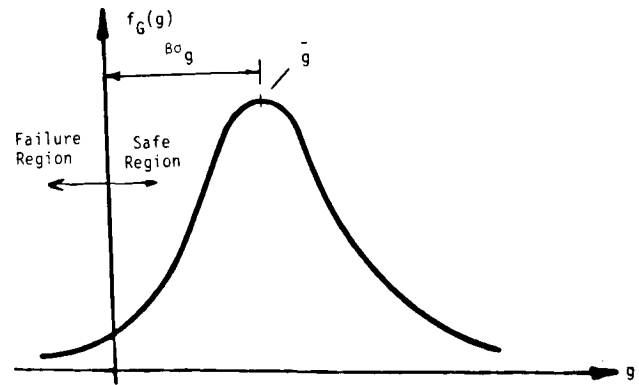


Figure 13. Probability density for failure function,  $g$ .

balances the risk reduction of future failures. A problem here is expressing the cost of failure in present worth terms. Another approach is to compile historical failure rates. If the rate is deemed acceptable (or no public outcry is evident which seeks to reduce the rate), this can be considered the societal target risk. A difficulty here is to isolate failures truly related to code checks. Most structural failures occur because of blunders or gross errors in design concept, analysis or construction and are *not* related at all to the code checking or safety factors employed. Control of such failures must be done by improvement in review procedures and other quality assurance operations.

The approach usually adopted by code writers for establishing the target beta is to assess the present design provisions and perform safety index calculations over a wide range of representative practice (e.g., for different bridge spans, geometries, attachments). In general, there will be a wide range observed in computed  $\beta$ 's because uncertainties were not always considered in the original development of the specifications. The aim in any new code provisions should be uniform or consistent target reliabilities. Thus, an average beta based on present standards is selected and this becomes the target for future code provisions.

## FATIGUE RELIABILITY MODEL

This section formulates a reliability approach to express the risk that the fatigue life of steel beam attachments will be less than the predicted life. Several points to note are: (1) the assumptions of the model, (2) the random variables expressing the uncertainty in knowing the true fatigue life, and (3) the sensitivity of the risk to the statistical parameters of these random variables.

The safety margin is defined simply as:

$$Z = Y_F - Y_S \quad (27)$$

where failure does not occur if  $Z > 0$ ,  $Y_F$  is life at which failure actually occurs (a random variable), and  $Y_S$  is specified or calculated life (deterministic).

A linear Miner cumulative damage rule assumption will be made, so that failure will occur when the nondimensional dam-

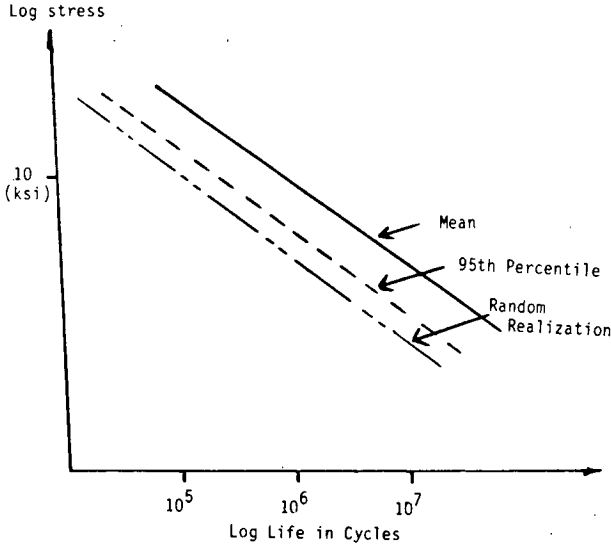


Figure 14. Illustration of fatigue SN curve plotted on log-log paper.

age accumulation sum equals 1.0. Letting the damage accumulation per year be denoted as  $D$ , we have for the variable,  $Y_F$ :

$$Y_F = \frac{X}{D} \quad (28)$$

where  $X$  is a random variable accounting for model uncertainty (mainly Miner's law assumption).

According to Miner's rule the accumulated damage is:

$$D = \sum \frac{1}{N(S_i)} \quad (29)$$

where the sum is over each of the stress cycles  $S_i$  for one year.  $N(S_i)$  is the number of cycles to failure at a constant amplitude stress range of  $S_i$ . The fatigue curve may be described as the straight line  $\log S$  vs.  $\log N$  curve as discussed in Chapter Two and shown in Figure 14. Figure 14 illustrates three lines including the mean SN curve, the commonly used nominal 95th percentile curve and a random realization of the SN line. As discussed in Chapter Two, the fatigue strength line is usually written as

$$NS^b = c \quad (30)$$

where the exponent  $b$  equals 3 (Chapter Two) for most welded attachments.

Substitution in Eq. 29 gives:

$$D = \frac{1}{c} \sum S_i^3 \quad (31)$$

where  $S_i$  is each of the nominal stress ranges occurring on the attachment detail.

The true stress range for any truck crossing depends on several variables and may be written as:

$$S_i = \frac{M_i}{S_x} = \frac{W_i g i m h}{S_x} \quad (32)$$

where  $M_i$  = maximum bending moment range of the  $i^{\text{th}}$  truck crossing event on the girder,  $W_i$  =  $i^{\text{th}}$  truck crossing gross vehicle weight,  $m$  = influence factor relating truck weight to maximum bending moment,  $i$  = impact amplification (same as AASHTO  $1 + I$ ),  $g$  = lateral girder distribution (expressed as percent of gross span moment carried by a single girder),  $h$  = account for closely spaced or multilane presence of vehicles which amplify the moment, and  $S_x$  = actual section modulus.

All of the foregoing random variables ( $M_i$ ,  $W_i$ ,  $m$ ,  $i$ ,  $g$ ,  $h$ , and  $S_x$ ) have been discussed in Chapter Two. Equation 32 gives the actual stress range due to the  $i^{\text{th}}$  truck crossing event. It relates to the design stress range through the selection of the section modulus, which is expressed using similar terms:

$$S_{XD} = \frac{\gamma W_D g_D i_D m_D h_D}{S_{rD}} \quad (33)$$

where  $\gamma$  is the reliability factor to be specified after calibration of the risk (this factor ensures an acceptable risk for the computed fatigue life of the member).  $W_D$ ,  $g_D$ ,  $i_D$ ,  $m_D$ ,  $h_D$  are the specified nominal or design values of  $W$ ,  $g$ ,  $i$ ,  $m$ , and  $h$ , respectively.  $S_{rD}$  is the design or allowable stress range (this is obtained from the fatigue strength curves (SN curves) corresponding to expected lifetime total number of cycles the member is subjected—Chapter Three).  $S_{XD}$  is the computed value of section. In general, the actual section modulus  $S_x$  is a random variable (Chapter Two).  $S_{XD}$  and  $S_x$  are related by a random variable  $Z_X$  by:

$$S_x = Z_X S_{XD} \quad (34)$$

$Z_X$  reflects the scatter in the true section modulus compared to computed nominal section modulus.

Substituting Eqs. 34, 33, and 32 into Eq. 31 gives:

$$\begin{aligned} D &= \frac{1}{c} \left( \frac{W_i g i m h}{\gamma Z_X W_D g_D i_D m_D h_D} S_{rD} \right)^3 \\ &= \frac{V}{c} \left( \frac{g m i h}{\gamma Z_X W_D g_D i_D m_D h_D} S_{rD} \right)^3 \sum \frac{W_i^3}{V} \end{aligned} \quad (35)$$

where  $V$  = number of trucks per year.

To simplify, let

$$W_{eq} = \left( \sum f(W_i) W_i^3 \right)^{1/3} \quad (36)$$

where  $W_{eq}$  = equivalent fatigue truck weight, and  $f(W_i)$  = percentage of trucks within weight interval  $W_i$ . Let:

$$V = ADTT (365) C \quad (37)$$

where  $V$  = volume, reflecting the total number of equivalent stress cycles in a year (a random variable),  $ADTT$  = average daily truck traffic in vehicles per day (a random variable),  $C$  = equivalent number of stress range cycles per truck crossing (a random variable).

Substituting Eqs. 36 and 37 into Eq. 35 gives:

$$D = \frac{1}{c} (ADTT) 365 C \left( \frac{W_{eq} g m i h}{\gamma Z_X W_D g_D i_D m_D h_D} S_{rD} \right)^3 \quad (38)$$



Simplifying further gives:

$$c = N_T S_r^3 = N_T \left( \frac{S_r}{S_{rD}} \right)^3 S_{rD}^3 \quad (39)$$

where  $S_r$  is the true stress range (a random variable) from the SN curve corresponding to  $N_T$  number of stress cycles.  $N_T$  is a reference number of cycles and is deterministic. For convenience, it is chosen to be numerically equal to the total number of expected stress cycles in the lifetime of the member.

From the definition of  $N_T$ ,

$$N_T = \overline{ADTT} (365) \bar{C} Y_S \quad (40)$$

where  $\overline{ADTT}$  and  $\bar{C}$  denote the mean values of random variables  $ADTT$  and  $C$ . Substituting Eqs. 40 and 39 into Eq. 38 gives:

$$D = \frac{\overline{ADTT} (365) C}{N_T} \left( \frac{W_{eq} g m i h}{\gamma W_D g_D m_D i_D h_D Z_X} \frac{S_{rD}}{S_r} \right)^3 \quad (41)$$

$$\text{Let: } G = g/g_D \quad (42)$$

$$I = i/i_D \quad (43)$$

$$M = m/m_D \quad (44)$$

$$W = W_{eq}/W_D \quad (45)$$

$$H = h/h_D \quad (46)$$

$$S = S_r/S_{rD} \quad (47)$$

Equations 42–47 define as random variables the ratio of the true value (random) to the nominal design value.

Substitution now gives:

$$D = \frac{365 (\overline{ADTT}) C}{N_T} \left( \frac{W G I M H}{\gamma Z_X S} \right)^3 \quad (48)$$

Substituting Eqs. 48 and 28 into Eq. 27, we have:

$$Z = \frac{X N_T}{365 (\overline{ADTT}) C} \left( \frac{\gamma Z_X S}{W G I M H} \right)^3 - Y_S \quad (49)$$

The random variables include material terms,  $Z_X$ ,  $X$ , and  $S$ , truck variables,  $W$ ,  $ADTT$ ,  $H$ ,  $M$ , and  $C$  and analysis uncertainties  $I$  and  $G$ . The function given by Eq. 49 is the input to the reliability program. The other input includes statistical parameters and distribution functions of each of the 10 variables. The statistical data base is discussed in the next section. The output is the safety index,  $\beta$ , and the design or most likely failure points,  $ADTT^*$ ,  $C^*$ ,  $W^*$ ,  $G^*$ ,  $I^*$ ,  $M^*$ , and  $H^*$ ,  $S^*$ ,  $Z_X^*$ , and  $X^*$ .

## STATISTICAL DATA BASE

**Random Variable  $X$ .** The random variable  $X$  reflects the uncertainty in the damage model, mainly due to Miner's Rule. The damage predicted by Miner's Rule is assumed herein to be unbiased (198). To account for possible test scatter with this rule, a coefficient of variation of 15 percent is used. This value had to be estimated because data on the accuracy of Miner's Rule for welded steel structures were insufficient. The sensitivity of the design factors to such selected statistical parameters is shown to be small in subsequent sections because of the cali-

bration procedure adopted herein. The coefficient of variation of 15 percent implies that there is a 95 percent probability that the predicted life of a specimen using Miner's damage rule will be within 70 percent and 130 percent ( $\pm 2$  sigma levels) of the actual life.

**Random Variable  $M$ .** The random variable  $M$ , called the moment ratio, reflects the effect of axle spacing and axle weight distribution on the fatigue life of the bridge. Moment ratio has been defined as the ratio of the average influence factor due to actual truck spectrum on the bridge to the influence factor of the fatigue design vehicle. Moment ratio varies considerably with span. However, the gross weight of the fatigue vehicle does not affect the moment ratio. Truck traffic data from 12 sites are used to calculate the average moment ratios for different spans. The results are summarized in Table 5. The table also shows the mean and coefficient of variation,  $cov$ , of moment ratio for four different spans of 30 ft, 60 ft, 90 ft, and 120 ft. Data from 5 sites (205) were used to calculate moment ratios for continuous spans, using Schilling's vehicle as the design vehicle. The results are summarized in Table 6. The mean and  $cov$  for 4 different spans of 30 ft, 60 ft, 90 ft, and 120 ft are given in the table. It should be noted that these means and  $cov$  are reasonably close to the corresponding means and  $cov$  obtained for simple spans in Table 5.

Table 5. Moment ratios based on Schilling's vehicle for simple spans.

Site	M			
	Spans			
	30'	60'	90'	120'
US 75 over 56	0.918	0.941	0.945	0.963
Renesselear	0.969	0.996	0.989	0.994
I40 & Prothro JNC.	0.894	0.896	0.926	0.949
NYC Thruway	1.036	1.068	1.025	1.018
SR 114 East Dallas	0.913	0.929	0.947	0.964
I10 & US77				
Schulenberg	0.903	0.920	0.929	0.952
SR21 East Caldwell	0.996	1.042	1.003	1.002
SR 89 & Spring				
Valley	0.913	1.014	1.008	1.006
SR51 @ ILL. River				
& Peru	0.872	0.910	0.937	0.958
I-880 Sacramento	0.926	0.975	0.955	0.970
IS @ Mokelumne River	0.871	0.925	0.948	0.966
US 67 @ LR AKB				
Jacksonville	0.889	0.965	0.970	0.981
Mean	0.925	0.965	0.965	0.977
Cov	5.2%	5.5%	3.3%	2.2%
Reference (205)				

Table 6. Moment ratios based on Schilling's vehicle for continuous spans.

Site	M			
	Spans			
	30'	60'	90'	120'
I40) & SR25	0.88	0.91	0.95	0.97
I10 & US27	0.87	0.91	0.94	0.96
I-70 @ Vandalia	0.86	0.91	0.95	0.97
US67 @ LRAFB	0.88	0.96	0.98	0.99
SR 17 @ Fruituae	0.87	0.96	0.97	0.98
Average	0.87	0.93	0.96	0.97
cov%	1%	3%	2%	1%

Reference (205)

**Random Variable  $W$ .** The random variable  $W$  reflects the uncertainty in the estimation of the gross weight of the equivalent fatigue truck. As explained before, the value of 54 kip for gross weight of the fatigue truck is obtained from WIM studies including 30 nationwide sites with over 27,000 truck samples. Therefore, the value of gross weight of the fatigue truck is assumed to be unbiased. Furthermore, a *cov* of 10 percent is assumed for the gross weight of fatigue truck in the reliability analysis. This implies that there is a 95 percent chance that the effective gross weight of the truck spectrum at a site will be between 43 kip and 65 kip. This assumption is in good agreement with the results of WIM studies (205), where effective gross weights in the range of 45 kip to 67 kip were found (see Table 7 and reported data in Appendix D).

**Random Variable  $H$ .** The random variable  $H$  reflects the effect of multiple presence of trucks on the bridge. Moses and Nyman (60, 161) simulated this factor using WIM data for free traffic flow. A mean value of 1.03 and coefficient of variation of only 0.6 percent were reported for the headway factor.

**Impact Ratio  $I$ .** The random variable  $I$  reflects the uncertainty in the estimation of impact factor for a given site. The proposed procedures utilize best estimates of the impact factor. Hence, a mean value of 1.0 is assumed for the random variable  $I$ . A *cov* of 11 percent is assumed for the random variable  $I$  as reported by Moses and Pavia (146). The uncertainty in  $I$  and also  $G$ , which follows, refers to site-to-site uncertainty of the mean impact or  $G$  value. Variations from truck to truck within the same site are not too important because fatigue is an averaging process and such variations almost cancel out.

**Lateral Distribution Ratio  $G$ .** The random variable  $G$  reflects the uncertainty in the estimation of girder lateral distribution factor. The proposed procedures use the best estimate of the distribution factors. Hence, the mean value of  $G$  is taken as 1.0. Moses and Pavia (146) reported a *cov* of 13 percent for lateral distribution factors from site to site from data collected for 10 bridges. The same value is used in the present study.

**Random Variable  $Z_X$ .** The random variable  $Z_X$  reflects the uncertainty in the effective section modulus. In general, the

Table 7. Effective gross weights.

Data Source/Site	Weff
Lucas	49.4k
Astabula	50.0k
Texas Iowapark	67.0k
1970 FHWA	52.0k
California SR99	51.3k
I-30 @ US67 Benton	53.5k
US67 Jacksonville	44.9k
I-40 @ SR25	52.5k
US-65 @ RT 256	54.8k
I-30 @ RT 25	55.5k
27,513 truck data from WIM (124)	53.7k

Reference (205)

proposed procedures recommend the use of the best estimate of the actual section modulus and, hence, the mean value of  $Z$  is taken as 1.0. However, in some specific cases, it is recognized that the effective section modulus is significantly above the actual section modulus because of beneficial effects not normally calculated in design. For example, in Chapter Two and Appendix E it has been shown that the effective section modulus is about 15 percent above the actual section modulus for composite sections. Such specific cases are taken care of by increasing the computed section modulus. This increased section modulus is assumed to represent an unbiased value of effective section modulus. Hence,  $Z_X$  is taken as 1.0. A *cov* of 10 percent is assumed for the random variable  $Z_X$ . It is shown in the sensitivity analysis in this chapter that such assumptions do not significantly affect the safety factors if the target beta is taken as the average safety index used in the present calibration.

**Random Variable  $C$ .** The random variable  $C$  represents the equivalent number of stress cycles due to a single truck passage on the bridge. The proposed procedures use the best estimates of  $C$ . The recommended values of  $C$  are given in Article 6.3.4 of the evaluation procedure (Appendix A). These values are taken as the mean values of  $C$ . The coefficient of variation for the random variable,  $C$ , is estimated to be 5 percent because little variation is expected in its value. There are insufficient statistical data available to define this parameter more precisely.

**Random Variable  $ADTT$ .** The random variable  $ADTT$  represents the true value of the lifetime average daily truck traffic in the shoulder lane at the site. The procedures recommend that the value of  $ADTT$  should be estimated from a knowledge of site conditions and should be unbiased. Therefore, the estimated value of  $ADTT$  would be a mean value. A  $COV$  of 10 percent (146) is assumed for the random variable  $ADTT$ . Two aspects should be noted regarding this value. (1) Volume uncertainty affects the safety factors much less than stress uncertainty because fatigue damage is linearly proportional to volume but is proportional to the cube of stress range. Thus, a 10 percent  $COV$  on volume is equivalent to an effect of 10 percent cubed, or 3.33 percent on a stress parameter, such as lateral distribution and impact. (2) Larger volumes than expected will truly shorten the bridge life. However, from an economic viewpoint, the bridge has still provided its intended service in terms of total number of truck passages.

**Random Variable  $S$ .** The random variable  $S$  reflects the uncertainty in the estimation of fatigue strength curves. As has been discussed in Chapter Two, the fatigue strength curves are linear log  $S$  vs. log  $N$  curves for all categories and they have a slope of 3.0 on a log-log plot. The statistical properties of the random variable  $S$  depend on the fatigue category and are obtained from the test results reported from Lehigh University (119). The mean values and  $COV$  of stress ranges at 2 million cycles for different detail categories have been obtained and are given in Table 8. The mean values of  $S$  can be obtained using Equation 47. For example, for detail category C

$$\bar{S} = \frac{\bar{S}_r}{S_{rD}} = \frac{16.7}{13.0} = 1.29 \quad (50)$$

The mean values of  $S$  for all the detail categories are also given in Table 8. It should be noted that the mean value of  $S$  is the same for any number of stress cycles for a given detail category. This is because the mean SN curve and the design SN curve are assumed to be parallel and have a slope of 3.0 (see Chapter Two) on a log-log plot. The mean SN curve is given by

$$N\bar{S}_r^3 = c \quad (51)$$

The design SN curve is given by

$$N\bar{S}_{rD}^3 = K \quad (52)$$

Dividing Eqs. 51 by 52 and substituting Eq. 47 gives:

$$\bar{S} = \frac{\bar{S}_r}{S_{rD}} = \left(\frac{c}{K}\right)^{1/3} \quad (53)$$

From Eq. 53 it can be seen that  $S$  is independent of the number of stress cycles.

#### EXAMPLE

To illustrate the use of reliability programs and the input statistical data an example is given here. The example considered is a 100-ft simple span and a Category C redundant attachment. The input statistical data discussed in the previous section are summarized in Table 9. All the variables are assumed to have a log normal distribution which is typically assumed in struc-

Table 8. Statistical data for  $S$ .

Detail Category	$S_r$ at $2 \times 10^6$ cycles	$S_D$ at $2 \times 10^6$ cycles	Intercept on the nominal S-N curves	COV	$\bar{S}$
A	33.0	23.2	$2.5 \times 10^{10}$	21.7%	1.42
B	22.8	18.1	$1.191 \times 10^{10}$	14.1%	1.26
B'	18.0	14.5	$6.109 \times 10^{10}$	13.2%	1.24
C	16.7	13.0	$4.446 \times 10^9$	15.3%	1.29
D	13.0	10.3	$2.183 \times 10^9$	14.2%	1.26
E	9.5	8.1	$1.072 \times 10^9$	9.7%	1.17
E'	7.2	5.8	$3.908 \times 10^8$	13.2%	1.24
Average				14.5%	1.27

Table 9. Input to reliability program for example.

Variable	Mean	COV	Distribution
X	1.0	0.15	Lognormal
S	1.297	0.153	Lognormal
M**	0.97	0.03	Lognormal
G	1.0	0.13	Lognormal
I	1.0	0.11	Lognormal
H	1.03	0.006	Lognormal
C	1.0	0.05	Lognormal
ADTT*	2500	0.10	Lognormal
W**	1.0	0.10	Lognormal
$Z_x$	1.0	0.10	Lognormal

\*On outer lane

\*\* Normalized to fatigue truck (Figure 6.2.2A of Appendix A)

tural reliability research. For a given reliability factor,  $\gamma$ , the statistical input of Table 9 and the Z function (Eq. 49), the reliability program will output the safety index. Figure 15 shows a plot from the reliability program between reliability factor  $\gamma$  and safety index  $\beta$ . For example, a  $\gamma$  of 1.5 leads to a  $\beta$  of 2.3. Some more plots of  $\gamma$  versus  $\beta$  are shown in Figure 16 for different spans and different fatigue detail categories.

An examination of Figure 16 shows that the reliability factor as a function of safety index ( $\gamma$  versus  $\beta$ ) is not very sensitive to changes in span and fatigue detail categories, especially in the range of beta of 1 to 3. An average or typical curve is chosen to represent all spans and categories and is shown in Figure 17.

The  $\gamma$  versus  $\beta$  relationship shown is applicable for any values of the parameters related to truck volume, namely  $ADTT$ ,  $C$ , or  $Y_s$ . This can be seen by recalling Z and substituting Eq. 40 into Eq. 49. We obtain:

$$Z = Y_s \left[ X \left( \frac{ADTT}{ADTT} \right) \left( \frac{C}{C} \right) \left( \frac{Z_x S}{W G I M H} \right)^3 - 1.0 \right] \quad (54)$$

To further simplify, let:

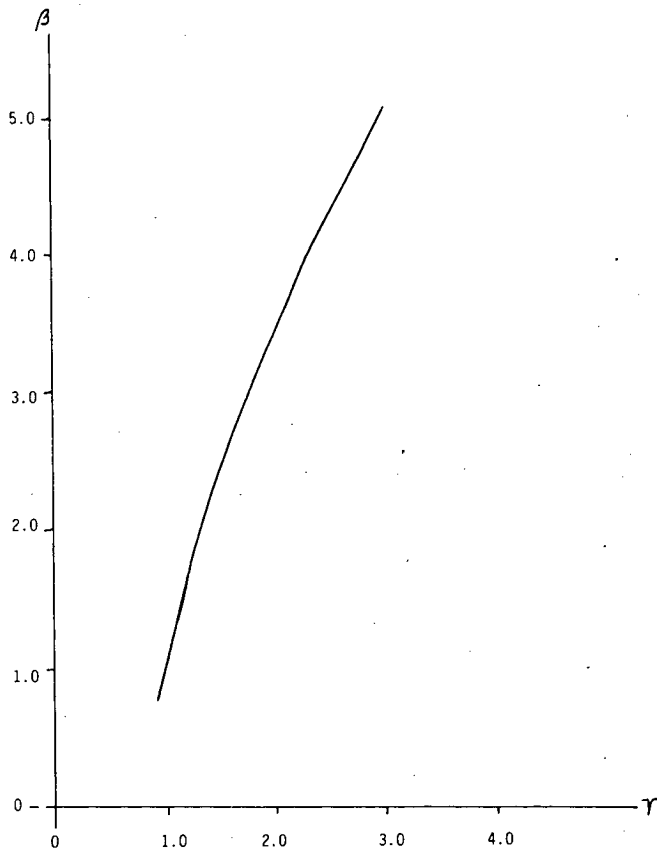


Figure 15.  $\gamma$  vs.  $\beta$  for example.

$$A = \frac{ADTT}{ADTT} \quad (55)$$

$$B = \frac{C}{C} \quad (56)$$

Substituting Eqs. 55 and 56 into Eq. 54, we have:

$$Z = Y_S \left[ X A B \left( \frac{Z_X S}{W G I M H} \right)^3 - 1.0 \right] \quad (57)$$

From the definitions of A and B, their statistical means and *cov* are independent of the estimated value of *ADTT* and *C* for the site. The means of A and B are always equal to 1.0 and their *cov* are 10 percent and 5 percent, respectively (see section on "Statistical Data Base"). Hence, it can be inferred from Eq. 57 that in the  $\gamma$  versus  $\beta$  relationship obtained using the *Z* function (Eq. 49),  $\gamma$  is independent of the estimated values of *ADTT*, *C*, and *Y<sub>S</sub>*.

#### TARGET BETAS FOR EVALUATION PROCEDURE

It can be seen from Figure 15 that different safety factors achieve different expected beta's or different probabilities that

the actual life will be shorter than predicted. The safety factor to be selected is sensitive to the target beta and, hence, to the statistical parameters of the variables in the reliability expression. In a calibration approach, the target beta is selected as an average of the betas implicit in present design practice. The typical calibration study finds (as also indicated herein) that the reliability levels (betas) in present design practices are *not* uniform. There is considerable spread in the betas which is not intended. Thus, the calibration is intended to achieve more uniform reliability (beta) levels. The target beta can be the average of present design practices as long as there is no obvious need to either raise or lower existing calibration risk levels based on performance experience. This was the philosophy adopted in the recent AISC-LRFD and is also appropriate for the bridge fatigue example herein.

Fourteen AASHTO design cases with different truck volumes, detail categories, spans, impact factors, lateral distribution factors, and support conditions (simply supported or continuous) were used to evaluate an average beta implicit in the present AASHTO design practice. This is done by taking sections which just satisfy the AASHTO fatigue criteria (see Table 10a) and computing the implicit reliability factor,  $\gamma$ , by the methods described herein. The designs selected were intended to be both representative of typical cases and also to represent possible extreme occurrences. For example, case H has a mean impact of 1.20 and a mean girder distribution of 0.50. Hence, this case is used to represent an extremely unlikely case to observe what values of beta would result. The  $\gamma$ 's and the corresponding  $\beta$ 's found from the mean  $\gamma$  versus  $\beta$  graph for each case are given in Table 10(b) and Figure 18. Each point in the figure corresponds to a  $\gamma$  versus  $\beta$  case. To illustrate how the points were obtained a sample calculation is given below.

#### Sample Calculation

1. *Given*
- 100-ft simple span, Category C, 2,500 ADTT, 8-ft girder spacing.
2. AASHTO HS-20 Bridge Design Calculations:
- Impact factor =  $1 + (50)/(100 + 125) = 1.222$ .
- Moment range = 1,524 kip-ft (HS-20 vehicle on 100-ft simple span).
- Lateral distribution =  $8/14 = 0.571$  8-ft spacing).
- Allowable stress range = 10 ksi (Category C for over 2 million cycles).
- $S_{XD} = Mgi/S_{rD} = 1,524 (12) 0.571 (1.222)/(10) = 1,276$  in.<sup>3</sup> (AASHTO Design Section).
- Referring to Eq. 33:

$$\gamma = \frac{S_{rD} S_{XD}}{W_D g_D i_D m_D h_D} \quad (58)$$

- For the proposed evaluation:

$W_D = 54$  kip (refer to Chapter Two);

$g_D = \frac{8}{D} = 0.36$ ;  $D = 22.33$  (refer to Chapter Two);

$i_D = 1.10$ ; assuming smooth surface (refer to Chapter Two);

$m_D =$  maximum moment range on bridge/gross vehicle weight

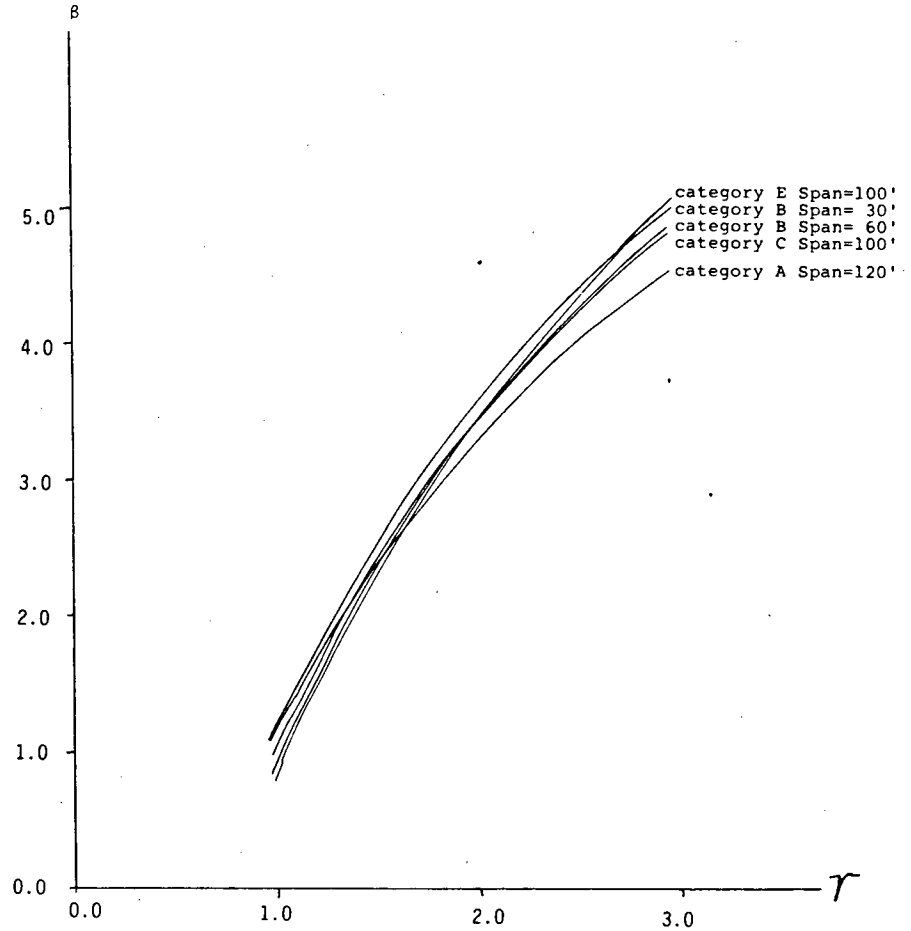


Figure 16.  $\gamma$  vs.  $\beta$  plots.

= 214.8 in. (for vehicle shown in Appendix A, Figure 6.2.2A);

$h_D = 1.0$  (refer to Chapter Two);

$S_{XD} = 1,276 \times 1.15 = 1,501 \text{ in.}^3$  (the section modulus is increased 15 percent as recommended in the proposed methods for composite sections with shear connectors); and

$S_{rD}$  = allowable stress range corresponding to expected total number of cycles during the lifetime of the bridge (taken from the 95th percentile line).

- Assuming that a 75-year life is desired for the member (consistent with the proposed design), Eq. 40 gives  $N_T = ADTT$  (365)  $C Y_s$  in which  $ADTT = 2,500$  (given in the problem);  $Y_s = 75$  years;  $C = 1.0$  (for 100-ft simple spans, see the table in guidelines); and  $N_T = 2,500 (365) 1.0 (75) = 68.4 \times 10^6$  cycles.
- The equation for the 95th percentile fatigue strength line is written as

$$S_{rD}^3 N_T = K \quad (59)$$

where  $K$  is the intercept of the 95th percentile line;  $K = 4.446 \times 10^9$  (for Category C, see Table 7).

- Substitution gives  $S_{rD} = 4.02 \text{ ksi}$ .

- Substituting in Eq. 58 gives the corresponding reliability factor for this design example.

$$\gamma = \frac{(4.02)(1501)}{54(0.36)(1.10)(214.8)(1.0)}$$

$$\gamma = 1.32 \text{ (Point B on Figure 18)}$$

Thirteen other cases are given in Figure 18. As explained in the previous section, the mean  $\gamma$  versus  $\beta$  curve in Figure 17 is assumed to represent all the cases. This can be justified by examining Figure 16 in the normal range of  $\beta$ ' of 1.0 to 3.0. Therefore, the evaluation points are all marked on the mean  $\gamma$  versus  $\beta$  curve. This helps to put all the evaluation points on a single graph and gives a perspective of reliability levels in present design. It can be seen from Figure 18 that most of the design points fall around a beta of 2.0, which is midway in the range of the betas (0.7–3.6) corresponding to all the design points including the extreme design situations cited earlier. This corresponds to a reliability factor,  $\gamma$ , of 1.35. The same analysis is repeated for nonredundant details and the results are given in Table 11 and Figure 19. The mean of the range of betas (1.5–5.3) for nonredundant details appears to be about 3.0. This

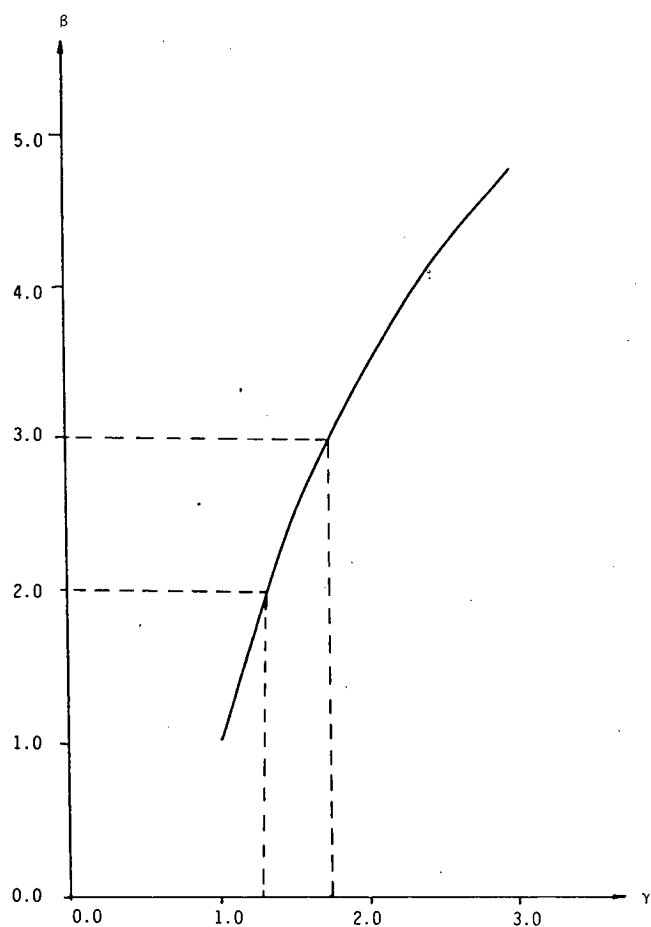


Figure 17. Mean  $\gamma$  vs.  $\beta$  curve.

corresponds to a reliability factor,  $\gamma$ , of 1.75. From this analysis the target safety index for redundant and nonredundant members was fixed as 2.0 and 3.0, respectively, in the proposed evaluation procedure.

These examples demonstrate quite strongly the advantages of the proposed format. For redundant spans, we try and achieve our target  $\beta$  of 2 (the actual variation is shown later) for all the design cases, while AASHTO produced betas ranging from 0.7 to 3.6. Design with high betas is uneconomical, while the low betas will have relatively low probabilities that the actual fatigue life will exceed the predicted life. Similarly for the non-redundant cases, the proposed evaluation methods try to achieve a target  $\beta$  of 3.0 for all cases compared to AASHTO betas that range from 1.5 to 5.3.

The target betas (using the proposed safety factors of 1.35 and 1.75 for redundant and nonredundant cases respectively) will not be achieved exactly even for the proposed method procedures. More factors would be needed to make this possible. The scatter in beta, however, will be much smaller as shown in Table 12 for the above 14 design cases. To compare the scatter in beta the same 14 cases (used for target beta selection) were designed as per the proposed methods. The corresponding betas for these sections are shown in columns (5) and (7) of Table 12 for redundant and nonredundant members respectively. The

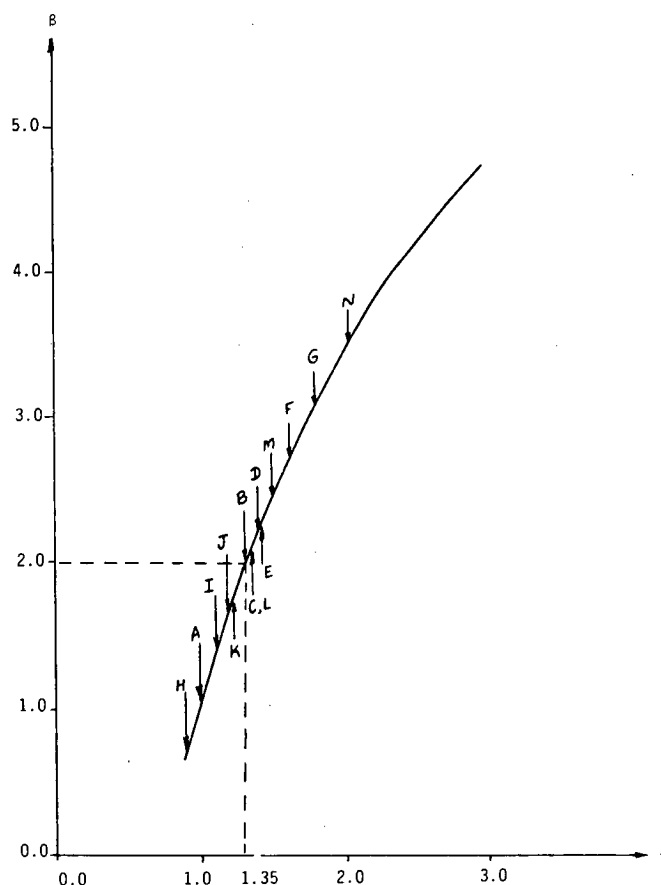


Figure 18.  $\beta$ 's in present design for redundant members.

scatter in beta for redundant members is between 1.85 and 2.17 (as against 0.7 to 3.6 for AASHTO methods) and for nonredundant members it is between 2.85 and 3.10 (as against 1.5 to 5.3 for AASHTO methods). Hence, the proposed procedures provide a more uniform safety index.

#### SAFETY FACTORS FOR EVALUATION PROCEDURE

The evaluation procedures have been developed with the following aims: (1) consistent and uniform reliability over the range of application (all spans, categories, lives, volumes); (2) flexible to incorporate site-specific data; (3) flexible to provide the Engineer with a better (usually longer) fatigue life estimate if more effort is applied.

The first aim was satisfied by the calibration process. A target safety index has been fixed to achieve consistent and uniform reliability. The other two goals are obtained by incorporating several alternatives to the basic procedure. Some of the alternatives need site-specific data, while some other alternatives require more analysis effort by the Engineer. It should also be noted that in the evaluation, the Engineer can also obtain the mean fatigue life as well as the safe life. This should help clarify

Table 10(a).  $\beta$ 's in present design (redundant members).

(1)	(2)	(3)	(4)	(5)	AASHTO DESIGN PARAMETERS				(10)
					(6)	(7)	(8)	(9)	
Designations	Span	Bridge Type	Detail Category	Truck Volume	Impact	D.F.*	Moment Range	Allowable Stress	AASHTO Design Section
A	120'	S.S.	C	4000	1.20	0.571	1879	10	1545
B	100'	S.S.	C	2500	1.22	0.571	1519	10	1270
C	60'	S.S.	A	2500	1.27	0.727	800	24	369
D	60'	S.S.	B	2500	1.27	0.727	800	18	492
E	60'	S.S.	C	2500	1.27	0.571	800	10	696
F	60'	S.S.	D	2500	1.27	0.571	800	7	995
G	60'	S.S.	E	2500	1.27	0.571	800	5	1392
H	30'	Cont.	C	1500	1.30	0.571	272	10	242
I	100'	Cont.	A	2500	1.22	0.727	1512	24	671
J	100'	Cont.	B	2500	1.22	0.727	1512	18	894
K	100'	Cont.	C	2500	1.22	0.571	1512	10	1264
L	100'	Cont.	D	2500	1.22	0.571	1512	7	1806
M	100'	Cont.	E	2500	1.22	0.571	1512	5	2528
N	60'	Cont.	C	4000	1.27	0.571	799	10	695

Cases A-M: Composite

Case N: Noncomposite

Table 10(b). Continued

(1)	(2)	(3)	(4)	(5)	(6)	(7)	(8)
Designation	$S_{XD}$	$W_{D^mD}$	$g_D$	$i_D$	$S_{rD}$	$\gamma$	$\beta$
A	1777	1217	0.35	1.20	3.44	1.03	1.05
B	1461	947	0.36	1.10	4.02	1.32	2.00
C	424	408	0.40	1.10	7.15	1.38	2.05
D	566	408	0.40	1.10	5.58	1.43	2.15
E	800	408	0.40	1.10	4.02	1.46	2.20
F	1144	408	0.40	1.10	3.17	1.65	2.75
G	1601	408	0.40	1.10	2.50	1.81	3.10
H	242	179	0.50	1.20	4.17	0.91	0.70
I	772	962	0.36	1.20	7.15	1.16	1.45
J	1028	962	0.36	1.20	5.58	1.20	1.60
K	1454	962	0.36	1.20	4.02	1.23	1.65
L	2077	962	0.36	1.20	3.17	1.32	2.05
M	2907	962	0.36	1.20	2.50	1.52	2.40
N	904	444	0.30	1.10	3.44	2.05	3.55

$$\gamma = \frac{S_{XD} S_{rD}}{W_{D^mD} g_D i_D}$$

\*\* $S_{XD}$  = 1.15 x AASHTO design section for composite sections  
 = 1.30 x AASHTO design section for noncomposite sections with no visual separation

and explain why a span, which does not satisfy a safe life check, may in fact not yet show any visual signs of fatigue cracking. Typically, the mean life will be about 5 times the computed safe life for redundant spans and 10 times the safe life for nonredundant spans. Depending on the situation, for a span not meeting the required safe life, the Engineer can select different options including more frequent inspection or control on permit vehicles.

Most of the alternatives in the evaluation lead to lower safety factors which, in turn, will increase the estimated fatigue life of the member. The concept here is that risk is influenced by both the safety factor and the uncertainty. The same target safety index can therefore be achieved by reducing uncertainties and using a smaller safety factor. The safety factor or reliability factor is given by

$$R_s = R_{s0} F_{s1} F_{s2} F_{s3} \quad (60)$$

where  $R_s$  = reliability or safety factor (this factor is used to

multiply the nominal calculated design stress to achieve the needed safety index);  $R_{s0}$  = basic reliability factor which depends on whether component is redundant or nonredundant; and  $F_{sn}$  = factor for procedure  $n$  ( $F_{sn} = 1.0$  if the procedure  $n$  is not used).

In the previous section the target betas were fixed at 2.0 and 3.0 for redundant and nonredundant members, respectively. Using the mean (reliability factor)  $\gamma$  vs.  $\beta$  (safety index) curve developed previously (Figure 17), the reliability factors corresponding to target betas of 2.0 and 3.0 are obtained as 1.35 and 1.75 respectively.

These values of 1.35 and 1.75 are used as the basic reliability factors in the proposed evaluation procedures for redundant and nonredundant members, respectively. The procedures specify several alternatives that could be used to incorporate site-specific data in evaluation. These alternatives usually require more effort and consequently lower the uncertainties associated with the random variables. Therefore, lower safety factors may still provide the required target safety indices. A partial safety factor is

Table 11(a).  $\beta$ 's in present design (nonredundant members).

(1)	(2)	(3)	(4)	(5)	AASHTO DESIGN PARAMETERS					(10)
					(6)	(7)	(8)	(9)		
Designations	Span	Bridge Type	Detail Category	Truck Volume	Impact	D.F.*	Moment Range	Allowable Stress	AASHTO Design Section	
A	120'	S.S.	C	4000	1.20	0.727	1879	10	1967	
B	100'	S.S.	C	2500	1.22	0.727	1519	10	1617	
C	60'	S.S.	A	2500	1.27	0.727	800	24	369	
D	60'	S.S.	B	2500	1.27	0.727	800	16	554	
E	60'	S.S.	C	2500	1.27	0.727	800	10	886	
F	60'	S.S.	D	2500	1.27	0.571	800	5	1393	
G	60'	S.S.	E	2500	1.27	0.571	800	2.5	2784	
H	30'	Cont.	C	1500	1.30	0.727	272	10	308	
I	100'	Cont.	A	2500	1.22	0.727	1512	24	671	
J	100'	Cont.	B	2500	1.22	0.727	1512	16	1006	
K	100'	Cont.	C	2500	1.22	0.727	1512	10	1609	
L	100'	Cont.	D	2500	1.22	0.571	1512	5	2528	
M	100'	Cont.	E	2500	1.22	0.571	1512	2.5	5056	
N	60'	Cont.	C	4000	1.27	0.727	799	10	885	

\*The given impact and D.F. values are assumed to be the mean values for the site.

Girder spacing is assumed to be 8 feet.

Table 11(b). Continued

(1)	(2)	(3)	(4)	(5)	(6)	(7)	(8)
Designation	$S_{XD}$	$W_{D'D}$	$g_D$	$i_D$	$S_{rD}$	$\gamma$	$\beta$
A	2262	1217	0.35	1.20	3.44	1.31	1.85
B	1860	947	0.36	1.10	4.02	1.71	2.90
C	424	408	0.40	1.10	7.15	1.38	2.10
D	637	408	0.40	1.10	5.58	1.61	2.65
E	1019	408	0.40	1.10	4.02	1.86	3.20
F	1602	408	0.40	1.10	3.17	2.31	3.90
G	3202	408	0.40	1.10	2.50	3.62	5.35
H	354	179	0.50	1.20	4.17	1.16	1.50
I	772	962	0.36	1.20	7.15	1.16	1.50
J	1157	962	0.36	1.20	5.58	1.35	2.00
K	1850	962	0.36	1.20	4.02	1.57	2.80
L	2907	962	0.36	1.20	3.17	1.93	3.45
M	5814	962	0.36	1.20	2.50	3.04	4.80
N	1018	444	0.30	1.10	3.44	2.61	4.10

Table 12. Comparison of  $\beta$ 's in proposed methods and AASHTO methods.

Designation	Span	Detail Category	$\beta$		$\beta$	
			Redundant Members		Nonredundant Members	
			AASHTO -	Proposed -	AASHTO -	Proposed -
(1)	(2)	(3)	(4)	(5)	(6)	(7)
A	120'S.S	C	1.05	1.99	1.85	2.93
B	100'S.S	C	2.00	2.02	2.90	2.96
C	60'S.S	A	2.05	2.03	2.10	2.85
D	60'S.S	B	2.15	1.97	2.65	2.92
E	60'S.S	C	2.20	2.01	3.20	2.93
F	60'S.S	D	2.75	1.97	3.90	2.91
G	60'S.S	E	3.10	1.85	5.35	2.87
H	30'S.S	C	0.70	2.16	1.50	3.09
I	100'CONT	A	1.45	2.06	1.50	2.89
J	100'CONT	B	1.60	2.01	2.00	2.98
K	100'CONT	C	1.65	2.05	2.80	2.99
L	100'CONT	D	2.05	2.01	3.45	2.97
M	100'CONT	E	2.40	1.90	4.80	2.96
N	60'CONT	C	3.55	2.17	4.10	3.10

given for each alternative procedure, which lowers the reliability factor, but still provides the same safety index (probability that an actual life will be below the predicted life). The various alternatives and the associated partial safety factors are discussed in the following paragraphs.

**Measured Stresses ( $F_{S1}$ ).** This alternative allows the Engineer to use a stress histogram obtained through field measurements at critical sections. Because of the lesser uncertainty associated with measurements compared to nominal calculated values, a

lower coefficient of variation of 3 percent is used for  $W$ ,  $I$ ,  $G$ , and  $Z_x$ . The  $cov$  are not reduced to zero by the field measurements since uncertainties result from (1) measurement scatter, (2) differences in truck weights over different time periods and seasons (assuming a test is completed in a few days), (3) changes in impact with possible surface roughness changes, etc. These 3 percent  $cov$  are much smaller than the corresponding values of 10 percent, 11 percent, 13 percent, and 10 percent for  $W$ ,  $I$ ,  $G$ , and  $Z_x$  used earlier. The mean value of  $M$  is taken as 1.0



and the *cov* of  $M$  was reduced to 1 percent (from 3 percent) since the effects of different vehicle dimensions are included in the stress measurements. These changes were incorporated in the input data for the reliability program. Output from the reliability program indicated that a safety factor of 1.14 (against 1.35 earlier) was required to reach a beta of 2.0 with the reduced *cov* mentioned above. Referring to Eq. 60, it can be seen that the partial safety factor is the ratio of the reliability factor (used to multiply the nominal stress range) to the basic reliability factor. Therefore,  $F_{s1} = 1.14/1.35 = 0.85$ .

**Site Truck Weight Data ( $F_{s2}$ ).** The alternatives in this section deal with the gross weight of the fatigue truck. The first alternative permits the Engineer to modify the gross weight based on judgment and local site conditions. The "judgment" here implies the use of best estimate for the vehicle gross weight. The fatigue prediction model already assumed that the best estimate of effective gross weight is used. Therefore, there is no change in the safety factor. However, the Engineer could still benefit from this alternative if the local conditions suggest an effective gross weight less than 54 kip. Conversely, if the local condition suggests a higher effective gross weight, this weight should be used. The effective gross weight should be calculated from a gross weight histogram by

$$W_{eq} = (\sum f_i W_i^3)^{1/3} \quad (61)$$

where  $W_{eq}$  = effective gross weight of fatigue truck;  $f_i$  = fraction of gross weights within an interval  $i$ ; and  $W_i$  = gross weight at midwidth of interval  $i$ .

The histogram of truck traffic should exclude panel, pickup, and other 2-axle/4-wheel trucks. This same definition of truck is to be used for truck volume. As explained in Chapter Two it is important that the definition of truck used for calculating effective gross weight should be consistent with the definition of truck used for estimating truck volume.

The second alternative permits the Engineer to use weigh station measurements. Because this type of measurement is detectable to the truck drivers, heavy weight trucks generally tend to evade the measuring stations. Therefore, the estimated effective gross weight (from Eq. 59) tends to be biased and hence  $\bar{W}$  is taken as 1.05. However, there is less uncertainty in effective gross weight and, therefore, a lower *cov* of 3 percent is used. With this change in input data, the reliability program found that a safety factor of 1.34 is required for a beta of 2.0. Hence, the partial safety factor for this alternative procedure is  $1.34/1.35 \approx 1.0$ . The decrease in uncertainty, *cov*, was offset by the unconservative bias in the measurement. As a net result, there is no significant change in the safety index and, hence, the same safety factor is required to attain the target safety index.

A third alternative allows the Engineer to obtain gross weight histograms through a planning department's weigh-in-motion measurements. As this type of measurement is undetectable to the truck drivers, the results are unbiased. Hence,  $\bar{W}$  is taken as 1.0 and a *cov* of 3 percent is used to signify lower uncertainty. With this change in input to the reliability program, the output indicated that a safety factor of 1.28 is required for a beta of 2.0. Hence, the partial safety factor for this alternative procedure is  $1.28/1.35$ , or 0.95.

**Improved Lateral Distribution Factors ( $F_{s3}$ ).** This partial safety factor relates to estimation of the lateral distribution factor. The first alternative permits the evaluator to use either

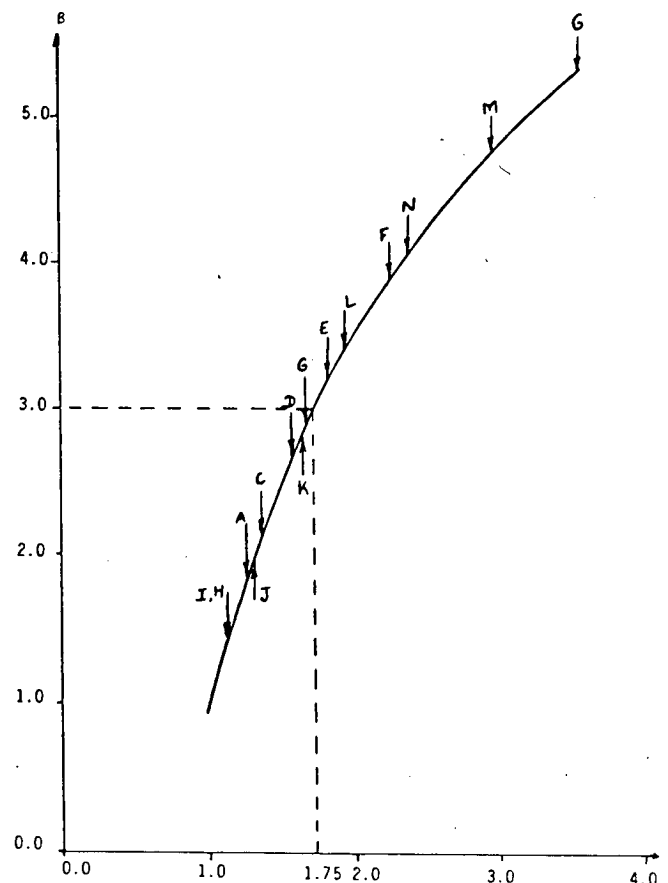


Figure 19.  $\beta$ 's in present design for nonredundant members.

the procedure proposed by Bakht (Appendix C) or the procedure proposed by Schilling (Appendix C). The basic procedure is the equation proposed in Chapter Two based on a conservative estimate for these two methods. Both of the methods give a more accurate estimate of lateral distribution factor, which is usually lower than that given by the basic procedure. Any benefit in lower uncertainty with these methods is offset, however, by removing the conservative bias deliberately put into the factors from the basic procedure. Hence, the same safety factors are recommended for this alternative.

A second alternative permits the use of rigorous methods, such as finite element methods, to calculate the lateral distribution factor. The factor is calculated from the moment range carried by each beam, girder, or stringer when a single fatigue truck is moved along the center of the outer traffic lane that results in the highest moment in the member under consideration. When rigorous methods are used to compute the moment range carried by the girder, the uncertainty in the distribution factor is lower and, therefore, a *cov* of 7 percent is used (as against 13 percent used earlier). The modified data were input to the reliability program. The output indicated that a safety factor of 1.30 is required for a beta of 2.0. Thus, the partial safety factor for this alternative is  $1.30/1.35$ , or 0.96.

## SAFETY FACTORS FOR DESIGN PROCEDURE

The target safety indices for the evaluation procedure were fixed at 2.0 and 3.0 for redundant and nonredundant members, respectively. These safety indices correspond to a probability of failure of 2.3 percent and 0.1 percent respectively. As explained earlier, failure here means a lower fatigue life and not collapse of the bridge. Moreover, in the evaluation of existing bridges the Engineer is usually concerned with short periods of life, say, the next 10 to 30 years. In the design of new bridges the Engineer is usually concerned with longer periods, typically in the range of 75 to 100 years. Hence, the fatigue design of new bridges inherently involves a large amount of uncertainty, especially with respect to future traffic conditions. Fortunately, however, predictions of the life of the bridges can be updated in the future to reflect changes in these traffic conditions. Therefore, it would not be reasonable to use an unduly high safety index that could add significantly to the cost of the bridge.

In the proposed design procedures, therefore, a lower target safety index of 1.0 is used for redundant members. For non-redundant members the same target safety index of 3.0 is used. The target index of 1.0 for redundant members corresponds to a probability of about 15 percent that the actual life will be less than the design life. This is acceptable because the bridge can be evaluated in the future using the site-specific data to ensure a desired safe life for the bridge. It should be noted that the recommended design truck volumes tabulated in the design procedure have built-in growth factors not presently included in AASHTO truck volumes.

In evaluation, the Engineer may have a better knowledge of the present traffic conditions than he has in design. Hence, higher *cov* are used to model the design conditions. A *cov* of 30 percent is used for *ADTT* and a *cov* of 15 percent is used for *W*. In addition, a bias of 5 percent is assumed in *W* ( $W = 1.05$ ) to reflect the growth in effective truck weights over the life span of the bridge. The reliability program with the above changes in the data base gave reliability factors of 1.10 and 2.00 for redundant and nonredundant members, respectively, which are recommended in the proposed design procedure. These reliability factors correspond to target safety indices of 1.0 and 3.0, respectively.

## FATIGUE LIMIT

It is generally accepted that a constant amplitude fatigue limit exists for typical bridge details. If all cycles in a variable amplitude spectrum are below this constant amplitude fatigue limit, the fatigue life for that spectrum would be infinite.

In an NCHRP study on variable amplitude loading Fisher (Ref. 119, p. 25) concluded that "if any of the stress cycles in a stress spectrum exceeded the constant amplitude fatigue limit, the fatigue life could be predicted by the cumulative damage laws assuming all cycles contributed to the damage." ECCS specifications (Ref. 172, p. 16) recommend "if any nominal stress range in the design spectrum exceeds the constant amplitude fatigue limit, the nominal stress ranges below the constant amplitude fatigue limit should also be considered in the fatigue assessment." A recent study on variable amplitude loading at the University of Texas, Austin (Ref. 251, pp. 207, 208) concluded that "all cycles in the complex spectrum are damaging, including those below the threshold stress intensity."

More research is still required to determine if a fatigue limit exists for a variable amplitude stress spectrum when only several stress cycles exceed the constant amplitude fatigue limit. Long life fatigue tests being conducted at Lehigh, TRRL, Maryland, and elsewhere may help resolve this issue.

It should be noted, however, that even if a variable amplitude fatigue limit exists for any stress spectrum, it may not significantly affect the reliability factors developed herein. This is because the reliability factors recommended in the proposed evaluation and design procedures are calibrated to existing design practices and the average reliability levels implied in these practices. To illustrate this point a fatigue limit coinciding with the constant amplitude fatigue limit was assumed to exist even for a variable amplitude loading. Therefore, only those stress cycles falling above the constant amplitude fatigue limit were assumed to contribute to damage. This approach represents an extreme assumption regarding fatigue damage since most theories recognize some damage accumulation on variable amplitude loading from stress cycles below the fatigue limit.

The reliability program was modified to exclude all the stress cycles below the constant amplitude fatigue limit while computing the fatigue damage. The assumed fatigue limits for each fatigue category are given in Table 13. Five different cases (with different spans and fatigue categories) were chosen and designed as per AASHTO specifications. The betas implicit in these 5 cases were obtained from the modified reliability program. The same 5 cases were designed again, using the proposed specifications for a life of 75 years. An average lifetime ADTT of 2,500 trucks and a girder spacing of 8 ft were assumed in each design. Betas for the sections obtained by the proposed method were evaluated using the modified reliability program. The sections obtained by AASHTO design and the proposed design methods were then used to evaluate the beta, in each case, using a linear SN model without a fatigue limit (original reliability program).

The results are summarized in Table 14. Columns 3 and 5 of Table 14 show the betas for sections designed according to the AASHTO specifications without and with fatigue limits, respectively. Columns 4 and 6 of Table 14 show the betas for sections designed according to the proposed design method without and with fatigue limits respectively. The average betas from the proposed method and the AASHTO design methods for the model without fatigue limit were matched perfectly for the five different cases. It can be seen that even after the model has been changed (a fatigue limit is introduced), the average betas from the proposed method and the AASHTO method are still almost the same. Therefore, it can be deduced that calibration to present design practice makes the assumptions in the fatigue model less important. Another point to note here is that the betas for the proposed design for the model without fatigue limit are more uniform (range from 1.87 to 2.02) than the corresponding betas for the AASHTO design (range from 1.58 to 2.36). This is the goal of the reliability approach. The betas for the AASHTO design for the model with fatigue limit are more uniform than the corresponding betas for the proposed methods. This is because the different fatigue categories are assumed to have fatigue limits at a different number of cycles. This has not been taken into account in the calibration of the target safety index. However, more uniform betas can be obtained for the model with fatigue limit by introducing a partial safety factor for each fatigue detail category. These partial safety factors can be so obtained as to provide uniform betas for all fatigue cat-

egories and can be derived for a given set of SN curves with given fatigue limits.

The need to determine the evidence of a variable amplitude fatigue limit still exists because it will lead to a more accurate fatigue model and may, in the future, allow one to reduce the target betas below historical values. For the present, a linear SN model is used to model the fatigue life. However, in those cases where the probability is small that only a few cycles over the lifetime will exceed the fatigue limit, a provision is given which provides for an infinite life check. This will, at most, affect only Categories A, B and C. The probability analysis to control the likelihood of exceeding the fatigue limit stress is given in the next section.

### INFINITE LIFE SAFETY MARGIN

As explained in Chapter Two, there is a need to establish a fatigue limit, so that any section subjected to a maximum stress range less than this fatigue limit does not need a fatigue check (consistent with current AASHTO practice). A typical SN curve with a fatigue limit,  $S_L$ , is shown in Figure 2 of Chapter Two.

If  $S_r$  is the nominal effective stress range (best estimate) obtained in the evaluation or design method, the maximum stress range,  $S_{max}$ , can be obtained as:

$$S_{max} = X S_r \quad (62)$$

where  $X$  is the ratio of the maximum stress range to effective stress range.

A reliability failure function can be written to estimate the probability of  $S_{max}$  exceeding the fatigue limit,  $S_L$ . This fatigue limit is also taken as a random variable.

From Eqs. 21 and 62,

$$Z = S_L - S_{max} = S_L - X S_r \quad (63)$$

From Eq. 26, the log normal reliability format gives the safety index,  $\beta$ , as

$$\beta = \frac{\text{Ln} [\bar{S}_L / (\bar{X} S_r)]}{\sqrt{V_{S_L}^2 + V_X^2 + V_{S_r}^2}} \quad (64)$$

where the bar denotes the mean, and  $V$  is the coefficient of variation. Because there are only two variables, the log normal format is exact.

The data for the fatigue limit for each category used in the proposed method corresponds to permissible stresses used for the "over 2 million cycles" case in the AASHTO method for redundant members. It is assumed that these values have the same bias and  $cov$  (random properties) as the stress range design values used in evaluation or design. Hence, the code value for "over 2 million cycles" corresponds to 95 percent probability level for the random variable  $S_L$ . From Table 8 it can be seen that bias and  $cov$  vary depending on the detail category.

The average bias is obtained as 1.27 from Table 8. It should be noted that category E has a bias of only 1.17, but it will be shown in Chapter Five, with some examples, that the fatigue limit never governs for Categories E and E'. If the design fatigue limit (95<sup>th</sup> percentile value) is denoted as  $S_{FD}$ , the mean is  $\bar{S}_L = 1.27 S_{FD}$ . Similarly, the average  $cov$  from Table 8 gives:  $V_{S_L} = 14.5$  percent.

Table 13. Assumed fatigue limits.

Detail Category	Mean $S_r$ at $2 \times 10^6$ cycles (ksi)	Nominal $S_r$ at $2 \times 10^6$ cycles (ksi)	cov	Fatigue Limit Stress Range	
				Mean (ksi)	Nominal (95% (ksi)
A	33.0	23.2	21.7%	34.1	24.0
B	22.8	18.1	14.1%	20.2	16.0
B'	18.0	14.5	13.2%	14.9	12.0
C	16.7	13.0	15.3%	12.8	10.0
D	13.0	10.3	14.2%	8.8	7.0
E	9.5	8.1	9.7%	5.3	4.5
E'	7.2	5.8	13.2%	3.2	2.6

The values cited here are consistent with SN curves proposed by Fisher (26)

Table 14.  $\beta$ 's with fatigue limit.

S.S. Span	Fatigue Category	$\beta$		$\beta$	
		Linear SN Model Without Fatigue Limit	Linear SN Model With Fatigue Limit	Linear SN Model Without Fatigue Limit	Linear SN Model With Fatigue Limit
(1)	(2)	AASHTO (3)	Proposed (4)	AASHTO (5)	Proposed (6)
60	C	1.78	2.00	4.89	5.22
90	C	1.58	2.02	4.68	5.33
60	D	2.15	1.99	5.16	4.91
90	D	1.96	2.01	4.94	5.02
60	E	2.36	1.87	5.19	4.39
Average		1.97	1.98	4.97	4.97

Assumptions: Safe Life = 75 years

Average ADIT = 2500 trucks/day

Girder Spacing = 8'

Redundant Structure

Taking the data in Table E-1 for the ratio of maximum measured stress to effective stress, one can obtain the data for  $X$ . Using these data,  $\bar{X} = 2.67$ , and  $V_X = \sigma_X / \bar{X} = 0.41 / 2.67 = 0.15$ .

From the previous section, the data for effective stress range can be estimated. Since  $S_r$  is a product of several random variables,

$$V_{S_r} = \sqrt{V_G^2 + V_I^2 + V_W^2 + V_{Z_x}^2 + V_M^2 + V_H^2}$$

where  $V_G$ ,  $V_I$ ,  $V_W$ ,  $V_{Z_x}$ ,  $V_M$ , and  $V_H$  are the coefficients of variation of the random variables  $G$ ,  $I$ ,  $W$ ,  $Z_x$ ,  $M$ , and  $H$ , respectively.

$$V_S = \sqrt{(0.13)^2 + (0.11)^2 + (0.1)^2 + (0.1)^2 + (0.03)^2 + (0.006)^2} = 22.3 \text{ percent}$$

Substituting in Eq. 64

Table 15. Sensitivity of calibration to database.

S.S Span (1)	Detail Category (2)	8			
		Data Base 1		Data Base 2	
		AASHTO (3)	Proposed (4)	AASHTO (5)	Proposed (6)
60	C	1.78	2.01	1.91	2.15
90	C	1.58	2.02	1.72	2.16
60	D	2.15	1.99	2.30	2.13
90	D	1.96	2.01	2.10	2.15
60	E	2.36	1.87	2.50	2.01
Average		1.97	1.98	2.11	2.12

Notes:

Data Base 1 was used for target beta calibration.

Data Base 2 was the same as Data Base 1 except that the COV for G was changed from 13% to 5%.

$$\beta = \frac{\ln [(1.27 S_{FD}) / (2.67 S_r)]}{\sqrt{(0.145)^2 + (0.15)^2 + (0.223)^2}}$$

$$\beta = \frac{\ln [0.476 (\overline{S_{FD}} / S_r)]}{0.305} \quad (65)$$

Using Eq. 65, for  $\beta = 1$ ,  $S_{FD}/S_r = 2.85$ ; for  $\beta = 2$ ,  $S_{FD}/S_r = 3.87$ ; and for  $\beta = 3$ ,  $S_{FD}/S_r = 5.24$ .

This would mean that if a beta of 2.0 is required, an infinite life would be obtained if the expected effective stress is less than  $S_{FD}/3.87$ , where  $S_{FD}$  is the present "over 2 million" AASHTO value. However, there is a safety factor already incorporated in our procedure to account for effective stress range variability. Therefore, this reduces the margin needed for infinite life as follows:

$$\text{Evaluation-Redundant: } \frac{S_{FD}}{R_s S_r} = \frac{3.87}{1.35} = 2.87$$

$$\text{Evaluation-Nonredundant: } \frac{S_{FD}}{R_s S_r} = \frac{5.24}{1.75} = 2.99$$

$$\text{Design-Redundant: } \frac{S_{FD}}{R_s S_r} = \frac{2.85}{1.10} = 2.60$$

$$\text{Design-Nonredundant: } \frac{S_{FD}}{R_s S_r} = \frac{5.24}{2.00} = 2.62$$

The infinite life fatigue margin ranges from 2.60 to 2.99. Given the limited data base for such variable amplitude fatigue life estimation, a single value is selected for all four cases. This value is the average and equals 2.75. The value of 2.75 may be justified in several other ways.

For example, in Table E-1 the maximum observed stress range is typically 2.5 to 3.0 times the effective stress range.

It is also seen that the check for infinite life based on the reliability procedure compares closely with values derived from calibrating to existing AASHTO procedures. It is shown in Chapter Five, following a discussion of examples that the average ratio of AASHTO design stresses for "over 2,500 ADTT" to the proposed unfactored design stress is about 3.0. (This can

Table 16. Sensitivity of random variables.

Random Variable (Y)	Mean Y	cov of Y Y*	10% Increase in Mean Value of Y		20% Increase in cov of Y	
			(R = 2.0)	Y*	R	Y*
X	1.0	0.15	.936	2.15	1.03	1.99
S	1.297	0.153	1.08	2.39	1.16	1.89
M	0.97	0.03	.98	1.68	1.08	2.0
G	1.0	0.13	1.12	1.69	1.21	1.95
I	1.0	0.11	1.09	1.69	1.18	1.98
H	1.03	0.006	1.03	1.69	1.13	2.0
P	1.0	0.005	1.0	1.92	1.11	2.0
ADTT	2500	0.10	2550	1.92	2800	2.0
Z <sub>x</sub>	1.0	0.10	0.92	2.38	1.00	1.97
W	1.0	0.10	1.07	1.69	1.16	1.99

be seen in Table 25 (a) by taking the ratio of columns 11 and 9, which are the respective AASHTO and proposed design stresses.) Dividing by the safety factor of 1.1 gives a corresponding ratio needed to produce infinite life of 3.0/1.1, or 2.73 which is close to 2.75.

Similarly, a ratio of 3.0 corresponds closely to the ratio of maximum truck weight (about 155 kip) and the effective maximum truck weight (54 kip) as obtained in the FHWA weight spectrum. Thus, if the assumption is made that fatigue is governed by individual truck occurrences, the expected maximum truck weight will be approximately 3 times the effective truck weight.

In summary, the various approaches lead to similar values for a fatigue limit for variable amplitude loading. Recall the assumption that few cycles may be permitted that exceed this stress level without initiating a crack growth. This assumption still needs to be validated by test programs now underway. It is, however, implicitly accepted in the present AASHTO fatigue design rules.

## SENSITIVITY STUDIES

In most reliability studies, sufficient data on each variable are not available and some "reasonable" assumptions must be made. The assumptions do not significantly affect the reliability factors when the target beta is chosen by the calibration procedures as the average  $\beta$  implicit in the current practice. This reasoning can be illustrated with the assumptions in values of means and cov of the random variables used in the reliability program. Five design cases as given in Table 15 are chosen. Initially, the data base assumed for target beta calibration is used to find the betas in the sections designed by the AASHTO and the proposed methods. These betas are shown in columns 3 and 4, respectively, of Table 15. As expected, the average  $\beta$ 's from the AASHTO method and the proposed method are equal and close to 2.0. A change is now introduced in the data base. The cov of the random variable G (girder distribution ratio) is changed to 5 percent from 13 percent. The betas for the same sections are now evaluated using the new data base. These betas are shown in columns 4 and 5 for the AASHTO designed sections and the sections designed by the proposed methods. It

can be seen that the average betas for each method obtained from the modified data base are the same. Therefore, it can be inferred that assumptions in data base are less important, when the target beta is made equal to the average of betas implicit in the current design practice.

To provide insight into the data needs, Table 16 shows the impact of changes in each parameter (mean value and *cov*) on

the  $\beta$  value.  $Y^*$  denotes the most likely failure point. As *cov* increases, there is greater uncertainty about the value of the random variable. Therefore  $Y^*$  moves farther away from the mean and, hence, the safety index decreases. Increase in mean value decreases  $\beta$  if it is a load term and increases  $\beta$  if it is a resistance term. From Table 16 it can be seen that data for  $G$ ,  $S$ ,  $I$ , and  $W$  are most sensitive in their influence on  $\beta$ .

## CHAPTER FIVE

# EXAMPLES

This chapter gives examples to illustrate the application of the proposed fatigue evaluation and design procedures and to compare these procedures with existing AASHTO methods. For some of these examples, plots are given to show how the safe life varies with the desired level of safety (safety index,  $\beta$ ). These plots also show how the probability of realizing less than the safe life varies with the safe life. An important fact to note in all the examples is that the stresses described are well below current fatigue design stresses. However, they are consistent with reported measured values.

## EVALUATION

### Example E.1

This example utilizes an H20-type bridge on a 60 ft simply supported span. Redundant structure, spacing of girders = 8 ft; noncomposite construction Girder-W36  $\times$  160,  $S_x = 542$  in.<sup>3</sup>

**Fatigue Truck.** Vehicle in Appendix A, Figure 6.2.2A is used; therefore,  $F_{S2} = 1.0$ .

**Impact.** The inspection report stated that the road surface is in "good condition." The gross weight of the truck is therefore only increased by 10 percent to 59.4 kip to allow for impact.

**Moment Range.** Maximum moment range caused by the fatigue truck on a 60-ft simple span is 5,796 kip-in. (for a gross weight of 59.4 kip).

**Lateral Distribution.** See Article 6.2.6 in Appendix A for recommended values.  $DF = S/D = 8/20.0 = 0.40$  ( $D = 20.0$  for 60-ft span);  $F_{S3} = 1.0$ .

**Section Modulus.** The section is being evaluated as a non-composite section.  $S_x = 1.30 \times 542 = 705$  in.<sup>3</sup> (no visual indication of slab separation).

**Nominal Stress Range.**  $S_r = (\text{Moment range} \times DF) / (\text{Section modulus})$

$$= (5,796 \times 0.40) / 705 = 3.28 \text{ ksi.}$$

**Reliability Factor.**  $R_{S0} = 1.35$  (redundant),  $F_{S1} = 1.0$  (no measurements),  $F_{S2} = 1.0$  (standard fatigue truck is used), and  $F_{S3} = 1.0$  (the basic procedure is used for estimating girder

distribution);  $R_S = (1.35)(1.0)(1.0)(1.0) = 1.35$ .

**Check for Infinite Life.**  $S_{FL} = 4.4$  ksi (Category C—Stiffener). Factored stress:  $1.35 \times 3.28 = 4.43$  ksi  $> 4.4$  ksi. Therefore, the section has finite life. In this instance the section almost satisfies infinite life. This may be achieved by a more rigorous analysis for  $DF$  as will be done in Example E.2.

**Truck Traffic.** For the finite life check, the lifetime average daily truck volume in the outer lane is estimated to be 2,500 trucks per day.

**Cycles Per Truck Passage.**  $C = 1$  (span above 40 ft).

**Fatigue Life Calculation.**  $K = 12$  (Category C); present age,  $a = 50$  years. Substituting in equation given in Art. 6.3.2 in Appendix A the remaining safe life is:  $Y_f = (12 \times 10^6) / [2,500(1.0)((1.35)(3.28))^3] - 50 = 6$  years.

**Remaining Mean Life Calculation.**  $Y_m = [(2)(12 \times 10^6)] / [2,500(1.0)(3.28)^3] - 50 = 222$  years.

The total safe fatigue life for the bridge and traffic conditions in Example E.1 is 56 years (the present age of 50 years plus the remaining safe life of 6 years). "Safe" as used here implies a safety index of 2.0 (redundant member) and a corresponding probability of 2.3 percent that the actual fatigue life will be shorter than 56 years. The safe lives corresponding to other levels of safety (safety indexes) are plotted in Figure 20. The probability that the actual life will be less than the safe life is also given in this plot. (The safety index and probability scales are related by the data in statistical normal distribution tables.)

As shown in the figure, the safe life for a safety index of 3.0, which is used for nonredundant members, is only 20 years and the corresponding probability that the actual life will be less than this safe life is only 0.001 percent. On the other hand, safety indexes less than 2.0 correspond to longer safe lives and higher probabilities that the actual lives will exceed these safe lives. For example, there is a 9 percent probability that the actual life will exceed a safe life of 100 years. The expected mean life corresponds to a safety index of 0 and a probability of 50 percent that the actual life will be less than the expected mean life. For this example, the mean life is 272 years—far greater than the safe life of 56 years corresponding to a safety index of 2.0.

Example E.1 uses the basic procedure to evaluate the re-

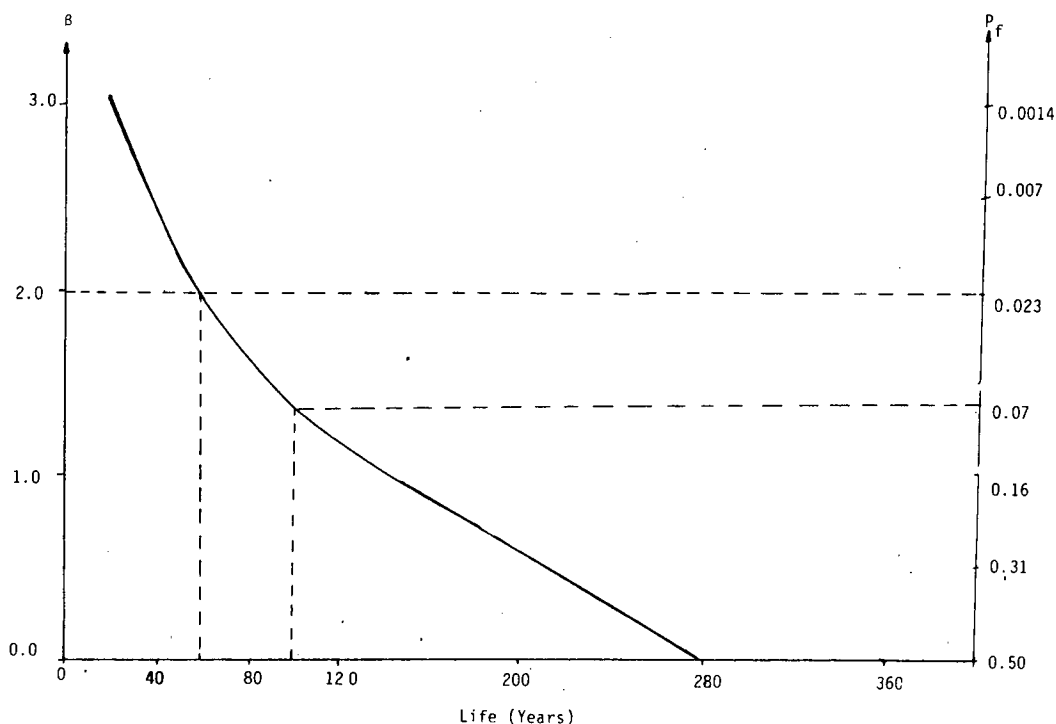


Figure 20. Life vs. probability of failure for Example E.1.

maintaining safe life of the member. As explained in previous chapters, the evaluation procedure includes a number of alternatives, which may be used to obtain a more accurate and usually higher estimate of the remaining life for the same section. To illustrate the use of alternative methods, two examples are shown below. Example E.2 uses an alternative method to obtain a better estimate of the lateral distribution factor; and Example E.3 uses an alternative method to calculate safe remaining life using past and future periods of truck traffic and truck volume.

### Example E.2

**Fatigue Truck.** The same fatigue truck as in Example E.1 is used.

**Moment Range.** Maximum moment range = 5,796 kip-in.

**Lateral Distribution.** Alternative I of Art. 6.2.6 in Appendix A is used. The original curves given by Bakht (Figures C1-C6) are used to estimate lateral distribution. Relevant details of the bridge are as follows: span = 60 ft; number of design lanes = 2; design lane width = 12 ft; vehicle edge distance = 10 ft (refer to Chapter Two for definition of vehicle edge distance); spacing of girders = 8 ft;  $\mu = (12 - 11)/2 = 0.5$  (Eq. C-8).

Assuming that the critical girder is an interior girder,  $D = 7.75$  (Figure C-2);  $C_f = 3.50$  (Figure C-3); and  $C_e = 40$  (Figure C-5). Equation C-7 gives:

$$DF = \frac{50 S}{D(100 + \mu C_f + C_e)}$$

$$= \frac{50 (8.0)}{7.75 (100 + 0.5 \times 3.5 + 40)}$$

$$= 0.36 \text{ (compares with 0.40 given in Example E.1)}$$

$$F_{S3} = 1.0 \text{ (see guidelines in Appendix A)}$$

**Section Modulus.** The section modulus is being evaluated as a noncomposite section.  $S_x = 1.30 \times 542 = 705 \text{ in.}^3$  (no visual indications of slab separation).

**Nominal Stress Range.**  $S_r = (\text{Moment range} \times DF) / (\text{Section modulus}) = (5,796 \times 0.36) / 705 = 2.96 \text{ ksi}$ .

**Reliability Factor.**  $F_{S0} = 1.35$  (redundant member),  $F_{S1} = 1.0$  (no measurements),  $F_{S2} = 1.0$  (standard fatigue truck), and  $F_{S3} = 1.0$  (Alternative I for estimating girder distribution);  $R_s = 1.35(1.0)(1.0)(1.0) = 1.35$ .

**Check for Infinite Life.**  $S_{FL} = 4.4 \text{ ksi}$  (Category C—Stiffener). Factored stress =  $1.35 \times 2.96 = 4.0 \text{ ksi} < 4.4 \text{ ksi}$ . Therefore, the section has infinite life and no further fatigue check is required.

### Example E.3

The same nominal fatigue truck as in Examples E.1 and E.2 is used. The same impact and distribution factors of E.2 are used. Hence, the same nominal stress range and reliability factors as in Example E.2 are obtained here. However, the detail category is assumed as category C (but not a stiffener). Therefore,  $S_{FL}$  will be 3.6 ksi and the section will have finite life.

**Nominal Stress Range.**  $S_r = 2.96 \text{ ksi}$  (see Example E.2).

*Reliability Factor.*  $R_s = 1.35$  (see Example E.2).

*Check for Infinite Life.*  $S_{FL} = 3.6$  ksi. Factored stress =  $1.35 \times 2.96 = 4.0$  ksi  $> 3.6$  ksi. Therefore, the section has finite life.

*Truck Traffic.* The fatigue life of the bridge is divided into two periods in which truck volume and equivalent fatigue truck weight remain constant: (a) a past period from opening of the bridge to the present (average truck volume in shoulder lane = 2,000/day and equivalent truck weight = 50 kip—reflects lower weights and volume in past); (b) a future period from the present to the end of fatigue life (average truck volume in shoulder lane = 2,500/day and equivalent truck weight = 60 kip—assumes growth in future truck weights and volume).

*Cycles Per Truck Passage.*  $C = 1.0$  (above 40-ft span).

*Safe Fatigue Life Calculation.*

$$K = 12 \text{ (Category C)}$$

$$Y_1 = \frac{12 \times 10^6}{2,000(1.0) [1.35 \times 2.96 \times (50/54)]^3}$$

$$= 120 \text{ years}$$

$$Y_p = 50 \text{ years (present age)}$$

$$Y_N = \frac{12 \times 10^6}{2,500(1.0) [1.35 \times 2.96 \times (60/54)]^3}$$

$$= 56 \text{ years}$$

$$Y_f = 56 [1 - (50/120)]$$

$$= 33 \text{ years (Expected Safe Future Life).}$$

*Remaining Mean Life.*  $Y_m = (2 \times 12 \times 10^6)/(2,500(2.96)^3) - 50 = 370$  years.

Example E.1 gave a remaining safe life of 6 years, while Example E.2 using a rigorous  $DF$  value gave an infinite fatigue life. Hence, there was substantial gain in using the alternative method. The remaining safe life increased to 33 years when another additional alternative method was used in Example E.3.

The proposed evaluation procedure was used to estimate the remaining safe life of two bridges which had recently been inspected. Example E.4 shows the estimations of safe remaining life of a stringer bridge in Connecticut. (The present calculations were done by A.G. Lichtenstein, Consulting Engineers, using this project's proposed fatigue evaluation guidelines and are reproduced here.)

#### Example E.4

This example uses a stringer rolled beam with cover plate; W36 $\times$ 150 w/10 in.  $\times$  9/16 in. cover plate; span = 57 ft 9 in.; girder spacing = 7.5 ft.

*Fatigue Truck.* Vehicle in Figure 6.2.2A (Appendix A) is used;  $F_{S2} = 1.0$ .

*Impact.* The Engineer decided that the road surface is "smooth." The gross weight of the fatigue truck is therefore increased by 10 percent to 59.4 kip to allow for impact.

*Moment Range.* The detail at cover plate cut-off point is being evaluated here. The maximum moment range at this detail due to the fatigue truck is calculated to be 279.4 kip-ft as per Art. 6.2.5. (for a gross weight of 59.4 kip).

*Lateral Distribution.* The basic procedure is used:  $DF = S/D = 7.5/20 = 0.375$  ( $D = 20.0$  for 57 ft 9 in. span from Art. 6.2.6);  $F_{S3} = 1.0$  (as per Art. 6.2.6).

*Section Modulus.* There are shear connectors between slab and beam. Hence, composite section modulus (as per AASHTO specifications) is calculated at the detail under consideration and increased by 15 percent as per Art. 6.2.7.1.  $S_x = 677 \times 1.15 = 779$  in.<sup>3</sup>

*Nominal Stress Range.*  $S_r = (\text{Moment range} \times DF)/(\text{Section modulus}) = (279.4(12) \times 0.375)/(779) = 1.61$  ksi.

*Reliability Factor.*  $R_{S0} = 1.35$  (redundant),  $F_{S1} = 1.0$  (no measurements),  $F_{S2} = 1.0$  (standard fatigue truck), and  $F_{S3} = 1.0$  (basic method for  $DF$ );  $R_S = (1.35)(1.0)(1.0)(1.0) = 1.35$ .

*Check for Infinite Life.*  $S_{FL} = 0.9$  ksi (Category E'). Factored stress:  $1.35 \times 1.61 = 2.17 < 0.9$  ksi; therefore, the section has finite life.

*Truck Traffic.* An ADTT of 685 trucks per day on the bridge was given. The number of trucks per day in the shoulder lane is obtained by multiplying the total ADTT on the bridge by a factor  $F_L$  (see Art. 6.3.5.1). Note that in Examples E.1 to E.3, the truck volume in the shoulder lane was directly estimated by the engineer. Therefore, the factor  $F_L$  has not been applied.  $F_L$  is equal to 0.85 for two-lane one-way traffic. The present truck traffic in shoulder lane,  $T$ , is  $0.85(685) = 582$  trucks per day. A growth rate of 4 percent was determined by the engineer. Using Figure 6.3.5A, for a  $g$  of 4 percent and a present age of 28 years,  $T_a/T$  is obtained as 1.25. Therefore  $T_a = 582(1.25) = 730$  trucks per day.

*Cycles Per Truck Passage.*  $C = 1.0$  (Art. 6.3.4 of Appendix A).

*Safe Fatigue Life Calculation.* The detail category was decided as category E' by the engineer.  $K = 1.1$  (Art. 6.3.3 of Appendix A). Present age,  $a = 28$  years. Substituting in equation given in Art. 6.3.2, the remaining safe life is  $Y_f = (1.1 \times 10^6)/(730(1.0)(1.35 \times 1.61)^3) - 28 = 119$  years.

*Mean Life Calculation.*  $Y_m = (2 \times 1.1 \times 10^6)/(730(1.0)(1.61)^3) - 28 = 694$  years.

The 147 years for total safe life ( $119 + 28$ ) compares to 367 years computed using the Connecticut rating specifications. Their procedure is somewhat similar to the procedure herein except that site truck classification is used as well as the AASHTO distribution and impact factors. The Connecticut rules also do not indicate whether the computed life is a mean expected life or a reliable safe life. It also does not have the options outlined in the proposed guidelines herein. Tables 17(a) through 17(c) show three proposed worksheets which summarize the evaluation procedure contained herein. The first sheet is called the Data sheet (Table 17a). This sheet contains the data regarding bridge geometry, the traffic conditions, and the element detail where the fatigue evaluation is to be done. The second sheet is called the Analysis sheet (Table 17b). In this sheet all of the required analysis parameters are calculated and entered in the appropriate places. The third sheet is called the Calculation sheet (Table 17c) and is used to calculate the remaining mean and safe life for the detail under consideration. These sheets lead the Engineer through the evaluation procedure in a systematic manner. Tables 18(a) through 18(c) demonstrate the use of the worksheets for Example E.4.

Example E.5 shows the remaining life calculations for a plate girder bridge. (These calculations were also done by A.G. Lichtenstein consulting engineers and are reproduced here.)

Table 17(a). Fatigue evaluation example—data sheet.

BRIDGE:		FILE:	DATE:
BRIDGE GEOMETRY		COMMENTS	
SPANS			
GIRDER SPACING			
REDUNDANCY			
DECK TYPE	POSITIVE OR NEGATIVE W/CONNECTORS W/O CONNECTORS SEPARATION YES NO		
CONDITION OF ROAD SURFACE			
TRAFFIC		COMMENTS	
ADTT			
GROWTH RATE (if available)			
UNUSUAL TRAFFIC CONDITIONS IF ANY			
TRAFFIC TYPE			
ELEMENT		COMMENTS	
ELEMENT SECTION			
CRITICAL DETAIL LOCATION			
SECTION SIZE			
ADDITIONAL REMARKS:			

Table 17(c). Calculation sheet.

BRIDGE:		FILE:	DATE:
REMAINING LIFE CALCULATION		COMMENTS	
SAFE NO. OF CYCLES			
SAFE LIFE OF MEMBER/ MEAN LIFE			
PRESENT AGE			
SAFE REMAINING LIFE			
COMMENTS			

Table 17(b). Analysis sheet.

BRIDGE:		FILE:	DATE:
ANALYSIS		PARAMETERS	REFERENCE
FATIGUE TRUCK			
TRUCK SUPERPOSITIONS			
IMPACT FACTOR			
LATERAL DISTRIBUTION			
MOMENT RANGE ON MEMBER			
SECTION MODULUS			
NOMINAL STRESS RANGE			
RELIABILITY FACTOR	$R_{s0}$ $F_{s1}$ $F_{s2}$ $F_{s3}$ $R_s$		
FACTORED STRESS RANGE			
FATIGUE CATEGORY/ FATIGUE LIMIT			INFINITE LIFE FINITE LIFE
CYCLES PER TRUCK PASSAGE			
LIFETIME AVG. TRUCK VOLUME IN OUTER LANE			
COMMENTS			



Table 18(a). Fatigue evaluation Example E.4—data sheet.

BRIDGE: Steel stringer bridge FILE: in Connecticut		DATE:
BRIDGE GEOMETRY		COMMENTS
SPANS	S. S. - 57' 9"	
GIRDER SPACING	75'	
REDUNDANCY	Redundant Member	$R_{50} = 1.35$
DECK TYPE	POSITIVE X OR NEGATIVE W/CONNECTORS <u>X</u> W/O CONNECTORS SEPARATION YES NO	Increase section modulus by 15%
CONDITION OF ROAD SURFACE	Smooth Surface	$I = 1-1$
TRAFFIC		COMMENTS
ADTT	685	Total ADTT on bridge
GROWTH RATE (if available)	4%	
UNUSUAL TRAFFIC CONDITIONS IF ANY	-	
TRAFFIC TYPE	2 lanes - 1 way traffic	
ELEMENT		COMMENTS
ELEMENT SECTION	Rolled Beam	
CRITICAL DETAIL LOCATION	@ 8'10 1/2" from left support	Cover plate cut off category E'
SECTION SIZE	w36 x 150 w/10" x 9/16" Cov PL	
ADDITIONAL REMARKS:		

Table 18(c). Calculation sheet.

BRIDGE: Steel stringer bridge FILE: in Connecticut		DATE:
REMAINING LIFE CALCULATION		COMMENTS
SAFE NO. OF CYCLES	$4.5 \times 10^7$ cycles	Fig. 6.3.2A
SAFE LIFE OF MEMBER/ MEAN LIFE	147 years / 722 years	REF 6.3.2
PRESENT AGE	28 years	
SAFE REMAINING LIFE	119 years	
COMMENTS  Conn DOT - Estimate 367 years Total Safe life prediction herein is <u>147</u> years		

Table 18(b). Analysis sheet.

BRIDGE: Steel stringer bridge FILE in Connecticut		DATE:
ANALYSIS	PARAMETERS	REFERENCE
FATIGUE TRUCK	Fig. 6.2.2 A	Standard fatigue truck
TRUCK SUPERPOSITIONS	-	No unusual site conditions
IMPACT FACTOR	1.10	Smooth road surface Ref. 6.2.4
LATERAL DISTRIBUTION	0.375	Ref. 6.2.6
MOMENT RANGE ON MEMBER	105 kft	
SECTION MODULUS	$1.15 \times 677 = 779 \text{ in}^3$	Composite section with shear connectors
NOMINAL STRESS RANGE	1.61 ksi	
RELIABILITY FACTOR	(redundant) $R_{50} F_{s1} F_{s2} F_{s3} = R_s$ $1.35 \ 10 \ 10 \ 10 = 1.35$	Ref. 6.2.8
FACTORED STRESS RANGE	2.17 ksi	
FATIGUE CATEGORY/ FATIGUE LIMIT	E'/0.9 ksi	INFINITE LIFE FINITE LIFE <u>X</u>
CYCLES PER TRUCK PASSAGE	1.0	Ref. 6.3.4
LIFETIME AVG. TRUCK VOLUME IN OUTER LANE	730	Ref 6.3.5
COMMENTS		

**Example E.5**

Given in this example are plate girder bridge; 6-span continuous bridge, each span = 184.3 ft; critical detail in the second span at 134 ft from left pier, where stiffeners are welded to bottom flange and web of the girder.

*Fatigue Truck.* Vehicle in Figure 6.2.2A is used;  $F_{S2} = 1.0$ .

*Impact.* The Engineer decided that the road surface is "smooth." The gross weight of the fatigue truck is therefore increased by 10 percent to 59.4 kip to allow for impact.

*Moment Range.* The maximum moment range at the critical detail is 2,588 kip-ft as per Art. 6.2.5 (for a  $GW$  of 59.4 kip).

*Lateral Distribution.* There are two longitudinal plate girders supporting the entire deck; therefore, simple beam distributions are used to estimate  $DF$ . The truck is placed such that the centerline of the truck coincides with the centerline of outermost lane. Spacing of girders was 23 ft. The distance from the centerline of the truck to the critical girder was 5.5 ft. Therefore,  $DF = (23 - 5.5)/(23) = 0.761$ .

*Section Modulus.* There are no shear connectors between slab and beam. Hence, steel section alone is used to compute a nominal section modulus. Section modulus using steel section alone was found to be 4,590 in.<sup>3</sup> for the detail under consideration. There was no visual separation of deck and girder. Hence, we take  $S_x = 1.30 \times 4,590 = 5,967$  in.<sup>3</sup>

*Nominal Stress Range.*  $S_r = (\text{Moment range} \times DF) / (\text{Section Modulus}) = [2,588.3 (12) (0.761)] / (5,967) = 3.96$  ksi.

*Reliability Factor.* The member is taken as a nonredundant member because only two girders support the entire deck. Thus:  $R_{S0} = 1.75$  (nonredundant),  $F_{S1} = 1.0$  (no measurements),  $F_{S2} = 1.0$  (standard fatigue truck),  $F_{S3} = 1.0$  (basic method for  $DF$ ), and  $R_s = (1.75)(1.0)(1.0)(1.0) = 1.75$ .

*Check for Infinite Life.*  $S_{FL} = 1.6$  ksi (Category E); factored stress:  $1.75 \times 3.96 = 6.9$  ksi  $> 1.6$  ksi. Therefore, the section has finite life.

*Truck Traffic.* An ADTT of 2,600 trucks per day on the bridge was given. The number of trucks in the shoulder lane is obtained by multiplying the total ADTT on the bridge with a factor  $F_L$  (Art. 6.3.5.1). For two-lane one-way traffic,  $F_L$  is 0.85. Therefore, the present truck traffic in the shoulder lane,  $T$ , is  $0.85 (2,600) = 2,210$  trucks per day. A growth rate of 2 percent was selected by the Engineer. Using Figure 6.3.5.2A, for a  $g$  of 2 percent and a present age of 14 years,  $T_a/T$  is obtained as 1.15. Therefore,  $T_a = 2,210 (1.15) = 2,550$  trucks per day.

*Cycles per Truck Passage.*  $C = 1.0$  (Art. 6.3.4 of Appendix A).

*Safe Fatigue Life Calculation.* The detail category for the section was decided as E by the Engineer.  $K = 2.9$  (Art 6.3.3 of Appendix A). Present age,  $a = 14$  years. Substituting in equation given in Art. 6.3.2, the remaining safe life is  $Y_f = (2.9 \times 10^6) / [2,550 (1.0) (1.75 \times 3.96)^3] - 14 = -10.5$  years.

*Remaining Mean Fatigue Life Calculations.*  $Y_m = (2 \times 2.9 \times 10^6) / (2,550 (1.0)(3.96)^3) - 14 = 23$  years.

The negative safe remaining life here indicates that the safe life of the member is exhausted. Similar conclusions were drawn for the same member when the Connecticut DOT procedures were used to evaluate the fatigue life of the bridge. However, it should be noted that "safe life" in the proposed procedure corresponds to a beta of 3.0 (for nonredundant members) or a probability of a failure of 0.1 percent. Figure 21 shows the plot between the safe life of the member and safety index (and probability that the actual life will be less than the safe life).

The plot shows a probability of only 8.4 percent that the actual life will be less than the present age of 14 years. The plot also shows a mean life ( $P_f = 0.50$ ) of 37 years for the member.

The evaluator can now use Art. 6.4 to either: (a) institute frequent inspections (6.4.5); (b) restrict traffic (6.4.3); (c) recalculate life with better estimates of  $DF$ ,  $ADTT$ , gross weight of fatigue truck, etc. (6.4.2); and (d) repair (6.4.4).

In this instance the owner selected to repair some details and in other cases to field measure stresses. For the above detail, measurements were reported to produce a "maximum stress range below 5 ksi" (exact values including the effective stress are not available to us). From Table E-1 of Appendix E, we may deduce that the effective stress is usually 20 to 60 percent of the maximum stress range. Hence, the effective stress range in this case is likely to be below 2.5 ksi. This compares with the calculated nominal (before the safety factor is applied) effective stress range of 3.96 ksi. Several reasons may exist for differences between measured and the computed effective nominal stresses contained herein. (1) The truck traffic weight at the site may differ from the prescribed 54-kip equivalent weight. (2) The range of extreme heavy trucks at the site may be less than at other sites. Appendix E demonstrates there is a large scatter reported between the maximum and the effective stress range. This scatter is between 1.5 and 5, which would indicate that this site falls in the lower band of the scatter. (3) The section modulus may differ from our nominal bias reflecting typical average conditions. Parapets, curbs, walls, deck steel have all been known to contribute to the true section property. (4) The end condition for the bridge may not correspond to a simply supported case as assumed. Thus, end restraint may dramatically reduce stress levels.

In this instance the Engineer found significant benefits in terms of increased safe life estimation by using accurate field measurements.

The data, calculations, and conclusions of Example E.5 are summarized into the worksheets and are shown in Tables 19(a) through 19(c).

It should be noted that one project consultant believed that the detail in Example E.5 more correctly belongs in detail Category C and not Category E as determined by the Engineer. Example E.6 shows the calculations for the same detail assuming a detail Category C.

**Example E.6**

*Check for Infinite Life.* Factored stress range = 6.9 ksi (see Example E.5).  $S_{FL} = 4.4$  ksi (Category C Stiffener). The section has finite life since  $6.9$  ksi  $> 4.4$  ksi.

*Safe Fatigue life Calculations.*  $K = 12$  (Art 6.3.3 of Appendix A for Category C);  $T_a = 2,250$  trucks per day (see example E.5);  $C = 1.0$  (Art 6.3.4 of Appendix A); and  $a = 14$  years (present age).

Substituting in equation given in Art 6.3.2, the remaining safe life is  $Y_f = (12 \times 10^6) / (2,250 (1.0)(6.9)^3) - 14 = 0$  years.

*Remaining Mean Fatigue Life Calculation.*  $Y_m = (2 \times 12 \times 10^6) / (2,250 (1.0)(6.9)^3) - 14 = 138$  years.

This indicates that the safe life of the structure is just over. This estimate of safe life is also quite low, whereas the mean life calculation shows that there is a remaining mean life of 138 years. The large remaining mean life indicates why no fatigue cracks were observed. However, the safe life calculation is es-

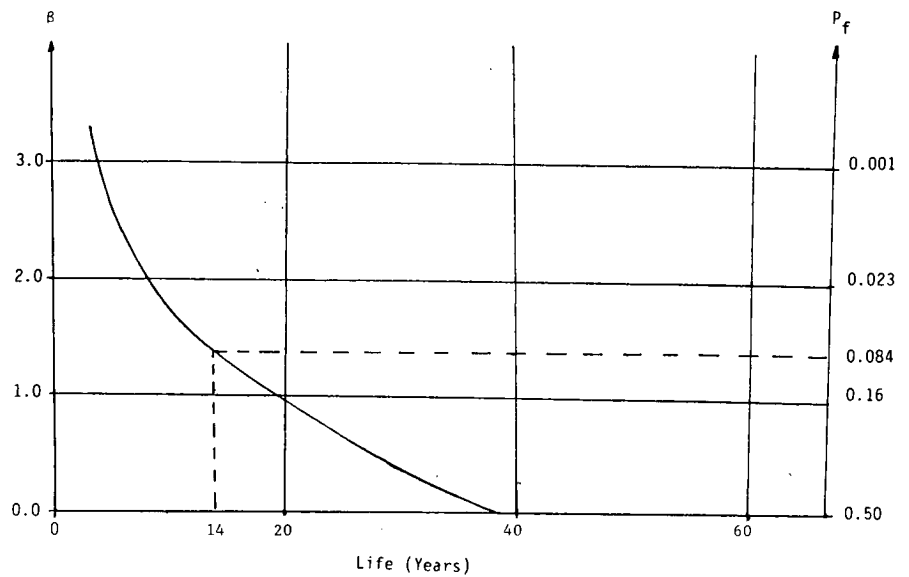


Figure 21. Life vs. probability of failure for Example E.5.

Table 19(a). Fatigue evaluation Example E.5—data sheet.

BRIDGE: Moshannon East Bound		FILE:	DATE:
BRIDGE GEOMETRY		COMMENTS	
SPANS	2 Span continuous - 184+3'/184+3'		
GIRDER SPACING	23'		
REDUNDANCY	Nonredundant		$R_{50} = 1.75$
DECK TYPE	POSITIVE X OR NEGATIVE _____ W/CONNECTORS _____ W/O CONNECTORS <u>X</u> SEPARATION YES _____ NO <u>X</u>		The section should be increased by 30%
CONDITION OF ROAD SURFACE	Smooth surface		$I = 110$
TRAFFIC		COMMENTS	
ADTT	2600		Total ADTT on bridge
GROWTH RATE (if available)	2 %		
UNUSUAL TRAFFIC CONDITIONS IF ANY	-		
TRAFFIC TYPE	2 lanes - 1 way traffic		
ELEMENT		COMMENTS	
ELEMENT SECTION	Plate girder		
CRITICAL DETAIL LOCATION	@ 134' from left support		Stiffeners welded to bottom flange and web *
SECTION SIZE	$I_x = 289198 \text{ in}^4$		Mof inertia is given at the section
ADDITIONAL REMARKS:			
* Category E determined by consultant			

Table 19(b). Analysis sheet.

BRIDGE: Moshannon East Bound		FILE	DATE:
ANALYSIS		PARAMETERS	REFERENCE
FATIGUE TRUCK	Fig. 6.2.2A	Standard fatigue truck	
TRUCK SUPERPOSITIONS	-	No unusual site conditions	
IMPACT FACTOR	1.10	Smooth road surface Ref. 6.2.4	
LATERAL DISTRIBUTION	0.761	Ref. 6.2.6	
MOMENT RANGE ON MEMBER	1970 kft		
SECTION MODULUS	1.30 x 4590 = 5967	Steel section alone; no visual separation of deck & girder	
NOMINAL STRESS RANGE	3.96 ksi		
RELIABILITY FACTOR	(nonredundant) $R_{s0} F_{s1} F_{s2} F_{s3} = R_s$ 175 10 10 10 = 175	Ref. 6.2.8	
FACTORED STRESS RANGE	6.9 ksi	(=1.75 x 3.96)	
FATIGUE CATEGORY/ FATIGUE LIMIT	E / 1.6 ksi	INFINITE LIFE FINITE LIFE <u>X</u>	
CYCLES PER TRUCK PASSAGE	1.0	Ref. 6.3.4	
LIFETIME AVG. TRUCK VOLUME IN OUTER LANE	2550	Ref. 6.3.5	
COMMENTS			

pecially important in this example because the member is non-redundant and a fatigue crack could lead to bridge failure. To be satisfied that the fatigue life is consistent with AASHTO safety levels, the zero remaining safe life indicates that the Engineer must adopt one of the remedial options.

#### Other Examples

The evaluation procedure was used to evaluate a number of hypothetical bridges to show the effect of various analysis parameters on the calculation of safe life of the member. Table 20 shows the effect of impact factor on calculation of safe life. The bridge is designed for H-15 loading and has a simple span of 60 ft. The other assumptions regarding the bridge are given in Table 20. The safe life for this hypothetical bridge is estimated as 33 years for an impact factor of 1.10 (Example E.7) and 20 years for an impact factor of 1.30 (Example E.8). The impact factor of 1.10 corresponds to smooth road surfaces, while the impact factor of 1.30 is the maximum allowed impact factor for a rough road surface. An intermediate value of impact factor of 1.20 gave a safe life of 25 (Example E.9) years for the same bridge. Therefore, impact factor has a significant effect on the safe life of the member.

Table 21 shows the effect of fatigue detail category on the

safe life of the member. The hypothetical bridge for these examples is assumed to be designed for H-15 loading. The bridge is assumed to have two equal spans of 90 ft each. The other assumptions about the bridge and traffic conditions are given in Table 21. The safe life of the member varies from 2 years for Category E' details to infinity for Category A details. Therefore, the determination of the appropriate detail category is quite important.

In Examples E.10 to E.16 (Table 21), the section used to estimate the safe life of the bridge was the section at which the positive bending moment was maximum (point A on Figure 22). Example E.17 (Table 22) gives the safe life for a detail at point B for the same hypothetical bridge (Figure 22). Example E.17 is compared with Example E.13 (both assume Category C and same bridge geometry, traffic conditions etc.) in Table 22. The detail at point B (Figure 22) has infinite life, while the safe life for the detail at point A (Figure 22) is only 21 years. This is mainly because of the lower moment range at the interior support due to the fatigue truck.

Examples E.18 and E.19 (Table 22) show the effect of the gross weight of the equivalent fatigue truck on the safe life of the bridge. The bridge considered here is a 60-ft simply supported bridge designed for H-15 loading. There were no shear connectors and no visual separation of deck and girder was observed. Steel section alone yielded a section modulus of 409

Table 19(c). Calculation sheet.

BRIDGE: Moshannon East Bound		FILE:	DATE:
REMAINING LIFE CALCULATION		COMMENTS	
SAFE NO. OF CYCLES	$3.4 \times 10^6$ cycles	Fig. 6.3.2A	
SAFE LIFE OF MEMBER	30.5 years/ 37 years	Ref. 6.3.2	
PRESENT AGE	14 years		
SAFE REMAINING LIFE	-10 + 5 years	Ref. 6.3.2	
COMMENTS			
<p>Safe life of 4 years corresponds to a safety index of 3 for nonredundant members. Figure 22 shows a mean life (<math>P_f = 0.50</math>) of <u>37</u> years. For present age of <u>14</u> years, <math>P_f</math> (probability of failure) is only <u>8.4%</u>. The evaluator can now use section 6.4 to either:</p> <ol style="list-style-type: none"><li>(1) Institute frequent inspections (6.4.5)</li><li>(2) Restrict traffic (6.4.3)</li><li>(3) Recalculate life (6.4.3)</li><li>(4) Repair (6.4.4)</li></ol> <p>In this instance owner selected to repair some details and in other cases to field measure stresses. For the above detail, measurements produced a maximum stress below 5 ksi. The effective stress is usually half the maximum stress. This compares with calculated of <math>5.2 \times 0.75 = 3.9</math> ksi. Thus tests may show satisfactory life. (complete data not available for comparison and safe life estimation using test data).</p>			

Table 20. Effect of impact factor on safe life.

Example No.	Span	Impact Factor	Unfactored Effective Stress Range (ksi) $S_r$	Fatigue Limit (ksi) $S_{FL}$	Safe Life (years)	Mean Life (years)
	Length					
E.7	60'	1.10	4.63	3.6	33	162
E.8	60'	1.20	5.04	3.6	25	123
E.9	60'	1.30	5.46	3.6	20	98

## Assumptions -

- The lifetime average volume in shoulder lane is 1500 trucks/day
- Girder spacing = 8ft; D.F. =  $8/20 = 0.40$
- Detail Category is C
- There are no shear connectors and there is no visual separation of deck and girder.
- The section is designed for H-15 loading. Steel section alone gives  $S_x$  of 409 in<sup>3</sup>, at the midspan of the bridge, for which the safe life is predicted.

Table 21. Effect of fatigue detail category on safe life.

Example No.	Span(s) Length	Continuous Fatigue Category	Unfactored Effective Stress Range (ksi)	Fatigue (ksi) $S_{FL}$	Safe Life (years)	Mean Life (years)
H-15 Bridges						
E.10	90/90	A	5.37	8.8	Infinite	
E.11	90/90	B	5.37	5.9	54	266
E.12	90/90	B'	5.37	4.4	28	138
E.13	90/90	C	5.37	3.6	21	103
E.14	90/90	D	5.37	2.6	10	49
E.15	90/90	E	5.37	1.6	5	25
E.16	90/90	E'	5.37	0.9	2	10

## Assumptions:

- Average Lifetime volume in outerlane is 1500 trucks/day
- Smooth road surface; I = 1.10
- Girder spacing = 8'; D.F. =  $8/22 = 0.36$
- There are shear connectors between deck and girder. The section modulus is calculated according to AASHTO specifications and includes the deck. Composite Section modulus is 615 in<sup>3</sup>;  $S_x = 1.15 \times 615 = 707$  in<sup>3</sup>.
- Section is designed for H-15 loading; at 36 from left support (0.4L)

in<sup>3</sup> for the critical girder, which is increased by 30 percent as per Art. 6.2.7.1 of the evaluation procedure. In Example E.18, the proposed fatigue truck in Figure 6.2.2A (Appendix A) was used. To show the effect of gross weight, it was hypothetically

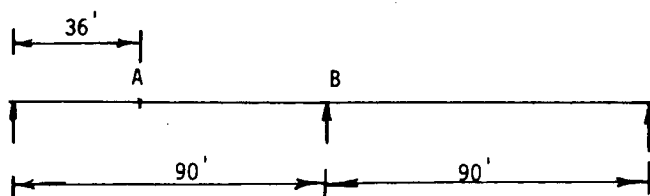


Figure 22. Bridge geometry and critical detail locations for Examples E.10 to E.17.

Table 22. Comparison of fatigue lives at midspan and support.

Example No.	Spans of Detail	Location of Detail	Calculated Composite $S_x$ (IN)	Moment Range (ksi)	Unfactored Effective Stress Range (ksi) $S_e$	Fatigue Limit (ksi)	Safe (years)	Mean Life (years)
E.13	90/90	At 36' from left support	615	833	5.37	3.6	21	103
E.17	90/90	over the center support	735	396	2.57	3.6	Infinite	

Assumptions:

- Lifetime average volume in shoulder lane is 1500 trucks/day
- Category C
- Smooth road surface;  $I = 1.10$
- Girder Spacing = 8'; D.F. =  $8/22 = 0.36$
- There are shear connectors between deck and girder. The calculated section modulus includes deck as per AASHTO specifications. This section modulus is increased by 15% for Example E.13. No such increase is made in example E.17 as the detail is in negative bending region.

Table 23. Effect of gross weight on safe life.

Example No.	Simple Span Length	Gross Weight of Fatigue Truck	Unfactored Effective Stress Range (ksi) $S_e$	Fatigue Limit (years)	Safe Life (years)	Mean Life (years)
E.18	60'	54 kips	4.62	3.6	33	162
E.19	60'	50 kips	4.28	3.6	42	207

Assumptions

- The average lifetime volume in outer lane is 1500 trucks/day
- Girder spacing = 8ft; D.F.  $8/20 = 0.40$
- Fatigue detail category is C
- Impact factor = 1.10

assumed that the actual traffic conditions suggested a lower effective truck weight of 50 kip. The safe life calculated for the same bridge with the lower effective gross weight is shown in Example E.19 in Table 23, as 42 years. This compares with the estimated safe life of 33 years for Example E.18 with the standard fatigue truck. Therefore, the gross weight of the fatigue truck has a significant effect on the safe life of the bridge.

Examples E.20 to E.22 in Table 24 show the effect of the estimated lifetime average ADTT in the outer lane of the bridge.

Table 24. Effect of ADTT on safe life.

Example No.	Simple Span Length	Estimated ADTT in outer lane (trucks/day)	Unfactored Effective Stress Range (ksi) $S_e$	Fatigue Limit (ksi) $S_{FL}$	Safe Life (years)	Mean Life (years)
E.20	60'	1000	4.62	3.6	50	246
E.21	60'	2000	4.62	3.6	25	123
E.22	60'	3000	4.62	3.6	16.5	81

Assumptions

- Girder Spacing = 8ft; D.F. =  $8/20 = 0.40$
- Impact factor = 1.10
- Fatigue Detail Category is C
- Standard fatigue truck from fig. 6.2.2A in Appendix A.

The bridge considered in these examples is a 60-ft simple span bridge designed for H-15 loading. The deck is a noncomposite deck. The steel section alone gave a section modulus of 409 in.<sup>3</sup> Because no visual separation of deck and girder was observed, the section modulus was increased by 30 percent as per Art. 6.2.7.1 of the proposed evaluation procedure. Examples E.20 to

E.22 show the calculated safe life for the same bridge, but with varying estimates of the ADTT in the shoulder lane of the bridge. Examples E.20 to E.22 are evaluated for lifetime average ADTT's of 1,000, 2,000, and 3,000 trucks per day, respectively, in the shoulder lane. These are hypothetically assumed to show the effect of the estimated lifetime average ADTT. Table 24 shows that the safe life for Examples E.20 to E.22 are 50 years, 25 years, and 16.5 years, respectively. It can be seen that the safe life decreases proportionally with increase in the estimated ADTT for the bridge. Therefore lifetime average ADTT is an important parameter and has a significant effect on the estimated safe life of the bridge.

### Example E.23

This example became available at the end of the project because the bridge described developed a fatigue crack across the entire tension flange. Because the bridge was nonredundant, it has been taken out of service.

The three-span bridge with spans 150 ft, 180 ft, and 150 ft is evaluated. A cover plate detail at 60 ft from the intermediate support in the middle span is being checked.

**Fatigue Truck.** The fatigue vehicle proposed in the evaluation procedure is used (see Figure 6.2.2A);  $F_{S2} = 1.0$ .

**Impact.** The Engineer decided that the road surface is "smooth." The gross weight of the fatigue truck is, therefore, increased by 10 percent to 59.4 kip to allow for impact.

**Moment Range.** The maximum moment range at the critical detail is 1,452 kip-ft as per Art. 6.2.5.

**Lateral Distribution.** There are two longitudinal plate girders supporting the entire deck so simple beam distribution is used to estimate  $DF$ . The truck is placed such that the centerline of the truck coincides with the centerline of outermost lane. The distance from the centerline of the truck in the outermost lane to the critical girder is 9.5 ft. Spacing of girders was 34 ft. Therefore,  $DF = (34 - 9.5)/(34) = 0.72$ .

**Section Modulus.** There are no shear connectors between the deck and the girder. The steel section alone is used in computing the section modulus. The steel section alone yielded a section modulus of 3,345 in.<sup>3</sup> for the detail. The bridge is no longer in service, so the Engineer felt that to be conservative there was a separation of deck and girder and therefore did not further increase the section modulus.

**Nominal Stress Range.**  $S_r = [1,452 (12) (0.72)]/(3,345) = 3.8$  ksi.

**Reliability Factor.** The member is taken as a nonredundant member because only two girders support the entire deck.  $R_{S0} = 1.75$  (nonredundant),  $F_{S1} = 1.0$  (no measurements),  $F_{S2} = 1.0$  (standard fatigue truck), and  $F_{S3} = 1.0$  (basic method for  $DF$ );  $R_S = (1.75)(1.0)(1.0)(1.0) = 1.75$ .

**Infinite Life Check.** The detail category was decided as E by the Engineer.  $S_{FL} = 1.6$  ksi. Factored stress:  $(1.75)(3.8) = 6.65$  ksi > 1.6 ksi; therefore, the section has finite life.

**Truck Traffic.** The traffic is estimated as 7,000 veh per day. The bridge is a two-lane, two-way traffic-type bridge. Therefore  $F_L$  is 0.60 from Art. 6.3.5.1.  $F_T$  is taken as 0.20 from Art. 6.3.5.1. The present truck volume is calculated as  $T_a = 7,000 (0.2)(0.6) = 840$  trucks per day. The Engineer decided not to use any growth rate for this site.

**Cycles Per Truck Passage.**  $C = 1.0$  (see Art. 6.3.4).

**Safe Fatigue Life Calculation.**  $K = 2.9$  (for Category E—

Art. 6.3.3). Present age  $a = 25$  years (estimate). Remaining safe life,  $Y_f = (2.9 \times 10^6)/(840(1.0)(1.75 \times 3.8)^3) - 25 = -13$  years.

**Mean Life Calculation.** Remaining mean life  $Y_m = (2 \times 2.9 \times 10^6)/(840(1.0)(3.8)^3) - 25 = 101$  years.

The foregoing calculations show that the detail has a total safe life of only 12 years ( $Y_f + a$ ) (corresponding to a probability of failure of 0.1 percent) and a total mean life of 126 years ( $Y_m + a$ ) corresponding to a probability of failure of 50 percent). Cracks were detected in the structure at the present age of about 25 years, which is in between the safe life and the mean life. It should be noted that there were many details of this nature in the bridge. Thus, even if each had a mean life of 126 years, the likely time to failure for any single attachment is less than the mean. The exact calculation of this "system" effect is complicated since the time to failure for each attachment is statistically correlated due to common load and load effect occurrences. Nevertheless, it is not unlikely that a bridge of this type with many similar details with mean lives of 126 years but safe lives of only 12 years would, in fact, have experienced a crack after only 25 years.

## DESIGN

Design examples consistent with the proposed design procedure are shown below.

### Example D1

A 100-ft simple span with two lanes and two-way traffic is illustrated. A "very heavy traffic" volume conditions is assumed for the bridge.

**Fatigue Truck.** The fatigue truck shown in Figure 10.3.2.1A is used. The gross weight is taken as 54 kip.

**Impact.** The gross weight is increased by 15 percent to account for impact.  $GW = 62.1$  kip (as per Art. 10.3.2.3).

**Moment.** The maximum moment range on the bridge due to the passage of fatigue truck is 1,111.6 kip-ft (for a  $GW$  of 62.1 kip).

**Lateral Distribution.**  $DF = S/D$ , where  $D = 22.33$  (from table interpolating for 100-ft span),  $S = 8$  ft (spacing of girders = 8 ft), and  $DF = 8/22.33 = 0.36$ . Moment range for the girder =  $1,111.6 \times 0.36 = 400.2$  kip-ft.

**Reliability Factor.**  $R_S = 1.10$  (assuming redundant structure).

**Permissible Stress Range.**  $T_d = 2,400$  trucks per day (Table 10.3.3.5A),  $C = 1.0$  (above 40-ft span),  $K = 12.0$  (assume Category C detail),  $S_{FL} = 3.64$  ksi (for Category C), and  $S_{rp} = [(12.0 \times 10^6)/(2,400(1.0)75)]^{1/3} = 4.08$  ksi > 3.64 ksi. Since the computed permissible stress (4.08 ksi) is above the fatigue limit stress, it governs the design.

**Nominal Stress Range.**  $R_S S_r \leq S_{rp}$ . Nominal effective stress,  $S_r \leq S_{rp}/R_S = 4.08/1.10 = 3.71$  ksi.

**Composite Section Modulus.**  $S_x = (\text{Moment range})/(\text{Nominal stress range} \times 1.15)$ . (A 15 percent increase in computed AASHTO Section Modulus is permitted for composite decks.) Therefore, the required section is  $S_x = (400.2(12))/(3.71(1.15)) = 1,126$  in.<sup>3</sup>

Comparisons of section modulus obtained by the proposed procedure and the current AASHTO method are shown in Table 25(a) and 25(b) for a number of hypothetical cases including

Table 25(a). Comparison of proposed design methods with AASHTO procedures.

Case No. (1)	AASHTO DESIGN PARAMETERS				PROPOSED METHOD PARAMETERS										
	G (2)	I (3)	M (4)	ALLOWABLE		G (7)	I (8)	C (9)	M (10)	R <sub>s</sub> (11)	ALLOWABLE				
				S <sub>FL</sub> (5)	S <sub>RP</sub> (6)						S <sub>FL</sub> (12)	VHT (13)	HT (14)	LT (15)	VLT (16)
D2	0.73/0.73			36	24						8.73	(6.44)	(6.79)	(8.0)	12.54
D3	0.73/0.73			27.5	18	0.36	1.15	1.0	967	1.10	5.82	(5.06)	(5.33)	6.29	9.85
D4	0.73/0.57			19	10						3.64	(3.61)	3.81	4.49	7.03
D5	0.73/0.57	1.22	1523	16	7						2.55	2.87	3.02	3.56	5.58
D6	0.73/0.57			12.5	5						1.64	2.25	2.37	2.80	4.38
D7	0.73/0.57			9.4	2.6						0.95	1.63	1.72	2.02	3.17
D8				36	24						8.73	(6.44)	(6.79)	(8.0)	12.54
D9	0.73/0.73			27.5	18						5.82	(5.06)	(5.33)	6.29	9.85
D10	0.73/0.57			19	10						3.64	(3.61)	3.81	4.49	7.03
D11	0.73/0.57	1.27	799	16	7	0.40	1.15	1.0	439	1.10	2.55	2.87	3.02	3.56	5.58
D12	0.73/0.57			12.5	5						1.64	2.25	2.32	2.80	4.38
D13	0.73/0.57			9.4	2.6						0.95	1.63	1.72	2.02	3.17
D14	0.73/0.73			36	24						8.73	(5.29)	(5.58)	(6.58)	10.31
D15	0.73/0.73			27.5	18						5.81	(4.16)	(4.38)	(5.17)	8.10
D16	0.73/0.57	1.30	282	19	10						3.64	(2.97)	(3.13)	3.69	5.78
D17	0.73/0.57			16	7	0.47	1.15	1.8	185	1.10	2.55	(2.36)	(2.48)	2.93	4.59
D18	0.73/0.57			12.5	5						1.66	1.85	1.95	2.30	3.60
D19	0.73/0.57			9.4	2.6						0.95	1.34	1.41	1.66	2.61

( ) - denotes cases where S<sub>FL</sub> governsIn proposed method, use larger of S<sub>FL</sub> or S<sub>RP</sub>

Table 25(b). Continued

Design Case (1)	Span (2)	Detail Category (3)	Sx as per AASHTO - IN <sup>3</sup>		Sx as per Proposals - IN <sup>3</sup>				Sx as per strength HS 20 & WSD (10)
			ADTT < 2500 (4)	ADTT > 2500 (5)	VHT (6)	HT (7)	LT (8)	VLT (9)	
D2		A	452	678	526	526	526	366	
D3		B	592	904	789	789	731	466	
D4		C	857	1271	1263	1206	1024	653	1905
D5	100'	D	1017	1816	1601	1521	1290	823	
D6		E	1302	2542	2042	1938	1641	1049	
D7		E'	1732	4888	2819	2671	2275	1649	
D8		A	247	370	266	266	266	185	
D9		B	323	494	398	398	368	235	
D10		C	468	694	636	608	516	330	
D11	60'	D	556	992	808	767	651	415	809
D12		E	711	1388	1030	999	828	529	
D13		E'	946	2670	1422	1347	1148	732	
D14		A	89	134	131	131	131	111	
D15		B	117	178	197	197	197	141	
D16	30'	C	169	251	316	316	311	198	
D17		D	201	358	450	450	392	250	226
D18		E	257	502	621	588	499	318	
D19		E'	342	964	847	814	692	440	

- Redundant Structure, composite deck

- Spacing of girders = 8ft.

- 2 lane - 1 way traffic

different spans, fatigue detail categories, and truck volume categories.

The design examples considered in these tables are numbered D2 through D19. Three different simple spans of 30 ft, 60 ft, and 100 ft are considered as indicated in Table 25(b). Table 25(a) summarizes the various design parameters used in the proposed procedure and the AASHTO method. Columns (2) to (6) of Table 25(a) give the values of AASHTO lateral distribution factor, AASHTO impact factor, maximum moment caused by an HS-20 truck, and the AASHTO permissible stresses for the two volume categories permitted by the AASHTO specifications. The first listed value of the lateral distribution factor applies when the first volume category is used, and the second listed factor applies when the second volume category is used. The value of 0.73 is based on  $S/5.5$ ;

the value of 0.57 is based on  $S/7$  and, as indicated in AASHTO Table 10.3.1A, applies only to the over 2 million cycle category. Columns (7) to (11) of Table 25(a) give the values of lateral distribution factor, impact factor, number of cycles per truck passage, maximum moment range caused by the proposed fatigue truck (54 kip), and reliability factor for the proposed procedure. Column (12) gives the fatigue limit for the detail category. Columns (13) to (16) of Table 25(a) give the permissible stresses for the four truck volume categories in the proposed procedure: Very Heavy Traffic, Heavy Traffic, Light Traffic, and Very Light Traffic. The *larger* of the values obtained from column (12) and columns (13) to (16) based on volume, shall be used in design.

Table 25(b) shows the section moduli required for the design cases D2 through D19 as per both the proposed and the



AASHTO methods. Columns (4) to (5) of Table 25(b) give the required section modulus for each AASHTO design case for the two volume categories. Column (5) corresponds to AASHTO "Case I", which is for an ADTT of 2,500 or more in one direction, while column (4) corresponds to "Case II", which is for an ADTT of less than 2,500 in one direction. Columns (6) to (9) of Table 25(b) give the required section moduli for each case designed by the proposed procedures. Columns (6) to (9) correspond to the four truck volume categories in the proposed procedure, namely the Very Heavy Traffic (VHT), Heavy Traffic (HT), Light Traffic (LT), and Very Light Traffic (VLT), respectively. Column (10) of Table 25(b) shows the required section modulus for strength static (nonfatigue) design by the AASHTO specifications (using HS-20 and working stress design method).

Table 25(b) shows that for the 100-ft span, fatigue governs only for Categories E and E'. For these two detail categories, the section moduli required for the highest AASHTO volume category are well above those required for the highest volume category in the proposed procedure. For the 60-ft span, fatigue governs only for Categories D, E, and E'. Again, the section moduli required for the highest AASHTO volume category were well above those required for the highest volume category in the proposed procedure.

For the 30-ft span, fatigue governs for Categories C to E' in both the proposed method and the AASHTO method. The required section is higher for the proposed method for detail categories C, D, and E. There are two main reasons for this. First, the proposed method accounts for the fact that the passage

of a truck across a very short bridge causes two independent cycles (corresponding to the main axles); the present AASHTO method does not account for these independent cycles. Second, the proposed procedure requires an increase in lateral distribution as the span decreases; the present AASHTO method does not. For example, in the proposed procedure the lateral distribution factor for a given girder spacing is about 35 percent greater for a 30-ft span than for a 120-ft span. This is consistent with extensive analytical studies as discussed in Chapter Two and Appendix E. Thus, the larger effect of fatigue at very short spans is real, and the requirements of the proposed procedures are appropriate. Inasmuch as not many steel bridges with very short spans are being built, however, these requirements should not cause many problems.

### Standard Bridge Designs

Tables 26(a) and 26(b) show comparisons of the proposed design procedure with the AASHTO design method for standard bridge designs taken from "Composite Steel Plate Girder Bridge Superstructures" (USS), "Highway Structures Design Handbook" Vol. II (USS), "Short Span Steel Bridges" (USS), and "Standard Plans for Highway Bridges, Vol. II" (FHWA), which are denoted in Table 26 as R1, R2, R3, and R4 respectively. Table 26(a) gives the design parameters including bridge type, spans, steel yield stress, static design method, girder spacing, and the critical detail location being investigated, for design cases D20 through D31.

Table 26(a). Comparison using standard design sections.

Case No. (1)	Ref/Page (2)	Bridge Type (3)	Spans (4)	Steel Yield Stress (5)	Static Design Procedure (6)	Girder Spacing (7)	Critical detail locations (8)	Proposed Fatigue Design Stress (9)	AASHTO Stress		Ratio of (11)/(9)
									ADTT<2500 (10)	ADTT>2500 (11)	
D20	R2/II4.69	CPG	80	36	HS20/WSD	8.33	Midspan	2.42	7.03	5.52	2.28
D21	R4/302	CPG	100	50	HS20/WSD	8.00	Midspan	2.37	9.42	7.40	3.12
D22	R4/302	CPG	180	50	HS20/WSD	8.00	Midspan	1.67	5.89	4.63	2.77
D23	R1/III3	CPG	80/80	36	HS20/LFD	9.25	0.4L/SUP	4.7/1.47	18.63/4.71	14.04/3.70	2.98/2.52
D24	R1/III30	CPG	80/80	50	HS20/LFD	9.25	0.4L/SUP	4.43/1.84	17.56/5.87	13.8/4.61	3.12/2.51
D25	R1/III11	CPG	120/120	36	HS20/LFD	9.25	0.4L/SUP	4.24/1.10	16.16/3.37	12.7/2.65	3.0/2.41
D26	R3/70	CRB	50	36	HS20/LFD	9.25	Midspan	3.10	13.17	13.17	4.25
D27	R3/70	CRB	50	50	HS20/LFD	9.25	Midspan	4.19	17.8	17.8	4.25
D28	R3/70	CRB	80	36	HS20/LFD	9.25	Midspan	2.73	11.3	11.3	4.14
D29	R3/70	CRB	80	50	HS20/LFD	9.25	Midspan	3.83	15.8	15.8	4.13
D30	R3/93	CRB	50/50	36	HS20/LFD	9.25	Cover Pt.	4.37	16.7	13.1	3.00
D31	R1II3.27	CRB	70/70	36	HS20/WSD	8.33	Cover Pt.	2.04	7.1	5.58	2.74

#### Notes:

CPG = continuous plate girder  
 CRB = continuous rolled beam  
 WSD = working stress design  
 LFD = load factor design

#### References:

- R1 = "Composite Steel Plate Girder Bridge Superstructures-Load Factor Design", United States Steel Corporation, Pittsburgh, PA, 1982.
- R2 = "Short span Steel Bridges-Load Factor Design," United States Corporation, Pittsburgh, PA, 1978.
- R3 = "Highway Structures Design Handbook, Volume II, "United States Steel Corporation, Pittsburgh, PA, 1985.
- R4 = "Standard Plans for Highway Bridges-Volume II," Federal Highway Administration, Washington, D.C., 1968.

Table 26(b). Continued

Case (1)	Detail Category (2)	Cycles Per truck (3)	Permissible Stress Range						
			AASHTO		$S_{FL}/R_s$ (6)	Proposed Method		Srp/Rs [4-lane 2-way traffic]	
			ADTT < 2500 (4)	ADTT > 2500 (5)		VHT (7)	HT (8)	LT (9)	VLT (10)
D20	C	1.0	19.0	10.0	3.30	3.22	3.40	4.00	6.26
D21	C	1.0	19.0	10.0	3.30	3.22	3.40	4.00	6.26
D22	C	1.0	19.0	10.0	3.30	3.22	3.40	4.00	6.26
D23	C	1.0/1.0	19.0/19.0	10.0/10.0	3.30	3.22/3.22	3.40/3.40	4.00/4.0	6.26/6.26
D24	C	1.0/1.0	19.0/19.0	10.0/10.0	3.30	3.22/3.22	3.40/3.40	4.00/4.00	6.26/6.26
D25	C	1.0/1.10	19.0/10.0	10.0/10.0	3.30	3.22/3.12	3.40/3.29	4.00/3.87	6.26/6.07
D26	B	1.0	27.5	18.0	5.29	4.51	4.76	5.60	8.77
D27	B	1.0	27.5	18.0	5.29	4.51	4.76	5.60	8.77
D28	B	1.0	27.5	18.0	5.29	4.51	4.76	5.60	8.77
D29	B	1.0	27.5	18.0	5.29	4.51	4.76	5.60	8.77
D30	E	1.0	12.5	5.0	1.65	2.00	2.11	2.50	3.90
D31	E	1.0	12.5	5.0	1.65	2.00	2.11	2.50	3.90

AASHTO DESIGN ACCEPTABLE for fatigue if columns 10 or 11 from table 5.10a is below Column 4 or 5, respectively

PROPOSED DESIGN ACCEPTABLE for fatigue if column 9 in Table 5.10a is below either column 6 or column 7-10 based on traffic

Column (9) gives the design stress range calculated by the proposed procedure and columns (10) and (11) give the design stress range calculated by present AASHTO methods for the two different volume categories. The calculated stress ranges can be different for these two volume categories because a lateral distribution of  $S/7$  is used for "Case I" (if over 2 million cycle category governs) and a factor of  $S/5.5$  is used for "Case II".

Table 26(b) shows the permissible stresses for the above design cases (D20 through D31) by the AASHTO method and the proposed procedure. The permissible stress depends on the truck volume on the bridge and the fatigue limit. Columns (5) and (4) give the permissible stresses according to the AASHTO method for the "Case I" and "Case II" volume categories. The design stresses from columns (10) and (11) of Table 26(a) must be less than the permissible stresses from columns (4) and (5) of Table 26(b), respectively, according to the AASHTO design method. The proposed procedure requires a check given by

$$R_s S_r < S \text{ (if } S_{rp} > S_{FL}); R_s S_r < S_{FL} \text{ (if } S_{FL} > S_{rp}) \quad (66)$$

or

$$S_r < S_{rp}/R_s \text{ (if } S_{rp} > S_{FL}); < S_{FL}/R_s \text{ (if } S_{FL} > S_{rp}) \quad (67)$$

$S_r$  is given in column (9) of Table 26(a) as explained before.  $S_{FL}/R_s$  is given in column (6).  $S_{rp}/R_s$  is given in columns (7) to (10) of Table 26(b) for the four different truck volume categories in the proposed procedure. The traffic is assumed to be four-lane two-way traffic for all the design cases. Therefore,  $S_r$  from column (9) of Table 26(a) must be less than either the fatigue limit  $S_{FL}/R_s$  value or the permissible  $S_{rp}/R_s$  values from columns (7) to (10) of Table 26(b) in a fatigue check.

The design stress ranges calculated by the proposed procedure are much lower than those calculated by present AASHTO methods, but are within the range normally measured in actual bridges. Specifically, these stress ranges varied from 1.1 to 4.7 ksi. Thus, the proposed procedures reflect the actual stress conditions in bridges as intended.

A comparison between the calculated design stress ranges from Table 26(a) and the permissible stress ranges from Table 26(b) shows that fatigue governs in the same five design cases according to either the proposed procedure or the present

AASHTO method: D23, D24, D25, D30, D31. The first three cases were two-span continuous plate girder bridges. A Category C stiffener was checked at the 0.4 point and at the interior support; fatigue did not govern at the support by either method. At the 0.4 point, fatigue governed for the "Case I" AASHTO volume category and for the VHT, HT, and LT volume categories in the proposed procedure. Fatigue did not govern for the Lighter Traffic categories by either method.

The last two cases were continuous span rolled beam bridges and a Category E cover plate end was checked in both cases. For Case D30, fatigue governed for all volume categories in both methods. For Case D31, fatigue governed for "Case I" by the AASHTO method and for the VHT volume category in the proposed procedure.

For cases governed by fatigue, the proposed design method permits much more flexibility in adjusting the design and provides methods of assessing the effects of various options the Engineer can pursue. For example, the Engineer could obtain better information on the expected truck volume and growth rate at the site, or he could accept a shorter design life. The equations given in the proposed procedure permit him to calculate the effects of different volumes, growth rates, and design lives on the permissible stress range.

## SUMMARY

The conclusions from the evaluation and design examples are summarized here. The evaluation and design examples show that the proposed methods are easy to use and utilize stress calculation procedures similar to that of AASHTO procedures.

Examples E.1 to E.3 demonstrate the flexibility incorporated into the evaluation procedures to use site-specific data regarding traffic volumes and bridge dimensions. Using such site-specific data, the proposed methods give a better (usually longer) estimate of the safe remaining life. The mean remaining life is also provided, so the engineer can appreciate the range of fatigue life safety margin intended by AASHTO safety factors. Examples E.4 to E.6 and E.23 demonstrate how the methods have been used for actual bridges. The methods yielded reasonable estimates of safe remaining life and compared well with the predictions made using CONN-DOT rating specifications. It should, however, be noted that the CONN-DOT procedures are

not calibrated to yield consistent reliability in the range of application. Examples E.7 to E.22 illustrate the effect of impact factor, fatigue detail category, gross weight, critical detail location, and truck volume on the estimated safe remaining life. These factors were found to significantly influence the estimated safe remaining life.

Example D1 demonstrates a typical design calculation using the proposed design methods. The proposed method is quite simple to use and employs similar stress calculations as the present AASHTO method. The fatigue truck in the proposed method has fixed axle spacing, and is easier to compute the design stress range especially for continuous spans. In comparison, variable axle spacing of the HS-20 truck requires a lot of "bookkeeping" to establish maximum moment ranges. Examples D2 to D19 compare the proposed method with the AASHTO method based on the required section modulus for a given design case. It was found that the proposed methods are more flexible because they have four different volume categories as opposed to two volume categories used in the AASHTO method. Also the proposed method allows more exact distribution analysis, accounts for local site traffic, volume growth, and selection of bridge life. The latter is especially important in rehabilitation projects.

The proposed methods are more economical (require less section modulus) for spans above 50 ft and for fatigue detail

Categories E and E'. For fatigue detail Categories A and B the proposed methods require higher section modulus. However, for these categories, the strength design typically governs the design section modulus. For fatigue detail Categories C and D, both AASHTO and the proposed methods yield comparable section moduli.

For short spans (typically 30 to 40 ft) the AASHTO methods yield smaller design sections. For short spans, it was found that a single truck passage causes more than one cycle (typically 1.5 to 1.8 cycles, see Appendix E) per truck passage. The AASHTO methods do not take this into account and, therefore, may be unconservative compared to longer spans. Examples D20 to D31, comparing standard design sections from different design handbooks, further reinforces the above conclusions on the proposed design methods. It was also found that the stress ranges described in both the proposed evaluation and design procedures are well below the fatigue design stresses in current AASHTO procedures. They are, however, consistent with reported measured values. Column (12) of Table 26(a) shows the ratio of AASHTO design stresses to the proposed design stresses. The ratio is found to vary between 2.28 and 4.25. The average ratio is 3.15. This value was used in Chapter Four to show that the reliability calibration for the fatigue limit stresses,  $S_{FL}$ , are reasonable and consistent with present procedures and the proposed margin of 2.75 for the infinite life check.

## CHAPTER SIX

# CONDITIONS NOT CONSIDERED IN THE EVALUATION PROCEDURE

## SECONDARY BENDING

Secondary bending results from either (1) partial fixity at beam or truss joints that are assumed to be pinned, or (2) distortions of various members of the bridge, especially bracing members (187). Secondary bending stresses usually have little effect on the static strength of the bridge and are not calculated in the design. They can, however, cause fatigue cracking in either secondary bracing members or main members. In fact, many of the fatigue cracks that have occurred in actual bridges have resulted from secondary bending (54, 67, 127).

Because secondary bending stresses are not normally calculated, provisions pertaining to secondary bending are not included in the proposed fatigue design and evaluation procedures. Instead, a systematic review must be made either during the design of a new bridge or the evaluation of an existing bridge, to identify and correct potential fatigue problems due to secondary bending. To provide guidance for such a review, the relevant general principles are discussed in subsequent paragraphs. Further guidance can be obtained elsewhere (56, 57, 127). A study to develop specific fatigue design and evaluation

criteria pertaining to secondary bending is in progress at Lehigh University. Criteria developed in this study could be added to the proposed design and evaluation procedures.

### Partial End Fixity

The behavior of a typical "pinned" joint connecting a beam to a girder web is illustrated in Figure 23 (60). The moment/rotation relationship for the joint is given by the solid curved line, which is specifically for a simple web connection. The relationship between the end moment and end rotation for the beam is represented by the solid straight line. The intersection of the straight and curved lines defines the actual end moment and rotation for the case under consideration. A stiffer connection type, such as the double seat angle represented by the dashed line, results in a higher end moment and lower rotation.

The end moment can cause fatigue cracking in (1) the connecting angle or plate, (2) the beam itself, or (3) the bolts (or weld) attaching the connecting angle to the girder web. Reducing joint stiffness improves fatigue behavior with respect to all three failure modes. This can be accomplished by using (1) the most

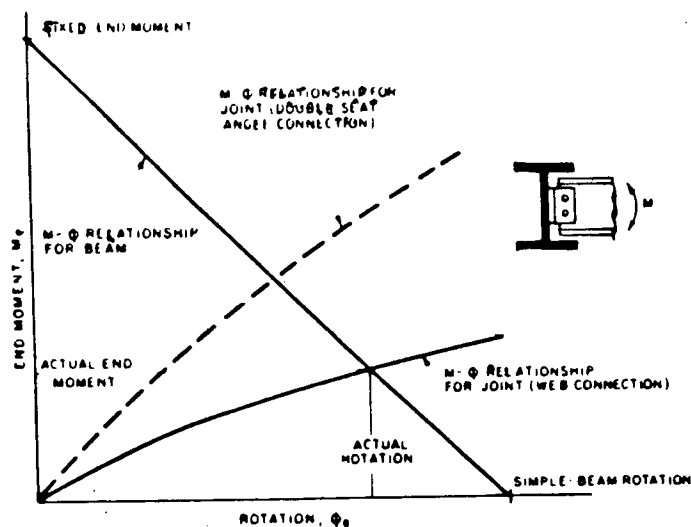


Figure 23. Behavior of simple-beam end connections.

flexible type of connection (simple web connection), (2) the smallest connecting angle thickness consistent with static design, and (3) the minimum number of bolts necessary to carry the shear.

Cracking in the connecting angle can be further minimized by using a large gage for the outstanding leg (distance from angle corner to first row of rivets) in the top third of the beam; a minimum value of

$$g = \sqrt{\frac{Lt}{12}} \quad (68)$$

is recommended (50). In the equation,  $g$  is the gage in the top third of the beam depth (and also in the bottom third if tensile stresses can develop in that region),  $L$  is the span in inches, and  $t$  is the thickness of the angle in inches.

Cracking in the beam itself usually occurs when the bending strength of the beam has been greatly reduced by coping the flanges to facilitate the connection. Therefore, avoiding such copes, or suitably strengthening coped beams, prevents such cracking (57).

Fatigue failures of the bolts attaching the angle to the girder web result from direct tension loads caused by the end moment. To avoid such failures, the bolts must be properly tightened because this reduces the variation of stress caused in the bolt by the cyclic tension loads (60).

The end moments that develop due to partial fixity in "pinned" truss joints are similar to those in "pinned" beam joints. However, the joint rotations that must be accommodated in truss joints result from member shortening rather than lateral loading on the members and, therefore, are much smaller.

### Member Distortions

Distortions of various members in a bridge can cause lateral bending of webs and gusset plates. Usually the lateral bending in the web results from twisting of the flange, lateral movement of the flange, or out-of-plane distortion of the web. Lateral

bending in gusset plates usually results from out-of-plane movements imposed on these plates by the members connected to them. Several specific cases are shown in Figure 24; most of these are discussed in detail elsewhere (57, 187).

Cross bracing (and to a lesser extent, diaphragms) between adjacent girders cause out-of-plane movements in the girder webs when the girders deflect different amounts. Similarly, traffic loadings can cause lateral bracing members to impose out-of-plane movements on the horizontal gusset plates to which they are attached, even though such bracing is designed only to resist lateral buckling or wind loading. The out-of-plane movements caused by both types of bracing are usually much greater in curved and skewed bridges than in straight bridges. Vibration of lateral bracing excited by traffic loadings can also cause out-of-plane movements and fatigue cracking (57). Horizontal loadings, especially on curves, can cause lateral movements of the flanges of floor beams supporting the deck.

As illustrated (187) in Figure 24 lateral forces or movements imposed at locations away from the girder supports can usually be accommodated by twisting of the cross section as a whole without the development of large lateral bending stresses in the web. At supports where twisting of the cross section is prevented, however, large lateral bending stresses can occur in the web, especially if a portion of the web is restrained by stiffeners, connection plates, or connection angles, so that all of the imposed rotation must be accommodated in a short length of the web. The magnitude of the stress varies inversely with the gap distance between the flange/web weld and the end of the stiffener, connection plate, or connection angle weld. Thus, lateral bending stresses in the web can be minimized by providing an adequate gap. A minimum gap of 4 in. has been recommended (57). Alternatively, lateral bending stresses in the web can be eliminated by welding the stiffener or connection plate to the flange.

Similarly, the lateral bending stresses caused in bracing gusset plates were thought to vary inversely with the gap between the end of the bracing and the girder web or flange to which the gusset is attached. However, a recent finite-element study and fatigue tests of web gusset plates suggest that the lateral bending

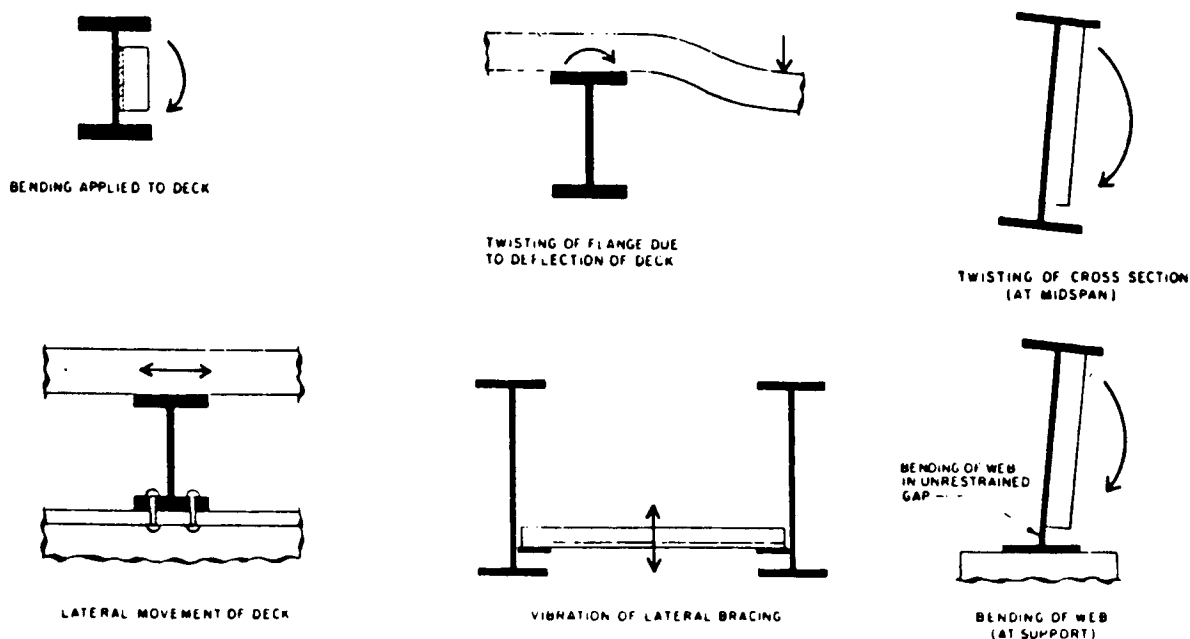


Figure 24. Lateral bending of curb.

stresses imposed by the bracing are small and are not greatly affected by the gap (68).

The lateral-bending fatigue strength depends on the type of fillet provided at the intersection of the web and flange or of the gusset plate and web. For rolled shapes that have a smooth generous fillet, the fatigue strength approaches that of Category A (57). For fillet welded or complete-penetration groove welded flange/web or gusset/web joints, the fatigue strength is probably equal to that of Category C (57). Partial-penetration groove welds, such as are used at the corners of box girders, usually do not have a fillet and often have a lack of fusion that is equivalent to a crack at the corner. Consequently, such joints have a low lateral-bending fatigue strength and are particularly susceptible to secondary bending problems.

## CRACKED MEMBERS

Once visible fatigue cracks are detected in a bridge member the remaining fatigue life of the bridge is usually short. This is true because the rate of growth accelerates rapidly as a crack increases in size; thus, most of the fatigue life occurs while the crack is very small (or not yet initiated) (190). Because the remaining life of a cracked member is short, it is usually desirable to repair the crack as soon as possible. Nevertheless, it is sometimes useful to estimate the remaining fatigue life of a cracked member to indicate the urgency of repairs or replacement. Therefore, methods of estimating the remaining life of a cracked member are discussed briefly in the next section, and methods of repairing the cracks are discussed briefly in the following section.

## Estimating Remaining Life

Usually, fracture-mechanics crack-growth procedures (54, 83, 113, 178, 245) are used to estimate the remaining life of cracked members. According to these procedures the crack growth rate and remaining life depend primarily on the stress-intensity range,  $K_r$ , at the crack tip. This stress intensity range varies with the crack depth (or width),  $a$ , as defined by the following equation:

$$K_r = CS_r \sqrt{\pi a} \quad (69)$$

where  $C$  is a dimensionless geometric parameter discussed in the next paragraph,  $S_r$  is the applied stress range in ksi, and  $a$  is in inches. Thus,  $K_r$  has the rather unusual dimensions of ksi  $\sqrt{\text{in}}$ . For variable-amplitude loading, the applied stress spectrum can be represented by the effective stress range defined in Chapter Two and the corresponding effective stress-intensity range is given by

$$K_{re} = CS_{re} \sqrt{\pi a} \quad (70)$$

Again,  $S_{re}$  is in ksi,  $a$  is in inches, and  $K_{re}$  is in ksi  $\sqrt{\text{in}}$ .

The parameter  $C$  represents stress gradient effects and depends primarily on the geometry of the crack and of the detail. It may also vary with the crack depth,  $a$ . Often  $C$  is treated as the product of several individual geometric parameters that define different geometric characteristics (3, 245, 250). Usually, one of these factors defines the nominal stress concentration in the region of the crack and another is related to the type of crack. Figure 25 shows four main types: (1) elliptical surface crack, (2) full-width surface crack, (3) through crack, and (4)

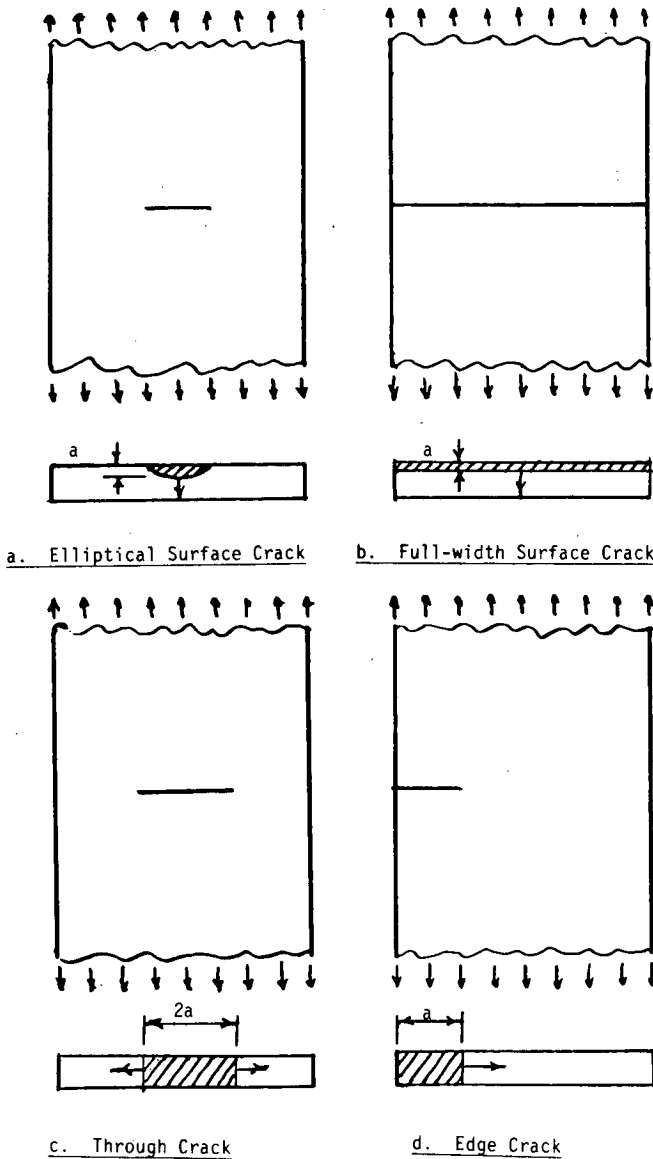


Figure 25. Types of fatigue cracks.

edge crack. An elliptical surface crack can start at a surface defect, such as a nick, or at a stress raiser, such as the end of a longitudinal attachment. It propagates through the thickness to the opposite surface. It then becomes a through crack and propagates toward both edges. A full-width surface crack often occurs along a transverse weld across the end of a cover plate (198, 199) and propagates toward the opposite surface. An edge crack can start at a defect or stress raiser on the edge of a plate and propagate toward the opposite edge.  $C$  factors are available (3, 199, 245, 246, 250) for these types of cracks located in regions affected by various stress raisers that typically occur in bridge details. Simplified methods of developing factors for other cases have also been proposed (3, 250).

The crack growth rate varies with  $K_{re}$  as shown in Figure 26. This behavior can be idealized by three straight lines on a log plot. The lower horizontal line represents the crack growth

threshold; if  $K_{re}$  is below this level, no crack growth occurs. Usually, however, the size of cracks that can be detected in bridges is large enough so that the corresponding  $K_{re}$  exceeds this threshold. For the structural steels (excluding A514 steel) and weldments in these steels, the sloping central portion of the curve can be conservatively (54, 178) defined as

$$\frac{da}{dN} = 3.6 \times 10^{-10} K_{re}^3 \quad (71)$$

in which  $a$  is in inches,  $K_{re}$  is in ksi  $\sqrt{\text{in.}}$ , and  $da/dN$  is the change in crack length per stress cycle.

The remaining portion of the curve represents the very rapid growth that occurs near the end of the fatigue life; it is idealized as a horizontal line corresponding to an infinite growth rate. The level of this horizontal line has not been well established. However, an approximate relationship that depends on the yield and tensile strengths of the material has been proposed (178); for structural steels, this relationship reduces to

$$K_{rel} = 7 \sqrt{\frac{S_y + S_t}{2}} \quad (72)$$

in which  $S_y$  is the yield strength in ksi,  $S_t$  is the tensile strength in ksi, and  $K_{rel}$  is the limiting  $K_{re}$  in ksi  $\sqrt{\text{in.}}$ . For structural steels with yield strengths up to 50 ksi,  $K_{rel}$  is about 50 ksi  $\sqrt{\text{in.}}$

An equation defining the remaining life of a cracked member can be obtained by combining Eq. 70 and Eq. 71 and integrating  $a$  from an initial crack depth,  $a_o$ , to a final crack depth,  $a_f$ . If  $C$  is assumed to remain constant over this range of  $a$ , the following equation results

$$N = \frac{10^9}{C^3 S_{re}^3} \left[ \frac{1}{\sqrt{a_o}} - \frac{1}{\sqrt{a_f}} \right] \quad (73)$$

where  $S_{re}$  is the effective stress range in ksi and  $a_o$  and  $a_f$  are in inches. The final crack depth should be taken as the lower of (1) the maximum value possible in the detail or (2) the value of  $a$  corresponding to  $K_{rel}$ . This latter value of  $a_{max}$ , to be calculated from Eq. 70, also depends on the static threshold  $k_{th} = C S_{max} \sqrt{\pi a_{max}}$ , where  $S_{max}$  is the maximum tensile stress in the stress cycle.

If  $C$  varies significantly over the crack depth range under consideration, this range can be subdivided into increments in which  $C$  is assumed to remain constant and Eq. 73 can be applied to each increment. Alternatively, the following finite-difference equation, obtained by combining Eqs. 70 and 71, can be applied incrementally as illustrated in Ref. 198:

$$\Delta N = \frac{5 \times 10^8 (\Delta a)}{C^3 S_{re}^3 a^{3/2}} \quad (74)$$

in which  $\Delta N$  is the number of cycles required to propagate the crack over the increment  $\Delta a$ ,  $a$  is the midpoint of that increment,  $C$  is the value of the geometric parameter at  $a$ , and  $S_{re}$  is the effective stress range. The parameters  $a$  and  $\Delta a$  are in inches and  $S_{re}$  is in ksi.

If the type of crack changes during the remaining life, the analysis must be made in separate stages. For example, a crack initiating at the surface at the center of a plate grows as an

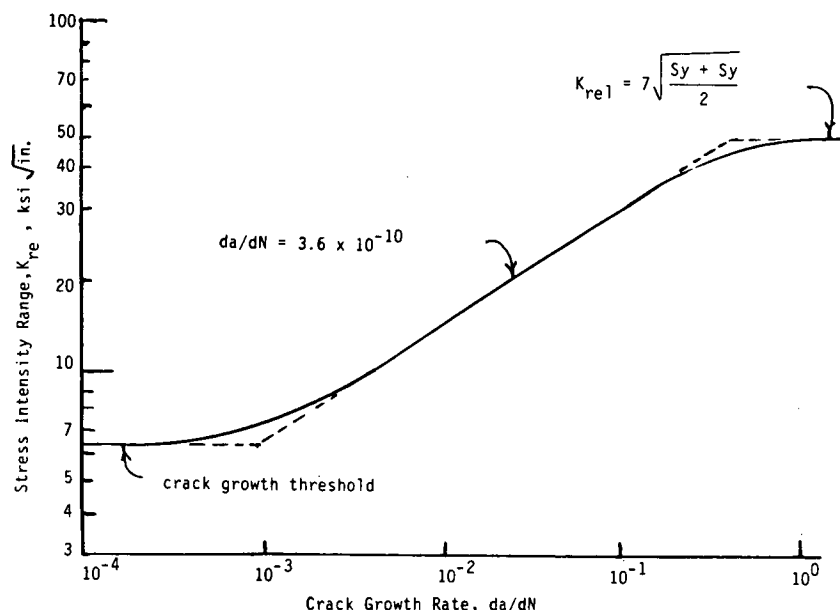


Figure 26. Crack growth rate vs. stress intensity range for structural steels.

elliptical surface crack until it reaches the opposite surface and then grows as a through crack toward the plate edges.

### Repairing Cracks

The best method for repairing a fatigue crack in a bridge member depends primarily on the crack's size and location (187). Large cracks may require major repairs such as replacing members, adding bracing to redistribute load, or adding bolted splice plates. In certain cases, it may be desirable to leave the crack unaltered and merely monitor its future growth (215). Several different methods are available for repairing or arresting cracks that fall between these two extremes. These methods are discussed here.

### Grinding

Steel producers are permitted (208) to remove surface or edge imperfections up to  $\frac{1}{8}$  in. deep by grinding without replacing the removed metal. Edge or surface fatigue cracks (probably initiated by a nick) not exceeding this depth can easily be repaired in the same way. In fact, even deeper edge cracks could be safely removed by grinding, provided that the ground area is well faired with gentle changes in contour. Grind marks perpendicular to the direction of stress should be avoided. Fatigue cracks at the toe of a fillet weld are more difficult to remove successfully by grinding (70) because more abrupt changes in contour are required at the weld.

Grinding can be done with either a rotary disk (typically a 4-in. disk with a 60 to 150 grit) or a conical burring bit. Burr grinding is preferred for treating fillet weld toes because disk grinding tends to be erratic and can cause worse conditions than existed before grinding (204). Some investigators used three

successive 30 to 200 grit polishes after burr grinding to further improve the surface. The cost of burr grinding without and with polishing is estimated (204) to be 3 to 4 and 12 times, respectively, that of single point peening.

Fisher (70) applied burr grinding without subsequent polishing to cover-plate ends, and did not achieve a significant improvement in fatigue strength. Other investigators were able to achieve 40 to 200 percent improvements in the fatigue strengths of various fillet welded details by burr grinding either with or without polishing (204). Because of its higher cost and less reliable results, however, burr grinding is a less attractive alternative than peening or TIG remelting for improving fillet welded details containing shallow cracks.

### Peening

Peening has been used successfully to improve the fatigue strength of uncracked or cracked members in many different applications. To be effective, the peening should be uniform in intensity and coverage. Three types of peening have been used (89, 204): (1) shot peening (129) in which pellets are shot at the surface, (2) single point peening (70, 81) in which a single  $\frac{1}{2}$ -in. diameter rod is applied pneumatically, and (3) multiple point peening (52, 81) in which 0.08-in.-diameter rods are applied pneumatically. In all of these methods, the peening cold works the surface and causes a thin layer of compressive residual stresses that are balanced by low tensile residual stresses below this layer. The peening also closes shallow surface imperfections or cracks.

The surface compressive residual stresses are superimposed on the applied stresses and thereby improve the fatigue strength (190). The improvement is greatest when the applied tensile stresses, both constant and cyclic, are low enough so that the net cyclic stresses are always in compression. High tensile dead

load stresses tend to reduce the effectiveness of peening unless it is done while the member is under dead load stresses. Usually, the tensile residual stresses below the surface are very low and consequently have little detrimental effect.

For bridge applications, peening is most often applied to the toes of transverse or longitudinal welds, and to transverse groove welds with the reinforcement in place. For uncracked details of this type, increases in fatigue strength (at 2,000,000 cycles) of about 20 to 200 percent have been reported (204). For fillet-welded details, the improvement in fatigue strength that can be achieved by peening the toe is often limited by fatigue cracking at the root of the weld (70). Root cracking is normally less critical than toe cracking, but becomes more critical when the toe is improved. Peening requires a lesser degree of operator skill, and is generally cheaper than the other treatments used to improve fatigue strength. Of the three peening methods, the single point method is generally preferable with respect to both cost and effectiveness (204).

Single point peening has been used successfully to repair fatigue cracks up to  $\frac{1}{8}$  in. deep at the toe of a fillet weld (70). It is a simple, effective, and economical way of making repairs provided that the cracks are not deeper than  $\frac{1}{8}$  in. and that the peening is uniform in coverage and severity. Otherwise, a buried crack will remain and severely limit the remaining fatigue life.

#### *TIG Remelting.*

The gas tungsten arc (TIG) welding process can be used to remelt the toe of a previously deposited fillet weld and thereby eliminate shallow imperfections or fatigue cracks that occur at that location. TIG remelting is generally regarded (70, 204) as the most reliable treatment for improving the fatigue strength of fillet welded details, but requires greater operator skill and is more costly than peening. In fact, it is estimated that the cost of TIG remelting is about 3 times that of single point peening. Usually, it is necessary to remove mill scale by sand blasting before TIG remelting (70) and to use appropriate procedures (70, 138) to help avoid weld craters at critical locations.

Because the improvement due to this treatment is caused by the removal of imperfections, it is not significantly affected by dead load stresses. The amount of improvement, however, may be limited by root cracking. Increases in fatigue strength (at 2,000,000 cycles) of 40 to 250 percent and 15 to 35 percent, respectively, have been reported (204) for uncracked transverse and longitudinal fillet welds. Fisher (70) indicated that fillet welded details, such as cover-plate ends, can be improved by one AASHTO detail category (from E to D, etc.) by TIG remelting. Gas tungsten arc remelting has also been shown (70) to be effective in removing fatigue cracks up to  $\frac{3}{16}$  in. deep at the toe of a fillet weld. However, caution is needed to avoid buried cracks.

#### *Rewelding.*

Larger fatigue cracks can often be repaired in the same way that unacceptable welds and internal imperfections are repaired during fabrication. The AWS specifications (214) cover such repairs. First, the crack is completely removed by air carbon-arc gouging, oxygen gouging, chipping, grinding, or machining. It may sometimes be desirable to use dye-penetrant or magnetic-particle inspection to assure that the crack has been completely

removed. Next, the gouge is rewelded to its original contour. Subsequent grinding to a smooth contour may sometimes be desirable.

Generally, this is the most reliable method of repairing a fatigue crack because the crack can be fully removed and the repaired region restored to its original condition or an improved condition better than the original. (However, if the condition that caused the fatigue crack is not removed as part of the repair, there is no point in repairing the girder.) The repair will extend the remaining fatigue life of the detail, but will not always fully restore the original life because of the effects of accumulated cycles outside of the repaired region. Treatments such as peening, TIG remelting, and grinding can be used after rewelding to further extend the remaining life of the detail. Residual stresses caused by extensive rewelding on an existing bridge could affect the fatigue strength of adjacent details and should be considered in selecting an appropriate repair method. An NCHRP Project 12-27, "Welded Repair of Cracks in Steel Bridge Members," is currently developing detailed guidelines for the weld repair of large cracks in existing bridges.

#### *Drilling Holes*

The growth of full-thickness fatigue cracks in steel plates can be arrested by drilling holes at the crack ends. This technique has been successfully used in many different applications including bridges (68, 70, 215). The purpose of the hole is to reduce the very high stress intensity that occurs at the crack tip. Therefore, it is essential that the hole include the crack tip. Because the actual end of a fatigue crack is difficult to detect visually, it is suggested the near edge of the hole be placed at the apparent crack end to assure that the actual end will be within the hole. Also, it is advisable to dye-penetrant inspect the hole to verify that the crack tip has been removed. Hole diameters between 0.5 and 1.0 in. have been used (68, 70, 215).

The fatigue category for a circular hole in a plate generally ranges from B to D depending on the smoothness of the hole edges (215). A carefully reamed hole qualifies as Category B (215). Because it is not important that the hole be precisely circular, hand filing can be used if needed to improve smoothness.

The fatigue strength of a crack with circular holes at both ends is less than that of a single circular hole and depends on the length between the outer edges of the holes. If this length is below a limiting value ( $L_{limit}$ ), further cracking will not occur. The following equation has been proposed (187) to define the limiting length:

$$L_{limit} = 200/S_r^2 \text{ for } L_{limit} \geq 1 \text{ in.} \quad (75)$$

where  $L_{limit}$  is in inches and  $S_r$  is the applied stress range in ksi. The actual maximum stress range occurring in the bridge, rather than an artificially high design value, should be used in this equation. The equation was derived (187) from a stress-intensity threshold developed (68) from a rather limited number of data and, therefore, should be regarded as approximate. The equation implies a fatigue limit of 14 ksi for a single 1-in. diameter hole; this is slightly below the fatigue limit of 16 ksi for Category B.

High-strength bolts with washers can be placed in the drilled holes and tightened by the turn-of-nut method to further reduce the possibility of cracking (68, 215). This produces compressive



stresses around the hole, but makes it more difficult to inspect for new cracks. The nonburr side of the washer should be placed against the plate to avoid cracks initiated by the burr (215).

### *Replacing Rivets*

The fatigue life of riveted joints in existing bridges can be considerably extended by merely replacing some of the rivets with high strength bolts. The maximum extension can be achieved by replacing all rivets, and repairing all observed cracks in the joint plates. However, life extensions of 2 to 6 times can be obtained by merely replacing rivets at locations where cracks can be observed in the adjacent plate material (174). With this approach, cracks in the plates need not be repaired unless they extend more than 1 in. beyond a rivet head. The bolts should be tightened by the turn-of-nut method as specified for bolted joints. Washers under the turning elements should be placed with the nonburr side against the plate (215).

## **CORROSION AND MECHANICAL DAMAGE**

### **Corrosion**

For most steel bridges, the fatigue life is not significantly affected by corrosion. Therefore, corrosion is not considered in the proposed fatigue evaluation and design procedures. For some steel bridges, however, the fatigue life can be significantly reduced by corrosion. Therefore, the effects of corrosion on fatigue life are discussed briefly in the following paragraphs.

Unsuitable design details and unusual environmental conditions that increase susceptibility to corrosion have been identified (11) in NCHRP Project 10-22. This study was made specifically for weathering steels, but most of the conditions that contribute to corrosion of such steels also apply to painted steels. An NCHRP Project 12-28(7), "Guidelines for Evaluating Corrosion Effects in Existing Steel Bridges," is currently developing guidelines for evaluating corrosion effects in existing steel bridges. The guidelines developed in these NCHRP studies should be helpful in identifying particular bridges for which corrosion might need to be considered in the fatigue evaluation. The guidelines, of course, should also be helpful in avoiding corrosion problems in new bridges. In general, joints and other locations where moisture and contaminants can collect are most susceptible to corrosion.

### *Painted Steel*

Corrosion of steel members can generally be prevented by painting and proper maintenance, but does occur in many bridges because of neglected maintenance. Light uniform rusting generally has little effect on the fatigue life of a member or detail. Heavy corrosion, in contrast, can cause a large reduction in fatigue life. Such corrosion can cause several detrimental effects. First, it reduces the cross sectional area and thereby increases the nominal stresses. Second, it can roughen the surface, especially if it occurs nonuniformly. Third, it can cause a notch, or make an existing stress raiser more severe if it is concentrated in a small area at a critical location, such as the end of a cover plate. On the other hand, corrosion can sometimes improve fatigue life by blunting a sharp crack or notch (215).

Only a few fatigue tests are available (166) to indicate the magnitude of the detrimental effects that can occur. Specifically, fatigue tests were performed on four riveted stringers that had been in service on a railroad bridge for about 80 years. At the most severely corroded locations along the stringers, the areas of the legs of the flange angles were reduced by 5 to 40 percent. One of the stringers did not develop visible fatigue cracking at the corroded location within 40 million cycles when the test was stopped. The other three stringers, however, developed cracks near the angle tip that caused eventual failure. Based on net section stresses, the failures corresponded to detail categories ranging from C to E. The uncorroded angle should correspond to a Category A detail (based on crack initiation at the flange tip away from rivets). Thus, severe corrosion caused a much greater reduction in fatigue life than would be predicted by the reduction in net section alone.

In addition to its direct effect on a member cross section, corrosion can also cause indirect detrimental effects on fatigue strength as well as on static strength. Thermal expansion of members connected to pinned joints "frozen" by corrosion can impose stresses that would not otherwise occur. Similarly, build-up of corrosion products can cause local forces and distortions, usually perpendicular to the plane of a plate element, that might affect fatigue. Reductions in thickness at locations that do not significantly affect the primary stresses in a member can lead to fatigue failures due to secondary bending that otherwise would not cause a problem. For example, a fatigue failure occurred in a rolled beam stringer in a railroad bridge because of lateral bending in combination with a reduction in web thickness caused by localized corrosion (215).

### *Weathering Steel*

At present, AASHTO (209) does not mention weathering steel in its fatigue provisions; consequently, weathering steel details can be assigned to the same categories as similar painted steel details. The proposed fatigue evaluation and design procedures follow this same approach because they utilize the present AASHTO detail categories.

Tests (9, 11) indicate that normal weathering can reduce fatigue strengths in the higher detail categories, such as A and B. However, there has been considerable controversy on whether these results justify special AASHTO fatigue provisions for weathering steels, and, if so, what these provisions should be. If AASHTO decides to adopt new fatigue provisions for weathering steels, the most convenient way would be to assign various types of weathering steel details to existing detail categories. Whatever new provisions AASHTO considers appropriate, however, should be incorporated into the proposed fatigue evaluation and design procedures.

### **Corrosion Fatigue**

Corrosion fatigue refers to combined action of corrosion and cyclic loading that produces detrimental effects greater than either acting alone (190). Generally, paint adequately protects against corrosion fatigue; therefore, corrosion fatigue is not considered in the proposed fatigue evaluation and design procedures. However, a bridge member could be subjected to corrosion fatigue if it is unpainted or if the paint deteriorates.

Therefore, corrosion fatigue is discussed briefly in the following paragraphs.

The most important corrosive agent that affects bridges is salt water. In an NCHRP study (18), crack growth tests of structural steel specimens continuously immersed in salt water (3 percent solution) did not show any significant corrosion fatigue effect; the crack growth rates for the immersed specimens were essentially the same as those for similar specimens in air. Furthermore, the growth rates were retarded significantly by alternate wet and dry environmental conditions. Therefore, it was concluded (18) that the crack propagation life of bridge-steel components under actual wet/dry conditions should not be less than that in air.

In contrast, another NCHRP study (11) indicated that the initiation, propagation, and total fatigue life for structural steels is less under continuously immersed (salt water) conditions than in air. The relationship between these continuously immersed conditions and service conditions in actual bridges, however, has not been adequately established. Therefore, the precise effect of corrosion fatigue in actual bridges is difficult to predict.

As mentioned earlier, unsuitable design details and unusual environmental conditions that increase susceptibility to corrosion have been identified (11). If these severe conditions are present, the steel generally should have a satisfactory paint coating to guard against corrosion fatigue. If the steel in the bridge under investigation does not have such a paint coating either because the paint has deteriorated or because unpainted weathering steel was used, it usually should be painted. Suitable painting procedures for existing bridges are described in the NCHRP study (11). Otherwise, the remaining fatigue life calculated by the proposed fatigue evaluation procedure should be reduced to account for possible corrosion fatigue effects.

The suggestions in the preceding paragraph are for severe corrosion conditions. For bridges under normal conditions, the effects of corrosion fatigue are generally small enough to be covered by the reliability factor even when there is no satisfactory paint coating. This reliability factor provides a margin of safety to account for various detrimental effects that could occur, including environmental effects. As discussed in earlier chapters, the probability is very low that all detrimental effects will occur simultaneously in a particular bridge.

### Fretting

- Fretting is an unusual type of fatigue that does not occur often in bridges; therefore, it is not covered in the proposed fatigue evaluation and design procedures. Fretting has occurred in laboratory fatigue tests of structural members and connections, but has not been reported in actual bridges. Specifically, the fretting in laboratory tests has occurred at loading fixtures, bearing plates, and bolted connections in A514 steel.

Fretting can occur when two metal surfaces in contact are subjected to small repetitive sliding movements (190). These movements cause the initiation of surface cracks that eventually may grow into ordinary fatigue cracks. Fretting can greatly reduce the fatigue life of a member or cause a fatigue failure that would not otherwise occur. The mechanism of fretting is very complex and apparently involves both mechanical and chemical action (74, 105). Fretting produces a powder consisting of oxides of the metals in contact; for steels in contact, the powder is rust. The powder provides a warning that fretting is occurring.

There are insufficient quantitative data available on fretting to permit accurate fatigue design calculations. However, the effects of some important factors are known (74, 105). As the contact pressure increases, the fretting fatigue life decreases to a minimum value, and remains close to that minimum value until the pressure becomes high enough to prevent sliding movements (105, 109). Corrosive environments tend to reduce fretting life. High hardness, higher strength steels appear to be more susceptible to fretting than lower strength structural steels.

Fretting can be prevented or minimized by (1) inserting a soft material (such as wood, brass, or copper) between the contact surfaces, (2) applying a surface treatment to induce compressive residual stresses in the contact surfaces, (3) preventing relative movement by high contact pressure, keyways, adhesives, or other means, and (4) reducing the cyclic stresses that propagate the fretting cracks. Lubrication by oils or greases normally provides only small improvements (74).

### Mechanical Damage

Several types of mechanical damage can occur to steel bridges: (1) nicks and gouges, (2) bent members, and (3) fire damage (202). Normally, such mechanical damage is repaired soon after it is found; alternatively, the damaged member or bridge may be replaced. Therefore, mechanical damage is not considered in the proposed fatigue evaluation and design procedures. However, the effect of such damage and subsequent repairs on fatigue are discussed briefly in the following paragraphs.

#### *Nicks and Gouges*

Nicks and gouges are stress repairs that reduce fatigue life; therefore, they should generally be repaired by grinding or one of the other methods described earlier for repairing cracked members. The remaining fatigue life for a member containing a nick or gouge can be conservatively estimated by treating it as a crack and applying the crack growth procedures described earlier. If the contour of the nick or gouge is smooth and gentle, the actual remaining life may be considerably higher.

#### *Bent Members*

Bent members due to overheight vehicles, overwidth vehicles, overweight vehicles, out-of-control vehicles, and marine collisions are fairly common. For example, a recent survey of 33 states reported that 815 steel bridges were damaged in a 5-year period; 94 percent included damage due to overheight vehicles (202). Usually, bent members either are replaced or are straightened by flame or mechanical procedures. These straightening procedures generally do not have a significant effect on fatigue behavior, although they could conceivably alter residual stresses in such a way as to affect fatigue behavior in a few unusual cases. No such cases, however, have been reported. The unusual situations in which residual stresses affect the fatigue behavior of fabricated members are discussed elsewhere (190).

#### *Fire Damage*

Occasionally, steel bridge members are subjected to high tem-

peratures as a result of a fire on or near the bridge. Generally, such temperatures cause permanent distortions, but do not adversely affect the mechanical properties unless quenched and tempered steels, such as A514 steels, are involved. Therefore, fire damage usually does not affect fatigue behavior, although it could conceivably have an effect in a few unusual cases by altering residual stresses as discussed in the preceding paragraph.

## CASE HISTORIES

A study of case histories can sometimes be helpful in assessing unusual conditions that could affect fatigue evaluations. Such case histories have been compiled in a book (54) and numerous papers (20,55,58,59,61,63–67,69,120–121,126–127,165,215,234,

249). Most of the fatigue failures that have occurred in bridges have resulted from (1) secondary bending, (2) improper fabrication, (3) severe details such as cover plate ends, or (4) stresses in elements that were not intended to carry stress. Fatigue failures have not been reported in detail Categories of A to C.

## CHAPTER SEVEN

# CONCLUSIONS AND SUGGESTED RESEARCH

## CONCLUSIONS AND IMPLEMENTATION

The proposed fatigue evaluation procedure for existing steel highway bridges provides the following advantages:

1. It realistically reflects the actual fatigue conditions in highway bridges.
2. It gives an accurate estimate of both the remaining mean and safe fatigue lives of a bridge and permits this estimate to be updated in the future to reflect changes in traffic conditions.
3. It uses the same detail categories and corresponding fatigue strength data as the present AASHTO specifications.
4. It uses procedures similar to those in the present AASHTO specifications to calculate stress ranges.
5. It provides consistent and reasonable levels of reliability.
6. It permits different levels of effort to reduce uncertainties and improve predictions of remaining life.
7. It is based on extensive recent research and can be conveniently modified in the future to reflect any new research results.
8. It is suitable for inclusion in the present AASHTO maintenance inspection manual.
9. It presents options that can be pursued by the engineer if he considers the calculated remaining life to be inadequate.

The proposed fatigue design procedure for new steel highway bridges provides the following advantages:

1. It is consistent with the proposed fatigue evaluation procedure for existing bridges.
2. It realistically reflects the actual fatigue conditions in highway bridges.

3. It uses the same detail categories and corresponding fatigue strength data as the present AASHTO specifications.

4. It uses procedures similar to those in the present AASHTO specifications to calculate stress ranges.

5. It provides simple procedures based on assumed conservative traffic conditions, but permits less conservative procedures based on the expected present and future traffic conditions at the site.

6. It relates a permissible stress range to a desired design life and permits the engineer to select this design life.

7. It provides consistent and reasonable levels of reliability.

8. It is based on extensive recent research and can be conveniently modified in the future to reflect any new research results.

9. It is suitable for inclusion in the present AASHTO bridge design specifications.

The proposed fatigue evaluation and design procedures do not cover secondary members, cracked and/or repaired members, or corrosion and mechanical damage. Some guidance on these effects, however, is given in the present report.

## SUGGESTED RESEARCH

The proposed fatigue evaluation and design procedures depend on (1) the traffic loadings applied to bridges, (2) the response of bridges to such loadings, and (3) the fatigue behavior of bridge members. Therefore, additional information on all aspects of these subjects would be useful in upgrading these procedures in the future. Some of the information on traffic loadings and even bridge response can be obtained as part of

the new Strategic Highway Research Program (SHRP). To improve the reliability calibration, additional data are needed on the variability of the parameters that were considered in this calibration. These included: (1) effective truck weight, (2) stress cycles per truck passage, (3) truck superpositions, (4) lateral distribution, (5) impact, (6) effective section modulus, (7) moment ratio, (8) constant-amplitude fatigue strength, and (9) cumulative damage relationship. More important, however, specific research is needed to clarify several points that directly affect particular provisions. Such research is discussed below.

### Fatigue Limit

It is generally accepted that the fatigue life will be infinite if all of the stress cycles in a variable-amplitude spectrum are below the constant-amplitude fatigue limit,  $S_{rLC}$ . As shown in Figure 27, this occurs when the effective stress range,  $S_r$ , for the spectrum is less than  $S_{rLC}/R_p$ , and this level of  $S_r$  can be considered the variable-amplitude fatigue limit,  $S_{rLV}$ , for the spectrum.  $R_p$  is the peak ratio for the spectrum and is defined as the peak stress range,  $S_{rp}$ , in the spectrum divided by the effective stress range.

If  $S_{re} > S_{rLV}$ , some of the cycles,  $S_{ra}$ , are above the constant-amplitude fatigue limit and others,  $S_{rb}$ , are below. In the past, it was thought that the cycles,  $S_{rb}$ , below the constant-amplitude fatigue limit cause no fatigue damage and can be ignored. The dashed SN curve in Figure 27 is based on this assumption and represents an upper bound on the fatigue life. It becomes asymptotic to the variable-amplitude fatigue limit at a very long life.

More recently, it was concluded that the  $S_{rb}$  cycles cause damage by propagating cracks initiated by the  $S_{ra}$  cycles. At

worst, these  $S_{rb}$  cycles cause the same fatigue damage as if the constant-amplitude fatigue limit did not exist. Therefore, the solid SN curve in Figure 27 defines the lower bound for fatigue life. The actual SN curve must lie between these two limiting curves, but sufficient data are not available to define its position precisely.

The difference between the upper- and lower-bound SN curves depends primarily on the peak ratio and the shape of the probability-density curve defining the stress spectrum. If this curve has a long low tail,  $R_p$  will be large and  $S_{rLV}$  will be well below  $S_{rLC}$ . The long tail, however, has only a small effect on the upper-bound curve. Consequently, the difference between the two curves will be large if the tail is long.

The effect of the fatigue limit on the evaluation and design procedures depends on the level of the actual SN curve at a practical design life of, say, 100 to 150 million cycles. If the actual SN curve is well above the SN curve assumed in the proposed procedures, the effect will be large. Therefore, tests are needed to define the actual SN curves for certain details.

For two reasons, Category C is the most important detail category that needs to be tested. First, Categories C and above (A through C) can generally not be eliminated from bridges, but the lower categories (D through E') generally can be eliminated if necessary by design changes. Second, the effect of the fatigue limit is expected to be greater for the less severe details (C and above) because the sloping SN curve must be projected further below the constant-amplitude fatigue limit to reach the design life for such details.

To define the actual SN curve for Category C, several girders should be tested at different  $S_{re}$  levels corresponding to various design lives between 100 million and 10 million cycles. To provide replication, five or six identical details should be included

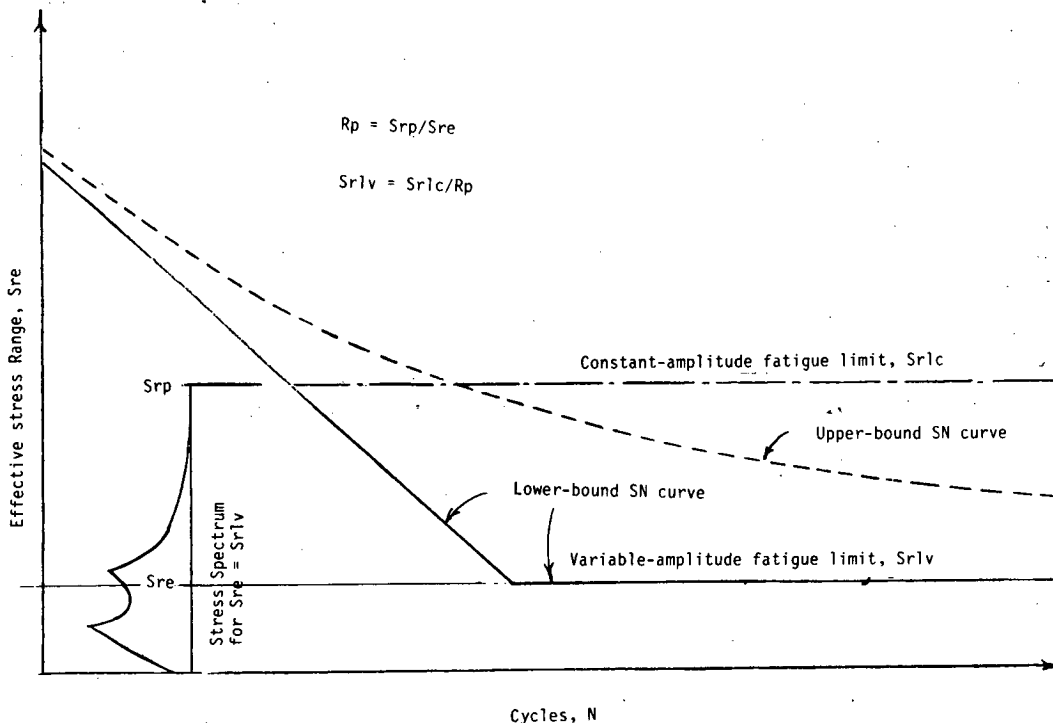


Figure 27. Effect of fatigue limit on variable-amplitude fatigue behavior.

in each girder. The tests should be continued to 100 million cycles or more. The stress spectrum for typical traffic (as described in Appendix D) should be used in these main tests. To show the effect of  $R_p$ , and the shape of the tail of the probability-density curve, additional tests should be performed on small specimens under two or more spectrums, similar to the spectrum shown on Figure D-18 in Appendix D, but with the tail modified. Similar tests on other detail categories would also be desirable but should have a lower priority than the tests on Category C details.

### Compression Cycling

In the proposed fatigue evaluation and design procedures, it was assumed that the fatigue life will be infinite if all of the stress cycles in the spectrum are completely in compression. This is consistent with present AASHTO procedures. Furthermore, no fatigue problems have been reported in actual bridges under these conditions. On the other hand, extensive fatigue cracking has occurred in some laboratory tests under these conditions, and the European fatigue specifications generally treat compression cycling of welded details the same as tension cycling.

With the present approach, the fatigue life of a detail is assumed to be infinite even if it is subjected to a high cyclic stress range provided that the compressive dead load stress is equal to this stress range. If the dead load stress is reduced slightly below this stress range, however, the life is assumed to be reduced to a relatively low finite value. This slight change in dead load stress probably does not actually have such a large effect on the fatigue life. Therefore, further study, perhaps including tests, should be applied to this provision.

### Long-Span Bridge Loadings

In long-span bridges, the traffic loading causes long periods of continuous stresses of varying magnitude rather than large

numbers of individual cycles. The magnitudes of these continuous traffic stresses, of course, are low and judgment, as well as the available evidence discussed in Chapter Two, suggests that no special fatigue loadings need to be considered for such bridges. An exception may be in the case of cable stayed bridges with significant live to dead load stress ratios. Further study of fatigue loadings in long-span bridges would be desirable to provide more definitive data on the nature and effects of such loadings.

Continuous stress vs. time curves could be generated from available data on (1) the percentage of vehicles of various weights and types in typical traffic and (2) the variation of traffic volume with time over a 24-hour period. The Monte Carlo method could be applied to these data to determine the positions of the vehicles on the bridge at any time, and appropriate influence lines could be used to calculate the resulting stresses. The effects of the continuous stress-time curves on fatigue behavior could be assessed by the methods discussed under "Equivalent Cycles" in Appendix C.

### Vibration Cycles for Unusual Bridges

For most bridge types, the effects of vibration stresses on fatigue behavior are generally small enough to be neglected as discussed in Chapter Two. The vibration cycles, however, have been shown to be significant in cantilever (suspended span) girder bridges. Also, large vibration stresses were reported in a bridge consisting of two steel girders, transverse steel floor beams, and a prestressed concrete deck.

Vibration stresses have not been measured on many other types of steel bridges and may be significant in some of these types. Therefore, a study, probably including field measurements, is needed to identify any other types of bridges where these vibration stresses need to be considered or what specific site conditions including grade, bump, and surface roughness may cause large vibration stresses.

## APPENDIX A

### PROPOSED FATIGUE EVALUATION PROCEDURES

Section numbers correspond to the 1983 AASHTO *Manual for Maintenance Inspection of Bridges* and would appear as a separate Section 6.

#### 6.0 FATIGUE EVALUATION OF STEEL BRIDGES

##### 6.1 GENERAL

###### 6.1.1 Development

The development and use of the fatigue evaluation procedures in this chapter are explained in *NCHRP Report 299*.

###### 6.1.2 Scope

The evaluation procedures in this chapter apply to uncracked steel members subjected to primary stresses. The procedures do not apply to members that have sustained severe corrosion or mechanical damage or that have been repaired after sustaining fatigue cracking. *NCHRP Report 299* gives information and references on the fatigue behavior of such members and on the possibility of fatigue due to secondary bending stresses that are not normally calculated.

###### 6.1.3 Evaluation Procedures

Section 6.2 gives procedures for calculating the stress range at a detail. Section 6.3 gives procedures for calculating both the remaining mean fatigue life and the remaining safe fatigue life for this stress range, and Section 6.4 gives options that may be pursued if the Engineer considers the remaining life to be inadequate. Each different detail must be checked individually. Some articles give one or more alternative procedures that may be used instead of the basic procedure. Most of the alternative procedures require more effort than the basic procedure but provide an improved precision that generally results in a longer calculated remaining safe life. A factor,  $F_{Sn}$ , is applied for each alternative procedure used in calculating the stress range.

The remaining mean life is the best possible estimate of the actual remaining life; there is a 50 percent probability that the actual remaining life will exceed the remaining mean life. The remaining safe life provides a much higher degree of safety; the probability that the actual remaining life will exceed the remaining safe life is 97.7 percent for redundant members and 99.9 percent for nonredundant members. These probabilities are comparable to the safety levels in the fatigue provisions of the 1983 AASHTO *Standard Specifications for Highway Bridges*.

#### 6.2 STRESS RANGE

##### 6.2.1 General Procedure

Calculate the nominal stress range,  $S_r$ , for the fatigue evaluation by following the steps in Articles 6.2.2 through 6.2.7.

*Alternative 1.* Through field measurements while the bridge is under normal traffic, obtain stress-range histograms for critical details. Calculate the effective stress range for each histogram from  $S_r = (\sum f_i S_{ri}^3)^{1/3}$ ; where  $f_i$  = fraction of stress ranges within an interval, and  $S_{ri}$  = midwidth of the interval;  $F_{S1} = 0.85$ .

If this alternative is used, omit Articles 6.2.2 through 6.2.7.

##### 6.2.2 Fatigue Truck

Use the dimensions and axle weights of the fatigue truck shown in Figure 6.2.2A to calculate the stress range.  $F_{S2} = 1.0$ .

*Alternative 1.* Adjust the gross weight of the fatigue truck based on judgment supported by a knowledge of truck traffic in the region. Distribute the gross weight to axles in accordance with Figure 6.2.2A.  $F_{S2} = 1.0$ .

*Alternative 2.* Through weigh station measurements at an appropriate location close to the site, obtain a gross-weight histogram for the truck traffic excluding panel, pickup, and other 2-axle/4-wheel trucks. Calculate the gross weight of the fatigue truck from  $W = (\sum f_i W_i^3)^{1/3}$  where  $f_i$  = fraction of gross weights within an interval, and  $W_i$  = midwidth of the interval;  $F_{S2} = 1.0$ .

Distribute the gross weight to axles in accordance with Figure 6.2.2A.

*Alternative 3.* Through weigh-in-motion measurements at the site, obtain a gross-weight histogram for the truck traffic excluding panel, pickup, and other 2-axle/4-wheel trucks. Calculate the gross weight of the fatigue truck by the equation in Alternative 2. Distribute the gross weight to axles in accordance with Figure 6.2.2A or use site data to provide a more appropriate distribution and axle spacing.  $F_{S2} = 0.95$ .

*Alternative 4.* Use the procedure given in *NCHRP Report 299* to evaluate the weight of the fatigue truck from traffic survey data that includes the percentage of various types of trucks.  $F_{S2} = 1.0$ .

##### 6.2.3 Truck Superpositions

If special site conditions are expected to cause unusual bunching of trucks, increase the gross weight of the fatigue truck by 15 percent. Such special conditions include (1) a traffic signal on or near the bridge and (2) a steep hill when the bridge is on a two-lane highway. Omit this step if such special conditions do not exist.

### 6.2.4 Impact

Increase the gross weight of the fatigue truck by 10 percent to account for impact on smooth road surfaces. If an inspection reveals unusual conditions, such as a poor joint or pavement roughness, that are expected to increase impact, increase the gross weight of the fatigue truck above 10 percent, but not above 30 percent.

### 6.2.5 Moment Range

Calculate the moment range (or axial force range for truss members) caused at the detail under consideration by a passage of the fatigue truck across the bridge. For longitudinal beams, girders, stringers, or truss members, place the fatigue truck at different positions that cause the algebraic maximum and minimum moments (or axial forces); the algebraic difference between the two is the moment (or axial force) range. For transverse bending members, the moment range equals the moment at the detail when the fatigue truck is at the center of the traffic lane that results in the highest moment.

### 6.2.6 Lateral Distribution

For straight longitudinal beams, girders, or stringers, calculate the moment range carried by the member under consideration by multiplying the total moment range due to the fatigue truck from Article 6.2.5 by a lateral distribution factor,  $DF$ , from Article 6.2.6.1 or Article 6.2.6.2.  $F_{S3} = 1.0$ .

**Alternative 1.** Calculate  $DF$  by one of the approximate methods in Appendix C of *NCHRP Report 299*.  $F_{S3} = 1.0$ .

**Alternative 2.** Use a rigorous method, such as the finite element method, to calculate the moment range carried by each beam, girder, or stringer when a single fatigue truck is moved along the centerline of the shoulder traffic lane.  $F_{S3} = 0.96$ .

**6.2.6.1 I-Shaped Members.**—If the deck is supported by two members, determine  $DF$  by assuming that the deck acts as a simple beam supporting a single truck at the center of the outer traffic lane. If the deck is supported by more than two members, determine  $DF$  as follows.

For interior members, use  $DF = DF_i = S/D$ , but not more than  $(S - 3)/(S)$ , where  $S$  = girder spacing in feet and  $D$  = factor defined below; values for intermediate span lengths may be interpolated. For positive and negative bending regions in continuous span bridges, the span length may be taken as the corresponding distance between points of dead load contraflexure:

Span (ft)	$D$
30 or less	17
40	19
60	20
90	22
120 or more	23

For exterior members, use  $DF = DF_e = DF_i$  if either (a) the inner face of the curb or parapet is less than 1 ft outside the centerline of the exterior member or (b) the width of the shoulder for the outside lane is more than 4 ft; otherwise:

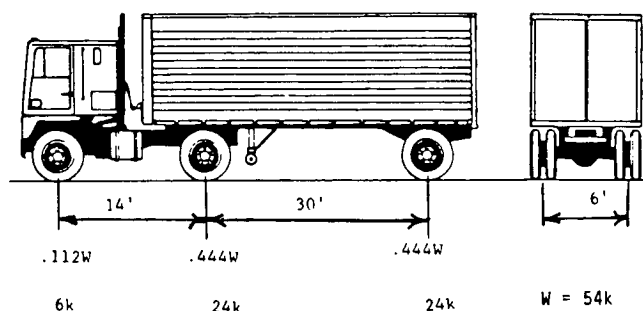


Figure 6.2.2A. Fatigue truck. (Note: A variable spacing of 14 to 30 ft can be used instead of the 30-ft main axle spacing, but this will significantly reduce the calculated remaining life.)

If  $P > 0.5$ ,  $DF_e = 0.7 - 0.4P$  but not less than  $DF_i$

If  $P \leq 0.5$ ,  $DF_e = 0.9 - 0.8P$  but not less than  $DF_i$

$P$  = distance from exterior member to centerline of (nearest) outer lane divided by girder spacing;  $P$  is negative if centerline is outside the exterior girder

**6.2.6.2 Box-Shaped Members.**— $DF$  may be conservatively calculated by dividing each box into two equivalent I-beams, each consisting of one-half of the box, and applying the procedures for I-shaped members.

### 6.2.7 Member Section

**6.2.7.1 Bending Members.**—Divide the moment range by the section modulus (moment of inertia divided by distance from neutral axis to expected crack initiation location) of the detail under consideration to get  $S_r$ .

**Composite Concrete Decks.** If the deck is attached to the steel section by shear connectors, use the full composite section (as defined in Article 10.38 of the *AASHTO Standard Specifications for Highway Bridges*) increased by 15 percent in positive bending regions (taken as the portion between the points of dead load contraflexure) and a section including the longitudinal rebars in negative bending regions.

**Noncomposite Concrete Decks.** If the deck is not attached to the steel section by shear connectors, use one of the following options. In positive bending regions where there is no visual indication of separation between the deck and steel section, use either the full composite section or the steel section alone increased by 30 percent. In positive bending regions, where there is a visual indication of separation, and in negative bending regions use the steel section alone.

**6.2.7.2 Truss Members.**—Divide the axial load range by the cross sectional area to get  $S_r$ .

### 6.2.8 Reliability Factor

To determine the remaining safe life, multiply the computed stress range,  $S_r$ , by a reliability factor:

$$R_S = R_{S0} (F_{S1}) (F_{S2}) (F_{S3})$$

where  $R_S$  = reliability factor associated with calculation of stress range;  $R_{S_0}$  = basic reliability factor; 1.35 for redundant members and 1.75 for nonredundant members; at the option of the Engineer, other levels of reliability described in *NCHRP Report 299* may be used;  $F_{S_n}$  = factor for procedure  $n$ ;  $F_{S_n} = 1.0$  unless otherwise specified.

Classify a member as nonredundant if, in the judgment of the Engineer, a failure of this member alone would cause collapse of the bridge.

To determine the remaining mean life, use  $R_S = 1.0$ .

### 6.3 REMAINING LIFE

#### 6.3.1 Infinite Remaining Life

The remaining safe fatigue life is infinite and no further fatigue calculations are required if (a)  $R_S S_r < S_{FL}$  or (b)  $2R_S S_t < S_c$ , in which  $S_r$  = stress range from Article 6.2;  $S_t$  = tension portion of stress range from Article 6.2;  $S_c$  = compressive dead load stress;

$S_{FL}$  = limiting stress range for infinite life from Article 6.3.3.

#### 6.3.2 Finite Remaining Life

Calculate the remaining fatigue life for an estimated lifetime average daily truck volume using the equations:

$$Y_f = \frac{fK \times 10^6}{T_a C (R_S S_r)^3} - a$$

where  $Y_f$  = remaining fatigue life in years;  $K$  = detail constant from Article 6.3.3;  $T_a$  = estimated lifetime average daily truck volume in the outer lane, and may be estimated by the Engineer or obtained from Article 6.3.5;  $C$  = stress cycles per truck passage from Article 6.3.4;  $S_r$  = stress range from Article 6.2 in ksi;  $R_S$  = reliability factor from Article 6.2.8;  $a$  = present age of bridge in years;  $f = 1.0$  for calculating safe life and 2.0 for calculating mean life.

*Alternative 1.* Calculate the remaining life by dividing the total fatigue life into two periods in which the truck volume and equivalent fatigue truck weight remain constant: (a) a past period from the opening of the bridge to the present,  $Y_p$ , and (b) a future period from the present to the end of the fatigue life,  $Y_f$ .

$$Y_f = Y_N [1 - (Y_p/Y_1)]$$

$$Y_1 = \frac{fK \times 10^6}{T_p C (R_S S_r W_p/W)^3}$$

$$Y_N = \frac{fK \times 10^6}{T_N C (R_S S_r W_N/W)^3}$$

where  $Y_f$  = remaining fatigue life in years;  $Y_p$  = present age of bridge in years;  $Y_1$  = fatigue life in years based on past volume,  $T_p$ , and fatigue truck weight  $W_p$ ;  $Y_N$  = fatigue life in years based on future volume,  $T_N$ , and fatigue truck weight  $W_N$ ;  $T_p$  = average daily truck volume in the outer lane for the past period;  $T_N$  = average daily truck volume in the outer lane for future remaining life period (an estimate including a growth

rate may be obtained from Figure 6.3.5.2A by letting  $T = T_p$  and  $a = 0$ );  $W_p$  = fatigue truck weight for the past period;  $W_N$  = fatigue truck weight for future remaining life period;  $W$  = gross weight of fatigue truck in Article 6.2.2;  $f = 1.0$  for calculating safe life and 2.0 for calculating mean life.

*Alternative 2.* Use one of the procedures given in *NCHRP Report 299* to (a) calculate the remaining fatigue life when the total fatigue life is divided into more than two periods, (b) calculate the remaining fatigue life when either past or future truck volume growth rates can be estimated, or (c) maintain a record of accumulated fatigue damage that can be updated at 4-year intervals and used to calculate the remaining fatigue life.

#### 6.3.3 Detail Constants

For the detail categories defined in Table 10.3.1B of the *AASHTO Standard Specifications for Highway Bridges*, use the following values:

Detail Category	Detail Constant, $K$	Limiting Stress Range, $S_{FL}$ (ksi)
A	68	8.8
B	33	5.9
B'	17	4.4
C	12	3.7*
D	6.0	2.6
E	2.9	1.6
E'	1.1	0.9
F	2.9	2.9

\* Use 4.4 ksi for stiffeners.

#### 6.3.4 Cycles Per Truck Passage

Use the following values for  $C$ , the number of stress cycles per truck passage:

For longitudinal members:

- (a) Simple-span girders:
  - 40-ft or above = 1.0
  - Below 40-ft = 1.8
- (b) Continuous-span girders within a distance equal to 0.1 of the span on each side of an interior support (take span equal to distance between supports):
  - 80-ft or above =  $1 + (\text{span} - 80)/400$  in feet
  - 40-ft or above but below 80-ft = 1.0
  - Below 40-ft = 1.5
- (c) Continuous-span girders elsewhere:
  - 40-ft or above = 1.0
  - Below 40-ft = 1.5
- (d) Cantilever (suspended span) girders = 2.0 (This type of bridge may have large vibrations which increase the stress cycles per truck passage. This should be investigated by the Engineer.)
- (e) Trusses = 1.0

For transverse members:

- (a) 20-ft or above spacing = 1.0
- (b) Below 20-ft spacing = 2.0



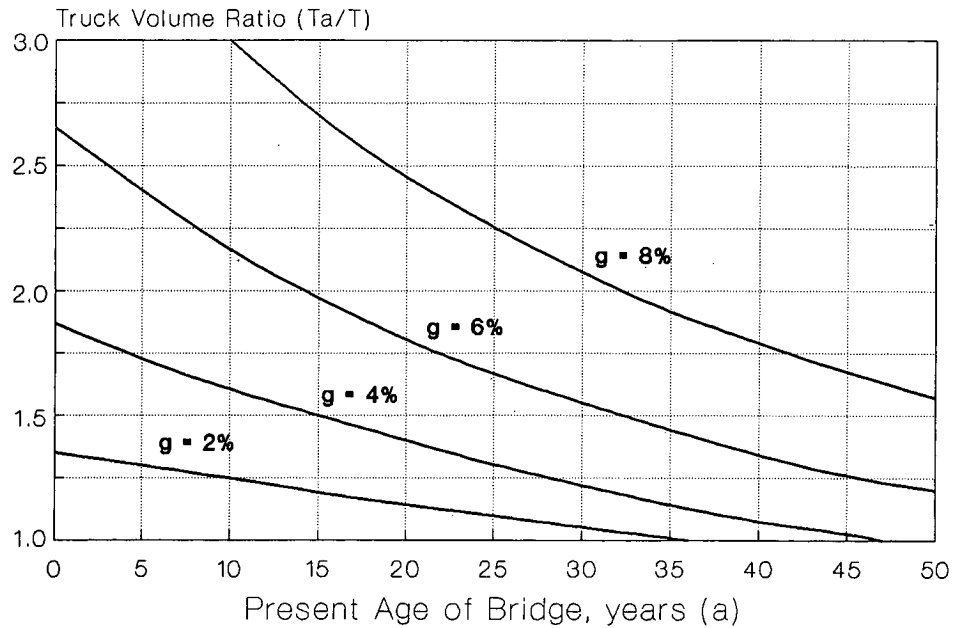


Figure 6.3.5A. Lifetime average truck volume chart.

**Alternative 1.** Use an influence line to determine the complex stress cycle caused by the passage of the fatigue truck across the bridge. Use the procedure given in Appendix C of *NCHRP Report 299* to determine the equivalent number of simple cycles.

**Alternative 2.** If the stress range is determined by field measurements, use the procedure given in *NCHRP Report 299* to determine the equivalent number of simple cycles from a stress-time plot of a typical truck passage.

No. of Lanes	2-Way Traffic	1-Way Traffic
1	—	1.00
2	0.60	0.85
3	0.50	0.80
4	0.45	0.80
5	0.45	0.80
6 or more	0.40	0.80

### 6.3.5 Lifetime Average Daily Truck Volume

Figure 6.3.5A can be used to estimate the lifetime average daily truck volume in the outer lane,  $T_a$ , from the present average daily truck volume in the outer lane,  $T$ , the present age of the bridge,  $a$ , and the annual growth rate,  $g$ . Extensive data on typical annual growth rates are given in *NCHRP Report 299* to provide guidance in selecting an appropriate value.

**6.3.5.1 Present Truck Volume.**—The present average daily truck volume in the outer lane can be calculated from the ADT at the site as follows:

$$T = (ADT) F_T F_L$$

where  $ADT$  = present average daily traffic volume (both directions) on the bridge;  $F_T$  = fraction of trucks (excluding panel, pickup, and other 2-axle/4-wheel trucks) in the traffic; if unknown, use 0.20 for rural Interstate highways, 0.15 for other rural highways and urban Interstate highways, and 0.10 for other urban highways;  $F_L$  = fraction of trucks in outer lane from table below.

### 6.4 OPTIONS IF REMAINING LIFE IS INADEQUATE

#### 6.4.1 General

Articles 6.4.2 through 6.4.5 give options that may be pursued if the Engineer considers the calculated remaining life to be inadequate. The effects of each of these options on the calculated remaining life can be determined by the procedures in Articles 6.2 and 6.3.

#### 6.4.2 Recalculate Life

Recalculate the remaining fatigue life using one or more of the alternative procedures in Articles 6.2 and 6.3.

#### 6.4.3 Restrict Traffic

Restrict the weight and/or volume of trucks passing over the bridge in critical lanes by posting and enforcement.

#### 6.4.4 Modify Bridge

Modify the bridge to improve its fatigue strength by (a) retrofitting the particular details that controlled the life, (b) adding cross section to reduce the stresses, or (c) other means.

#### 6.4.5 Institute Inspections

Institute thorough periodic inspections of the particular details that controlled the life to assure adequate safety without other changes.

## APPENDIX B

### PROPOSED FATIGUE DESIGN PROCEDURE

Section numbers correspond to present Article 10.3.1 and 10.3.2

#### 10.3 REPETITIVE LOADING AND TOUGHNESS CONSIDERATIONS

##### 10.3.1 Fatigue Check

The safe fatigue life of each detail shall exceed the desired design life of the bridge. The safe life exceeds the design life when either  $2R_S S_t < S_c$  or  $R_S S_r < S_{rp}$ , in which:

- $S_t$  = tension portion of the design stress range from Article 10.3.2
- $S_c$  = compressive dead load stress at the expected crack initiation location in the detail
- $S_r$  = design stress range from Article 10.3.2
- $S_{rp}$  = permissible stress range from Article 10.3.3
- $R_S$  = reliability factor; 1.1 for redundant members and 2.0 for nonredundant members

A member shall be considered nonredundant if, in the judgment of the Engineer, a failure of this member alone would cause collapse of the bridge.

##### 10.3.2 Design Stress Range

The design stress range,  $S_r$ , for each detail shall be calculated by following the steps in Articles 10.3.2.1 through 10.3.2.6.

**10.3.2.1 Fatigue Truck.**—A fatigue truck with the axle spacings and weight distribution shown in Figure 10.3.2.1A shall be used. If a gross-weight histogram for the truck traffic excluding panel, pickup, and other 2-axle/4-wheel trucks is available for the site, the gross weight of this truck shall be calculated from

$$W = (\sum f_i W_i^3)^{1/3}$$

where  $W$  = gross weight of fatigue truck;  $f_i$  = fraction of gross weights within an interval  $i$ ;  $W_i$  = gross weight at midwidth of interval  $i$ .

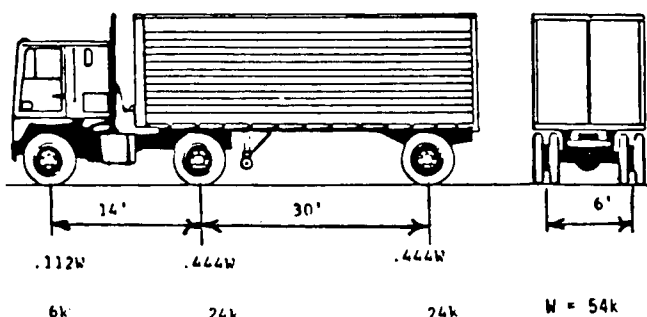


Figure 10.3.2.1A. Fatigue truck. (Note: A variable spacing of 14 to 30 ft can be used instead of the 30-ft main axle spacing, but this will significantly increase the design stress range.)

If such a histogram is not available, the gross weight shall be 54 kip.

**10.3.2.2 Truck Superpositions.**—If special site conditions are expected to cause unusual bunching of trucks, the gross weight of the fatigue truck shall be increased by 15 percent. Such special conditions include (a) a traffic signal on or near the bridge and (b) a steep hill when the bridge is on a two-lane highway.

**10.3.2.3 Impact.**—The gross weight of the fatigue truck shall be increased by 15 percent to account for impact.

**10.3.2.4 Moment.**—The moment range (or axial force range for truss members) caused at the detail under consideration by a passage of the fatigue truck across the bridge shall be calculated. For longitudinal beams, girders, stringers, or truss members, the truck shall be placed at positions that cause the algebraic maximum and minimum moments (or axial forces); the algebraic difference between the two is the moment (or axial force) range. For transverse bending members, the moment range shall equal the moment at the detail when the fatigue truck is at the center of the traffic lane that results in the highest moment.

**10.3.2.5 Lateral Distribution.**—For straight longitudinal beams, girders, or stringers, the moment range carried by the member under consideration shall be calculated by multiplying

the total moment range from Article 10.3.2.4 by a lateral-distribution factor,  $DF$ , or shall be determined by a rigorous analysis.

10.3.2.5.1 I-shaped members. If the deck is supported by two members,  $DF$  shall be determined by assuming that the deck acts as a simple beam supporting a single truck at the center of the outer traffic lane. If the deck is supported by more than two members,  $DF$  shall be determined as follows.

For interior members,  $DF = DF_i = S/D$ , but not more than  $(S - 3)/S$ ;  $S$  = girder spacing in feet; and  $D$  = factor defined below; values for intermediate span lengths may be interpolated. For positive and negative bending regions in continuous span bridges, the span length may be taken as the corresponding distance between points of dead load contraflexure.

Span (ft)	$D$
30 or less	17
40	19
60	20
90	22
120 or more	23

For exterior members,  $DF = DF_e = DF_i$  if either (a) the inner face of the curb or parapet is less than 1 ft outside the centerline of the exterior member or (b) the width of the shoulder for the outside lane is more than 4 ft; otherwise

If  $P > 0.5$ ,  $DF_e = 0.7 - 0.4P$  but not less than  $DF_i$

If  $P \leq 0.5$ ,  $DF_e = 0.9 - 0.8P$  but not less than  $DF_i$

$P$  = distance from exterior member to centerline of (nearest) outer lane divided by girder spacing; negative if centerline is outside the exterior girder

10.3.2.5.2 Box-shaped members.  $DF$  may be conservatively calculated by dividing each box into two equivalent I-beams, each consisting of one-half of the box, and applying the procedures for I-shaped members.

#### 10.3.2.6 Member Section.—

10.3.2.6.1 Bending members. The moment shall be divided by the section modulus (moment of inertia divided by distance from neutral axis to expected crack initiation location in the detail) to get  $S_r$ .

*Composite Sections.* If the deck is attached to the steel section by shear connectors, the full composite section (as defined in

Article 10.38) increased by 15 percent shall be used in positive bending regions (taken as the distance between points of dead load contraflexure) and a section including the longitudinal rebars shall be used in negative bending regions.

*Noncomposite Sections.* If the deck is not attached to the steel section by shear connectors, the steel section alone shall be used.

10.3.2.6.2 Truss members. The axial load range shall be divided by the cross sectional area to get  $S_r$ .

### 10.3.3 Permissible Stress Range For A Desired Design Life

The permissible stress range,  $S_{rp}$ , shall be determined by either (a) the simplified procedure given in Article 10.3.3.1 for a design life of 75 years or (b) the general procedure given in Article 10.3.3.2 for any desired design life.

10.3.3.1 *Simplified Procedure.*—For a design life of 75 years,

$$S_{rp} = \frac{(F)(S_{rpo})}{C^{1/3}} \text{ but not less than } S_{FL}$$

where  $F$  = detail factor from Article 10.3.3.3;  $S_{rpo}$  = normalized permissible stress range from Table 10.3.3.1A;  $C$  = cycles per truck passage from Article 10.3.3.4;  $S_{FL}$  = limiting stress range from Article 10.3.3.3.

10.3.3.2 *General Procedure.*—For any desired design life,

$$S_{rp} = \left[ \frac{K \times 10^6}{T_d C Y} \right]^{1/3} \text{ but not less than } S_{FL}$$

where  $Y$  = desired life in years;  $K$  = detail constant from Article 10.3.3.3;  $C$  = stress cycles per truck passage from Article 10.3.3.4;  $T_d$  = design truck volume from Article 10.3.3.5;  $S_{FL}$  = limiting stress range from Article 10.3.3.3.

Table 10.3.3.1A. Normalized permissible stress range.

Traffic Type	Lanes on Bridge	$S_{rpo}$ , ksi*			
		Very Heavy Traffic (ADT>8000/lane)	Heavy Traffic (ADT>2000/lane) (ADT<8000/lane)	Light Traffic (ADT>500/lane) (ADT<2000/lane)	Very Light Traffic (ADT<500/lane)
2-way	2	4.05	4.27	5.04	7.86
	4	3.54	3.74	4.40	6.89
	6	3.22	3.39	3.99	6.27
	8	2.92	3.08	3.63	5.69
1-way	1	4.31	4.54	5.36	8.40
	2	3.61	3.81	4.49	7.03
	3	3.22	3.39	3.99	6.27
	4	2.92	3.08	3.63	5.69

\* Based on (a) an annual ADT growth rate of 3%, (b) a design life of 75 years, and (c) 10% trucks for the Very Heavy and Heavy Traffic categories and 15% for the Light and Very Light Traffic categories.

10.3.3.3 *Detail Constants.*—For the detail categories defined in Table 10.3.3.3A\*, use the following values:

Detail Category	K	$S_{FL}$ (ksi)	F
A	68	8.8	1.78
B	33	5.9	1.40
B'	17	4.4	1.12
C	12	3.7**	1.00
D	6.0	2.6	.79
E	2.9	1.6	.62
E'	1.1	0.9	.45
F	2.9	2.9	.62

\* Table 10.3.3.3A of these specifications is the same as Table 10.3.1B of the 1983 AASHTO specifications and is not reproduced herein.

\*\* Use 4.40 ksi for stiffeners only.

10.3.3.4 *Cycles Per Truck Passage.*—The number of stress cycles per truck passage,  $C$ , shall be obtained from the following:

For longitudinal members:

(a) Simple-span girders:

40-ft or above = 1.0

Below 40-ft = 1.8

(b) Continuous-span girders within a distance equal to 0.1 of the span on each side of an interior support (take span equal to distance between supports):

80-ft or above =  $1 + (\text{Span} - 80)/400$  in feet

40-ft or above but below 80-ft = 1.0

Below 40-ft = 1.5

(c) Continuous-span girders elsewhere:

40-ft or above = 1.0

Below 40-ft = 1.5

(d) Cantilever (suspended span) girders = 2.0 (This type of bridge may have large vibrations which increase the stress cycles per truck passage. See *NCHRP Report 299*.)

(e) Trusses = 1.0

For transverse members:

(a) 20-ft or above spacing = 1.0

(b) Below 20-ft spacing = 2.0

10.3.3.5 *Design Truck Volume.*—The design truck volume,  $T_d$ , shall be either:

(a) Estimated by the Engineer as the average daily truck volume in the shoulder lane over the design life; use  $F_L$  to obtain trucks in shoulder lane.

(b) Obtained from Table 10.3.3.5A for the expected traffic volume at the bridge opening.

(c) Calculated by the following equations (graphs that facilitate these calculations for 75- and 100-year lives are provided in Chapter Three of *NCHRP Report 299*):

$$T = (ADT)F_TF_L; T_L = 20,000 nF_TF_L$$

$$Y_L = \frac{\log(1/R)}{\log G} \text{ where } R = \frac{T}{T_L}$$

$$\text{if } Y_L < Y, T_d = \frac{T[g(Y - Y_L) + 1 - R]}{gRY}$$

$$\text{if } Y_L > Y, T_d = \frac{T(G^Y - 1)}{gY}$$

where:

$ADT$  = expected average daily traffic volume (both directions) at the bridge opening;

$T$  = expected average daily truck volume in the outer lane at the bridge opening;

$F_T$  = fraction of trucks (excluding panel, pickup, and other 2-axle/4-wheel trucks) in the traffic; if unknown, use 0.20 for rural Interstate highways, 0.15 for other rural highways and urban Interstate highways, and 0.10 for other urban highways;

$F_L$  = fraction of trucks in shoulder lane from table below;

$n$  = number of traffic lanes on the bridge;

$Y$  = design life in years;

$Y_L$  = life in years to reach the limiting truck volume;

$G$  = truck-volume growth rate factor,  $1 + g$ ;

$g$  = truck-volume annual growth rate, percent;

$T_d$  = design truck volume; a constant  $T_d$  applied over the life of the bridge has the same effect as  $T$  growing at a rate  $g$ ;

$T_L$  = limiting truck volume.

Table 10.3.3.5A. Design truck volume.

Design Truck Volume*, $T_d$ - Trucks Per Day				
Traffic Type	Lanes on Bridge	Very Heavy Traffic** (ADT>8000/lane)	Heavy Traffic (ADT>2000/lane) (ADT<8000/lane)	Light Traffic (ADT>500/lane) (ADT<2000/lane)
2-way	2	2400	2050	1250
	4	3600	3070	1880
	6	4800	4100	2510
	8	6400	5460	3340
1-way	1	2000	1710	1040
	2	3400	2900	1770
	3	4800	4100	2510
	4	6400	5460	3340

\* Based on (a) an annual ADT growth rate of 3%, (b) a design life of 75 years, and (c) 10% trucks for the Very Heavy and Heavy Traffic categories and 15% for the Light and Very Light Traffic categories.

\*\* Based on an assumed limiting traffic volume (ADT) of 20,000 vehicles per lane.

No. of Lanes	$F_L$	
	2-Way Traffic	1-Way Traffic
1	—	1.00
2	0.60	0.85
3	0.50	0.80
4	0.45	0.80
5	0.45	0.80
6 or more	0.40	0.80

## APPENDIX C

### ALTERNATIVE PROCEDURES

This appendix gives several alternative procedures that are referred to, but not covered in detail, in the proposed fatigue evaluation and design procedures given in Appendixes A and B. Specifically, alternative procedures are given for calculating (1) the effective weight of the fatigue truck from traffic survey data, (2) lateral-distribution factors, (3) the remaining fatigue life, and (4) the equivalent number of simple cycles corresponding to a complex stress cycle for the passage of the fatigue truck across the bridge.

Two different approximate procedures are given for calculating lateral-distribution factors. One is based on a finite-element study (192, 194) and the other is based on an orthotropic-plate study (14). Both studies are described in Appendix E.

Four different procedures are given for calculating the remaining fatigue life. In the first, the remaining life is calculated by dividing the total fatigue life into two periods in which the truck-volume growth rate and the fatigue truck weight are both constant; the first period is from the opening of the bridge to the present and the second is from the present to the end of the fatigue life. In the second, the remaining life is calculated by

dividing the total fatigue life into several (more than two) periods in which the truck-volume growth rate and the fatigue truck weight are both constant. In the third, the remaining life is calculated by dividing the total fatigue life into several (more than two) periods in which the truck volume and the fatigue truck weight both remain constant. In the fourth, a procedure is presented for maintaining a record of accumulated fatigue damage that can be updated at 4-year intervals and used at any time to calculate the remaining life.

#### WEIGHT OF FATIGUE TRUCK

Traffic survey data often includes the percentages of the various types of trucks in the traffic, and the average weight of each type, but not a gross-weight histogram. Sometimes, only the percentages of the various types of trucks, and not their average weights, are available. The effective weight of the fatigue truck can be calculated from such limited traffic data in the following way (195):

1. Combine the data for the various truck types into the six main truck categories defined in Table C-1 (reproduced from Appendix D, Table D-15); exclude panel, pickup, and other 2-axle/4-wheel trucks. If the average weight of each truck category is known, multiply this weight by the appropriate  $W_e/W_a$  ratio from Table C-1 to get the corresponding effective weight for

Table C-1. Characteristics of idealized trucks for fatigue checks (representing various truck categories).

Truck Category	Types	Axle Load, %				Axle Spacing, ft.			$W_e/W_a$	Average Weight, $W_a$ , kips
		1	2	3	4	1	2	3		
2-axle single	2 axle	40	60	--	--	16	--	--	1.15	13.3
3-axle single	3 axle 4 axle	30	70	--	--	18	--	--	1.21	30.1
3-axle semitrailer	2S-1	27	40	33	--	12	32	--	1.06	28.4
4-axle semitrailer	2S-2 3S-1	23	35	42	--	12	28	--	1.10	38.1
5-axle semitrailer	3S-2 2S-3 3S-3	18	45	37	--	14	32	--	1.11	53.9
semitrailer/trailer	2S-1-2 3S-1-2	17	29	42	12	10	25	25	1.12	53.8
fatigue truck	--	11.2	44.4	44.4	--	14	30	--	--	--

Notes:

- (1)  $W_a$  = average gross weight for this truck category from latest nationwide truck survey
- (2)  $W_e$  = effective gross weight for this truck category

each category. If the known average weights are separated into loaded and empty categories, combine the loaded and empty weights into a single average for each truck category by weighting values according to the fractions of loaded and empty trucks in the traffic. Usually, about two-thirds of the semitrailers and one-half of the single units are loaded. If the average weight of each truck category is not known, use the average weight given in Table C-1 for each truck category. These average weights are based on the latest available nationwide data (122, 123) and should be reasonably accurate because the average weights of various truck types have not been changing much with time in recent years.

2. Calculate the effective weight for the site by applying the following equation to the different truck categories:

$$W_e = [f_i W_i^3]^{1/3} \quad (C-1)$$

in which  $W_i$  is the effective weight for truck category  $i$  and  $f_i$  is the fraction of category  $i$  trucks in the truck traffic.

### Effect of Axle Configuration

Equation C-1 does not include the effect of axle configuration, which depends on the bridge, but is usually small enough to be neglected as discussed in Appendix E. If desired, however, the effect of axle configuration at a particular location in the bridge can be included by following Steps 3, 4, and 5.

3. For each of the idealized trucks in Table C-1, calculate the ratio of the moment,  $M$ , caused by a given truck to the moment,  $M_f$ , caused by a fatigue truck with the same gross weight. The moments should be calculated at the location under consideration when the truck is positioned for highest moment at that location.

4. For each idealized truck, multiply the effective weight from Step 1 by the corresponding  $M/M_f$  ratio to get a new effective weight for that truck. Using these new effective weights in Eq. C-1, calculate the fatigue truck weight including the effect of axle configuration.

5. For continuous-span bridges, a moment ratio at the location under consideration could be calculated with the truck at the location resulting in the highest negative-bending moment as well as the highest positive-bending moment. The moment ratios calculated for the two truck locations may differ, and could be used to calculate a moment ratio based on the moment range. This refinement, however, would rarely be justified because the effect of axle configuration is small and the effect of this refinement would be even smaller.

### LATERAL-DISTRIBUTION FACTORS

Two alternative procedures are given for calculating lateral-distribution factors. One is based on a finite-element study (192, 194) and the other is based on an orthotropic-plate study (14). Both studies are described in Appendix E. Both alternative procedures agree reasonably well with lateral-distribution factors measured on actual bridges as discussed in Appendix E.

#### Finite-Element Study

The following approximate equations can be used to calculate lateral-distribution factors when there are more than two beams,

girders, or stringers, and the spacing of these members does not exceed 14 ft.

For interior beams, girders, or stringers:

$$I_{max} = 3.3 L^{2.3} \quad (C-2)$$

$$a = -\log_{10} (0.23 L^{0.25}) \quad (C-3)$$

$$DF_i = 0.5 [I/I_{max}]^a \text{ but not greater than } 0.5 \quad (C-4)$$

For exterior beams, girders, or stringers:

$$\text{If } P \leq 0.5 \quad DF_e = 0.9 - 0.8P \text{ but not less than } DF_i \quad (C-5)$$

$$\text{If } P > 0.5 \quad DF_e = 0.7 - 0.4P \text{ but not less than } DF_i \quad (C-6)$$

In these equations,  $DF_i$  = lateral-distribution factor for interior members;  $DF_e$  = lateral-distribution factor for exterior members;  $P$  = lane position ratio—distance from exterior beam to the centerline of the (nearest) outer traffic lane divided by the spacing between the exterior beam and the first interior beam—negative if outer-lane centerline is outside the exterior beam;  $L$  = distance in feet between supports for span in which the truck (or heaviest wheel) is positioned; and  $I$  = moment of inertia, either composite or noncomposite, of the beam, girder, or stringer in the central positive-bending region in inches<sup>4</sup>—highest moment of inertia if beams are not all the same.

### Orthotropic-Plate Study

The following approximate equations can be used to calculate lateral-distribution factors when there are more than two beams, girders, or stringers:

$$DF = 50 S / \{ D (100 + C_f + C_e) \} \quad (C-7)$$

$$= (w - 11) / 2 \text{ but not greater than } 1.0 \quad (C-8)$$

where:  $DF$  = lateral-distribution factor;  $S$  = spacing of girders, beams, or stringers, in feet;  $D$  = a factor defined in Figures C-1 and C-2, in feet;  $C_f$  = a factor defined in Figure C-3, in percent;  $C_e$  = a factor defined in Figures C-4 and C-5, in percent;  $w$  = a factor related to the traffic lane width; and  $w$  = width of traffic lane, in feet.

The factors  $D$  and  $C_e$  differ for exterior and interior girders and depend on the span length and number of traffic lanes on the bridge. For continuous-span bridges, the equivalent span lengths defined in Figure C-6 should be used for the positive-bending and negative-bending regions.

### REMAINING LIFE

Four alternative procedures for calculating the remaining fatigue life are given here; these procedures are intended for use in conjunction with Appendix A. Three of these procedures use two or more time periods in which the weight of the fatigue truck is assumed to remain constant. In one of these, the truck volume is also assumed to remain constant during each time period. In the other two, the truck volume is assumed to grow at a constant compound rate during each period. The fourth alternative procedure facilitates the monitoring of fatigue damage at 4-year inspection intervals and the calculation of re-

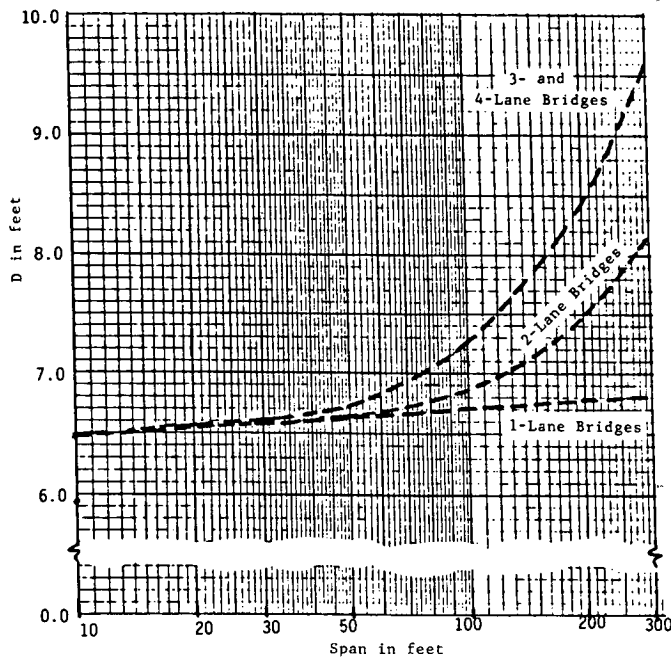


Figure C-1. Values of  $D$  for exterior girders.

maintaining life from these damage data. The symbols used in these four procedures are defined as follows:

- $S_r$  = stress range calculated for a fatigue truck weight,  $W$ , based on present traffic (see Appendix A)
- $K$  = detail constant (see Appendix A)
- $C$  = stress cycles per truck passage (see Appendix A)
- $R_s$  = reliability factor associated with the calculation of  $S_r$  (see Appendix A)
- $T$  = average daily truck volume in the shoulder lane; present volume if used without a subscript (see Appendix A)
- $W$  = gross weight of fatigue truck in kips; present weight if used without a subscript (see Appendix A)
- $Y$  = time period in years; total fatigue life based on present traffic conditions ( $T$  and  $W$ ) if used without a subscript;  $Y$  is generally different for each detail on the bridge
- $g$  = compound annual growth rate (expressed as a decimal) for  $T$
- $G$  = growth rate factor;  $1 + g$
- $D$  = fatigue damage (expressed in years) caused during a time period; when  $D_i = Y$ , the fatigue life is exhausted;  $D$  is the same for each detail in the bridge
- $e$  = 1.0 for calculating safe life and 2.0 for calculating mean life (see Appendix A)

Some of these variables have double subscripts. The first subscript refers to the following:

- $p$  = past period from the opening of the bridge to the present
- $f$  = final period; from the present to the end of the fatigue life if there are only two periods
- $i$  = incremental period
- $r$  = remaining period from present to end of the fatigue life
- $L$  = limiting value, or limiting period from the start of the

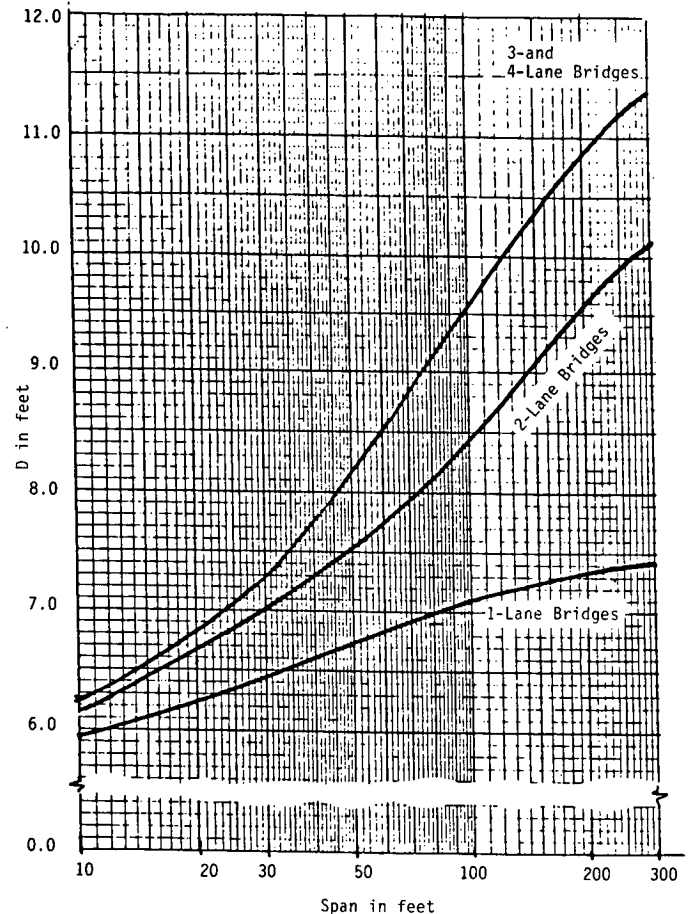


Figure C-2. Values of  $D$  for interior girders.

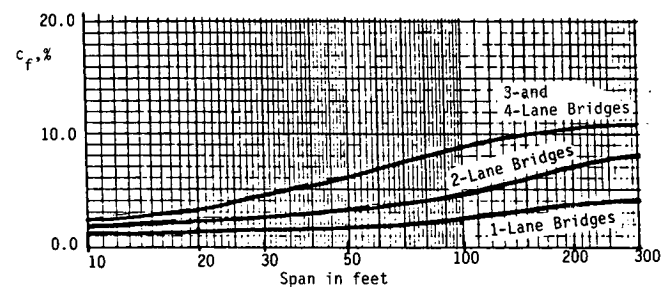


Figure C-3. Values of  $C_f$ .

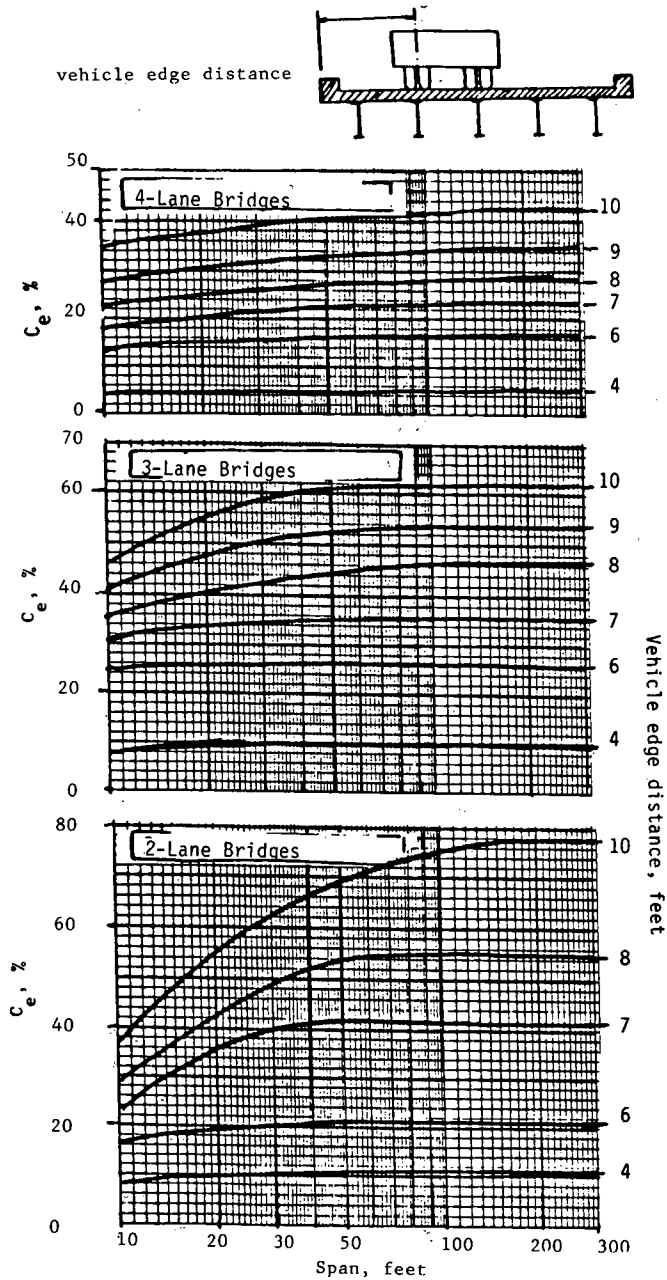
final period until the limiting truck volume is reached (see Appendix A)

$a$  = accumulated value; used in connection with  $D$

The second subscript (used in connection with  $T$ ) refers to the following:

- $s$  = value at start of a period
- $e$  = value at end of a period
- $a$  = average value for a period

The basic relationships are as follows:

Figure C-4. Values of  $C_e$  for exterior girders.

$$Y = e K \times 10^6 / \{C T (R_s S_r)^3\} \quad (C-9)$$

For a no-growth period:

$$D_i = (T_{ia}/T) (W_i/W)^3 Y_i \quad (C-10)$$

For a constant-growth period:

$$D_i = (T_{ia}/T) (W_i/W)^3 (G_i^Y - 1)/g_i \quad (C-11)$$

if  $g_i = 0$ ,  $(G_i^Y - 1)/g_i = Y_i$

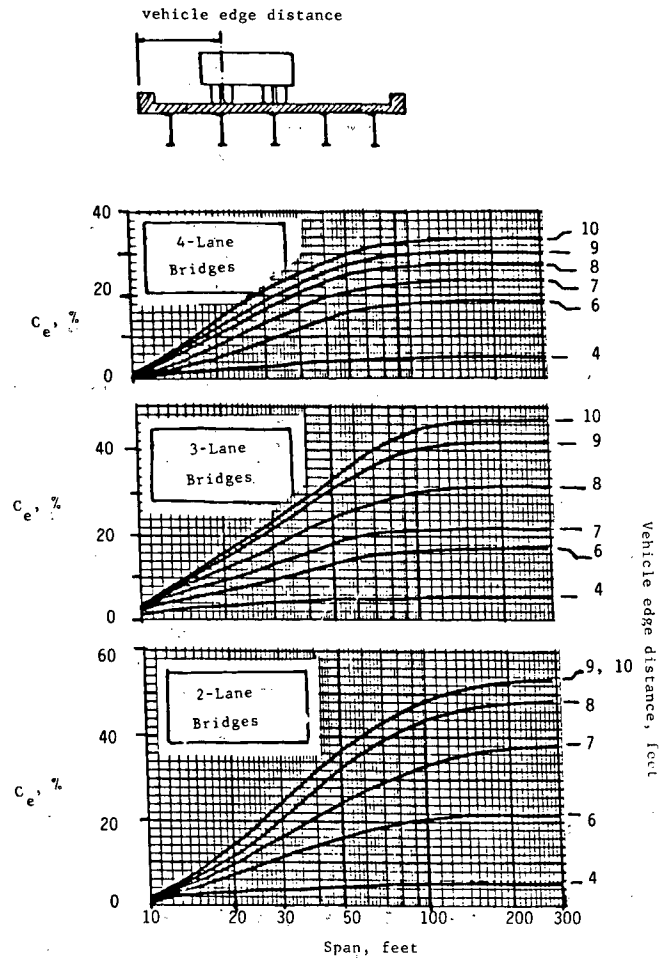
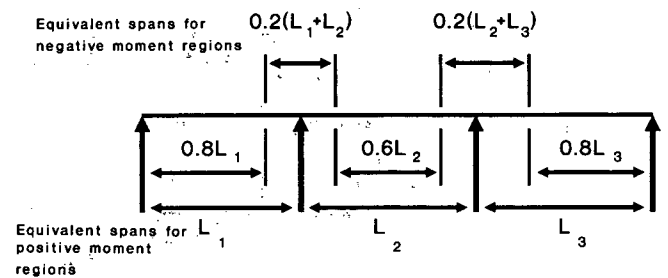
Figure C-5. Values of  $C_e$  for interior girders.

Figure C-6. Equivalent span lengths for continuous-span bridges.

#### Two Constant-Growth Time Periods

1. Divide the fatigue life into two time periods in which the truck-volume growth rate and fatigue-truck gross weight are both assumed to remain constant. One period extends from the opening of the bridge to the present and the other extends from the present to the end of the fatigue life.



2. Using Eq. C-9, calculate the fatigue life,  $Y$ , in years based on present traffic conditions.

3. Calculate the past fatigue damage,  $D_p$ .

$$D_p = (W_p/W)^3 (G_p^Y - 1)/(g_p G_p^Y) \quad (C-12)$$

if  $g_p = 0$ ,  $(G_p^Y - 1)/(g_p G_p^Y) = Y_p$

4. Calculate the time,  $Y_L$ , to reach the limiting truck volume,  $T_L$ .

$$Y_L = \log (T_L/T) / \log G_f \quad (C-13)$$

5. Calculate the fatigue damage,  $D_L$ , to reach the limiting truck volume,  $T_L$ .

$$D_L = (W_f/W) (G_f^Y - 1)/g_f \quad (C-14)$$

if  $g_f = 0$ ,  $(G_f^Y - 1)/g_f = Y_L$

6. Calculate the remaining fatigue life,  $Y_f$ .

$$\text{if } (D_p + D_L) > Y, Y_f = \log C / \log G_f \quad (C-15)$$

$$\text{where } C = 1 + g_f(Y - D_p)(W_f/W)^3 \quad (C-16)$$

$$\text{if } (D_p + D_L) \leq Y, Y_f = Y_L + (Y - D_p - D_L)(T/T_L)(W/W_f)^3 \quad (C-17)$$

#### More Than Two Constant-Growth Time Periods

1. Divide the fatigue life into any number of periods in which the truck-volume growth rate and fatigue-truck gross weight are both assumed to remain constant. The start of the final period must be defined, but the end is unknown.

2. Using Eq. C-9, calculate the fatigue life,  $Y$ , in years, based on present traffic conditions.

3. Calculate the truck volume,  $T_{is}$ , at the start of each period.

(a) Starting with the present truck volume as  $T_{ie}$ , work backward through time:

$$T_{is} = T_{ie}/G_f^Y \quad (C-18)$$

(b) Starting with the present truck volume as  $T_{is}$ , work forward.

$$T_{ie} = T_{is} G_f^Y \quad (C-19)$$

(c) If the truck volume at the start of any period exceeds the limiting truck volume, redefine the previous period to end when the truck volume equals the limiting value and use this end point as the start of the final period. Use the following equation to redefine the point.

$$Y_i = \log (T_L/T_{is}) / \log G_i \quad (C-20)$$

4. Calculate the fatigue damage,  $D_i$ , for each period except the last by using Eq. C-11.

5. Calculate the remaining fatigue life,  $Y_r$ , by adding the life for the final period,  $Y_f$ , to the time from the present to the start of the final period. (a) If  $D_i > Y$ , the fatigue life is exhausted

before the beginning of the final period; redefine the start of the final period so that  $D_i < Y$ . (b) If the truck volume,  $T_{fs}$ , at the start of the final period is less than the limiting truck volume,  $T_L$ , calculate the time,  $Y_L$ , to reach the limiting volume and the fatigue damage caused during this period.

$$\text{if } (D_i + D_L) > Y, Y_f = \log C / \log G_f \quad (C-21)$$

in which

$$C = 1 + g_f(Y - D_i)(T/T_f)(W/W_f)^3 \quad (C-22)$$

if  $(D_i + D_L) < Y$ ,

$$Y_f = Y_L + (Y - D_i - D_L)(T/T_L)(W/W_f)^3 \quad (C-23)$$

$$D_L = (T_{fs}/T)(W_f/W)^3 (G_f^Y - 1)/g_f \quad (C-24)$$

$$\text{if } g = 0, (G_f^Y - 1)/g_f = Y_L$$

The remaining life is equal to  $Y_f$  plus the time from the present to the start of the final period. (c) If the truck volume,  $T_{fs}$ , at the start of the final period equals the limiting truck volume,  $T_L$ ,

$$Y_f = (Y - D_i)(T/T_L)(W/W_f)^3 \quad (C-25)$$

#### More Than Two No-Growth Time Periods

1. Divide the fatigue life into any number of periods in which the truck-volume and fatigue-truck gross weight are both assumed to remain constant. The start of the final period must be defined, but the end is unknown. This case can be obtained from the preceding case by using a growth rate of 0, but is presented here in a simpler form.

2. Using Eq. C-9, calculate the fatigue life,  $Y$ , in years based on present traffic conditions.

3. Calculate the fatigue damage caused in each period except the last by using Eq. C-10.

4. Calculate the remaining life,  $Y_r$ , by adding the life for the final period,  $Y_f$ , to the time from the present to the start of the final period.

$$Y_f = (Y - D_i)(T/T_f)(W/W_f)^3 \quad (C-26)$$

#### Monitoring Fatigue Damage

In a bridge, truck traffic produces cyclic stresses that cause progressive fatigue damage. Generally, this damage can not be detected by inspection, but can be monitored by maintaining a record of the truck volume and weights that pass over the bridge. This can be conveniently done in connection with the routine inspections that are required at 2-year intervals according to the AASHTO maintenance-inspection manual (132). Specifically, the truck volume, and also the fatigue-truck weight if possible, are recorded at 4-year intervals (every other inspection).

The truck volume,  $T_{ia}$ , can be obtained from the ADT volume by the procedures given in Article 6.3.5.1 of Appendix A, and the fatigue-truck weight,  $W_i$ , can be obtained from truck-weight histograms, or other data, by the procedures given in Article 6.2.2 of Appendix A. The following procedures can then be

used to calculate (a) the incremental fatigue damage caused over each 4-year period, (b) the accumulated fatigue damage, and (c) the remaining safe fatigue life.

1. Using Eq. C-9, calculate the fatigue life,  $Y$ , of each detail in the bridge based on traffic conditions when the monitoring procedure is first started. These calculations need to be made only once.

2. Calculate the past fatigue damage,  $D_p$ , when the monitoring procedure is first started; if the bridge has just been opened at that time, there will be no fatigue damage. The calculated value of  $D_p$  is the same for all details in the bridge and does not need to be updated in the future.

$$D_p = (W_p/W)^3 (G_p^Y - 1)/(g_p G_p^Y) \quad (C-27)$$

if  $g_p = 0$ ,  $(G_p^Y - 1)/(g_p G_p^Y) = Y_p$

3. Calculate the incremental fatigue damage,  $D_i$ , for the latest 4-year period from the average truck volume,  $T_{ia}$ , and fatigue-truck weight,  $W_i$ , for the period. These values may be obtained by averaging the corresponding values at the start and end of the period. The incremental damage is the same for all details in the bridge.

$$D_i = (T_{ia}/T)(W_i/W)^3 Y_i = 4 (T_{ia}/T)(W_i/W)^3 \quad (C-28)$$

4. Calculate the fatigue damage,  $D_a$ , accumulated from the opening of the bridge to the end of the present period; this is the same for all details in the bridge.

$$D_a = D_p + D_i \quad (C-29)$$

5. Calculate the time,  $Y_L$ , from the end of the latest period to reach the limiting truck volume,  $T_L$ .

$$Y_L = \log (T_L/T_{ie})/\log G_f \quad (C-30)$$

6. Calculate the damage,  $D_L$ , to reach the limiting truck volume,  $T_L$ ; this is the same for all details in the bridge.

$$D_L = (T_{ie}/T)(W_f/W)^3 (G_f^Y - 1)/g_f \quad (C-31)$$

if  $g_f = 0$ ,  $(G_f^Y - 1)/g_f = Y_L$

7. Calculate the remaining safe fatigue life,  $Y_f$ .

$$\text{if } (D_a + D_L) > Y, Y_f = \log C/\log G_f \quad (C-32)$$

$$\text{in which } C = 1 + g_f(Y - D_a)(T/T_f)(W/W_f)^3 \quad (C-33)$$

$$\text{if } (D_a + D_L) \leq Y,$$

$$Y_f = Y_L + (Y - D_a - D_L)(T/T_L)(W/W_f)^3 \quad (C-34)$$

## Derivations

The basic growth equations used in the preceding alternative procedures are given in Appendix D. Other basic equations included in the preceding procedures are derived below.

## Basic Fatigue Life Equation

The total number of cycles to failure,  $N$ , is commonly defined as

$$N = A/(R_s S_r)^3 \quad (C-35)$$

in which  $A$  is a detail constant and the exponent 3 is the slope of the SN curve (119). The value of 3 is appropriate for typical bridge members (119). For a constant truck volume,  $T$ , and number of stress cycles per truck passage,  $C$ , the total number of cycles in  $Y$  years is

$$N = 365 T C Y \quad (C-36)$$

For convenience, a new detail constant  $K$  is defined as

$$K = A/(365 \times 10^6) \quad (C-37)$$

By combining, Eqs. C-35 through C-37

$$Y = e K \times 10^6 / \{ T C (R_s S_r)^3 \} \quad (C-38)$$

## Years to Reach Limiting Truck Volume

For truck volume growing at a constant compound rate,  $g$ , from a present value of,  $T$ , to a limiting value of,  $T_L$

$$T_L = T G^Y \quad (C-39)$$

in which  $G$  is the growth rate factor,  $1 + g$ , and  $Y_L$  is the number of years to reach  $T_L$ . Thus,

$$\log (T_L/T) = Y_L \log G \quad (C-40)$$

and

$$Y_L = \log (T_L/T)/\log G \quad (C-41)$$

## Damage Equations

It is convenient in the present study to express the fatigue damage,  $D_i$ , done during a given time period in terms of years; when  $D_i = Y$ , the fatigue life is exhausted. If the traffic conditions ( $T$  and  $W$ ) used in calculating  $Y$  remain constant over the entire life of the bridge, the damage caused during any time period is merely equal to the length of that time period in years,  $Y_i$ . However, for any time period,  $i$ , in which the  $T_i$  and/or  $W_i$  differ from the base values ( $T$  and  $W$ ) used in calculating  $Y$ , the damage for this period is greater or lesser than  $Y_i$ . Specifically,

$$D_i = (T_i/T)(W_i/W)^3 Y_i \quad (C-42)$$

for a period in which the truck volume is assumed to remain constant. As defined in Eq. C-35, the damage is proportional to the number of cycles that occur during the period and to the

cube of the stress range. The number of cycles, in turn, is proportional to the truck volume during the period, and the stress range, in turn, is proportional to the fatigue-truck weight.

If the truck volume varies at a constant compound growth rate,  $g$ , during the period, the number of cycles,  $N_i$ , that occur during the period is given by

$$N_i = 365 T_{is} (G^Y - 1)/g \quad (C-43)$$

The corresponding  $N$  for the base truck volume of  $T$  is

$$N = 365 T Y_i \quad (C-44)$$

Thus, the damage for the period is given by

$$D_i = (T_{is}/T) (W_i/W)^3 (G^Y - 1)/g \quad (C-45)$$

Similarly, the damage,  $D_L$ , that occurs from the start of the final period until the limiting truck volume,  $T_L$ , is reached is

$$D_L = (T_{fs}/T) (W_f/W)^3 (G^Y - 1)/g \quad (C-46)$$

#### Remaining Life Equations

The damage,  $D_f$ , for the final period combined with the damage for all previous periods must equal the fatigue life,  $Y$ . Thus,

$$Y = D_i + D_f \quad (C-47)$$

If the truck volume,  $T_f$ , is assumed to remain constant during the final period,  $D_f$  is given by Eq. C-42 and

$$Y = D_i + (T_f/T) (W_f/W)^3 Y_f \quad (C-48)$$

$$Y_f = (Y - D_i) (T/T_f) (W/W_f)^3 \quad (C-49)$$

If the truck volume,  $T_f$ , grows at rate  $g$  during the final period, two different cases must be considered. The choice between the two depends on the value of  $D_L$  from Eq. C-46. If  $(D_i + D_L) < Y$ ,  $T_f$  does not reach  $T_L$  before the fatigue life is exhausted and  $D_f$  is given by Eq. C-45. Thus,

$$Y = D_i + (T/T_f)(W/W_f)^3 (G^Y - 1)/g \quad (C-50)$$

Let,

$$C = 1 + g(Y - D_i)(T/T_f)(W/W_f)^3 \quad (C-51)$$

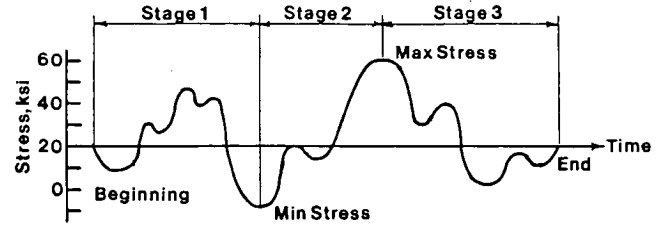
Then,

$$Y_f = \log C / \log G \quad (C-52)$$

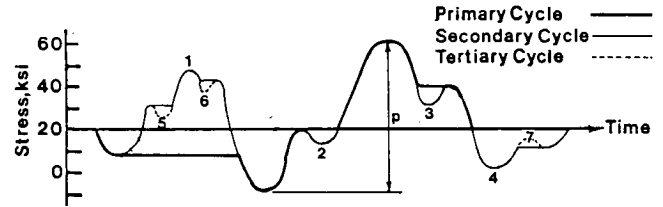
If  $(D_i + D_L) > Y$ ,  $T_f$  reaches  $T_L$  before the fatigue life is exhausted and  $D_f$  is the sum of the damage defined in Eqs. C-42 and C-46. Thus,

$$Y = D_i + D_L + (Y_f - Y_L)(T/T_f)(W_f/W)^3 \quad (C-53)$$

$$Y_f = Y_L + (Y - D_i - D_L)(T/T_L)(W/W_f)^3 \quad (C-54)$$



Complex Cycle



Decomposed Complex Cycle

Cycle Number	Cycle Order	Stress Range, ksi	Base Stress $S_b$ , ksi	$S_{ri}/S_{rp}$	$(S_{ri}/S_{rp})^3$
P	1	70	20	1.000	1.000
1	2	40	8	0.571	0.187
2	2	6	20	0.086	0.001
3	2	9	40	0.129	0.002
4	2	18	20	0.257	0.017
5	3	5	30	0.071	0.000
6	3	4	43	0.057	0.000
7	3	5	11	0.071	0.000
					1.207
					Equivalent Cycles

Figure C-7. Calculations of equivalent number of cycles.

#### EQUIVALENT CYCLES

The equivalent number of simple cycles for a complex cycle can be calculated (189, 193) in the following way (see also Figure C-7). The reversals included in a complex cycle cause the same amount of fatigue damage as individual simple cycles of the same size. Therefore, the complex cycle is first decomposed into several individual cycles of different sizes as shown in Figure C-7. These cycles of different sizes are then represented by an equivalent number of cycles of the same size. The method of decomposing the complex cycle is similar to the rain-flow method (47, 74).

The complex cycle begins and ends at the same stress—the base stress. The complex cycle consists of three stages. Stage 1 is between the beginning and the maximum or minimum stress

for the cycle, whichever is closer. Stage 2 is between the maximum and minimum stresses for the cycle. Stage 3 is between the end and the maximum or minimum stress, whichever is closer. If the entire curve is above or below the base stress, Stage 2 does not exist.

The complex cycle can be decomposed into a primary cycle and one or more higher order (secondary, tertiary, etc.) cycles. The algebraic difference between the maximum and minimum stresses is the stress range for the primary cycle. Each higher order cycle begins and ends at the same stress—the base stress for that cycle. Each higher order cycle has one peak or valley, and the algebraic difference between this peak or valley and the base stress for that cycle is the stress range for the cycle. A cycle of any order may include higher order cycles.

Within each stage, the primary cycle follows a path without reversal as shown in Figure C-7. When the path of the complex cycle reverses within a stage, the primary cycle moves horizon-

tally to intersect this path at a later point. This horizontal line is the base stress for the next higher order cycle.

Fatigue damage is proportional to the stress range,  $S_r$ , cubed. For example, the fatigue life at a stress range of 25 ksi is 8 times the life at a stress range of 50 ksi. Thus, each higher order cycle does  $(S_{ri}/S_{rp})^3$  times as much damage as the primary cycle, and the equivalent number of cycles (primary cycles) for a complex cycle is

$$N_e = 1 + (S_{r1}/S_{rp})^3 + (S_{r2}/S_{rp})^3 \dots + (S_{rn}/S_{rp})^3 \quad (C-55)$$

in which  $S_{rp}$  is the stress range for the primary cycle, and  $S_{ri}$  is the stress range for a higher order cycle. The equation conservatively neglects any effects of fatigue limit on the equivalent number of cycles.

## APPENDIX D AND APPENDIX E

Appendixes D and E contained in the report as submitted by the research agency are not published herein. Their titles are listed here for the convenience of those interested in the subject area. Qualified researchers may obtain loan copies of the unedited agency report by written request to the NCHRP, Transportation Research Board, 2101 Constitution Avenue, NW, Washington, DC 20418.

The titles are:

- Appendix D—Traffic Loading Data
- Appendix E—Bridge Response Data

## APPENDIX F

### REFERENCES AND BIBLIOGRAPHY

- (1) Abtahi, A., Albrecht, P., & Irwin, G. R., "Fatigue of Periodically Overloaded Stiffener Detail," *Journal of the Structural Division, ASCE*, Vol. 102, No. ST11, Nov., 1976.
- (2) Albrecht, P. A., & Simon, S., "Fatigue Notch Factors for Structural Details," *Journal of the Structural Division, ASCE*, Vol. 107, No. ST7, July, 1981.
- (3) Albrecht, P. A., & Yamada, K., "Rapid Calculation of Stress Intensity Factors," *Journal of the Structural Division, ASCE*, Vol. 103, No. ST2, Feb., 1977.
- (4) Albrecht, P., "Review of Fatigue Design Methods for Highway Bridges," Department of Civil Engineering, University of Maryland, College Park, MD, March, 1986.
- (5) Albrecht, P., "Fatigue Reliability Analysis of Highway Bridges," Department of Civil Engineering, University of Maryland, College Park, MD, May, 1982.
- (6) Albrecht, P., "Analysis of Fatigue Reliability," Department of Civil Engineering, University of Maryland, College Park, MD, Jan., 1981.
- (7) Albrecht, P., & Duerling, K., "Probabilistic Fatigue Design of Bridges for Truck Loading," Department of Civil Engineering, University of Maryland, College Park, MD, June, 1979.
- (8) Albrecht, P., & Friedland, I. M., "Fatigue-Limit Effect on Variable-Amplitude Fatigue of Stiffeners," *Journal of the Structural Division, ASCE*, Vol. 105, No. ST12, Dec., 1979.
- (9) Albrecht, P., & Naeemi, A. H., "Performance of Weathering Steel in Bridges," *NCHRP Report 272*, July, 1984.
- (10) Albrecht, P., & Yamada, K., "Simulation of Service Fatigue Loads for Short-Span Highway Bridges," *STP671, ASTM*, 1979.
- (11) Albrecht, P., et al. "Guidelines for the Design of Weathering Steel Bridges," *Sheladia Associates, Inc.*, Riverdale, MD, June, 1986.
- (12) Anderson, K. E., & Chong, K. P., "Least Cost Computer-Aided Design of Steel Girders," *Engineering Journal, AISC*, Vol. 23, No. 4, 4th Quarter, 1986.
- (13) Ang, A. H. S., & Munse, W. H., "Practical Reliability Basis for Structural Fatigue," presented at the April 14-18, 1975, *ASCE National Structural Engineering Conference* held in New Orleans, LA (Preprint 2494).
- (14) Aziz, T. S., & Alizadeh, A., "Transverse Distribution of Vehicle Loads on Highway Bridges," *Acres Consulting Services Limited, Toronto, Canada*, 1976.
- (15) Bakht, B., & Csagoly, P. F., "Bridge Testing," *Ministry of Transportation and Communications, Toronto, Ontario, Canada*, Aug., 1979.
- (16) Baldwin, J. W., Salame, H. J., & Duffield, R. C., "Fatigue Test of a Three-Span Composite Highway Bridge," *Report 73-1, Department of Civil Engineering, University of Missouri, Columbia, MO*, June, 1978.
- (17) Barsom, J. M., "Fatigue Considerations for Steel Bridges," *STP738, ASTM*, 1981.
- (18) Barsom, J. M., & Novak, S. R., "Subcritical Crack Growth and Fracture of Bridge Steels," *NCHRP Report 181*, 1977.
- (19) Beal, D. B., "Load Testing of Highway Bridges," *Quarterly R & D Digest No. 24, Engineering Research and Development Bureau, New York State Department of Transportation, Albany, NY*, 1983.
- (20) Bellenoit, J. R., Yen, B. T., & Fisher, J. W., "Stresses in Hanger Plates of Suspended Bridge Girders," *Transportation Research Record 950, TRB*, 1984.
- (21) Bellomo, S. J., et al., "Evaluating Options in Statewide Transportation Planning/Programming Techniques and Applications," *NCHRP Report 199*, 1979.
- (22) Benjamin, J. R., & Cornell, C. A., "Probability, Statistics and Decision for Civil Engineers," *McGraw Hill*, 1970.
- (23) Booth, G. S., "A Review of Fatigue Strength Improvement Techniques," *Welding Institute (England)*, 1983.
- (24) Booth, G. S., & Wylde, J. G., "Defect Assessment for Fatigue - Example Solutions Using the the Techniques Described in PD6493," *Welding Institute Research Bulletin (England)*, Vol 23, No. 3, March, 1982.
- (25) Boulton, C. F., "On the Influence of Tensile and Compressive Peak Overloads on Fatigue Crack Propagation in Structural Steels - A Progress Report," *Welding Institute Research Report 5/1976/E, (England)*, March, 1976.
- (26) Bowers, D. G., "Loading History Span No. 10 Yellow Mill Pond Bridge I-95, Bridgeport, Connecticut," *Research Report, Connecticut Department of Transportation, Wethersfield, CT*, May, 1972.

- (27) Bowman, M. D., & Yao, J. T. P., "Fatigue Damage Assessment of Welded Steel Structures," presented at the May 17, 1983, W. H. Munse Symposium, Behavior of Metal Structures, Research to Practice held in Philadelphia, PA.
- (28) "Bridge Inspection," OECD Road Research Group, Director of Information, OECD, 2 rue Andre-Pascel, 75775 Paris (France), 1976.
- (29) "Bridge Inspector's Training Manual," FHWA, 1979.
- (30) "Bridge Loading: Research Needed," by the ASCE Committee on Loads and Forces on Bridges, P. B. Buckland, Chmn., Journal of the Structural Division, ASCE, Vol. 108, No. ST5, May, 1982.
- (31) Burdette, E. G., Goodpasture, D. W., & Doyle, S. K., "Comparison of Measured and Computed Load-Deflection Behavior of Two Highway Bridges," Transportation Research Record 507, TRB, 1974.
- (32) Christiano, P. O., & Goodman, L. E., "Bridge Stress Range History," Highway Research Record 382, 1972.
- (33) Christiano, P., Goodman, L. E., & Sun, C. N., "Bridge Stress Range History and Diaphragm Stiffening Investigation," Department of Civil Engineering and Hydraulics, University of Minnesota, Minneapolis, MN, June, 1970.
- (34) Cicci, F., & Csagoly, P. F., "Assessment of the Fatigue Life of a Steel Girder Bridge," Transportation Research Record 507, TRB, 1974.
- (35) Crabtree, J., & Deacon, J., "Highway Sizing," Transportation Research Record 869, TRB, 1982.
- (36) Csagoly, P. F., Campbell, T. I., & Agarwal, A. C., "Bridge Vibration Study," Ontario Ministry of Transportation and Communications, Downsview, Ontario, Sept., 1972.
- (37) Cudney, G. R., "Stress Histories of Highway Bridges," Journal of the Structural Division, ASCE, Vol. 94, No. ST12, Dec., 1968.
- (38) Cudney, G. R., "The Effects of Loadings on Bridge Life," Research Report No. R-638, Michigan Department of State Highways, Lansing, MI, Jan., 1968.
- (39) Dally, J. W., & Panizza, G. A., "A New Fatigue Damage Indicator," Illinois Institute of Technology, Sept. 15, 1970.
- (40) Dederman, A. H., "Dynamic Tests of Two Cantilever Type, Deck Steel Girder Bridges," Nebraska Department of Roads, Lincoln, NE, Aug., 1961.
- (41) Deen, R. C., & Havens, J. H., "Fatigue Analysis from Strain Gage Data and Probability Analysis," Research Report 411, Kentucky Department of Transportation, Nov., 1974.
- (42) "Design Recommendations for Cyclic Loaded Welded Steel Structures, XIII-998-81/XV-494-81," International Institute of Welding, Joint Working Group XIII-XV, A. Hobbacher, Chmn., Welding Institute (England), June, 1982.
- (43) Desrosiers, R. D., "The Development of a Technique for Determining the Magnitude and Frequency of Truck Loadings on Bridges," Civil Engineering Department, University of Maryland, College Park, MD, April, 1969.
- (44) Dimmick, T. B., "Traffic Trends on Rural Roads in 1947," Public Roads, Vol. 25, No. 3, March, 1949.
- (45) Dorton, R. A., "The Conestogo River Bridge Design and Testing," presented at the 1976 Canadian Structural Engineering Conference, 1976.
- (46) Douglas, T. R., & Karrh, J. B., "Fatigue of Bridges Under Repeated Highway Loadings," Civil Engineering Department Report 54, University of Alabama, Tuscaloosa, AL, April, 1971.
- (47) Dowling, N. E., "Fatigue Failure Predictions for Complicated Stress-Strain Histories," Report 337, University of Illinois, Urbana-Champaign, IL, 1971.
- (48) Dubuc, J., et al., "Unified Theory of Cumulative Damage in Metal Fatigue," WRC Bulletin 162, Welding Research Council, June, 1971.
- (49) Edinger, J. A., "Influence of Increased Gross Vehicle Weight on Fatigue and Fracture Resistance of Steel Bridges," MS thesis submitted to the Department of Civil Engineering, Lehigh University, Bethlehem, PA, 1981.
- (50) Ellingwood, B., et al., "Development of a Probability Based Load Criterion for American National Standard A58," NBS Special Publication 577, National Bureau of Standards, June, 1980.
- (51) "Fatigue Analysis of Existing Bridges," Connecticut Department of Transportation, Wethersfield, CT, July, 1984.
- (52) Faulkner, M. G., & Bellow, D. G., "Improving the Fatigue Strength of Butt Welded Steel Joints by Peening," Welding Research International, Vol. 5, 1975.

- (53) Fenves, S. J., Veletsos, A. S., & Siess, C. P., "Dynamic Studies of Bridges on AASHTO Road Test," Publication 968, TRB, 1962.
- (54) Fisher, J. W., "Fatigue and Fracture in Steel Bridges," John Wiley & Sons, New York, NY, 1984.
- (55) Fisher, J. W., "Inspecting Steel Bridges for Fatigue Damage," Fritz Engineering Laboratory Report No. 386-15(81), Lehigh University, Bethlehem, PA, March, 1981.
- (56) Fisher, J. W., "Fatigue Cracking in Bridges from Out-of-Plane Displacements," Canadian Journal of Civil Engineering, Vol. 5, No. 4, 1978.
- (57) Fisher, J. W., "Bridge Fatigue Guide," AISC, 1977.
- (58) Fisher, J. W., & Mertz, D. R., "Hundreds of Bridges -- Thousands of Cracks," Civil Engineering, Vol. 55, No. 4, April, 1985.
- (59) Fisher, J. W., & Mertz, D. R., "Displacement Induced Fatigue Cracking of a Box Girder Bridge," IABSE Symposium on Maintenance, Repair, and Rehabilitation of Bridges held in Washington, DC, in 1982.
- (60) Fisher, J. W., & Struik, J. H. A., "Guide to Design Criteria for Bolted and Riveted Joints," John Wiley & Sons, New York, NY, 1974.
- (61) Fisher, J. W., & Yuceoglu, U., "A Survey of Localized Cracking in Steel Bridges," Interim Report DOT-FH-11-9506, FHWA, Dec., 1981.
- (62) Fisher, J. W., Mertz, D. R., & Zhong, A., "Steel Bridge Members Under Variable Amplitude Long Life Fatigue Loading," NCHRP Report 267, Dec., 1983.
- (63) Fisher, J. W., Pense, A. W., & Hausamann, H., "Fatigue and Fracture Analysis of Defects in a Tied Arch Bridge," IABSE Colloquium on Fatigue of Steel and Concrete Structures held in Lausanne, Switzerland, in 1982.
- (64) Fisher, J. W., Pense, A. W., & Roberts, R., "Evaluation of Fracture of Lafayette Street Bridge," Journal of the Structural Division, ASCE, Vol. 103, No. ST7, July, 1977.
- (65) Fisher, J. W., Yen, B. T., & Daniels, J. H., "Fatigue Damage in the Lehigh Canal Bridge from Displacement Induced Secondary Stresses," Transportation Research Record 607, TRB, 1977.
- (66) Fisher, J. W., Yen, B. T., & Marchica, N. V., "Fatigue Damage in the Lehigh Canal Bridge," Fritz Engineering Laboratory Report 386.1, Lehigh University, Bethlehem, PA, Nov., 1974.
- (67) Fisher, J. W., et al., "Distortion Induced Stresses in a Floorbeam-Girder Bridge: Canoe Creek," Fritz Engineering Laboratory Report 500-2(86) Lehigh University, Bethlehem, PA, April, 1986.
- (68) Fisher, J. W., et al., "Fatigue Behavior of Full-Scale Welded Bridge Attachments," NCHRP Report 227, Nov., 1980.
- (69) Fisher, J. W., et al., "Analysis of Cracking in Quinnipiac River Bridge," Journal of the Structural Division, ASCE, Vol. 106, No. ST4, April 4, 1980.
- (70) Fisher, J. W., et al., "Detection and Repair of Fatigue Damage in Welded Highway Bridges," NCHRP Report 206, June, 1979.
- (71) Fisher, J. W., et al., "Fatigue Strength of Steel Beams with Welded Stiffeners and Attachments," NCHRP Report 147, 1974.
- (72) Fisher, J. W., et al., "Effect of Weldments on the Fatigue Strength of Steel Beams," NCHRP Report 102, 1970.
- (73) Freudenthal, A. M., "Fatigue of Structural Metal Under Random Loading," Preprint 67b, ASTM, 1960.
- (74) Fuch, H. O., & Stephens, R. I., "Metal Fatigue in Engineering," John Wiley and Sons, New York, NY, 1980.
- (75) Galambos, C. F., "Highway Bridge Loadings," Public Roads, Vol. 43, No. 2, Sept., 1979.
- (76) Gersch, B. C., "Dynamic Testing Program of the T. & N. O. Railroad Overpass, El Paso County, Texas," Research Report 64-5, Texas Highway Department, Austin, TX, Sept., 1964.
- (77) Goble, G. G., Moses, F., & Pavia, A., "Field Measurements and Laboratory Testing of Bridge Components," Report 08-74, Ohio Department of Transportation, Columbus, OH, Jan., 1974.
- (78) Goodpasture, D. W., "Stress History of Highway Bridges," Department of Civil Engineering, University of Tennessee, Knoxville, TN, Dec. 31, 1972.
- (79) Goodyear, D., "Issues in Stay Cable Fatigue Design Loading," to be published.

- (80) Grundy, P., Heng, T. S., & Chitty, G. B., "Measurement Versus Estimation of Railway Bridge Fatigue," paper presented at the 1st Int. Conference of the Engr. Integrity Society held in Bournemouth, UK, on March 17 to 20, 1986.
- (81) Gurney, T. R., "The Effect of Peening and Grinding on the Fatigue Strength of Fillet Welded Joints in Two Steels," British Welding Journal, Vol. 15, 1968.
- (82) Gurney, T. R., "Fatigue Tests Under Variable Amplitude Loading," Report 220/1983, Welding Institute (England), July, 1983.
- (83) Gurney, T. R., "The Application of Fracture Mechanics to Fatigue of Welded Joints," presented at the June 8-11, 1982, ITBTP Fracture Mechanics Seminar held at St-Remy-les-Chevreuse, France.
- (84) Gurney, T. R., "Further Fatigue Tests on Fillet Welded Joints Under Simple Variable Amplitude Loading," Report 182/1982, Welding Institute (England), May 1982.
- (85) Gurney, T. R., "Fatigue Tests on Fillet Welded Joints to Assess the Validity of Miner's Cumulative Damage Rule," Proceedings of the Royal Society (England), 1982.
- (86) Gurney, T. R., "The Basis of the Revised Fatigue Design Rules in the Department of Energy Offshore Guidance Notes," Proceedings of the 1982 International Conference on Offshore Welded Structures, Welding Institute (Eng.), 1982.
- (87) Gurney, T. R., "Basis of Fatigue Design of Welded Joints," IABSE Colloquium on Fatigue of Steel and Concrete held in, Lausanne, Switzerland, in 1982.
- (88) Gurney, T. R., "Some Fatigue Tests on Fillet Welded Joints Under Single Variable Amplitude Loading," Report 144/1981, Welding Institute (England), May, 1981.
- (89) Gurney, T. R., "Fatigue of Welded Structures," 2nd ed., Cambridge University Press (England), 1979.
- (90) Gurney, T. R., "Some Recent Work Relating to the Influence of Residual Stresses on Fatigue Strength," Proceeding of the 1977 Conference on Residual Stresses in Welded Construction and Their Effects," Welding Institute (Eng.).
- (91) Gurney, T. R., "Fatigue Design Rules for Welded Steel Joints," Research Bulletin, Welding Institute (England), Vol. 17, No. 5, May, 1976.
- (92) Gurney, T. R., "Fatigue Design Rules for Welded Steel Joints," Welding Institute Research Bulletin (England), Vol. 17, No. 5, May, 1976.
- (93) Gurney, T. R., "Cumulative Damage Calculations Taking Account of Low Stresses in the Spectrum," Welding Institute Research Report 2/1976/E, March, 1976.
- (94) Gurney, T. R., "Cumulative Damage Calculations with the Proposed New Fatigue Design Rules," Welding Institute Research Report 4/1976/E, March, 1976.
- (95) Gurney, T. R., & Maddox, S. J.: "Comparison of British and American Fatigue Design Rules for Welded Structures," presented at the October 27-31, 1980, ASCE Annual Convention held at Hollywood-by-the-Sea, FL.
- (96) Gurney, T. R., & Maddox, S. J., "A Re-analysis of Fatigue Data for Welded Joints in Steel," Welding Research International, Vol. 3, No. 3, 1973.
- (97) Hamburg, J. R., Lathrop, G. T., & Kaiser, E. J., "Forecasting Inputs to Transportation Planning," NCHRP Report 266, 1983.
- (98) Harrison, J. D., "Acceptance Levels for Defects in Welds Subjected to Fatigue Loading," presented at the July 10, 1979, International Institute of Welding Colloquium held in Bratislava, Yugoslavia.
- (99) Hartgen, D. T., "What Will Happen to Travel in the Next 20 Years?" Transportation Research Record 807, TRB, 1981.
- (100) Hasofer, A. M., & Lind, N. C., "An Exact and Invariant Second-Moment Code Format," Journal of the Engineering Mechanic Division, ASCE, Vol. 100, No. EM1, Feb., 1974.
- (101) Heins, C. P., "LFD Criteria for Composite Steel I-Beam Bridges," Journal of the Structural Division, ASCE, Vol. 106, No. ST11, Nov., 1980.
- (102) Heins, C. P., & Galambos, C. F., "Bridge Fatigue Due to Daily Traffic," Transportation Research Record 507, TRB, 1974.
- (103) Heins, C. P., & Kuo, J. T. C., "Live Load Distribution on Simple Span Steel I-Beam Composite Highway at Ultimate Load," Civil Engineering Department, University of Maryland, MD, April, 1973.
- (104) Heins, C. P., & Sartwell, A. D., "Tabulation of 24 Hours Dynamic Strain Data on Four Simple Span Girder-Slab Bridge Structures," Progress Report 29, Civil Engineering Dept. University of Maryland, College Park, MD, June, 1969.
- (105) Heywood, R. B., "Designing Against Fatigue in Metals," Reinhold, New York, NY, 1962.



- (106) "Highway Capacity Manual," Special Report 209, TRB, 1985.
- (107) "Highway Capacity Manual," Special Report 87, TRB, 1965.
- (108) "Highway Statistics Summary to 1975," FHWA, 1976.
- (109) "Highway Statistics," FHWA, 1984.
- (110) "Highway Structures Design Handbook, Volume I," United States Steel Corporation, Pittsburgh, PA, 1985.
- (111) Hinkle, A. J., & Yao, J. T. P., "Fatigue and Corrosion Behavior of Structures," School of Civil Engineering, Purdue University, West Lafayette, IN, 1984.
- (112) Hirt, M. A., "Fatigue Considerations for the Design of Railroad Bridges," Transportation Research Record 664, TRB, Sept., 1978.
- (113) Hirt, M. A., & Fisher, J. W., "Fatigue Crack Growth in Welded Beams," Engineering Fracture Mechanics, Vol. 5, 1973.
- (114) Hirt, M., "Remaining Fatigue Life of Bridges," IABSE Symposium on Maintenance, Repair, and Rehabilitation of Bridges held in Washington, DC, in 1982.
- (115) Holcomb, R. M., "Distribution of Loads in Beam-and-Slab Bridges," PhD dissertation presented to the Iowa State University, Ames, IA, 1956.
- (116) "Interstate System Traveled-Way Traffic Map," FHWA, 1975.
- (117) Jacquemoud, J., "Analyse du Comportement a la Fatigue des Ponts - Routes," PhD thesis presented to the Ecole Polytechnique Federale de Lausanne, Lausanne, Switzerland, in 1981.
- (118) Jacquemoud, J., & Hirt, M. A., "Fatigue Behavior of Highway Bridges," (in French), IABSE Colloquium on Fatigue of Steel and Concrete Structures held in Lausanne, Switzerland, in 1982.
- (119) Keating, P. B., & Fisher, J. W., "Review of Fatigue Tests and Design Criteria on Welded Details," Fritz Engineering Laboratory Report 488-1(85), Lehigh University, Bethlehem, PA, Oct. 1985.
- (120) Keating, P. B., Fisher, J. W., Yen, B. T., & Frank, W. J., "Fatigue Behavior of Welded Wrought-Iron Bridge Hangers," Transportation Research Record 950, TRB, 1984.
- (121) Keating, P. B., et al., "Fatigue Behavior of Welded Wrought-Iron Bridge Hangers," Transportation Research Record 950, TRB, 1984.
- (122) Kent, P. M. & Robey, M. T., "1975-1979 National Truck Characteristics Report" FHWA, June, 1981.
- (123) Kent, P. M., & Bishop, H., "1974 National Truck Characteristics Report," FHWA, April, 1976.
- (124) Klippstein, K. H., & Schilling, C. G., "Stress Spectrums Short-Span Steel Bridges," Special Technical Publication 595, ASTM, 1976.
- (125) Knight, J. W., "Improving the Fatigue Strength of Fillet Welded Joints by Grinding and Peening," Report 8/1976/E, Welding Institute (England), 1976.
- (126) Koob, M. J., Hanson, J. M., & Fisher, J. W., "Post-Construction Evaluation of the Fremont Bridge," Transportation Research Record 950, TRB, 1984.
- (127) Lee, J. J., et al., "Displacement Induced Stresses in Multigirder Steel Bridges," Fritz Engineering Laboratory Report 500-1(86), Feb., 1986.
- (128) Levinson, H., "Characteristics of Urban Transportation Demand--A Handbook for Transportation Planners," Urban Mass Transportation Administration, Washington, DC, 1978.
- (129) Maddox, S. J., "Improving the Fatigue Lives of Fillet Welds by Shot Peening," IABSE, 1982.
- (130) Maddox, S. J., "Improving the Fatigue Lives of Fillet Welds by Shot Peening," IABSE Colloquium on Fatigue of Steel and Concrete Structures held in Lausanne, Switzerland, in 1982.
- (131) Maddox, S. J., "Assessing the Significance of Flaws in Welds Subject to Fatigue," Welding Research Supplement, Vol. 53, No. 9, Sept., 1974.
- (132) "Manual for Maintenance Inspection of Bridges," AASHTO, 1983.
- (133) Martin, B. V., Memmott, F. W., & Bone, A. J., "Principles and Techniques of Predicting Future Demand for Urban Area Transportation," Report R63-1, Dept. of Civil Engineering, Mass. Institute of Technology, Cambridge, MA, June, 1961.
- (134) Matson, T. M., Smith, W. S., & Hurd, F. W., "Traffic Engineering," McGraw-Hill, NY, 1955.
- (135) McDougale, E. A., Burdette, E. G., & Goodpasture, D. W., "Comparison of Measured and Computed Lateral Load Distribution for Two Continuous Steel Girder Highway Bridges," Dept. of C. E., Univ. of Tenn., Knoxville, TN, Jan., 1976.

- (136) McKeel, W. T., et al., "A Loading History Study of Two Highway Bridges in Virginia," Final Report VHRC70-R48, Virginia Highway Research Council, Charlottesville, VA, June, 1971.
- (137) Memmott, J. L., & Buffington, J. L., "Predicting Traffic Volume Growth Rates Resulting From Changes in Highway Capacity and Land Development," Report 225-23, Texas Trans. Inst., Texas A&M Univ., College Station, TX, Jan., 1981.
- (138) Millington, D., "TIG Dressing to Improve Fatigue Properties in Welded High-Strength Steels," Metal Construction and British Welding Journal, Vol. 5, No. 4, April, 1973.
- (139) Miner, M. A., "Cumulative Damage in Fatigue," Transactions of the American Society of Mechanical Engineers, Vol 67, 1945.
- (140) Morf, T. F., & Houska, F. V., "Traffic Growth Patterns on Rural Highways," Bulletin 194, Highway Research Board, Washington, DC, 1958.
- (141) Moses, F., "Load Spectra for Bridge Evaluation," IABSE Symposium on Maintenance, Repair, and Rehabilitation of Bridges held in Washington, DC, in 1982.
- (142) Moses, F., "Probabilistic Load Modelling for Bridge Fatigue Studies," IABSE Colloquium on Fatigue of Steel and Concrete Structures held in Lausanne, Switzerland, in 1982.
- (143) Moses, F., "Probabilistic Approaches to Bridge Design Loads," Transportation Research Record 711, TRB, 1979.
- (144) Moses, F., & Ghosn, M., "A Comprehensive Study of Bridge Loads and Reliability," Report No. FHWA/OH-85/005, Department of Civil Engineering, Case Western Reserve University, Cleveland, OH, Jan., 1985.
- (145) Moses, F., & Ghosn, M., "Instrumentation for Weighing Trucks-In-Motion for Highway Bridge Loads," Report FHWA/OH-83/001, Department of Civil Engineering, Case Western Reserve University, Cleveland, OH, Aug., 1983.
- (146) Moses, F., & Pavia, A., "Probability Theory for Highway Bridge Fatigue Stresses - Phase II," Report No. Ohio-DOT-02-76, Department of Civil Engineering, Case Western Reserve University, Cleveland, OH, Aug., 1976.
- (147) Moses, F., & Yao, J. T. P., "Safety Evaluation of Buildings and Bridges," presented at the November 14-18, 1983, Symposium on Structural Design, Inspection, and Redundancy held in Williamsburg, VA.
- (148) Moses, F., Ghosn, M., & Gohieski, J., "Weigh-In-Motion Applied to Bridge Evaluation," Report No. FHWA/OH-85/012, Department of Civil Engineering, Case Western Reserve University, Cleveland, OH, Sept., 1985.
- (149) Moses, F., Schilling, C. G., & Raju, K. S., "Commentary on New Fatigue Design and Evaluation Procedures," NCHRP Project 12-28(3), Feb., 1987.
- (150) Moses, F., Schilling, C. G., & Raju, K. S., "Fatigue Evaluation Procedures for Steel Bridges," NCHRP Interim Report, April, 1986.
- (151) Munse, W. H., "Predicting the Fatigue Behavior of Weldments for Random Loads," presented at the May 8 - 11, 1979, Offshore Technology Conference held at Houston, TX, (Paper 3300).
- (152) Munse, W. H., "Fatigue of Welded Steel Structures," Welding Research Council, New York, NY, 1964.
- (153) Munse, W. H., et al., "Fatigue Characterization of Fabricated Ship Details for Design," Report No. SSC-318, Department of Civil Engineering, University of Illinois, Urbana-Champaign, IL, Aug., 1982.
- (154) Mutanyi, T., "A Method of Estimating Traffic Behavior on All Routes in a Metropolitan County," Highway Research Record 41, TRB, 1963.
- (155) "National Transportation Policies through the Year 2000," National Transportation Policy Study Commission, Washington, DC, June, 1979.
- (156) Neumann, D. L., & Savage, P., "Truck Weight Case Study for the Highway Performance Monitoring System (HPMS)," Office of Highway Planning, FHWA, June 1982.
- (157) Neveu, A. J., "Quick-Response Procedures to Forecast Rural Traffic," Transportation Research Record 944, TRB, 1983.
- (158) Nieto-Ramviez, J. A., & Veletsos, A. S., "Response of Three-Span Continuous Highway Bridges to Moving Vehicles," Engineering Station Bulletin 489, University of Illinois, Urbana-Champaign, IL, 1956.
- (159) Nolan, C., & Albrecht, P., "Load and Resistance Factor Design of Steel Structures for Fatigue," Department of Civil Engineering, University of Maryland, College Park, MD, June, 1983.
- (160) Nyman, W. E., & Moses, F., "Calibration of Bridge Fatigue Design Model," Journal of Structural Engineering, ASCE, Vol. 111, No. 6, June, 1985.

- (161) Nyman, W. E., & Moses, F., "Load Simulation for Bridge Design and Life Prediction," Department of Civil Engineering, Case Western Reserve University, Cleveland, OH, May, 1984.
- (162) O'Connor, C., & Pritchard, R. W., "Impact Studies on Small Composite Girder Bridges," Journal of Structural Engineering, ASCE, Vol. 111, No. 3, March, 1985.
- (163) Oehler, L. T., "Vibration Susceptibilities of Various Highway Bridge Types," Journal of the Structural Division, ASCE, Vol. 83, No. ST4, July, 1957.
- (164) "Ontario Highway Bridge Design Code," and Commentary, Ontario Ministry of Transportation and Communications, Toronto, Ontario, Canada, 1983.
- (165) Osborn, A. E., & Koob, M. J., "Evaluation and Field Testing of the Dan Ryan Rapid Transit Structure," Transportation Research Record 950, TRB, 1984.
- (166) Out, J. M., Fisher, J. W., & Yen, B. T., "Fatigue Strength of Weathered and Deteriorated Riveted Numbers," Fritz Engineering Laboratory Report 483-3(84), Lehigh University, Bethlehem, PA, Oct., 1984.
- (167) Pass, J. D., Frank, K. H., & Yura, J. A., "Fatigue Behavior of Longitudinal Transverse Stiffener Intersection: Evaluation of the Fatigue Life of Structural Steel Bridge Details," CTR, University of Texas, Austin, TX, May, 1983.
- (168) Pavia, A., "Reliability Approach to Fatigue Design of Highway Bridges," PhD thesis submitted to Case Western Reserve University, Cleveland, OH, 1975.
- (169) Pedersen, N. J., & Samdahl, D. R., "Highway Traffic Data for Urbanized Area Project Planning and Design," NCHRP Report 255, 1982.
- (170) Pigman, J. G., & Mayer, J. G., "Characteristics of Traffic Streams on Rural, Multilane Highways," Research Report 444, Bureau of Highways, Kentucky Department of Transportation, Lexington, KY, April, 1976.
- (171) "Recommendations for Stay Cable Design and Testing," Ad. Hoc Committee on Cable-Stayed Bridges, Post-Tensioning Institute, Jan., 1986.
- (172) "Recommendations for the Fatigue Design of Structures," European Convention for Constructional Steelwork, Sept. 24, 1982.
- (173) "Recommended Design Loads for Bridges," by the ASCE Committee on Loads and Forces on Bridges, P. G. Buckland, Chmn., Journal of the Structural Division, ASCE, Vol. 107, No. ST7, July, 1981.
- (174) Reemsnyder, H. S., "Fatigue-Life Extension of Riveted Structural Connections," Journal of the Structural Division, ASCE, Vol. 101, No. ST12, Dec., 1975.
- (175) "Report of Subcommittee on Inspection of Steel Bridges for Fatigue," unpublished report of ASCE subcommittee, Dec. 1, 1970.
- (176) Roberts, R., et al., "Fracture Mechanics for Bridge Design," Fritz Engineering Laboratory, Lehigh University, Bethlehem, PA, July, 1977.
- (177) Robison, R., "Sunshine Skyway Nears Completion," Civil Engineering, Vol. 56, No. 11, Nov., 1986.
- (178) Rolfe, S. T., & Barsom, J. M., "Fracture and Fatigue Control in Structures," Prentice-Hall, Inc., Englewood Cliffs, NJ, 1977.
- (179) Ruhl, J. A., & Walker, W. H., "Stress Histories for Highway Bridges Subjected to Traffic Loadings," Structural Research Report 416, University of Illinois, Urbana-Champaign, IL, April, 1975.
- (180) Sahli, A. H., Albrecht, P., & Vannoy, D. W., "Fatigue Strength of Retrofitted Cover Plates," Journal of Structural Engineering, ASCE, Vol. 110, No. 6, June, 1984.
- (181) Sahli, A., & Albrecht, P., "Fatigue Life of Welded Stiffeners with Known Initial Cracks," STP 833, ASTM, 1984.
- (182) Sanders, W. W., "Distribution of Wheel Loads on Highway Bridges," NCHRP Synthesis 111, Nov., 1984.
- (183) Sanders, W. W., & Elleby, H. A., "Distribution of Wheel Loads on Highway Bridges," NCHRP Report 83, 1970.
- (184) Sanders, W. W., Elleby, H. A., & Klaiber, F. W., "Ultimate Load Behavior of Full-Scale Truss Bridges," Report RD-76-40, FHWA, Sept., 1975.
- (185) Sartwell, A. D., & Heins, C. P., "Tabulation of Dynamic Strain Data on a Three Span Continuous Bridge Structure," Progress Report 33, Civil Engineering Department, University of Maryland, College Park, MD, Nov., 1969.
- (186) Sartwell, A. D., & Heins, C. P., "Tabulation of Dynamic Strain Data on a Girder-Slab Bridge Structure During Seven Continuous Days," Progress Report 31, Civil Engineering Dept., Univ. of Maryland, College Park, MD, Sept., 1969.

- (187) Schilling, C. G., "Highway Structures Design Handbook, Chapter 1/6 - Fatigue, Section IV - Fatigue Design," United States Steel Corporation, Pittsburgh, PA., Feb., 1985.
- (188) Schilling, C. G., "A New Method for the Fatigue Design of Steel Highway Bridges," Civil Engineering for Practicing and Design Engineers, Vol. 3, No. 6, June, 1984.
- (189) Schilling, C. G., "Stress Cycles for Fatigue Design of Steel Bridges," Journal of Structural Engineering, ASCE, Vol. 110, No. 6, June, 1984.
- (190) Schilling, C. G., "Highway Structures Design Handbook, Chapter 1/6 - Fatigue, Section III - Fatigue Behavior," United States Steel Corporation, Pittsburgh, PA, Jan., 1984.
- (191) Schilling, C. G., "Impact Factors for Fatigue Design," Journal of the Structural Division, ASCE, Vol. 108, No. ST9, Sept., 1982.
- (192) Schilling, C. G., "Lateral-Distribution Factors for Fatigue Design," Journal of the Structural Division, ASCE, Vol. 108, No. ST9, Sept., 1982.
- (193) Schilling, C. G., "Highway Structures Design Handbook, Chapter 1/6 - Fatigue, Section II - Fatigue Stresses," United States Steel Corporation, Pittsburgh, PA, March, 1982.
- (194) Schilling, C. G., "Lateral-Distribution Tables for Fatigue Design," Research Laboratory Report, United States Steel Corporation, Monroeville, PA, Dec. 31, 1981.
- (195) Schilling, C. G., "Highway Structures Design Handbook, Chapter 1/6 - Fatigue, Section I - Fatigue Loadings," United States Steel Corporation, Pittsburgh, PA, Jan., 1981.
- (196) Schilling, C. G., & Klippstein, K. H., "New Method for Fatigue Design of Bridges," Journal of the Structural Division, ASCE, Vol. 104, No ST3, March, 1978.
- (197) Schilling, C. G., & Klippstein, K. H., "Fatigue of Steel Beams by Simulated Bridge Traffic," Journal of the Structural Division, ASCE, Vol. 103, No. ST8, Aug., 1977.
- (198) Schilling, C. G., et al., "Fatigue of Welded Steel Bridge Members Under Variable-Amplitude Loadings," NCHRP Report 188, 1978.
- (199) Schilling, C. G., et al., "Low-Temperature Tests of Simulated Bridge Members," Journal of the Structural Division, ASCE, Vol. 101, No. ST1, Jan., 1975.
- (200) Shaaban, H., & Albrecht, P., "Collection and Analysis of Stress Range Histograms Recorded on Highway Bridges," Department of Civil Engineering, University of Maryland, College Park, MD, 20742, May, 1985.
- (201) Shakeri Manesh, A. A., & Ganga Rao, H. V. S., "Design Formulas for Slab-Stringer Bridges," Report 2025, Department of Civil Engineering, West Virginia University, Morgantown, WV, 1977.
- (202) Shanafelt, G. O., & Horn, W. B., "Guidelines for Evaluation and Repair of Damaged Steel Bridge Members," NCHRP Report 271, June, 1984.
- (203) Swallowitz, H., "Bridging the Gap in Bridges," Civil Engineering, Vol. 56, No. 11, Nov., 1986.
- (204) Smith, I. F. C., & Hirt, M. A., "Methods of Improving Fatigue Strength of Welded Joints," ICOM 114, Institut de Statique et Structures, Ecole Polytechnique Federale de Lausanne, Lausanne, Switzerland, April, 1983.
- (205) Snyder, R. E., Likins, G. E., & Moses, F., "Loading Spectrum Experienced by Bridge Structures in the United States," Report FHWA/RD-85/012, Bridge Weighing Systems, Inc., Warrensville, OH, Feb., 1985.
- (206) Sossau, A. B., et al., "Quick-Response Urban Travel Estimation Techniques and Transferable Parameters User's Guide," NCHRP Report 187, 1978.
- (207) Sossau, A. B., et al., "Travel Estimation Procedures for Quick Response to Urban Policy Issues," NCHRP Report 186, 1978.
- (208) "Standard Specification for Rolled Steel Plates, Shapes, Sheet Piling, and Bars for Structural Use," Designation A6-81b, ASTM, 1985.
- (209) "Standard Specifications for Highway Bridges," 13th ed., AASHTO, 1983 and Interim Specifications through 1986.
- (210) "Statistical Abstract of the United States: 1985," United States Bureau of the Census, Washington, DC, 1984.
- (211) "Steel Structures," Swiss Standard SIA 161, (in English), Schweiz. Ing.- und Architekten-Verein SIA, Zurich, Switzerland, 1981.
- (212) "Steel, Concrete, and Composite Bridges, Part 10: Code of Practice for Fatigue," BS1 BS 5400, British Standards Institution (England), 1980.

- (213) Strating, J., "Fatigue Under Random Loadings," Report 6-71-17, Department of Civil Engineering, Delft University of Technology, Delft, Netherlands, Nov., 1971.
- (214) "Structural Welding Code - Steel," and Commentary, AWS, 7th ed., 1983.
- (215) Sweeney, R. A. P., "Some Examples of Detection and Repair of Fatigue Damage in Railway Bridge Members," Transportation Research Record 676, TRB, 1978.
- (216) Swenson, K. D., & Frank, K. H., "The Application of Cumulative Damage Fatigue Theory to Highway Bridge Fatigue Design," Report 306-2F, Center for Transportation Research, University of Texas, Austin, TX, Nov., 1984.
- (217) Tang, J. P., & Yao, J. T. P., "Random Fatigue - A Literature Review," Technical Report CE-22(70)NSF-065, Department of Civil Engineering, University of New Mexico, Albuquerque, NM, June 1970.
- (218) Thoft-Christensen, P., & Baker, M. J. "Structural Reliability Theory and Its Application," Springer-Verlag, New York, NY, 1982.
- (219) Tilly, G. P., "Dynamic Response of Bridges," Transportation Research Record 665, TRB, 1978.
- (220) Tilly, G. P., & Nunn, D. E., "Variable Amplitude Fatigue in Relation to Highway Bridges," Proceedings of the Institute of Mechanical Engineers (England), Vol. 194, No. 27, 1980.
- (221) "Traffic Characteristics on Illinois Highways/1971," Illinois Department of Transportation, Springfield, IL, 1971.
- (222) "Traffic Volume Trends," FHWA, March, 1986.
- (223) "Transportation and Traffic Engineering Handbook," Institute of Transportation Engineers, Prentice-Hall, Englewood Cliffs, NJ, 1982.
- (224) "Transportation and Traffic Engineering Handbook," Institute of Transportation Engineers, Prentice-Hall, Englewood Cliffs, NJ, 1976.
- (225) Tung, C. C., "Fatigue Life of Multilane Highway Bridges," Journal of the Engineering Mechanics Division, ASCE, Vol. 96, No. EM5, Oct., 1970.
- (226) Tung, C. C., & Kusmez, K. M., "Statistical Evaluation of AASHTO Fatigue Specifications," Report No. FHWA-RD78-S0732, School of Engineering, North Carolina State University, Raleigh, NC, Nov., 1975.
- (227) Turner, H. T., & Manning, T. A., "A Loading History Study of Selected Highway Bridges in Louisiana, Division of Engineering Research, Louisiana State University, Baton Rouge, LA, April 1, 1972.
- (228) Varney, R. F., & Galambos, C. F., "Field Dynamic Loading Studies of Highway Bridges in the U. S., 1948-1965," Highway Research Record 76, TRB, 1965.
- (229) "Vehicle Classification and Truck Weight Survey: 1970-1985," New York Department of Transportation, Albany, NY, Jan., 1986.
- (230) Walker, W. H., "Lateral Load Distribution in Multi-Girder Bridges," Proceedings of the June 12-14, 1986, AISC National Engineering Conference held at Nashville, TN.
- (231) Walker, W. H., "Final Report, Highway Bridge Impact Investigation," Department of Civil Engineering, University of Illinois, Urbana-Champaign, IL, 1970.
- (232) Walker, W. H., & Veletsos, A. S., "Response of Simple-Span Highway Bridges to Moving Vehicles," Engineering Station Bulletin 486, University of Illinois, Urbana-Champaign, IL, 1966.
- (233) Wattar, F., Albrecht, P., & Chrysos, L., "End-Bolted Cover Plates," Journal of Structural Engineering, ASCE, Vol. 111, No. 6, June, 1985.
- (234) Watzman, A., "Program Averts Cracked Eyebars," Engineering News-Record, Vol. 217, No. 19, Nov. 6, 1986.
- (235) Wilson, W. M., et al., "Fatigue Strength of Fillet-Weld and Plug-Weld Connections in Steel Structural Members," Engineering Experiment Station Bulletin 350, University of Illinois, Urbana-Champaign, IL, March 14, 1944.
- (236) Winfrey, R., Howell, P. D., & Kent, P. M., "Truck Traffic Volume and Weight Data for 1971 and Their Evaluation," Report No. FHWA-RD-76-138, FHWA, Dec., 1976.
- (237) Wirsching, P. H., & Yao, J. T. P., "Statistical Methods in Structural Fatigue," Journal of the Structural Division, ASCE, Vol. 96, No. ST6, June, 1970.
- (238) Wolchuck, R., & Marybaur, R. M., "Stress Cycles for Fatigue Design of Railroad Bridges," Journal of the Structural Division, Vol. 102, No. 1, Jan., 1976.
- (239) Woodward, H. T., & Fisher, J. W., "Predictions of Fatigue Failures in Steel Bridges," Fritz Engineering Laboratory Report No. 386-12, Lehigh University, Bethlehem, PA, May, 1974.

- (240) Wright, D. T., & Green, R., "Highway Bridge Vibrations, Part II, Ontario Test Programme," Report No. 5, Department of Civil Engineering, Queen's University, Kingston, Ontario, Canada, 1964.
- (241) Wright, R. N., & Walker, W. H., "Criteria for the Deflection of Steel Bridges," Bulletin 19, AISI, Nov., 1971.
- (242) Wylde, J. G., & Booth, G. S., "Defect Assessment for Fatigue - The Techniques Described in PD6493," Welding Institute Research Bulletin (England), Vol. 22, No. 4, April, 1981.
- (243) Yamada, K., & Albrecht, P., "Fatigue Design of Welded Bridge Details for Service Stresses," Transportation Research Record 607, TRB, 1976.
- (244) Yamada, K., & Albrecht, P., "A Collection of Live Load Stress Histograms of U. S. Highway Bridges," Department of Civil Engineering, University of Maryland, College Park, MD, Dec., 1974.
- (245) Yamada, K., & Hirt, M. A., "Fatigue Life Estimation Using Fracture Mechanics," IABSE Colloquium on Fatigue of Steel and Concrete Structures held in Lausanne, Switzerland, in 1982.
- (246) Yamada, K., & Hirt, M. A., "Fatigue Crack Propagation from Fillet Weld Toes," Journal of the Structural Division, ASCE, Vol. 108, No. ST7, July, 1982.
- (247) Yao, J. T. P., "Reliability Considerations for Fatigue Analysis and Design of Structures," Report No. NSF/RA-800206, School of Civil Engineering, Purdue University, West Lafayette, IN, June, 1980.
- (248) Yao, J. T. P., "Fatigue Reliability and Design," Journal of the Structural Division, ASCE, Vol. 100, No. ST9, Sept., 1974.
- (249) Yura, J. A., Frank, K. H., & Gupta, A. K., "Field Tests of a Continuous Twin Girder Steel Bridge," Report No. CTR-3-5-79-247-2, Center for Transportation Research, University of Texas, Austin, TX, Nov., 1981.
- (250) Zettlemoyer, N., & Fisher, J. W., "Stress Gradient Correction Factor for Stress Intensity at Welded Stiffeners and Cover Plates," Welding Journal, Vol. 56, Dec., 1977.
- (251) Zwerneman, F. J., "Fatigue Crack Growth in Steel Under Variable Amplitude Load-Time Histories," PhD thesis presented to the University of Texas, Austin, TX, Dec., 1985.

**THE TRANSPORTATION RESEARCH BOARD** is a unit of the National Research Council, which serves the National Academy of Sciences and the National Academy of Engineering. It evolved in 1974 from the Highway Research Board which was established in 1920. The TRB incorporates all former HRB activities and also performs additional functions under a broader scope involving all modes of transportation and the interactions of transportation with society. The Board's purpose is to stimulate research concerning the nature and performance of transportation systems, to disseminate information that the research produces, and to encourage the application of appropriate research findings. The Board's program is carried out by more than 270 committees, task forces, and panels composed of more than 3,300 administrators, engineers, social scientists, attorneys, educators, and others concerned with transportation; they serve without compensation. The program is supported by state transportation and highway departments, the modal administrations of the U.S. Department of Transportation, the Association of American Railroads, the National Highway Traffic Safety Administration, and other organizations and individuals interested in the development of transportation.

The National Academy of Sciences is a private, nonprofit, self-perpetuating society of distinguished scholars engaged in scientific and engineering research, dedicated to the furtherance of science and technology and to their use for the general welfare. Upon the authority of the charter granted to it by the Congress in 1863, the Academy has a mandate that requires it to advise the federal government on scientific and technical matters. Dr. Frank Press is president of the National Academy of Sciences.

The National Academy of Engineering was established in 1964, under the charter of the National Academy of Sciences, as a parallel organization of outstanding engineers. It is autonomous in its administration and in the selection of its members, sharing with the National Academy of Sciences the responsibility for advising the federal government. The National Academy of Engineering also sponsors engineering programs aimed at meeting national needs, encourages education and research, and recognizes the superior achievements of engineers. Dr. Robert M. White is president of the National Academy of Engineering.

The Institute of Medicine was established in 1970 by the National Academy of Sciences to secure the services of eminent members of appropriate professions in the examination of policy matters pertaining to the health of the public. The Institute acts under the responsibility given to the National Academy of Sciences by its congressional charter to be an adviser to the federal government and, upon its own initiative, to identify issues of medical care, research, and education. Dr. Samuel O. Thier is president of the Institute of Medicine.

The National Research Council was organized by the National Academy of Sciences in 1916 to associate the broad community of science and technology with the Academy's purpose of furthering knowledge and advising the federal government. Functioning in accordance with general policies determined by the Academy, the Council has become the principal operating agency of both the National Academy of Sciences and the National Academy of Engineering in providing services to the government, the public, and the scientific and engineering communities. The Council is administered jointly by both Academies and the Institute of Medicine. Dr. Frank Press and Dr. Robert M. White are chairman and vice chairman, respectively, of the National Research Council.

**TRANSPORTATION RESEARCH BOARD**

**National Research Council**

**2101 Constitution Avenue, N.W.**

**Washington, D.C. 20418**

**ADDRESS CORRECTION REQUESTED**